



The
University
Of
Sheffield.

**Solvolysis at Secondary and Tertiary Carbon
Centres in 50% TFE**

The University of Sheffield

Department of Chemistry

Dian Li

August 2017

Submitted to The University of Sheffield in part-fulfilment of the requirements for the degree of Doctor of Philosophy.

Declaration

The work described herein was undertaken at the Department of Chemistry, University of Sheffield from October 2014 to July 2017 under the supervision of Professor N. H.

Williams. This thesis and the data presented within it were completed solely by the author and have not been submitted previously for any degrees at this or any other institutions.

Chapter 2 has been included in the following paper: D. Li, N. H. Williams, *J. Phys. Org. Chem.* **2016**, 29, 709, and was also presented on the 15th European Symposium on Organic Reactivity (ESOR), Kiel, Germany, 2015 as a poster.

Dian Li

August 2017

Acknowledgements

I would like to thank Professor N. H. Williams firstly, for giving me the opportunity to undertake this PhD and secondly for his support over the past 3 years. And for having faith in me, especially when I did not.

Besides, thanks to all the current and past group members, who built an outstanding research and learning environment in the lab. Special thanks go to our UK-oldest postdoc fellow Professor Charles Stirling, who entertained us in a scientific way.

I would like to thank Professor T. T. Tidwell (University of Toronto), R. A. McClelland (University of Toronto), P. v. R. Schleyer (University of Georgia, in Athens), H. C. Brown (Purdue University), W. P. Jencks (Brandeis University), T. W. Bentley (Swansea University) and R. A. Moss (Rutgers University), for their excellent ideas and review papers. Also, the author wants to acknowledge Professor Y. Tsuji (Kurume National College of Technology) and Professor M. Novak (Miami University), for their kind data donation in Chapter 4.

More importantly, I want to express my greatest gratitude to Professor H. Mayr (Ludwig-Maximilians-Universität München), who enlightened my interest on carbenium ion study by laser flash photolysis and communicated with me on the 15th European Symposium on Organic Reactivity (ESOR), Kiel, Germany, 2015. Also, my greatest gratitude to Professor J. P. Richard (University at Buffalo), who inspired me to develop an interest on carbenium ion study by solvolysis and spent two days providing useful and valuable ideas on my talk.

Thanks to all the staff in the Department of Chemistry, for making the department a great place for researchers.

Thanks, go to the Department of Chemistry, University of Sheffield, for the financial support.

Finally, I would extend my thanks to my parents and girlfriend Jingying Peng (The University of Edinburgh); without their support and love, the work could not have been finished.

Abstract

Chapter 1 reviews the variety of sub pathways between classical S_N1 and S_N2 mechanisms and how to distinguish between them. Various mechanistic probes are discussed and their advantages and drawbacks evaluated.

Chapter 2 describes the measurement of the stereochemical outcome for substrates and products during the solvolysis of simple secondary tosylates in 50% TFE. Isotope labelling in the leaving group demonstrates that low levels of ¹⁸O scrambling occur in the substrate during the reaction. Analysing these data together, the mechanism is best described as an enforced uncoupled concerted pathway.

Chapter 3 addresses the solvolysis of endo-2-norbornyl tosylate. Thiocyanate trapping and deuterium labelling probes show that most of the products are derived from the non-classical norbornyl cation, and that the minor products are not consistent with the formation of the classical 2-norbornyl cation as an intermediate. The solvolysis mechanism is best described by both S_N1 and S_N2 pathways, where the S_N1 pathway directly generates the non-classical norbornyl cation.

Chapter 4 attempts to determine the viability of forming the 1-(3-nitrophenyl)ethyl cation in 50% TFE. Its lifetime in 50% TFE has been estimated to be shorter than 10⁻¹³ s, indicating that solvolysis of its precursor should be enforced to follow a concerted pathway. Azoxytosylate is a nucleofuge that experiences less nucleophilic assistance than tosylates and was used in the precursor. The concentration dependence of the product analysis of thiocyanate trapping experiments showed that complete trapping is not experimentally

accessible. Analysing these data leads to the conclusion that the mechanism is still ambiguous, but indicates that a pathway without a cation intermediate is more credible.

Chapter 5 re-examines a very classical substrate family: simple tertiary substrates. It is well accepted that solvolysis of simple tertiary substrates should occur by a step-wise mechanism. However, previous analysis indicates that the lifetime of simple tertiary cations in 50% TFE is about 1 ps, suggesting a solvent-reorganization dominated pathway. Since previous methods used to estimate these cations' lifetime have some significant limitations, we designed a thiono-thiolo exchange probe which allowed us to observe competing O-to-S isomerisation in the substrate during solvolysis. By using 1-adamantyl substrates, a more accurate estimation of a simple tertiary cation's lifetime as 3-7 ps was deduced.

Chapter 6 considers the 3,5-bis(trifluoromethyl)cumyl cation, which has an estimated lifetime shorter than 10^{-13} s. This is not long enough to support a step-wise pathway, but a thiono-thiolo probe shows about 8% O-to-S rearrangement during solvolysis. We propose that the solvolysis mechanism can be a step-wise pathway with a lifetime of about 10 ps for the corresponding intermediate. The reason why the correlation between solvolysis rates and cations' lifetimes is not always valid is discussed.

Chapter 7 provides the author's personal perspective on cation reactivity study. The direct observation of these intermediates by ultra-fast techniques may well be necessary to fully describe these systems and will benefit both synthetic and biological chemistry in the future.

Abbreviations

$A_N D_N$	Concerted mechanisms	$D_N + A_N$	Step-wise mechanisms
A_N	Associative	D_N	Dissociative
$A_N^* D_N$	Uncoupled concerted mechanisms	ns	Nanosecond (10^{-9} s)
ps	Picosecond (10^{-12} s)	fs	Femtosecond (10^{-15} s)
ρ	Hammett constant	σ^+	Brown-Okamoto substituent constant
NMR	Nuclear magnetic resonance	RT	Room temperature
KIE	Kinetic isotopic effect	Nu	Nucleophile
Cupferron	N-nitroso-N-phenylhydroxylamine	Y_{Cl}	Grunwald–Winstein solvent scale
HFIP	Hexafluoroisopropanol	DMAP	4-Dimethylaminopyridine
TsCl	Tosyl chloride	TFE	2,2,2-trifluoroethanol
EtOAc	Ethyl acetate	NaOAc	Sodium acetate
TFA	Trifluoroacetic acid	B_{AC}	Base-catalysed acyl hydrolysis mechanism
DCM	Dichloromethane	THF	Tetrahydrofuran
OPms	Pemsylate (pentamethylbenzenesulfonate)	OBs	Brosylate (4-bromobenzenesulfonate)

Contents

Declaration	I
Acknowledgements	II
Abstract	IV
Abbreviations	VI
Chapter 1 General Introduction	1
1.1 Why study the effect of organic structure on reactivity towards solvolysis?.....	1
1.2 The two simplest solvolysis mechanisms: S_N1 ($D_N + A_N$) and S_N2 ($A_N D_N$).....	1
1.3 Borderline solvolysis mechanisms: step-wise with unstable intermediates, solvent pre-organization or uncoupled concerted ($A_N^* D_N$) pathways?.....	3
1.4 Concurrent S_N2 with S_N1 pathways.....	7
1.5 How to study borderline solvolysis mechanisms (step-wise with unstable intermediates <i>vs</i> uncoupled concerted)?.....	8
1.6 Aims and approach.....	19
1.7 Projects and purposes.....	20
1.8 Conclusion remarks.....	22
Chapter 2 The Solvolysis Mechanism of Simple Secondary Tosylates in 50% (v : v) Aqueous TFE	23
2.1 Introduction.....	23

2.2 Experimental.....	24
2.3 Results.....	32
2.4 Discussion	36
2.5 Conclusion	48
Chapter 3 The Solvolysis Mechanism of endo-2-norbornyl Tosylate in 50% Aqueous (v : v) TFE.....	51
3.1 Introduction.....	51
3.2 Experimental.....	54
3.3 Results.....	60
3.4 Discussion.....	63
3.5 Conclusion.....	72
Chapter 4 Can 1-(3-nitrophenyl)ethyl Cation Be Formed in 50% (v : v) TFE? On the Study of Solvolysis Reaction of 1-(3-nitrophenyl)ethyl Azoxytosylate.....	74
4.1 Introduction.....	74
4.2 Experimental.....	77
4.3 Results and Discussion.....	84
4.4 Conclusion.....	101
Chapter 5 The Solvolysis Mechanism of Simple Tertiary Substrates in 50% (v : v) TFE.....	102
5.1 Introduction.....	102
5.2 Experimental.....	105
5.3 Results and Discussion.....	125
5.4 Conclusion.....	140

Chapter 6 Solvolysis of 3,5-Bis(trifluoromethyl)Cumyl Substrates and On the Search for Thiono-Thiolo Rearrangement of Thionophosphates in 50% (v : v) TFE.....	142
6.1 Introduction.....	142
6.2 Experimental.....	144
6.3 Results.....	150
6.4 Discussion.....	154
6.5 Conclusion.....	158
Chapter 7 Summary and Perspective.....	161
References.....	166
Appendices.....	176
Chapter 2.....	176
Chapter 3.....	182
Chapter 4.....	185
Chapter 5.....	191

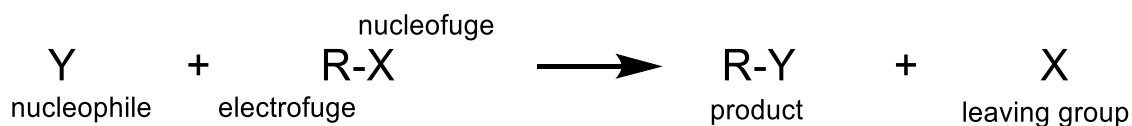
Chapter 1: General Introduction

1.1 Why study the effect of organic structure on reactivity towards solvolysis?

Organic chemists are well trained to understand the factors that control the reactivity of heterolysis reactions in polar solvents: the electrofugality and nucleofugality of corresponding precursors¹⁻³; solvents' ionising and hydrogen-bonding abilities³ and their nucleophilicity⁴. However, the question that arises is whether can one predict the stability and reactivity of a particular compound in a specified solvent? Most chemists may be stuck, but this is important in daily laboratory work since one may wonder if a certain substrate can be handled in aqueous or alcoholic solvents without being significantly solvolysed; is it moisture sensitive so that it must be stored under a dry atmosphere or can a bioactive amine or azole be generated from a precursor in aqueous solutions at a convenient rate. These daily chemistry questions are all related to structure and reactivity study in the field called physical organic chemistry. Thus, by studying solvolysis mechanisms in a systematic way, one may use the knowledge to solve synthetic and biological problems efficiently.

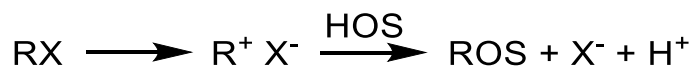
1.2 The two simplest solvolysis mechanisms: S_N1 ($D_N + A_N$)⁵ and S_N2 ($A_N D_N$)⁵

In nucleophilic substitution reactions, nucleophiles (Y) react with substrates (R-X) in a heterolysis pathway, giving products (R-Y) and leaving groups (X). Within the substrates, the leaving groups that depart with a pair of electrons are also called nucleofuges⁶ and the sites that receive a pair of electrons from the nucleophiles are called electrofuges⁶ (Scheme 1.1).



Scheme 1.1. The participants in nucleophilic substitution reactions

If the solvent can participate in the substitution reaction as a nucleophile, then this reaction type is referred to as solvolysis⁷. The S_N1 solvolysis mechanism (also called a step-wise or ionization pathway) requires that the substrate RX dissociates (D_N) to an intermediate (free R⁺ or R⁺ X⁻) first, then is trapped by solvents (A_N) to form the corresponding product. In water, alcohol or carboxylic acid (HOS) (most common solvolysis solvents), the final product ROS after the loss of proton is shown in Scheme 1.2 (fast proton transfer is omitted). A typical energy profile representing this process is also shown in Fig. 1.1.



Scheme 1.2. The S_N1 (D_N + A_N) solvolysis mechanism

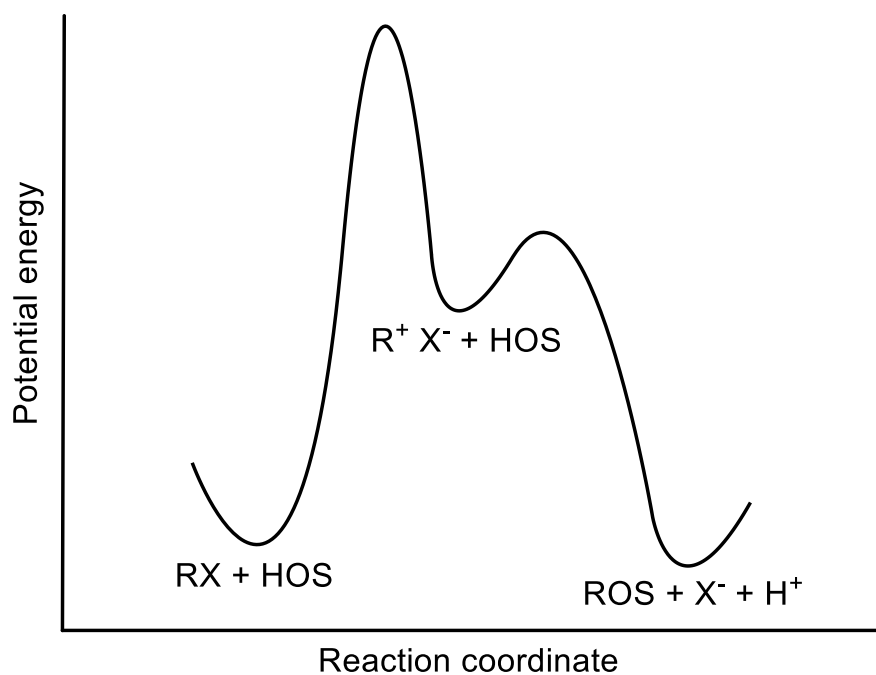


Figure 1.1. Reaction energy profile for S_N1 solvolysis pathways

The S_N2 solvolysis mechanism (also called a concerted pathway) does not include the formation of ion-pair intermediates and the attack by nucleophilic solvents (A_N) and the departure of leaving groups (D_N) take place in a single step. This might be asynchronous or synchronous, depending on the nucleophile and substrate's properties⁸. A typical energy profile for S_N2 solvolysis is shown in Fig. 1.2 (fast proton transfer is omitted).

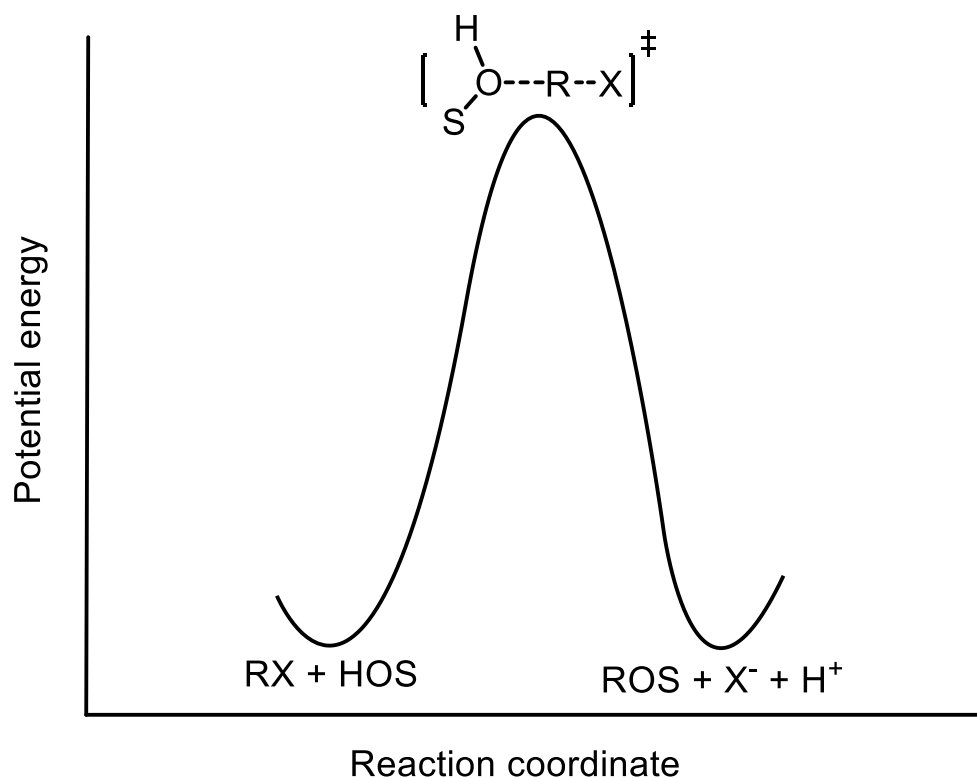


Figure 1.2. Reaction energy profile for S_N2 solvolysis pathways

1.3 Borderline solvolysis mechanisms: step-wise with unstable intermediates, solvent pre-organization or uncoupled concerted ($A_N^*D_N$)⁵ pathways?

Let's now consider solvolysis mechanisms in much more detail. The examples shown above as S_N1 and S_N2 mechanisms should be regarded as two limits (S_N1 (lim) and S_N2 (lim) in Fig. 1.3)⁹. As the cation's stability decreases, one can easily predict that the trend

will shift from S_N1 (lim) to S_N2 (lim) pathways. However, there are still a variety of subtle changes between these two extremes. Fig. 1.3 shows two representative borderline mechanisms described by Jencks⁹. The uncoupled concerted mechanism indicates that the highest energy species is mainly due to the ionization of the substrate without (or with little) nucleophilic assistance, followed by barrierless bond formation to the nucleophile¹⁰. Thus, this mechanism resembles an ionization pathway but no intermediates are formed; the two single steps shown in S_N1 (lim) now are slightly merged into a single asynchronous but still concerted step.

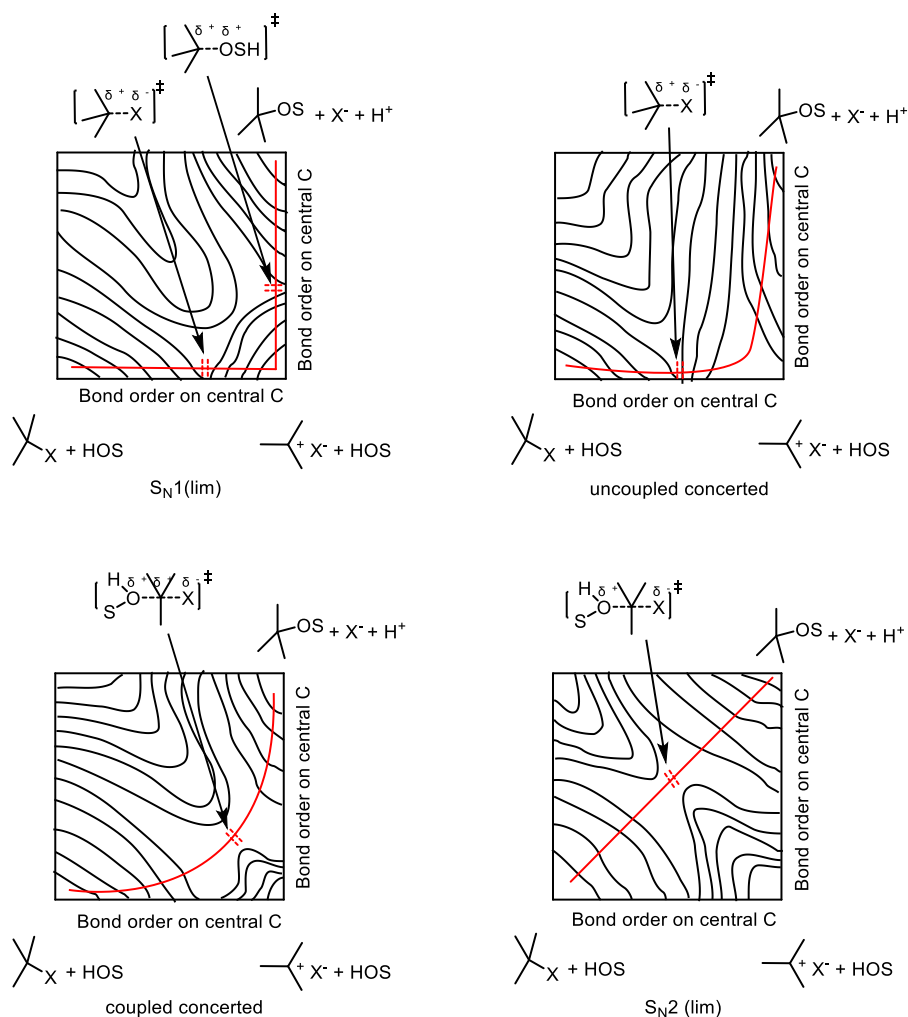


Figure 1.3. 2D reaction energy profiles showing the change from S_N1 (lim) to S_N2 (lim) mechanisms with decreasing carbenium ion stability

The coupled concerted pathway approaches the S_N2 (lim) mechanism as the cation's lifetime is further shortened. This represents more bond coupling between nucleophile and substrate but still not as much as the synchronous S_N2 (lim) mechanism. The electrofuge will accumulate partial positive charge that one can use to predict the effects of structural changes on solvolysis rates.

A key target over the last thirty years¹¹⁻¹³ has been to distinguish between 'mixed' mechanisms (S_N1 (lim) + S_N2 (lim)) and a single uncoupled concerted pathway for those borderline region substrates by a variety of useful probes (See 1.5). This aims to address the question of how and why solvolysis reaction mechanisms change with changing conditions and structures, and whether there is a relationship between intermediate's lifetime and the reaction pathways or not. Particularly, as pointed out by Jencks *et al.*¹¹⁻¹³, it is not clear whether all the S_N2 pathways are enforced to take place because the intermediates cannot exist in solutions (*i.e.* the intermediate's lifetime is shorter than bond vibration scale) (for the borderline region, this is referred to as a single uncoupled concerted pathway), or whether the S_N2 pathways provide an alternative lower or comparable energy pathway even if those intermediates are allowed to exist (for the borderline region, this is referred to as a 'mixed' mechanism). Trying to answer those questions will not only provide a more refined mechanism description (fundamental insights) but also will benefit synthetic chemists for choosing and designing synthesis strategies (synthetic insights).

Focusing back on the S_N1 (lim) mechanism shown in Fig. 1.3, the bimolecular reaction of cations with nucleophiles in solution cannot be faster than diffusion (*ca.* $k_{diff} = 5 \times 10^9 \text{ s}^{-1} \text{ M}^{-1}$ in 50% (v : v) TFE¹¹⁻¹⁴). If the intrinsic covalent bond formation barrier between

cations and solvents is lower than the diffusion barrier in solution (the barrier to form covalent bond between cations and strong nucleophiles will be even lower), then most of the cations will be quenched before nucleophiles can diffuse into the same solvent shell. Therefore, in order to overcome the barrier set by diffusion in solution, the nucleophiles need to associate with the substrates before their ionization. The ion-pair formed by nucleophile pre-association then will decay at a rate constant faster than $5 \times 10^9[\text{Nu}] \text{ s}^{-1}$, making the entire activation energy of product formation lower than a conventional step-wise pathway, where the second step is limited by diffusion control¹¹⁻¹³.

This can also be applied to solvolysis conditions without added nucleophiles. The reaction between cations and solvent molecules in the solvent shell cannot be faster than solvent reorganization (or relaxation). Thus, the energy barrier of the second step shown in Fig. 1.1 $\text{S}_{\text{N}}1$ (lim) requires further refinement. As most aqueous alcohol solutions' reorganization rate constants¹⁵ are about 10^{10} to 10^{11} s^{-1} (50% TFE (v : v) is suggested¹⁶ as 10^{11} s^{-1}), if the intrinsic energy of bond formation to generate solvolysis products from ion-pair intermediates is lower than the solvent reorganization barrier, then an alternative pathway which makes the entire activation energy lower than the step-wise pathway without pre-organization will be dominated. This pathway requires that the solvent molecules pre-organize first so that product formation from the ion and solvent can be faster than solvent reorganization. This subtle mechanism is referred to as a solvent pre-organized step-wise pathway¹⁶ as shown in Fig. 1.4.

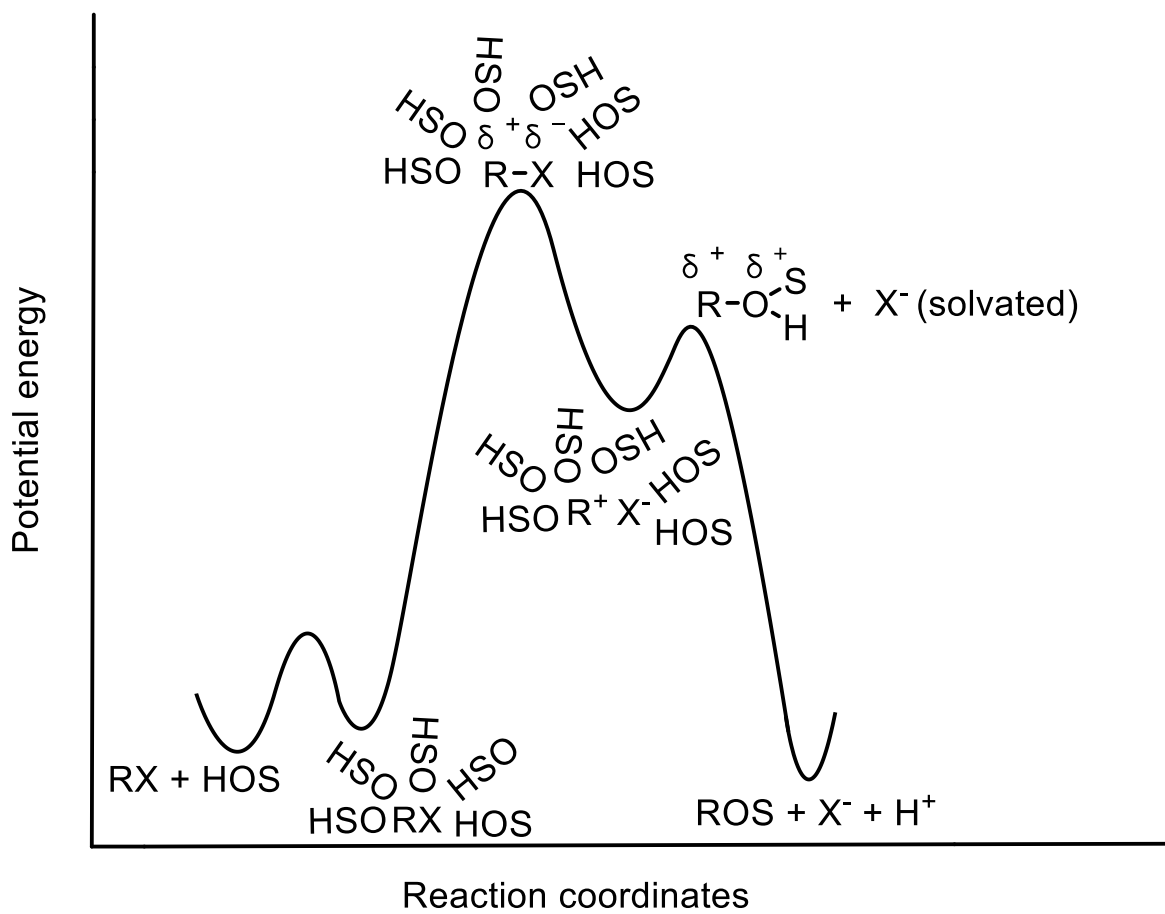


Figure 1.4. Reaction energy profile for solvent pre-organized step-wise mechanisms

1.4 Concurrent S_N2 with S_N1 pathways

Amyes and Richard¹⁷ reported that by solvolysing 4-methoxybenzyl chloride in 80% (v : v) as well as 70% (v : v) acetone/water, the azide reacts with the substrate in both S_N1 and S_N2 pathways. The evidence to support the concurrent pathways is the observation of two to three-fold rate acceleration in the presence of 0.1-0.2 M NaN_3 but with a higher azide adduct yield than calculated from the S_N2 contribution, indicating that part of the adduct yield is also from trapping an ion-pair intermediate.

Similarly, Tsuno *et al.*¹⁸ reported that the reactions between 1-arylethyl bromides and pyridine, substituted benzyl tosylates and N,N-dimethylaniline, as well as substituted

benzyl bromides and pyridine in acetonitrile, show a clear combination of first-order and second-order kinetic parameters. Based on Yukawa-Tsuno correlations, the unimolecular contribution is assigned to be S_N1 , while the bimolecular contribution is suggested to be S_N2 but with an electron-deficient central carbon (uncoupled or weakly coupled concerted mechanism shown in Fig. 1.3).

However, the concurrent S_N2 and S_N1 pathways have only been characterized for bimolecular reactions, simply because the nucleophiles' concentrations are known and can be varied. For solvolysis reactions, it is difficult or impossible to address the concurrent mechanisms since solvents' concentration cannot be varied.

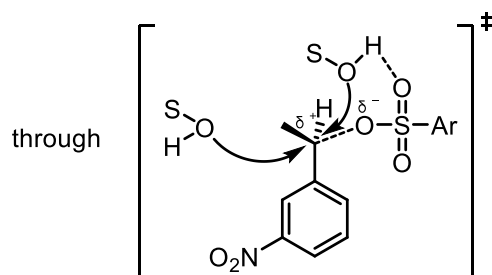
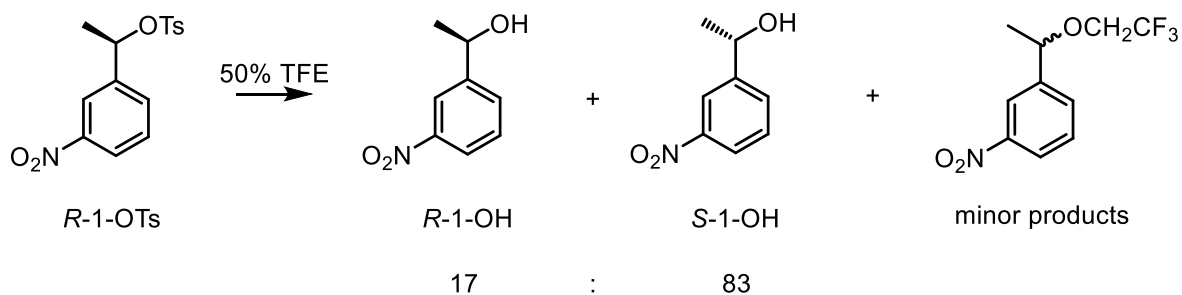
1.5 How to study borderline solvolysis mechanisms (step-wise with unstable intermediates vs uncoupled concerted)?

1.5.1 Stereochemistry of substrates and products

The product stereochemistry is not very useful to characterize borderline mechanisms, since the facial selectivity for this type of reaction is often between 50 : 50 and 100 : 0 (inversion : retention) and Richard *et al.*^{16,19} have pointed out that the leaving group can act as a general base to form products with retention of configuration in an uncoupled concerted pathway.

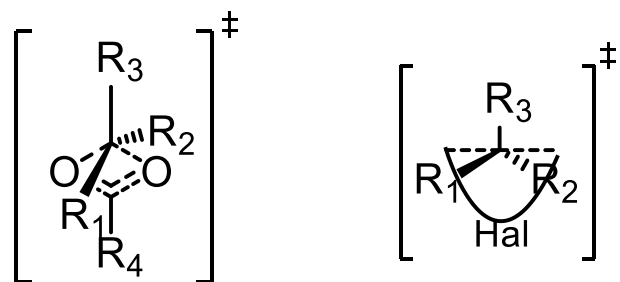
In a key example, Richard *et al.*^{16,19} reported that solvolysing (*R*)-1-(3-nitrophenyl)ethyl tosylate (**R-1-OTs**) in 50% (v : v) TFE (Scheme 1.3) gives products in a 17 : 83 ratio (retention : inversion) but other evidence indicates the solvolysis mechanism should be regarded as an uncoupled concerted pathway. Therefore, the facial selectivity alone cannot

be used as a criterion to distinguish between step-wise and uncoupled concerted mechanisms, since both pathways can generate products with some retention of configuration.



Scheme 1.3. Solvolysis of **R-1-OTs** in 50% (v : v) TFE

However, the stereochemistry of the substrates can be a useful tool to characterize the existence of ion-pair intermediates. Since the concerted racemization of esters or halides is impossible (Scheme 1.4), the step-wise racemization of a substrate directly indicates the formation of ion-pair intermediates that have long enough lifetimes to rotate the electrofuge before recombination²⁰.



Scheme 1.4. Impossible concerted intramolecular racemization for carboxylates and halides

Again, before making any conclusions, other pathways that can lead to racemization must be ruled out. The two most common pathways that can lead to substrate racemization are bimolecular reactions between substrates and leaving groups generated in the course of solvolysis (conventional S_N2 mechanisms) and the neighbouring group participation (see Chapter 2). These two processes do not require the formation of ion-pair intermediates, and can take place through concerted pathways (see Chapter 2). If these two processes are not significant then one can be confident about the existence of an ion-pair intermediate if racemization is observed.

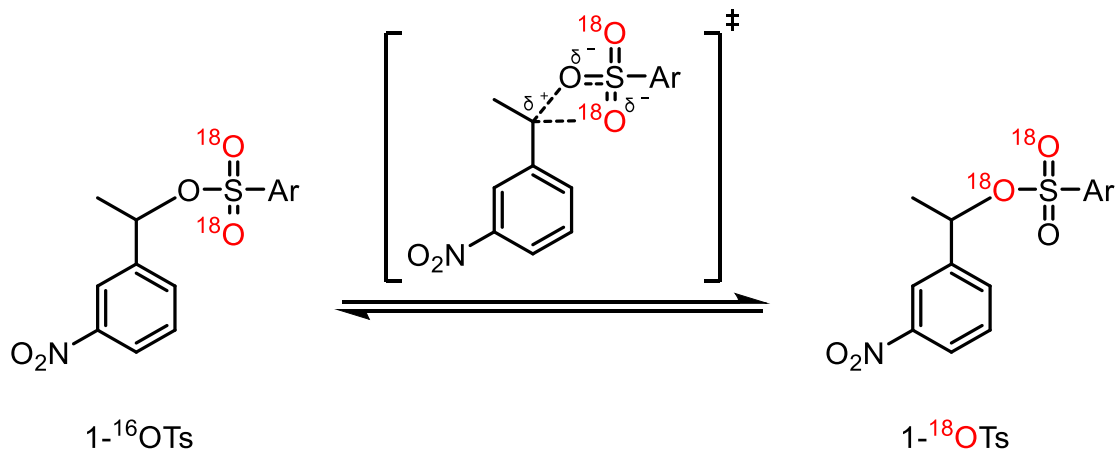
However, if racemization cannot be detected, this does not mean the solvolysis pathway has to be concerted. The electrofuge's rotation rate can be much slower than internal return (see Chapter 5) or internal return is much slower than other processes. Therefore, racemization is a sufficient but unnecessary observation to identify ion-pair formation.

1.5.2 Isotope exchange in ester-type leaving groups

Labelling one type of oxygen in an ester nucleofuge with ^{17}O or ^{18}O provides an additional tool to study ion-pair return. Since isotope exchange was believed to only take place in a step-wise pathway²¹ (the four-membered transition state was thought to be less likely), this

probe has been heavily used over the past twenty-five years as a test for the step-wise pathway²²⁻²⁴.

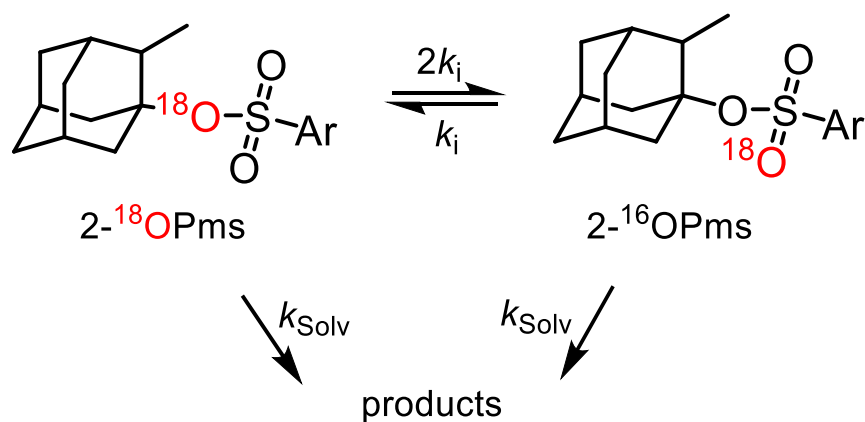
However, by studying the solvolysis of **1-OTs** in 50% (v : v) TFE, Tsuji and Richard^{16,19} pointed out that the isotope exchange was too fast relative to its racemization rate to be explained through a common intermediate. This was based on a tosylate anion exchange rate constant of 10^{11} s^{-1} and an estimation for the rate constant of $1.5 \times 10^{10} \text{ s}^{-1}$ for the rotation of 1-arylethyl cation in 50% (v : v) TFE²⁰. The observed ratio of isotope exchange to racemization was far greater than the maximum ratio calculated for a single ion-pair intermediate. Thus, it was concluded that the isotope exchange took place mostly in a concerted uncoupled pathway with a four-membered ring transition state that still accumulates significant charge on both electrofuge and nucleofuge as shown in Scheme 1.5.



Scheme 1.5. Isotope exchange of **1-OTs** in 50% (v : v) TFE in an uncoupled concerted pathway

Therefore, isotope exchange can only be mechanistically useful in some extreme cases. If no isotope exchange can be detected at all, this indicates a concerted pathway or a step-

wise pathway without internal return²⁵ (for more detailed discussions, see Chapter 3). If relatively fast isotope exchange is observed (empirically, $k_i / k_{\text{Solv}} > 1$), then this can be used as evidence to support the reversible formation of ion-pair intermediates. The latter case was reported by Shiner Jr *et al.*²⁶ when 2-methyl-1-adamantyl pemsylate (**2-OPms**) solvolyses in 95% (v : v) ethanol (Scheme 1.6). The isotope exchange k_i was measured as 1.3 times faster than k_{Solv} , indicating the reversible formation of ion-pair intermediates.



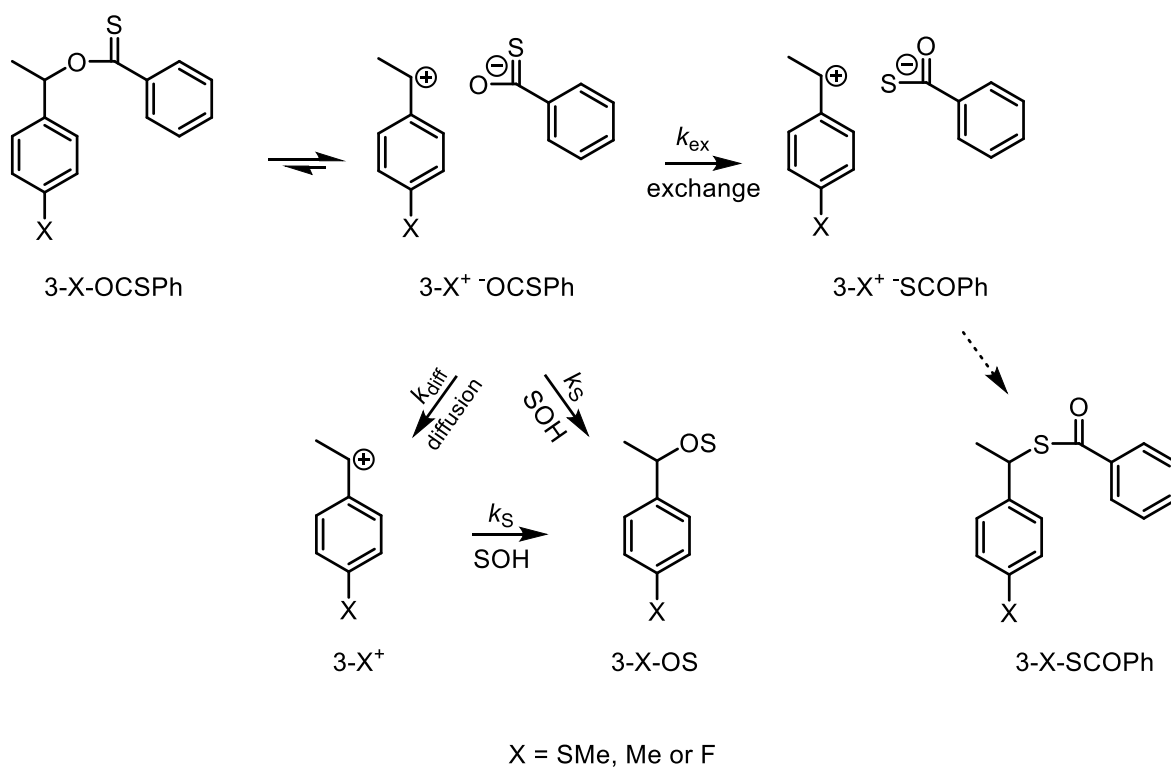
Scheme 1.6. Isotope exchange of **2-OPms** in 95% (v : v) ethanol/water

1.5.3 Thiono-thiolo rearrangement as an alternative probe to isotope exchange

As well as ¹⁷O or ¹⁸O labelling, an alternative probe to study ion-pair formation is to replace the acyl oxygen with sulfur, *i.e.* using a thiono ester^{27,28}. The advantage of this probe is that once the sulfur containing nucleofuge becomes a nucleophile and exchanges its position, the recombination between the nucleophile and the corresponding electrophile is barrierless (*i.e.* with a lifetime shorter than 100 ns in 50% (v : v) TFE, using the intrinsic bond formation rate constant ratio $k_{\text{strong nucleophile}} / k_{50\% \text{ TFE}} = 10^6 \text{ M}^{-1}$)^{11,14,28}. Thus, once the nucleophile exchanges its position, other processes (ion-pair separation or solvent trapping) cannot compete with the intramolecular recombination, which gives the rearranged product

(more stable) quantitatively. This probe overcomes the potential problem involved in using ^{17}O or ^{18}O labelling, where the ion-pair recombination rate constant is unknown and thus the ion-pair intermediate's lifetime cannot be derived directly. If the sulfur containing anion exchange rate constant is known, this thiono-thiolo rearrangement probe can directly derive the lifetime of such an ion-pair intermediate from the product competition (anion exchange versus ion-pair separation and solvent trapping); since after the sulfur-containing anion exchanges its position, the recombination is barrierless and no other processes can compete. Unfortunately, this probe has only been applied for carboxylates²⁸, phosphate triesters²⁷ and phosphinate esters, since other thionoesters are difficult to synthesize.

As a case study, Richard and Tsuji²⁸ reported using thionobenzoate as a nucleofuge to study the ion-pair recombination of three 1-arylethyl substrates (**3-X-OCSPh**) (Scheme 1.7).



Scheme 1.7. Thiono-thiolo rearrangement of **3-X-OCSPh** in 50% (v : v) TFE

Since the three cations' lifetimes have all been established by 'azide clock' methods²⁸ and the thiono-thiolo rearrangement is assigned to be step-wise (because the isomerization pathway gave a slightly more negative ρ value than solvolysis, based on a Yukawa-Tsuno correlation). Then the thionobenzoate anion exchange rate constant was obtained as 10^{11} s^{-1} by analysing the isomerised substrate yield (isomerization% = $\frac{k_{\text{ex}}}{k_{\text{ex}}+k_{\text{S}}+k_{\text{diff}}} \times 100\%$).

Therefore, thionocarboxylates rearrangement can be used as an efficient probe with a clock of 10^{11} s^{-1} to study the lifetimes of other ion-pair intermediates.

However, the formation of the isomerized substrate is a competition between anion exchange and other processes (ion-pair separation and solvent trapping), and ion-pair separation already has an established rate constant of $1.6 \times 10^{10} \text{ s}^{-1}$ in 50% (v : v) TFE²⁸. Therefore, this probe can only be used to characterize those relatively unstable cations ($k_{\text{S}} > i.e. 10^{10} \text{ s}^{-1}$ in 50% (v : v) TFE). Otherwise, when $k_{\text{S}} \ll k_{\text{diff}}$ but the isomerized ion-pair recombination is still faster than the anion exchange, the isomerization yield will be always about 86% ($\frac{k_{\text{ex}}}{k_{\text{ex}}+k_{\text{diff}}} \times 100\%$).

This probe has also been used with phosphate triesters. Compared with thionocarboxylates, thionophosphates are more reactive and easier to synthesize, which provide a chance to study those precursors which will generate unstable intermediates on a more convenient time scale. Unfortunately, previous work²⁷ only reported thiono-thiolo rearrangement for geranyl dimethylthionophosphate in 65% aqueous TFE (v : v) but did not provide the thionophosphate anion exchange rate constant. Thus, the thiono-thiolo rearrangement in thionophosphate triesters needs to be calibrated to establish the anion exchange rate

constant in 50% (v : v) TFE to be used in the study of the lifetimes of ion-pair intermediates (see Chapters 5 and 6).

1.5.4 'Azide clock' method

This method uses strong nucleophiles (NaN_3 and NaSCN are most commonly used) to study the relationship between the rate of reaction and the yield of trapping adducts¹¹⁻¹³. If the solvolysis mechanism is step-wise, these strong nucleophiles will only participate after the substrate's ionization. Thus, in principle, the observed rate constant should be insensitive to the concentration of added strong nucleophiles (ionic strength must be kept constant with other non-nucleophilic salts, but different salt effects still need to be considered as well), assuming the ionization step is the rate limiting step. However, the competition between solvents and added nucleophiles on the ion-pair intermediate will be directly related to the concentration of these strong nucleophiles.

If a large amount of new trapping adducts are formed (> 50%) without any significant change of solvolysis rates (empirically $\pm 10\%$), then this can be used as evidence to support rate limiting ion-pair formation in a step-wise pathway²⁹. Furthermore, at the product formation step, if the partitioning ratio between strong nucleophiles and solvents on the corresponding carbenium ions $\frac{k_N}{k_S} < 10^6 \text{ M}^{-1}$, it is highly likely that the ion-pair or free cation reacts with those strong nucleophiles by a diffusion controlled process (with a second order rate constant about $5 \times 10^9 \text{ s}^{-1} \text{ M}^{-1}$ in 50% (v : v) TFE²⁹). This was confirmed by directly observing of the decay cations using laser flash photolysis¹⁴. Therefore, the solvent attack rate constant on the ion-pair or free cation can be calculated based on the diffusion limit and partitioning ratio $\frac{k_N}{k_S}$ derived from product analysis.

However, the ‘azide clock’ method has serious limitations. For those substrates with borderline mechanisms, the partitioning ratio of the carbenium ions $\frac{k_N}{k_S}$ is often quite small and it is likely that some of the trapping adducts are from S_N2 or pre-association pathways (since the solvolysis belongs to the borderline region, stronger nucleophiles will shift the mechanism to conventional S_N2 to some extent). Therefore, not all the adducts are formed by trapping reactive intermediates^{30,31}, and a low adduct yield accompanied by a slightly faster solvolysis rate (masked by different salt effects) cannot distinguish between a real S_N2 pathway or an S_N1 pathway with a very reactive intermediate. This method can only be used reliably to characterize those intermediates whose lifetimes are longer than 1 ns in 50% TFE (empirically $\frac{k_N}{k_S} > 5 \text{ M}^{-1}$). More detailed discussions about this method can be found in Chapters 3-6.

1.5.5 Product-nucleophile concentration correlation

Following the ‘azide clock’ methods, the product-nucleophile concentration correlation focuses on the relationship between trapping adducts’ yields and the concentration of added nucleophiles in a different way.

As a key example, Maskill and Jencks³² reported that when benzyl azoxytosylate (**4-AzoOTs**) reacts in 50% (v : v) TFE with added NaSCN, the concentration of benzyl thiocyanate (**4-SCN**) and [NaSCN] are correlated by Equation 1 (the correlation is shown as Fig. 1.5):

$$\frac{[\mathbf{4-SCN}]}{[\text{all products}]} \times 100\% = \frac{[\text{NaSCN}]}{1.20 + 1.76[\text{NaSCN}]} \quad (1)$$

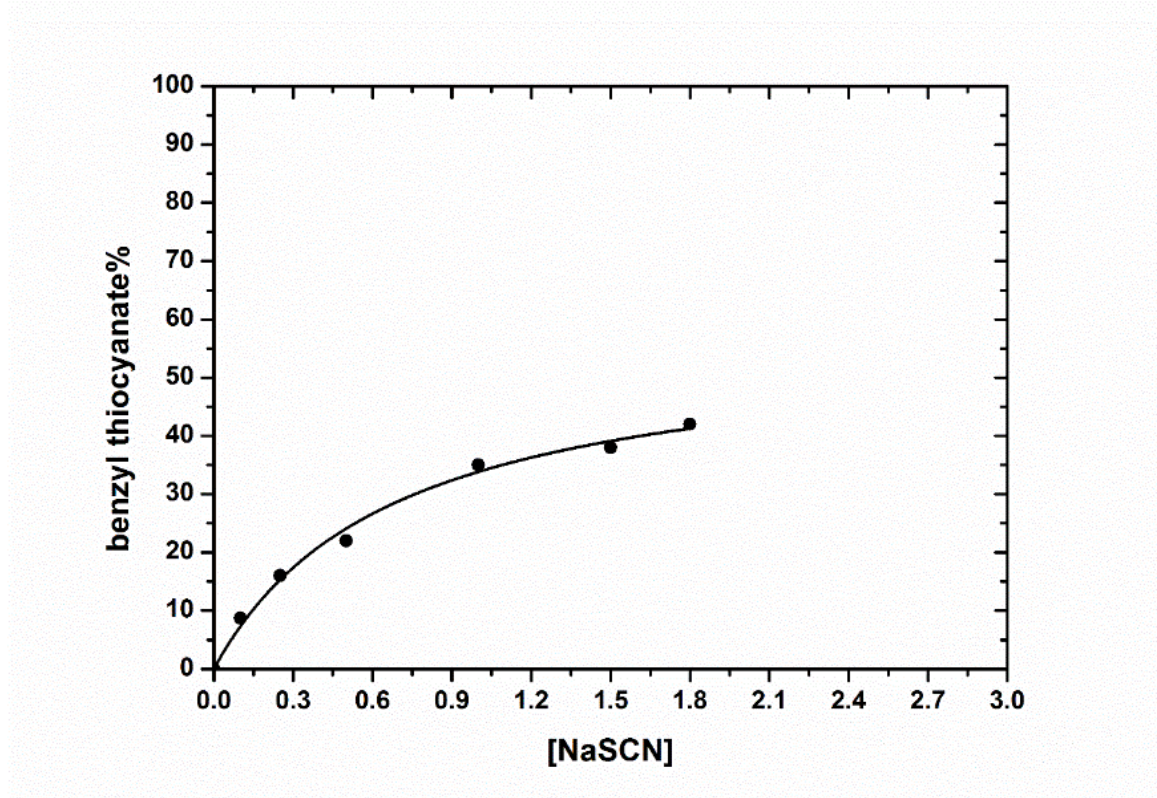
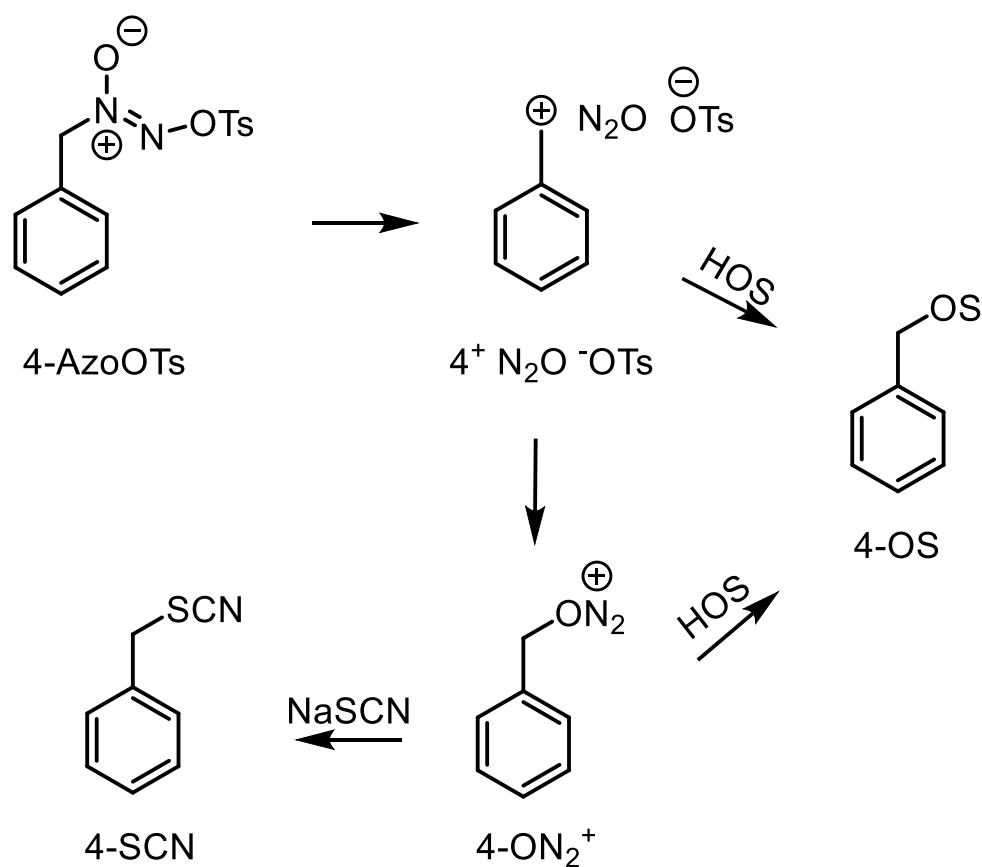


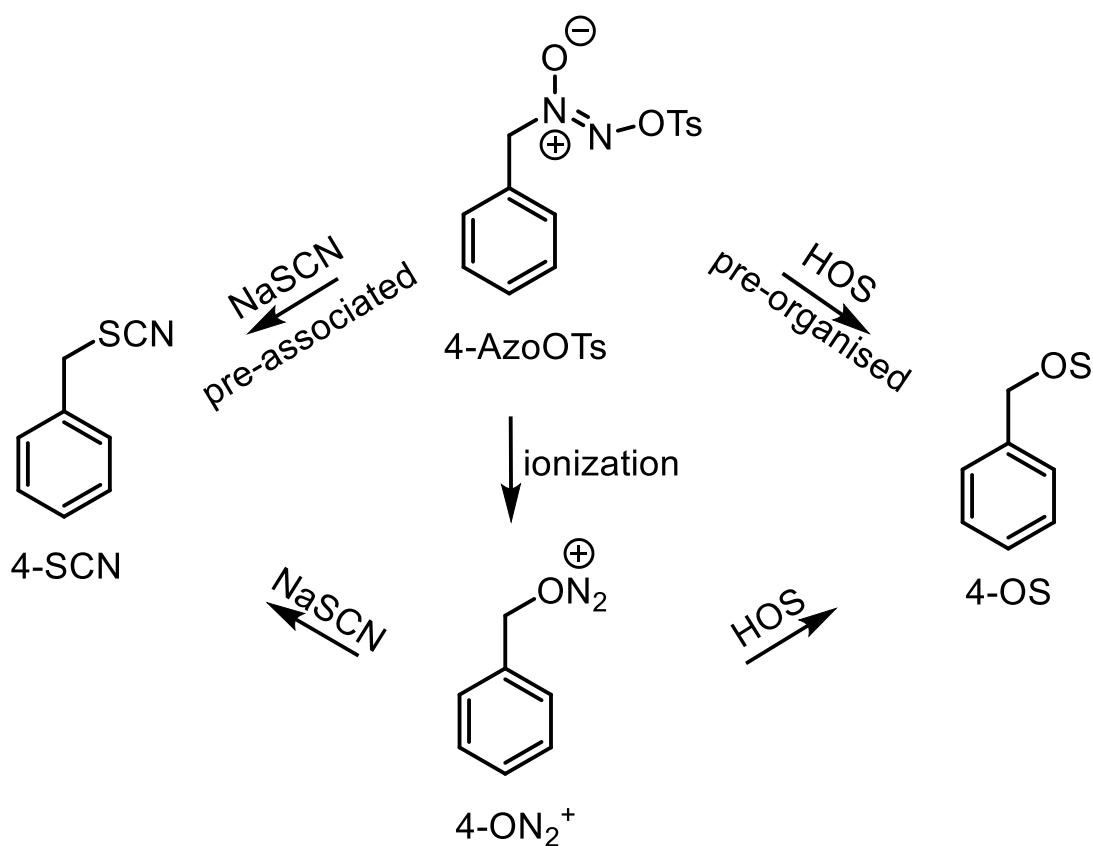
Figure 1.5. Correlation of [4-SCN] and [NaSCN] when **4-AzoOTs** reacts in 50% (v : v) TFE

This indicates that 100% trapping will not occur even if [NaSCN] becomes infinitely large. The limiting value for [4-SCN] formation is only 56%. Thus, they proposed a mechanism for the solvolysis reaction of **4-AzoOTs** in 50% (v : v) TFE that involves two reactive intermediates: the first one is too reactive to be trapped by NaSCN, and the second one can react with NaSCN³². The mechanism is shown below as Scheme 1.8.



Scheme 1.8. The solvolysis mechanism of **4-AzoOTs** in 50% TFE

However, as Maskill and Jencks pointed out³², if there is no energy barrier for the benzyl cation to react with solvent molecules, the first intermediate shown in Scheme 1.8 will become a transition state. Any processes involving the first intermediate then will become enforced uncoupled concerted pathways as shown in Scheme 1.9. Thus, the alternative route can then be described as three uncoupled parallel pathways, in which the nucleophiles are solvent molecules, NaSCN and the oxygen in N₂O moiety, respectively. Since the product ratio $\frac{[4\text{-OH}]}{[4\text{-OCH}_2\text{CF}_3]}$ is different to the solvent composition, those uncoupled processes must be pre-associated. While the alternative description is entirely compatible, they did not fit the product-nucleophile concentration correlation (Fig. 1.5) to the uncoupled pre-association scheme. More details about this method can be found in Chapter 4.



Scheme 1.9. Uncoupled nucleophile pre-association (and solvent pre-organised) pathways for the solvolysis of **4-AzoOTs** in 50% (v : v) TFE

1.6 Aims and approach

This chapter shows that between S_N1 (lim) and S_N2 (lim) solvolysis mechanisms, there are a series of sub pathways in the borderline region suggested by Jencks⁹, based on different lifetimes of carbenium ions. Among these, the uncoupled concerted and pre-association step-wise pathways not only play the most important role (since most of the substrates belonging to this region show behaviour consistent with either pathway) but also make the whole solvolysis reaction a continuous mechanistic spectrum rather than a sharp change from conventional S_N1 to S_N2 mechanisms.

On the other hand, it is known that concurrent S_N2 pathways can exist along with S_N1 pathways^{17,18}, which can mean that the lifetime of intermediates in S_N1 pathways is underestimated. The significance of the concurrent S_N2 contribution will depend on the balance of a more negative activation entropy (because of association) and a smaller activation enthalpy (because of bond coupling) to the free activation energy barrier of the reaction.

1.7 Projects and purposes

The existence of simple secondary cations in solutions has been debated for a long time, but no decisive conclusions have been made^{33,34}. Most of the probes used to study the solvolysis of secondary substrates have been applied under different conditions to each other, which makes analysis ambiguous. Therefore, we chose simple 2-alkyl tosylate and endo-2-norbornyl tosylate as two representative secondary cation precursors (Chapters 2 and 3) and applied several mechanistic probes under the same conditions (50% (v : v) TFE solvolysis with 1 M ionic strength) in order to gain more information about the possible existence of secondary cations in solutions.

Richard and Toteva³⁵ suggested that simple tertiary cations have a lifetime in 50% (v : v) TFE that is less than 1 ps, indicating that a step-wise pathway dominated by solvent reorganization or a solvent pre-organized pathway is necessary for solvolysis of tertiary substrates in aqueous solutions. However, the estimated lifetime of simple tertiary carbenium ions is based on the reactivity of substituted cumyl chlorides in 50% (v : v) TFE. The solvolysis rate constants (k_{SolV}) correlate well with the solvent attack rate constants (k_{S}) on corresponding cumyl cations as shown in Equation 2.

$$\log k_S = -0.53 \log k_{\text{solv}} + 10.6 \quad (2)$$

Due to the structural similarity, Equation 2 can be applied to simple tertiary chlorides in 50% (v : v) TFE and a rate constant k_S is obtained as 10^{12} s^{-1} , indicating a solvent pre-organized step-wise pathway or an uncoupled concerted pathway.

Meanwhile, McClelland *et al.*^{14a} reported that by using a correlation between pK_R and k_S of stable triarylmethyl and diarylmethyl cations in water (Scheme 1.10), the extrapolated k_S for simple tertiary cations is about $10^{10.6} \text{ s}^{-1}$.



Scheme 1.10. Acid-catalysed formation of cations in water

Apart from these correlations, we could not find any other supportive evidence about the lifetime of simple tertiary cations in aqueous solutions, which indicates the mechanism is still ambiguous. Thus, we chose 1-adamantyl bromide as a model for solvolysis with retention of configuration of simple tertiary substrates. The advantage of using the 1-adamantyl system is its structure similarity to simple tertiary systems, so the solvent attack rate constant should be quite close to that for front-side attack on simple tertiary ion-pairs and no side reactions need to be considered (*i.e.* eliminations or back-side S_N2 contributions). Based on that model (using the thiono-thiolo rearrangement probe) and product analysis (including stereochemical analysis) of solvolysis of simple tertiary substrates in 50% (v : v) TFE, we aim to obtain a more accurate value of the lifetime of

simple tertiary cations so that the corresponding solvolysis mechanism can be identified (see Chapter 5).

1.8 Conclusion remarks

There are a variety of useful probes and tools to study and distinguish between these sub pathways. However, no single one can be used to characterize ion-pair formation or support an uncoupled concerted pathway. Although each probe has its own limits and drawbacks, when they are used and analysed together, some more useful information may be obtained and may well be sufficient to draw a clear conclusion.

As the following chapters unfold, readers can recognize how the writer uses those specially designed probes to study those borderline solvolysis mechanisms case by case, from concerted to pre-association pathways, from secondary to tertiary substrates.

Chapter 2: The solvolysis mechanism of simple secondary tosylates in 50% (v : v) aqueous TFE*

2.1 Introduction

Whether simple secondary carbenium ions can be formed as intermediates in polar but weakly nucleophilic solvents through ground state solvolysis has been debated for a long time. No clear-cut conclusion has been reached except for a series of mechanistic studies with 2-propyl and 2-butyl substrates³⁶⁻⁴⁰.

Tidwell *et al.*³⁸, Kowalski *et al.*³⁹ and Farcaşiu⁴⁰ studied the solvolysis of 2-butyl tosylate in TFA by selective deuterium labelling. As a 1,2-hydride (deuteride) shift was observed during the reaction, these authors all agreed that a simple secondary substrate in TFA should undergo a stepwise mechanism ($D_N^*A_N$) with a true intermediate rather than through a concerted pathway (A_ND_N). However, they did not reach agreement on whether the intermediate was a hydride (deuteride) bridged cation or an 'open' carbenium ion. Furthermore, the reaction in TFA is complicated by the acid-catalysed reversible addition of trifluoroacetate and tosylate to the alkene product that also forms during solvolysis, which may contribute to the deuterium scrambling of substrates and products.

On the other hand, Khattak *et al.*³⁶ correlated the solvolysis rates of 2-propyl nosylate in pure HFIP with different nucleophiles against the same reactions with methyl iodide. Since the second-order rate constant of 2-propyl nosylate in pure HFIP was on the same straight line generated by other nucleophiles known to react via S_N2 mechanisms for both substrates, the solvolysis of 2-propyl substrates in HFIP was suggested to follow the same mechanism (A_ND_N). A change in mechanism from concerted to step-wise pathway would

be anticipated to give a positive deviation from the correlation. Dietze and Jencks³⁸ had also previously applied the same correlation method to the solvolysis reaction of 1-(4-nitrophenyl)-2-propyl derivatives in TFE and water/TFE mixtures³⁶. Their conclusion was that these simple secondary substrates reacted through a concerted solvolysis pathway, even in weakly nucleophilic solvents (such as TFE or HFIP), with an 'open' transition state. The mechanistic pathway was described as an enforced uncoupled concerted mechanism¹⁹ with a transition state that has similar properties to a true carbenium intermediate.

Thus, the evidence for either mechanism is not unambiguous, so we have investigated the reaction of 2-butyl tosylate in 50% (v : v) aqueous TFE by studying the stereochemistry of both substrates and solvolysis products and through selective ¹⁸O labelling^{19,41} in the tosylate group.

2.2 Experimental

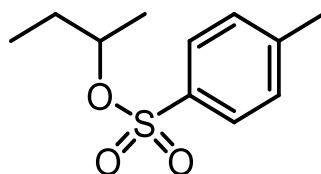
General

The alkyl tosylates, 4-nitrobenzoate ester and ¹⁸O labeled tosyl chloride were synthesized as described below. All other chemicals were purchased from Sigma-Aldrich, Alfa Aesar, Acros Organics or Santa Cruz Biotechnology. TFE was distilled from P₂O₅ and stored over 4Å molecular sieves. UHQ water was obtained from an ELGA PURELAB Option S-R 7-15 system. All other chemicals were used directly without further purification.

¹H NMR and ¹³C NMR spectra were recorded on Bruker AV-HD 400 and AV-HD 500 instruments. HPLC analysis to monitor reaction progress was carried out on a Waters 2690

(486 Tunable Absorbance Detector) and 2695 (2487 Dual λ Absorbance Detector) system with a Waters C8 column and UV detection at 265 nm. A gradient elution was used, changing from 95% water (containing 0.1% TFA) and 5% acetonitrile to 5% water (containing 0.1% TFA) and 95% acetonitrile over 20 mins followed by a further 10 mins of the final eluent mixture. Chiral HPLC analysis of the reactants and alcohol derivatives was recorded on a Gilson 805 manometric model (Gilson 811B Dynamic Mixer, Gilson 305 + 306 Pump and Applied Biosystems 757 Absorbance Detector) with a Phenomenex[®] Cellulose-2 chiral column and UV detection at 226 nm (for tosylates) and 265 nm (for 4-nitrobenzoates). The eluent for tosylate substrates was 12% isopropanol-88% hexane with a flow rate 0.8 mL/min, except for 2-octyl tosylate where 1% isopropanol-99% hexane was used with a flow rate of 1.0 mL/min. For 4-nitrobenzoate, 0.3% isopropanol-99.7% hexane was used with a flow rate 1.0 mL/min. GC analysis of 2-butanol, 2-octanol and 2-octene was determined with a Perkin Elmer ARNEL Auto System XL GC model. 2-butanol was analysed isothermally at 40 °C with a split ratio of 20. 2-octanol and 2-octene were analysed isothermally at 90 °C with a split ratio of 20.

Syntheses

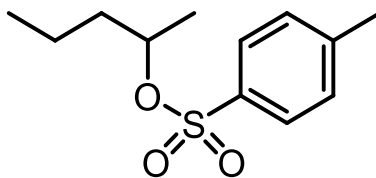


5-OTs

5-OTs^{47,48} was synthesised following a published procedure by Delaney *et al.*⁴⁷ 0.74 g (10 mmol) 2-butanol was dissolved in 10 mL anhydrous pyridine in an ice-water bath. 2.29 g (12 mmol) tosyl chloride was added portion wise within 10 mins. The solution was stirred

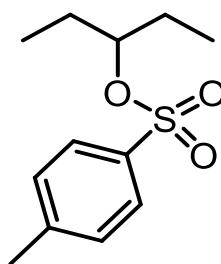
in the ice-water bath for another 6 hours before quenching with cold 3 M HCl solution (25 mL). After extracting with DCM (25 mL), the organic phase was washed with another 25 mL of 3 M HCl and the water phase was extracted with DCM (3 × 5 mL). The combined organic phase was washed with saturated NaHCO₃ solution, dried over Na₂SO₄ and filtered before removed under vacuum. The crude product was purified by flash chromatography using hexane: ethyl acetate (4:1), to yield 1.59 g (70%) of **5-OTs** as a colourless oil. ¹H NMR (400 MHz, CDCl₃): 7.81 (2H, d, J = 8.8 Hz), 7.35 (2H, d, J = 8.8 Hz), 4.51 – 4.60 (1H, m), 2.48 (3H, s), 1.52 – 1.78 (2H, m), 1.35 (3H, d, J = 6.5 Hz) and 0.82 (3H, t, J = 7.5 Hz). ¹³C NMR (100 MHz, CDCl₃): 144.4, 134.6, 129.7, 127.7, 81.8, 29.5, 21.6, 20.3 and 9.3.

S-5-OTs (ee 91%), **6-OTs**, **7-OTs**, **8-OTs** and **R-8-OTz** (ee 99.5%) were all synthesized by the same procedure⁴⁷ and purified by flash chromatography with the same eluent as above.



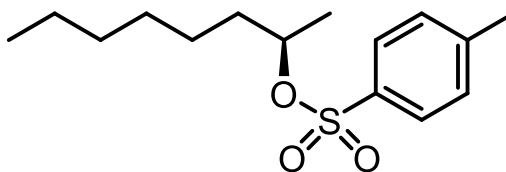
6-OTs

6-OTs⁴⁸: 65% yield as a colourless oil. ¹H NMR (400 MHz, CDCl₃): 7.81 (2H, d, J = 8.8 Hz), 7.35 (2H, d, J = 8.8 Hz), 4.59 – 4.74 (1H, m), 2.48 (3H, s), 1.51 – 1.76 (2H, m), 1.35 (3H, d, J = 6.6 Hz) and 0.67 (3H, t, J = 7.4 Hz). ¹³C NMR (100 MHz, CDCl₃): 144.3, 134.7, 129.66, 127.7, 80.4, 38.6, 21.6, 20.8, 18.1 and 13.6.



7-OTs

7-OTs^{49,50}: 50% yield as a colourless oil. ¹H NMR (400 MHz, CDCl₃): 7.81 (2H, d, J = 8.3 Hz), 7.34 (2H, d, J = 8.3 Hz), 4.42 – 4.73 (1H, m), 2.47 (3H, s), 1.67 – 1.80 (4H, m) and 0.85 (3H, t, J = 7.4 Hz). ¹³CNMR (100 MHz, CDCl₃): 144.3, 135.2, 129.7, 128.7, 66.8, 21.6, 20.2 and 11.1.

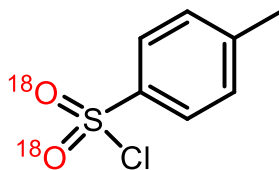


R-8-OTs

R-8-OTs^{51,52}: 60% yield as a colourless oil. ¹H NMR (400 MHz, CDCl₃): 7.79 (2H, d, J = 8.8 Hz), 7.35 (2H, d, J = 8.8 Hz), 4.52 – 4.67 (1H, m), 2.46 (3H, s), 1.65 – 1.08 (15H, m) and 0.85 (3H, t). ¹³CNMR (100 MHz, CDCl₃): 144.3, 134.7, 129.7, 127.7, 80.7, 36.5, 31.6, 28.8, 24.8, 22.4, 21.6, 20.8 and 14.0.

2-octyl 4-nitrobenzoate: After the solvolysis reaction of **R-8-OTs** (150 mL, 10 mM) was complete (at least 7 half-lives), the TFE was removed under vacuum and the aqueous solution extracted with 30 mL diethyl ether. After being washed with brine, the ether solution was concentrated under vacuum and the residue dissolved in 10 mL DCM charged with 2 eq DMAP in a water-ice bath. 1.5 equivalents of 4-nitrobenzoyl chloride were added

portion-wise within 5 mins and the reaction was kept in the ice bath for 2 hours before being slowly warmed to room temperature. The mixture was stirred at room temperature overnight before the solvent was removed under vacuum. The residue was dissolved in 1.5 mL hexane and diluted to a suitable concentration for chiral HPLC analysis. HPLC analysis gave two peaks with retention times of 20.2 and 22.1 minutes in a ratio of 92:8 that correspond to the 4-nitrobenzoate enantiomers as determined by analysis of racemic **2-octyl 4-nitrobenzoate** by the same method.



¹⁸O-tosyl chloride was synthesized by a modified procedure by Veisi *et al.*⁵³ To a 100 mL round bottom flask charged with 30 mL anhydrous acetonitrile, 1.86g (15 mmol) p-thiocresol and 1 mL H₂¹⁸O (97% isotope labelled, Santa Cruz Biotechnology) was added and stirred in an ice-water bath for 15 mins. 4.18g (18 mmol) trichloroisocyanuric acid (TCCA) was added portion-wise to the cooled solution within 10 mins and the reaction was kept at 0 °C for 1 h, then allowed to warm to room temperature and stirred overnight before the solvent was removed under vacuum. 30 mL diethyl ether was added and the mixture shaken violently. The solid was filtered off and washed with 5 × 2 mL diethyl ether; the combined filtrate was concentrated under vacuum to afford 2.86 g (14.7 mmol) of the **¹⁸O-tosyl chloride** (98%). The extent of labelling by ¹⁸O was been determined by GC-MS which showed that the tosyl chloride contained 93.5% doubly labelled **¹⁸O-tosyl chloride** and 6.5% singly labelled **¹⁸O-tosyl chloride**. The crude **¹⁸O-tosyl chloride** was used to

synthesise the tosylate esters immediately it was isolated, using the same synthetic and purification methods described above.

Kinetic analysis

The solvolysis reactions of all the tosylate esters were carried out under the same conditions: 5 mM tosylate, 5 mM 2,6-dimethyl pyridine, 1 mM 2,6-dimethyl-3-hydroxy pyridine (as an internal standard) and 1 M sodium perchlorate in 50% aqueous (v : v) TFE (v/v) at 30 °C. The solutions were immersed in a thermostated water bath, and the progress of the reactions was monitored by analysing aliquots of the reactions mixture using HPLC as described above for 72 hours. The peak areas in the chromatograms were integrated and a first order equation fit to these data; in all cases, $R^2 > 0.99$.

Stereochemical analysis

S-6-OTs (10 mM; initial ee 91%): At various time intervals, an appropriate volume of the reaction mixture (10 mM 2-*S*-butyl tosylate; 1.2 equivalents 2,6-dimethylpyridine; 1 M sodium perchlorate) was withdrawn and extracted with hexane. As the reaction proceeded, increasing volumes of the solution were required to ensure sufficient reactant was present for the analysis. The hexane layer was analyzed directly by chiral HPLC to measure the ratio of the tosylate enantiomers, and by chiral GC to measure the ratio of the 2-butanol enantiomers. Solutions with varying concentrations of tosylate anion present (5 mM S-6-OTs; 6 mM 2,6-dimethylpyridine; 0.1, 0.5 or 1.0 M sodium tosylate, with the total salt concentration made up to 1 M with sodium perchlorate; 1 M 15-crown-5) were analysed the same way.

R-8-OTs (5 mM (initial ee 99.5%); 6 mM 2,6-dimethylpyridine; 1 M sodium perchlorate) was analysed as above to determine the stereochemical changes in the reactant as the reaction progressed. To monitor the stereochemical changes in the alcohol product **R-8-OTs** (10 mM; 12 mM 2,6-dimethylpyridine; 1 M sodium perchlorate) was allowed to proceed to completion (7 half lives), and the 2-octanol isolated as above and converted to 4-nitrobenzoate ester before being analyzed by chiral HPLC.

Isomerisation of 7-OTs and 6-OTs: At various time intervals, an appropriate volume of the reaction mixture was withdrawn and extracted with hexane, which was directly analyzed by chiral HPLC. The signals for **7-OTs** and both enantiomers of **6-OTs** were completely resolved in the chromatogram, and the ratio was determined by integrating these peaks.

Product analysis

The products from the solvolysis of **5-OTs** and **6-OTs** were analysed by ^{13}C NMR. These reactions were carried out in 1 : 1 TFE/D₂O (v/v), with all other conditions the same as for the kinetic measurements. The ratio of the alcohol and ether products were measured by integrating peaks for the carbon at position 2. The products from the solvolysis of **8-OTs** were directly analysed by GC, using authentic 2-octene and 2-octanol as external standards to calibrate the yield of respective products. 2-octene was observed as a mixture of E/Z isomers, but 1-octene was not detected.

Product stability

When 2-octene was incubated under the solvolysis conditions (10 mM in 50% aqueous (v : v) TFE with 20 mM pyridinium tosylate, 10 mM 2,6-dimethyl pyridine and 1 M sodium perchlorate) for 5 days and then analysed by GC, no new peaks could be identified. When R-2-octanol was incubated under the solvolysis conditions (10 mM in 50% aqueous (v : v) TFE with 20 mM pyridinium tosylate, 10 mM 2,6-dimethyl pyridine and 1 M sodium perchlorate) for 2 weeks, then derivatized to the 4-nitrobenzoate ester, chiral HPLC analysis showed the ee had not changed.

¹⁸O isotope exchange analysis⁴¹

5-OS¹⁸O₂Ar (5 mmol) and **8-OS¹⁸O₂Ar** (5 mmol) were individually subjected to solvolysis under the conditions described above (with an initial reactant concentration of 10 mM). At different time intervals, an appropriate volume of solution (to be able to extract about 50 mg of the unreacted tosylate) was withdrawn and extracted with diethyl ether. The organic layer was separated and dried over Na₂SO₄ and the solvent removed under vacuum. The residue was dissolved in 1 ml CDCl₃ and analysed by ¹³C NMR at 125 MHz (pulse angle 45°, 10000 transients at 25 °C acquired with a 250 Hz sweep width, 8000 data points (0.031 Hz/pt) and a 16-s relaxation delay time) to determine the relative concentrations of tosylate esters with ¹⁸O in the bridging and nonbridging positions. The ¹³C signals at the 2-position were centred at 81.8 (**5-OS¹⁸O₂Ar**) and 80.8 (**8-OS¹⁸O₂Ar**) ppm, respectively. The peaks were sufficiently resolved (0.045 ppm difference) to allow the ratio of ¹³C bonded to ¹⁸O or ¹⁶O to be calculated by integration of the signals.

2.3 Results

The first-order rate constants for solvolysis of 2-butyl tosylate (**5-OTs**), 2-pentyl tosylate (**6-OTs**) and 2-octyl tosylate (**8-OTs**) are $1.15 \pm 0.05 \times 10^{-5} \text{ s}^{-1}$, $1.05 \pm 0.05 \times 10^{-5} \text{ s}^{-1}$ and $1.20 \pm 0.06 \times 10^{-5} \text{ s}^{-1}$, respectively (at 30 °C in 50% (v : v) aqueous TFE with 1 M NaClO₄). Within experimental error, these secondary tosylates all solvolyse at the same rate, whereas 3-pentyl tosylate (**7-OTs**) solvolyses approximately twice as fast and has a rate constant of $1.95 \pm 0.05 \times 10^{-5} \text{ s}^{-1}$, consistent with earlier reports⁴².

The solvolysis products of **5-OTs** are 2-butanol and 2-trifluoroethoxy butyl ether in a ratio of 5 : 1. As the molar ratio of water to TFE in the solvent mixture is about 4 : 1, the selectivity $\frac{k'_{\text{H}_2\text{O}}}{k'_{\text{TFE}}}$ is 1.25 : 1, which is similar to the solvolysis of a simple tertiary substrate³⁵ via an intermediate or a benzylic secondary substrate via a concerted pathway with a cation-like transition state in the same solvent mixture¹⁹. Under our reaction conditions, the elimination products could not be detected with confidence because of their volatility. GC analysis of the solvolysis products from **8-OTs**, where the potential elimination products are less volatile, showed that the ratio of alcohol : trifluoroethoxy ether : 2-octene is about 5 : 1 : 4. The yield of each product was analysed by calibrating with authentic samples (2-octanol and 2-octene) and also demonstrated a mass balance.

Thus, the solvolysis reaction under nearly neutral condition (1.2 eq weak base) still produced a significant amount of elimination products. Both E and Z isomers (yield E : Z about 4 : 1) of 2-octene were observed, but 1-octene could not be detected.

During the solvolysis of 10 mM (*S*)-2-butyl tosylate (*S*-5-OTs) in 50% (v : v) aqueous TFE, partial racemization of the substrate took place, with an observed first-order rate constant for racemization of $4.6 \pm 0.1 \times 10^{-7} \text{ s}^{-1}$ (Fig. 2.1(A)), corresponding to a first-order rate constant of $2.3 \pm 0.1 \times 10^{-7} \text{ s}^{-1}$ for the interconversion of both enantiomers.

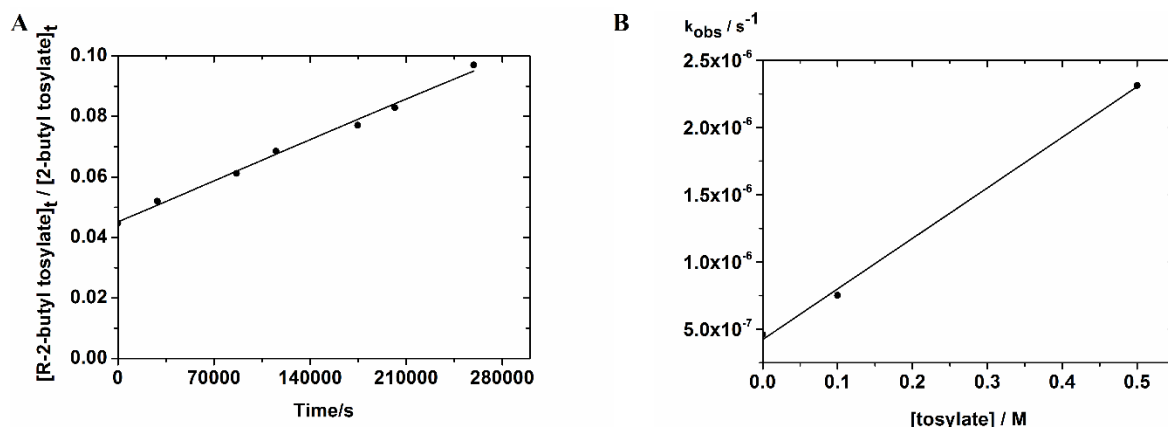
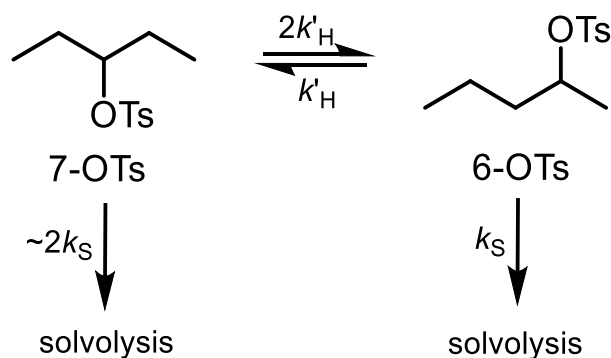


Figure 2.1. (A) Change in the ratio [*R*-5-OTs] / [5-OTs] with reaction time when the initial concentration of substrate is 10 mM. The solid line is the best fit of the equation [*R*-5-OTs] / [5-OTs] = $0.5 - 0.455e^{-2kt}$ with $k = 2.3 \pm 0.1 \times 10^{-7} \text{ s}^{-1}$. (B) Variation in observed first-order rate constant for racemization with concentration of tosylate anion. The solid line is the best fit and gives the equation $k_{\text{obs}} = 4.2 \pm 0.1 \times 10^{-7} + 3.8 \pm 0.2 \times 10^{-6} [\text{tosylate}] \text{ s}^{-1}$.

This racemization could be a result of the recombination of the substrate and the tosylate leaving group (generated during the solvolysis reaction), causing the inversion of the stereogenic centre in the substrate. To quantify its significance, the tosylate anion concentration was varied from 0 to 0.5 M (in the presence of 1 M 15-crown-5 to avoid ion pairing at high salt concentrations, and the ionic strength was adjusted to 1 M by NaClO₄). The first-order racemization rate increased linearly within this concentration range (Fig. 2.1(B)), giving a second-order rate constant of $3.8 \pm 0.2 \times 10^{-6} \text{ M}^{-1} \text{ s}^{-1}$, which corresponds to a second-order rate constant $1.9 \pm 0.1 \times 10^{-6} \text{ M}^{-1} \text{ s}^{-1}$ for the tosylate incorporation reaction.

In contrast, 10 mM (*R*)-2-octyl tosylate (**R-8-OTs**) only generated ~1% *S*-2-octyl tosylate (**S-8-OTs**) after 72 h, corresponding to a first-order rate constant $\sim 3.9 \times 10^{-8} \text{ s}^{-1}$ for racemization.

During the solvolysis of 3-pentyl tosylate (**7-OTs**), 2-pentyl tosylate (**6-OTs**) appears clearly in the reaction mixture. This can be explained by a 1,2-hydride shift mechanism (Scheme 2.1).



Scheme 2.1. Interconversion and solvolysis of **6-OTs** and **7-OTs**

By measuring the ratio of [**6-OTs**] : [**7-OTs**] (see Appendices Chapter 2 P. 180) at different time intervals by HPLC and applying numerical integration software (Berkeley Madonna W) to fit Scheme 2.1 to these data, k'_H (the first-order isomerization rate constant) was evaluated as $\sim 9 \times 10^{-7} \text{ s}^{-1}$. We assume that the 1,2-hydride transfer to the C_3 position in 7-OTs is twice as fast as to the C_2 position in 6-OTs due to a statistical factor of 2.

After solvolysis of **R-8-OTs**, 2-octanol was isolated and derivatised to the corresponding 4-nitrobenzoate ester to allow analysis by chiral HPLC using UV detection. The facial selectivity of the alcohol product is 8 : 92 (retention : inversion). This is much greater than

the fraction of substrate inverted ($\sim 1\%$ after 72 h) shown above and indicates a real facial selectivity (8 : 92) in the solvolysis reaction.

During the independent solvolysis of ^{18}O -labelled 2-butyl tosylate (**5-OS $^{18}\text{O}_2\text{Ar}$**) and 2-octyl tosylate (**8-OS $^{18}\text{O}_2\text{Ar}$**), scrambling of the isotopically labelled oxygen positions was detected by ^{13}C NMR from the recovered substrates (Fig. 2.2).

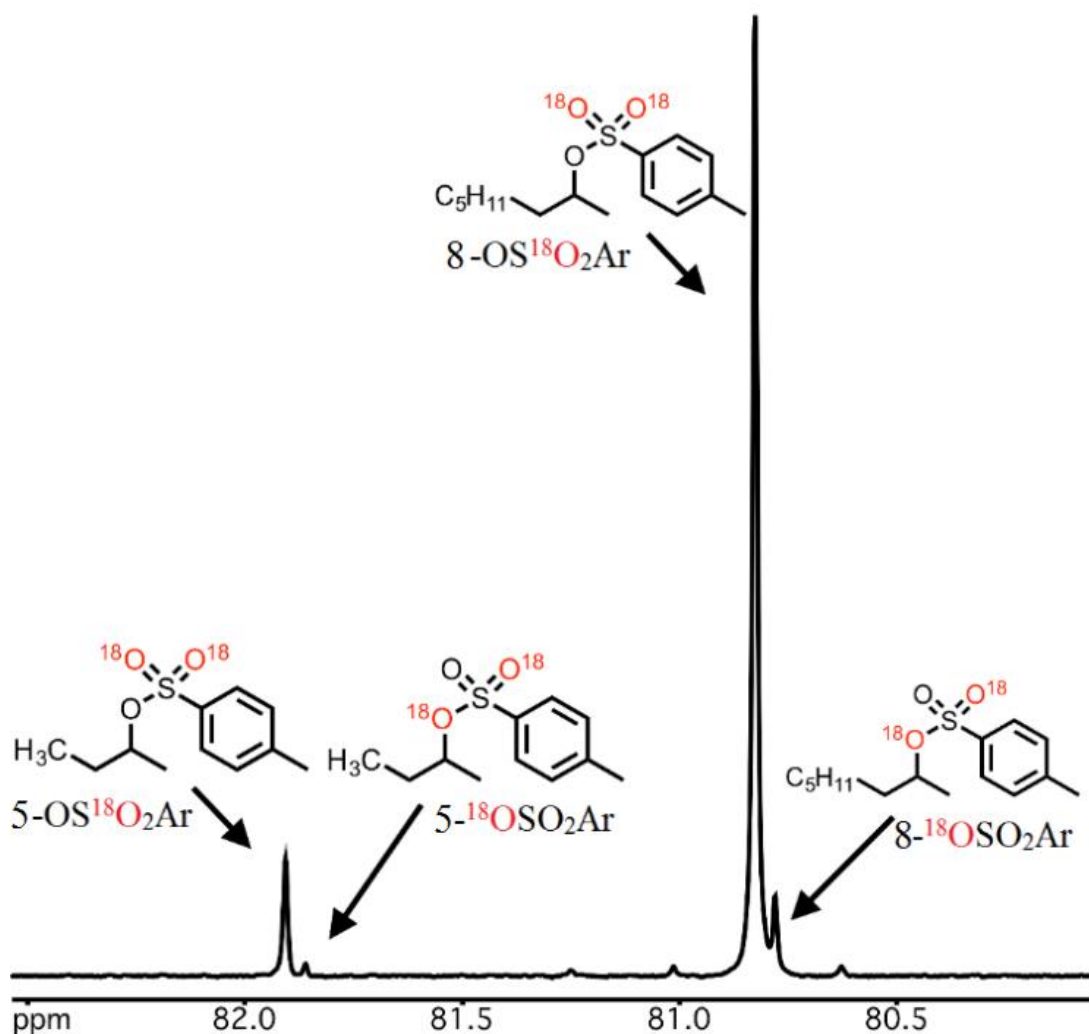
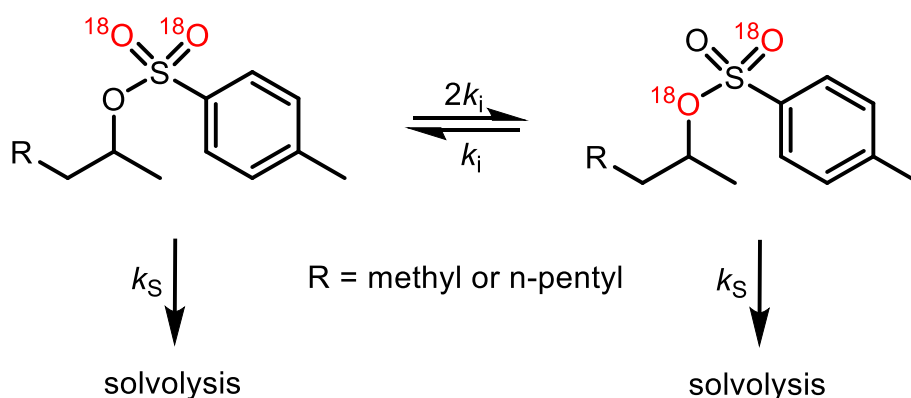


Figure 2.2. ^{13}C NMR spectrum of **5-OS $^{18}\text{O}_2\text{Ar}$** and **8-OS $^{18}\text{O}_2\text{Ar}$** recovered after 66.5 h

The extent of scrambling was similar in both cases (~8% after four half-lives), indicating similar first-order ^{18}O exchange rate constants (k_i in Scheme 2.2); the ratio of the two isotopomers at different time intervals is given in Table 2.1. Fitting with a first-order equation gives $k_i = 1.8 \pm 0.1 \times 10^{-7} \text{ s}^{-1}$ for **5-OS $^{18}\text{O}_2\text{Ar}$** , and $k_i = 1.4 \pm 0.1 \times 10^{-7} \text{ s}^{-1}$ for **8-OS $^{18}\text{O}_2\text{Ar}$** .



Scheme 2.2. Isotope exchange during solvolysis of **5-OS $^{18}\text{O}_2\text{Ar}$** and **8-OS $^{18}\text{O}_2\text{Ar}$**

Table 2.1. Results of isotope exchange for **5-OS $^{18}\text{O}_2\text{Ar}$** and **8-OS $^{18}\text{O}_2\text{Ar}$**

Time/s	C- ^{18}O : (C- ^{16}O + C- ^{18}O)	C- ^{18}O : (C- ^{16}O + C- ^{18}O)
0	0:100	0:100
57600	1.6:98.4	1.2:98.8
144000	4.6:95.4	3.8:96.2
239400	8.5:91.5	6.6:93.4

2.4 Discussion

Classical signs to suggest the formation of carbenium ion intermediates from simple secondary tosylates solvolysis are as follows: partial racemization of substrates; the non-equivalent oxygens in the tosylate group can exchange their positions; the formation of rearranged products and the substitution products of the tosylate do not show 100% inversion. These observations are all consistent with the data reported here. The products of the solvolysis reaction were proved to be stable: they neither reform the substrate nor

change their stereochemistry, unlike solvolysis in TFA³⁸⁻⁴⁰. Thus, these observations must be explained by the mechanism of the solvolysis pathway (kinetic control).

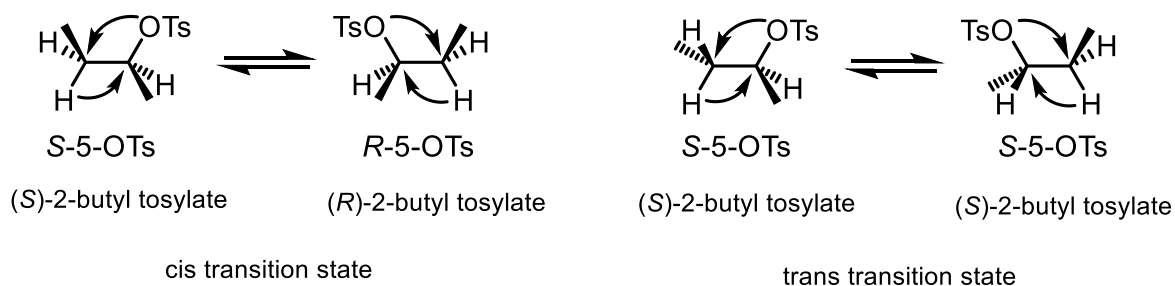
Racemization of both **5-OTs** and **8-OTs** is observed under the solvolysis conditions, but with different rates. It is possible that the tosylate anion generated in the course of the reaction can act as a competitive nucleophile and change the stereochemistry of the substrate. This process would also provide a pathway for oxygen isotope exchange in the labelled substrates. Measuring the rate of reaction between tosylate anion and **5-OTs** with different concentrations gives a second-order rate constant of $1.9 \pm 0.1 \times 10^{-6} \text{ M}^{-1} \text{ s}^{-1}$ for the bimolecular substitution reaction. If this pathway is the only process taken into account for racemization of **5-OTs** or **8-OTs**, the fraction of the minor enantiomer can be calculated from Equation 3 (P. 176),

$$\frac{[R - 5 - \text{OTs}]}{[5 - \text{OTs}]} = 0.5 - \frac{ee}{2} \exp\left(-2k_N[A]_0\left(t - \frac{1 - e^{-k'_S t}}{k'_S}\right)\right) \quad (3)$$

in which k_N is the second-order rate constant for the incorporation of tosylate generated during solvolysis, k'_S is the observed rate constant for solvolysis, $[A]_0$ is the initial concentration of the substrate and ee is the initial enantiomeric excess of **5-OTs** or **8-OTs** (expressed as a fraction of 1). After 72 h, Equation 3 predicts the formation of ~0.6% **S-8-OTs** in the remaining substrate from solvolysing 10 mM **R-8-OTs** (initially 0.25% *S*), close to the observed value of ~1%. However, for 10 mM **S-5-OTs** (initially 4.5% *R*), the predicted formation of **R-5-OTs** in the remaining substrate will be 4.8%, significantly smaller than the observed value of 9~10%.

It is evident that a significant additional pathway for racemization is required for **5-OTs**. A second process that can lead to racemization is a 1,2-hydride shift, coupled with 1,2 leaving group migration. In **5-OTs**, each migration still gives **5-OTs** but could lead to a change in stereochemistry. In **8-OTs**, racemization by 1,2-hydride transfer requires two steps—first to the C₃ position, then back to the C₂ position. The rate constant for the 1,2-hydride migration was measured by studying the solvolysis and isomerisation of **7-OTs**. Since **6-OTs** is approximately half as reactive as **7-OTs** towards solvolysis, and the rate of isomerisation to **6-OTs** benefits from a factor of 2 (for statistical reasons), detectable concentrations of **6-OTs** accumulate in the reaction mixture. Analysis of the accumulation of **6-OTs** using numerical integration gives a rate constant for the isomerization of $9 \times 10^{-7} \text{ s}^{-1}$ (Scheme 2.1).

Considering the stereochemistry of the reaction of **5-OTs**, the 1,2-transfer could happen through two transition states: cis and trans (Scheme 2.3). Both will contribute to the observed rate constant for the 1,2-hydride shift of $9 \times 10^{-7} \text{ s}^{-1}$, but only the cis transition state will lead to racemization.



Scheme 2.3. Stereochemical outcomes of isomerization through 1,2-migrations involving trans or gauche conformations of **S-5-OTs**

The ratio of the two transition states can be estimated to be about 4 : 1 by using cis and trans 2-butene as a model³, leading to a predicted rate constant of $1.8 \times 10^{-7} \text{ s}^{-1}$ for the

interconversion of the **5-OTs** enantiomers through this pathway. This value is close to the observed racemization rate constant for **5-OTs** (Fig. 2.1). Fitting Equation 4 (P. 177) to the best fit to obtain the isomerization rate constant (k'_H) using the independently measured rate constants for tosylate anion incorporation and solvolysis leads to the solid line given in Fig. 2.3, and k'_H is obtained as $2.1 \pm 0.1 \times 10^{-7} \text{ s}^{-1}$, in good agreement with the value from **7-OTs** (Fig. 2.3).

$$\frac{[R - 5 - \text{OTs}]}{[5 - \text{OTs}]} = 0.5 - \frac{ee}{2} \exp(-2k_N[A]_0(t - \frac{1 - e^{-k'_S t}}{k'_S}) - 2k'_H t) \quad (4)$$

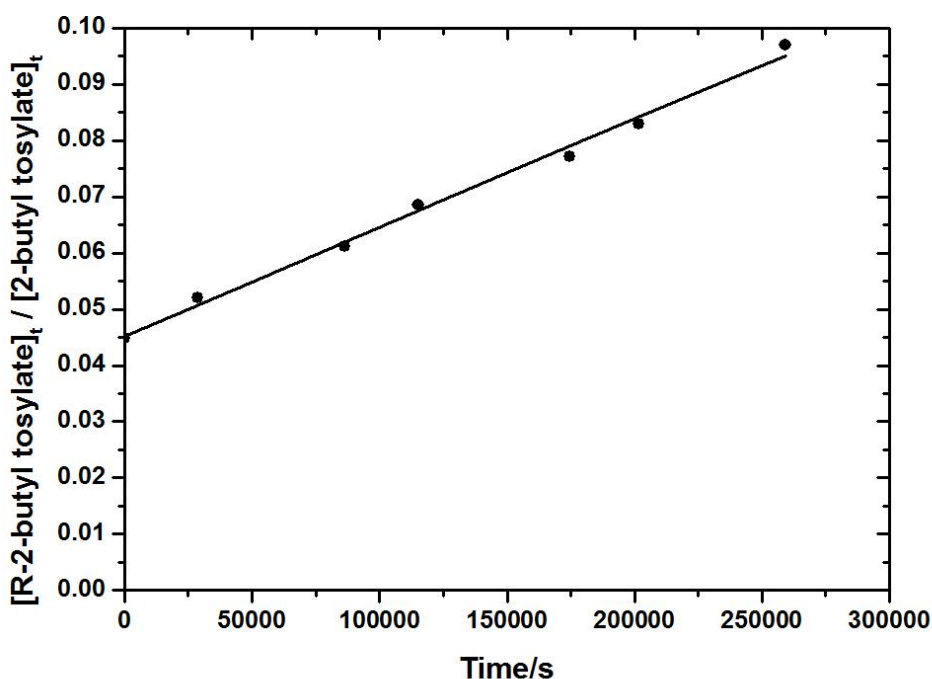
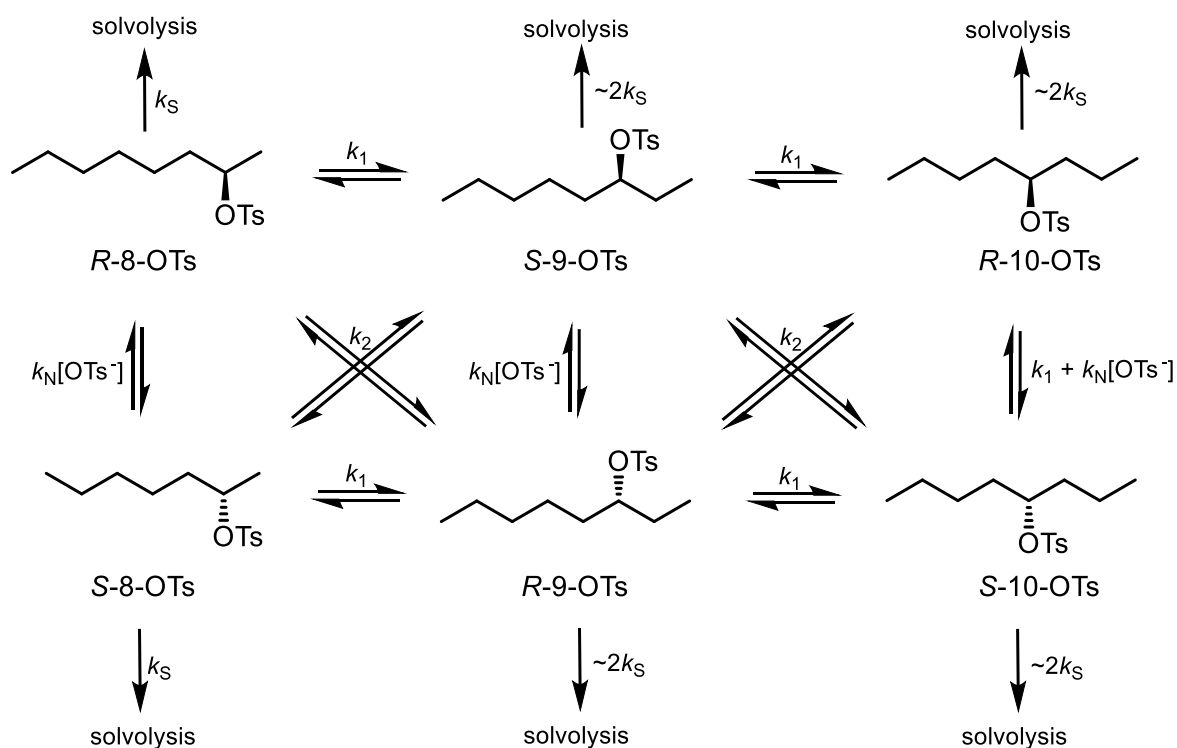


Figure 2.3. Racemization of 10 mM *S*-**5-OTs**. The solid line is the best fit of Equation 4, accounting for racemization through tosylate anion incorporation and 1,2 shifts.

Similarly, the racemization of **8-OTs** due to these factors can be predicted. In this case, the effect of 1,2 shifts on racemization is much reduced because (i) migration from the C₃ position is partitioned between the C₂ and C₄ positions and (ii) the solvolysis rates of **9-**

OTs and **10-OTs** are faster than that of **8-OTs**. We assume that **9-OTs** and **10-OTs** undergo solvolysis at least twice as fast as **8-OTs** (*i.e.* at the same rate as **7-OTs**, which is consistent with earlier reports⁴²). Numerical modelling of Scheme 2.4 (using Berkeley Madonna W) was used to predict $[S-8-OTs] : [8-OTs]$ against time, with $k_1 = 0.8k'_H = 7.2 \times 10^{-7} \text{ s}^{-1}$ and $k_2 = 0.2k'_H = 1.8 \times 10^{-7} \text{ s}^{-1}$, and $k'_S = 1.1 \times 10^{-5} \text{ s}^{-1}$ and $k_N = 2.2 \times 10^{-6} \text{ M}^{-1} \text{ s}^{-1}$. Each reaction arrow is accompanied by the corresponding rate constant shown in Scheme 2.4 (*i.e.* forward and reverse reactions have the same rate constant, shown only once for simplicity). This predicts that 1,2 migrations only lead to ~0.4% accumulation of **S-8-OTs** in the recovered **8-OTs** after 72 h. In contrast to **5-OTs**, migration away from the C₂ position and more rapid solvolysis of other isomers (**9-OTs** and **10-OTs**) suppresses the observation of racemization through the 1,2-migration pathway. In combination with the incorporation of tosylate anion formed during the solvolysis reaction, the ~1% fraction of **S-8-OTs** observed after 72 h can be satisfactorily accounted for.



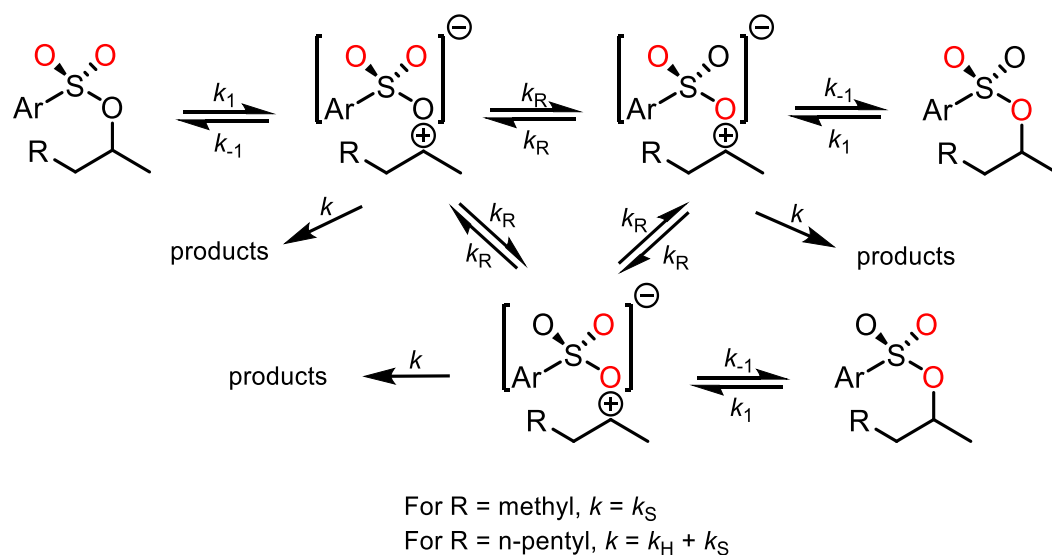
Scheme 2.4. Isomerisation and solvolysis of **8-OTs**

Based on these data, the major process that can compete with solvolysis to perturb the structure of **5-OTs** in dilute solution is 1,2-migration. When focusing on the stereochemical change in the **5-OTs**, most of the migrations (~80%) are invisible as they lead to the same enantiomer. This fact does not affect **8-OTs** significantly as discussed above. During this process, the bridging and non-bridging oxygen atoms in tosylate groups can still change their positions. Study of the isotope exchange for both **5-OS¹⁸O₂Ar** and **8-OS¹⁸O₂Ar** (¹⁸O labelled at the non-bridging positions) showed that both compounds exchanged ¹⁸O from bridging to non-bridging positions to a similar extent (6.6% and 8.5% after 72 h, with slightly greater exchange occurring for **5-OS¹⁸O₂Ar**). Taking the statistical factors into account and assuming heavy atom isotope effects are negligible, the rate constants for isotopic exchange are $1.8 \pm 0.1 \times 10^{-7} \text{ s}^{-1}$ (for **5-OTs**) and $1.4 \pm 0.1 \times 10^{-7} \text{ s}^{-1}$ (for **8-OTs**). Recovered **8-OTs** is not significantly affected by 1,2-hydride transfer or incorporation of tosylate released during solvolysis (< 1%), so ¹⁸O scrambling at the C₂ position of **8-OS¹⁸O₂Ar** requires a pathway independent of these processes.

¹⁸O scrambling in **5-OS¹⁸O₂Ar** will also include this pathway, plus a possible contribution from isotope exchange initiated by 1,2-migration. If 1,2-migration in **5-OTs** occurs by a pathway that selectively involves the non-bridging oxygen in the tosyl group, then the rate constant for isotopic exchange through this pathway would be predicted to be the same as for 1,2-migration ($\sim 9 \times 10^{-7} \text{ s}^{-1}$). If migrations occur selectively through the bridging oxygen, then 1,2-transfer will not cause any isotope exchange. As the rate constant for isotopic exchange in **5-OS¹⁸O₂Ar** is only greater by $\sim 0.4 \times 10^{-7} \text{ s}^{-1}$ than for **8-OS¹⁸O₂Ar**, isotopic exchange initiated by the 1,2 migration must be strongly selective (~95%) for the bridging

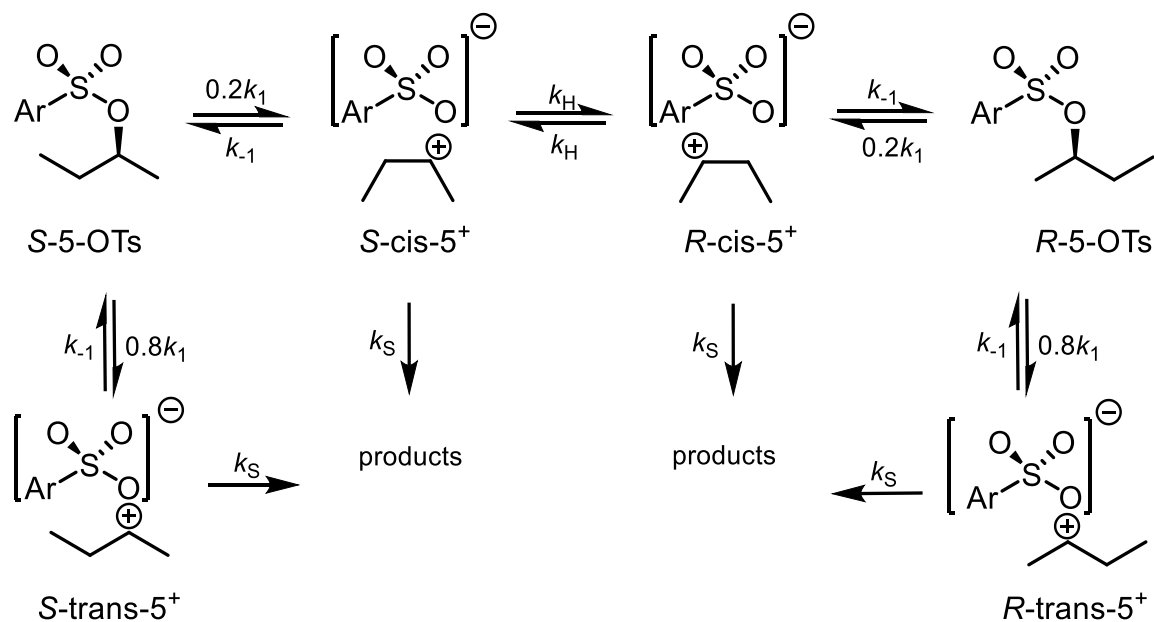
oxygen, assuming the contribution from direct exchange at the C₂ position is similar for both compounds.

The simplest detailed mechanism that can potentially account for all these data is the formation of a carbenium ion that can partition between solvolysis, reversion back to the substrate and a 1,2-hydride shift (followed by either solvolysis or reversion back to the substrate for **5-OTs**). For reversion back to the substrate accompanied by oxygen exchange, the non-equivalent oxygens exchange in tosylate is required. This process has a rate constant^{19,41} of $5 \times 10^{10} \text{ s}^{-1}$, slightly slower than the solvent reorganization rate constant of 10^{11} s^{-1} , which is the upper limit for carbenium ion generation without solvent pre-association³⁵. The 1,2-hydride transfer and isotope exchange could also take place in a coupled concerted process, with 1,2-hydride transfer accompanying isotope exchange. This must be a minor pathway, as shown by the similar isotope scrambling rates for **5-OS¹⁸O₂Ar** and **8-OS¹⁸O₂Ar**. Scheme 2.5 shows the isotope exchange by a step-wise pathway, involving the formation of carbenium ions. For **8-OTs**, 1,2-hydride shift contributes to formation of products, but in **5-OTs**, this is an ‘invisible’ reaction in terms of solvolysis that does not affect the rate. For simplicity, since the oxygen exchange coupled to 1,2-hydride transfer is small (see discussions earlier), this is not included in this scheme.



Scheme 2.5. Isotope exchange and solvolysis of **5-OS¹⁸O₂Ar** and **8-OS¹⁸O₂Ar** involving a common carbenium ion intermediate

Scheme 2.6 shows the step-wise mechanism for racemization of **5-OTs** initiated by 1,2-hydride transfer. The overall rate constant for ionization to the ion pair with the correct cis geometry is $0.2k_1$ based on a ratio of 4 : 1 of the trans and gauche forms.



Scheme 2.6. Racemization and solvolysis of **5-OTs** involving a common carbenium ion intermediate

The trans cation can also undergo 1,2-hydride transfer, but this does not change the sense of the stereogenic centre. Therefore, the trans cation contributes to solvolysis and oxygen exchange, but not to racemization. We assume that the 1,2-hydride transfer and ion recombination are not significantly affected by the different cation geometry (and so k_S and k_{-1} are the same for both ion-pairs). These schemes lead to a series of equations that relate the rate constants for each step. Equation 5 gives the observed rate constant for solvolysis for **5-OTs**:

$$k'_S = \frac{k_1 k_S}{k_{-1} + k_S} = 1.15 \times 10^{-5} \text{ s}^{-1} \quad (5)$$

The rate of isotope exchange in **5-OS¹⁸O₂Ar** is described in Equation 6

$$\frac{[^{18}\text{OTs}]}{[\text{ROTs}]} = \frac{2}{3}(1 - e^{-3k_i t}) \text{ where}$$

$$3k_i = \frac{3k_1 k_{-1} k_R}{(k_{-1} + k_S)(k_{-1} + k_S + 3k_R)} = 5.4 \times 10^{-7} \text{ s}^{-1} \quad (6)$$

Finally, the racemization of **S-5-OTs** initiated by 1,2-hydride transfer is described by the following expression (Equation 7):

$$\frac{[R - 5 - \text{OTs}]}{[5 - \text{OTs}]} = \frac{1}{2}(1 - 0.91e^{-2k'_H t}) \text{ where}$$

$$2k'_H = \frac{0.4k_1 k_{-1} k_H}{(k_{-1} + k_S)(k_{-1} + k_S + 2k_H)} = 4.2 \times 10^{-7} \text{ s}^{-1} \quad (7)$$

Combining Equations 5 and 6 and using a value^{19,41} of $k_R = 5 \times 10^{10} \text{ s}^{-1}$ gives

$$k_{-1} = \frac{3.13 \times 10^{-13} k_S^2 + 4.7 \times 10^{-2} k_S}{1 - \frac{k_S}{3.19 \times 10^{12}}} \quad (8)$$

This requires that $k_S < 3.2 \times 10^{12} \text{ s}^{-1}$ to give a positive value of k_{-1} . Combining Equations 5 and 7 and then using Equation 8 to replace k_{-1} by k_S gives

$$k_H = \frac{k_S(k_{-1} + k_S)}{11k_{-1} - 2k_S} = \frac{2.58 \times 10^{11} k_S}{k_S - 3.65 \times 10^{11}} \quad (9)$$

This requires that $k_S > 3.65 \times 10^{11} \text{ s}^{-1}$, so this leads to a limited range of values for k_S , $3.7 \times 10^{11} \text{ s}^{-1} < k_S < 3.2 \times 10^{12} \text{ s}^{-1}$, that are consistent with this scheme, the value of k_R and the data we have measured. Since k_S is larger than the solvent reorganization rate¹⁵ (10^{11} s^{-1}), then the mechanism of solvolysis either involves pre-organisation of the solvent prior to carbenium formation ($D_N^*A_N$) or is a true concerted pathway ($A_N D_N$). The pre-association stepwise mechanism ($D_N^*A_N$) requires that the rate constant of every elementary pathway should be slower than a bond vibration rate¹⁹ (10^{13} s^{-1}) in order to be kinetically meaningful. k_S includes several competing processes, with hydrolysis as the major pathway (50%). Thus, $1.6 \times 10^{12} \text{ s}^{-1} > k_{H_2O} > 1.8 \times 10^{11} \text{ s}^{-1}$, which is still below the upper limit for generating a carbenium intermediate.

Using the relationship in Equations 8 and 9, the dependence of the ratio of k_H / k_S and k_{-1} / k_S on k_S is shown in Fig. 2.4A, and the dependence of the values of k_H and k_{-1} on k_S is shown in Fig. 2.4B.

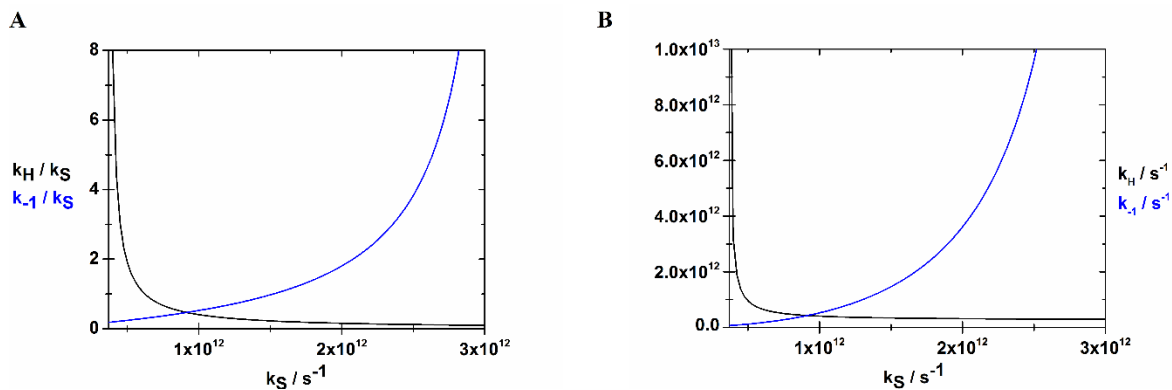


Figure 2.4. (A) Plot of k_H/k_S and k_{-1}/k_S against k_S . (B) Plot of k_H and k_{-1} against k_S . The limits of the x-axis correspond to the limits of k_S as described in the text.

If both k_H and k_{-1} are also limited to maximum values of 10^{13} s^{-1} , these plots show that the upper limit of k_S now becomes $2.5 \times 10^{12} \text{ s}^{-1}$ and that the lower limit remains the same at $3.7 \times 10^{11} \text{ s}^{-1}$ (note that k_H becomes very sensitive to k_S around the lower limit). These constraints and relationships may suggest that although the proposed carbenium ion cannot have a sufficiently long lifetime to allow solvent reorganisation, it can be an intermediate that might partition between solvent attack (k_S), 1,2-hydride migration (k_{-1} , k_H) and oxygen exchange (k_{-1} , k_R) within a pre-organised solvent shell.

Similar equations can be generated and applied to the observed rate constant for solvolysis of **8-OTs** (Equation 10) and oxygen exchange of **8-OS¹⁸O₂Ar** (Equation 11).

$$k'_S = \frac{k_1(k_H + k_S)}{k_H + k_S + k_{-1}} = 1.20 \times 10^{-5} \text{ s}^{-1} \quad (10)$$

$$\frac{[^{18}\text{OTs}]}{[\text{ROTs}]} = \frac{2}{3}(1 - e^{-3k_i t}) \text{ where}$$

$$3k_i = \frac{3k_1k_{-1}k_R}{(k_{-1} + k_S + k_H)(k_{-1} + k_S + k_H + 3k_R)} = 4.2 \times 10^{-7} \text{ s}^{-1} \quad (11)$$

Combining these equations and the $k_R = 5 \times 10^{10} \text{ s}^{-1}$ value^{19,41} applied earlier gives

$$4.29 \times 10^{12} k_{-1} = (k_S + k_H)(k_S + k_H + k_{-1} + 1.5 \times 10^{11}) \quad (12)$$

If we assume that k_S , k_H and k_{-1} have the same values for both **5-OTs** and **8-OTs** (*i.e.* that the two cations partition similarly between the respective processes), then Equations 8, 9 and 12 can be solved. This gives values of $k_S = 1.55 \times 10^{12} \text{ s}^{-1}$, $k_{-1} = 1.59 \times 10^{12} \text{ s}^{-1}$ and $k_H = 3.38 \times 10^{11} \text{ s}^{-1}$.

If the assumption is valid, then similar isotope exchange rates for the two compounds (Equations 6 and 11) require that k_H should be significantly smaller than k_S ; the ratio of k_H / k_S obtained from this analysis is ~ 0.2 , consistent with the slightly slower scrambling rate observed in **8-OS¹⁸O₂Ar**. Similarly, the values of k_R and k_H differ by about sevenfold. This suggests that hydride transfer competes more effectively with solvolysis and ion pair return than tosylate non-equivalent oxygen exchange. As we estimate that only $\sim 20\%$ of 1,2-hydride shifts lead to racemization for **5-OTs**, these values are all consistent with the measured oxygen exchange and racemization rates.

As the rate of **8-OTs** solvolysis is very similar as **5-OTs**, this also suggests that k_H cannot be as large as k_S ; the values obtained are consistent with this observation, predicting an increase in solvolysis rate of $\sim 12\%$ for **8-OTs** relative to **5-OTs** if k_1 s are identical for both compounds. We note that **6-OTs** solvolyses slightly more slowly than **5-OTs**, despite having an additional pathway for reaction (1,2-hydride transfer), so k_1 is unlikely to be identical for all these substrates. Comparing independently measured rate constants for

different substrates is subject to greater uncertainties than the competition processes that we have used to analyse the properties of the potential intermediate within the single substrate, so the rates of solvolysis are in good agreement with the model.

According to this analysis, the reaction of 2-alkyl tosylates in 50% aqueous (v : v) TFE can be adequately described by the stepwise mechanism shown in Schemes 2.5 and 2.6, where the intermediate has a lifetime just sufficient to exist kinetically. The solvent needs to be pre-organised to induce solvolysis, but the intermediate is not kinetically irrelevant as oxygen exchange and 1,2-hydride transfers can compete with the solvolysis pathway. The collapse of the carbenium ion through hydrolysis (to give alcohol) is estimated (from the product analysis) as $0.5k_s = 8 \times 10^{11} \text{ s}^{-1}$, which is approximately half the rate constant for collapse of the ion pair back to substrates (k_{-1}).

The stereochemistry of the product alcohol from **R-8-OTs** shows a significant amount of retention (8%), which requires an open transition state to allow enough space for front-side attack at the substituted carbon, presumably via the solvation shell of the leaving group (likely through hydrogen bonding), as observed in the solvolysis reaction of (*S*)-1-(3-nitrophenyl)ethyl tosylate in 50% aqueous (v : v) TFE, which showed a facial selectivity 17 : 83 (retention : inversion)¹⁹.

2.5 Conclusion

Overall, the data can be described in terms of a stepwise mechanism ($D_N^*A_N$) that allows 1,2-hydride transfer and oxygen exchange to compete inefficiently with solvolysis via pre-organised solvents. Of the two processes, 1,2-hydride transfer provides a faster ‘clock’

compared with oxygen exchange, although in the systems that we have studied here, this is not fully established since the process is only partially expressed in the observable isomerization that addresses its presence (racemization). The sum of our observations suggests that the reactions of 2-alkyl tosylates do not need to be described as a concerted mechanism, although solvent pre-organisation might be considered as an equivalent for an external nucleophile, and in which case the mechanism is similar to an uncoupled enforced concerted pathway. This interpretation can explain the contradictory conclusions outlined in the introduction: a pre-organisation requirement with an intermediate that can be identified by alternative isomerization processes can correlate well with other concerted mechanism in terms of observed reaction rates.

As the rate constants are so close to the vibrational limit for the kinetic existence of an intermediate, it is likely that the processes that dominate oxygen exchange and hydride transfer will be subject to dynamical effects, as has been suggested by Richard and Tsuji in the context of carbenium intermediates that are believed to have shorter lifetimes^{19,16,43}. In this case, the life-times of those carbeniums are shortened so much that the mechanistic description becomes one of competitive concerted processes with no common intermediates, but a series of closely related transition states on a shallow potential energy surface. This may be reasonable for the 2-alkyl tosylates but does not seem to be enforced by the analysis presented here. If this is the case, then a more realistic view of the reaction may as well be a series of competing processes over a potential surface that includes a shallow energy minimum (or just a saddle point) for the carbenium ion that influences the pathway⁴⁴. The transition state theory assumptions we have used to deduce the partitioning of the potential intermediate may not be valid in this case, but the computational analysis of

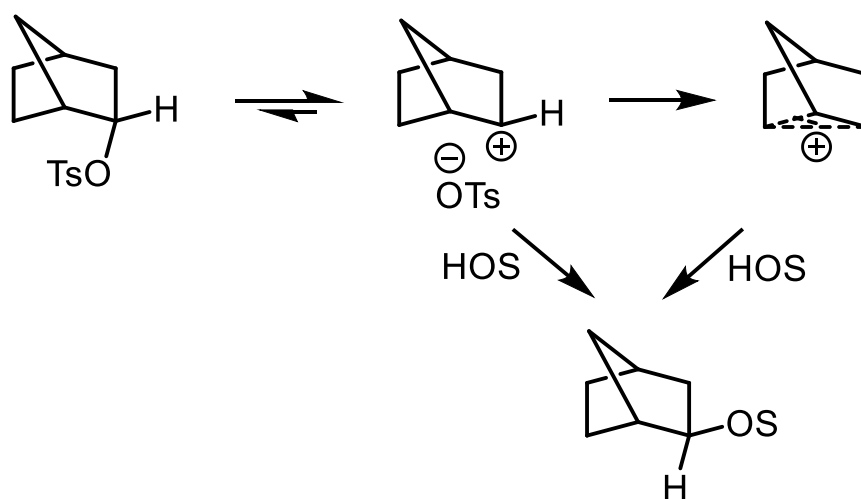
the lifetime of the methoxy methyl cation in water⁴⁵, which has a similar lifetime predicted by extrapolation of kinetic data⁴⁶, suggests that our suggestion of a carbenium ion in a shallow potential well is credible.

However, based on our succeeding discussions about norbornyl cation (see Chapter 3) and simple tertiary cations (see Chapter 5) in 50% aqueous (v : v) TFE, we suggest that the mechanism here should be best described as a true concerted mechanism (D_{NAN}), and different processes may be dominated by dynamical effects with a carbenium-like saddle point on the reaction potential surface.

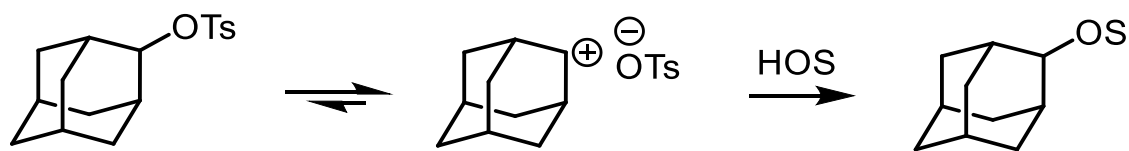
Chapter 3: The solvolysis mechanism of endo-2-norbornyl tosylate in 50% aqueous (v : v) TFE**

3.1 Introduction

Our recent research on solvolysis mechanisms of simple secondary tosylates in 50% (v : v) TFE suggests that the mechanism is best described as an enforced uncoupled concerted mechanism without forming a cation intermediate⁵⁴. However, when considering the solvolysis of endo-2-norbornyl sulfonates or 2-adamantyl sulfonates, most physical organic chemists still believe the solvolysis mechanism of both these types of substrates is a step-wise pathway, initially generating a classical cation as an intermediate^{34a-34e}. The reason these precursors are thought to involve classical secondary cations (Scheme 3.1) is that the front-side concerted σ participation is thought to be of higher energy than formation of classical secondary cations for the endo-2-norbornyl system⁵⁵; and back-side σ participation will introduce unfavourable strain energy for 2-adamantyl system (Scheme 3.2)^{56a,56b}.



Scheme 3.1. Solvolysis mechanism of endo-2-norbornyl tosylate initially involving a classical cation



Scheme 3.2. Solvolysis mechanism of 2-adamantyl tosylate involving a classical cation

Examining the literature, there is no clear evidence to support the step-wise mechanism of solvolysis of endo-2-norbornyl sulfonates. The first and most widely used criteria is the α secondary KIE; the relatively large ratio $k_H/k_D \approx 1.2$ was used as evidence for the step-wise pathway^{34c,34f-34h}. However, the α secondary KIE is only useful for indicating that in the rate-determining step, there is a hybridization change at the α carbon. A relatively large α secondary KIE is not sufficient to identify a classical cation intermediate. A transition state that resembles a classical cation can also account for the observed large α secondary KIE, which would be the case for the so-called enforced uncoupled concerted mechanism with a ‘carbenium ion like’ transition state^{16,19}.

Another tool that has been applied is ‘azide trapping’⁴¹. Unfortunately, the reported work relied on a low concentration of sodium azide (< 0.1 M) and analysed a very low yield of trapping products (< 10%) in order to support the step-wise pathway^{34i,34j} (because of no rate acceleration). Since the selectivity $\frac{k_{N_3^-}}{k_S}$ (M^{-1}) is quite low for endo-2-norbornyl sulfonates, a high concentration of trapping reagents must be used to obtain enough trapping products so that the relationship between solvolysis rate constants and the concentration of trapping reagents can be informative.

Deuterium or tritium scrambling in the products obtained by solvolysing the corresponding labelled endo-2-norbornyl sulfonates can address how significant the contribution of the non-classical cation is^{34k-34m}. However, the non-rearranged product is not useful for identifying the existence of classical cations unambiguously, simply because the fraction of non-rearranged products can also be generated through an S_N2 pathway that does not compete efficiently with S_N1 ionization.

Finally, isotope exchange at the sulfonate leaving groups probed by ¹⁷O labelling is also not helpful³⁴ⁿ. After solvolysing [ether-¹⁷O]-endo-2-norbornyl mesylate in refluxing ethanol, the lack of scrambling can be accounted by an S_N2 pathway or an S_N1 pathway without internal return. Since concerted isotope exchange has also been reported^{54,16,19}, this probe is difficult to interpret for cases where low levels of exchange are observed in any case.

The solvolysis mechanisms of endo-2-norbornyl sulfonates are still unambiguous after analysing these data listed above. Since the conditions of solvolysis were so different in each case it is difficult to draw a clear conclusion.

Therefore, we do not think there is compelling evidence to support the presence of classical 2-norbornyl cations when solvolysing endo-2-norbornyl sulfonates and we want to apply these probes under the same conditions to rationalize the solvolysis mechanism. By applying a modified trapping method as well as the deuterium scrambling analysis of the solvolysis products of 2-d-endo-norbornyl tosylate solvolysis in 50% (v : v) TFE, we suggest the mechanism should be regarded as a combination of S_N2 and S_N1 pathways. The

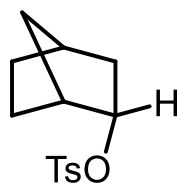
S_N1 pathway directly generates the non-classical cation without passing through the classical cation intermediate.

3.2 Experimental

General

All the chemicals were purchased from Sigma-Aldrich, Alfa Aesar or Acros Organics. Those used for synthesis purposes were used directly without further purification. TFE was distilled from P_2O_5 and stored over 4Å molecular sieves. UHQ water was obtained from an ELGA PURELAB Option S-R 7-15 system. 1H NMR and ^{13}C NMR spectra were recorded on Bruker AV-HD 400 instrument. HPLC analysis was carried out on Waters 2690 (486 Tunable Absorbance Detector) and 2695 (2487 Dual λ Absorbance Detector) systems with a Waters[®] SymmetryShield RP8 column (3.5 $\mu m \times 15$ cm) and UV detection at 265 nm. A gradient elution was used, changing from 95% water and 5% acetonitrile to 5% water and 95% acetonitrile over 20 mins followed by a further 10 mins of the final eluent mixture. GC analysis of exo-2-norborneol, exo-2-norbornyl trifluoroethyl ether, exo-2-norbornyl thiocyanate and exo-2-norbornyl azide was determined with a Perkin Elmer ARNEL Auto System XL GC model with Phenomenex Zebron[™] ZB-624 Column (30 m x 0.32 mm x 1.80 μm). The program is starting from 50 °C, 6 °C/min to 140 °C, holding for 5 mins and 45 °C/min to 220 °C, holding for another 9 mins with a split ratio 20 : 1.

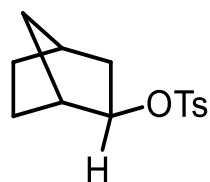
Syntheses



11-en-OTs

endo-2-norbornyl tosylate (11-en-OTs)⁶⁵. 0.56 g endo-2-norborneol (**11-en-OH**) (containing 4% exo-2-norborneol (**11-ex-OH**)) (5 mmol) and 1.22 g DMAP (10 mmol) were dissolved in 10 mL dry DCM and cooled to 0 °C in an ice-water bath with stirring. 1.43 g tosyl chloride (7.5 mmol) dissolved in 3 mL dry DCM and 2 mL dry diethyl ether was added dropwise within 5 mins. After addition, the ice-water bath was removed and the mixture was stirred under N₂ overnight before evaporating the solvent. The residue was dissolved in about 30 mL ethyl acetate and filtered through a short pad of Celite[®]. The filtrate was evaporated under vacuum and the yellow oil was dissolved in 30 mL 50% aqueous acetone to destroy 4% **11-ex-OTs**. The solution was stirred at RT for 15 mins before evaporating the acetone and the aqueous phase was extracted with 3 × 20 mL ethyl acetate. The organic phases were combined, dried over Na₂SO₄, filtered and evaporated under vacuum to afford a yellow oil, which was purified by silica chromatography, using DCM as eluent to afford 0.35 g **11-en-OTs** as a colourless oil (26.2%).

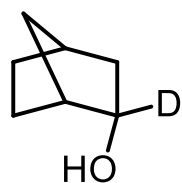
¹H NMR (400 MHz, CDCl₃): 7.77 (2H, d, J = 8.3 Hz), 7.32 (2H, d, J = 8.3 Hz), 4.78-4.73 (1H, m), 2.43 (3H, s), 2.33-2.31 (1H, m), 2.16-2.14 (1H, m), 1.87-1.77 (2H, m), 1.57-1.47 (1H, m), 1.36-1.18 (4H, m), 1.16-1.04 (1H, m). ¹³C NMR (100 MHz, CDCl₃): 144.5, 134.2, 129.8, 127.7, 83.1, 41.0, 37.0, 36.6, 36.2, 29.1, 21.6 and 20.6.



11-ex-OTs

exo-2-norbornyl tosylate (11-ex-OTs)⁶⁵. 0.56 g exo-2-norborneol (**11-ex-OH**) (5 mmol) and 1.22 g DMAP (10 mmol) were dissolved in 10 mL dry DCM and cooled to 0 °C in an ice-water bath with stirring. 1.43 g tosyl chloride (7.5 mmol) dissolved in 3 mL dry DCM and 2 mL dry diethyl ether was added dropwise within 5 mins. After addition, the ice-water bath was removed and the mixture was stirred under N₂ overnight before evaporating the solvent. The residue was dissolved in about 30 mL ethyl acetate and filtered through a short pad of Celite[®]. The filtrate was evaporated under vacuum and the yellow oil was purified by silica chromatography, using DCM as eluent to afford 0.15 g **11-ex-OTs** as a colourless oil (11.3%).

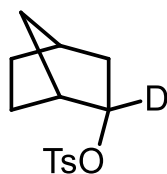
¹H NMR (400 MHz, CDCl₃): 7.76 (2H, d, J = 8.3 Hz), 7.32 (2H, d, J = 8.3 Hz), 4.45-4.40 (1H, m), 2.43 (3H, s), 2.36-2.32 (1H, m), 2.27-2.22 (1H, m), 1.62-1.33 (5H, m), 1.18-1.08 (1H, m), 1.02-0.93 (2H, m). ¹³C NMR (100 MHz, CDCl₃): 144.4, 134.6, 129.8, 127.6, 85.4, 42.1, 39.6, 35.3, 35.0, 27.9, 23.9 and 21.6.



d-11-en-OH

Endo-2-d-norborneol (d-11-en-OH). Following the procedure reported by Barden and Schwartz⁶⁶. 1.01 g sodium borodeuteride (23.9 mmol) and 2.86 g dichlorotitanocene (11.5

mmol) were dissolved in 30 mL dry dimethoxyethane and stirred at RT under nitrogen overnight. 1.04 g norcamphor (9.5 mmol) was dissolved in 3 mL dry dimethoxyethane and added dropwise to the mixture. After stirring for 10 mins at RT, TLC indicated all the norcamphor had been consumed. The solvent was evaporated under vacuum and the residue was dissolved in 30 mL 1 M NaOH and 30 mL diethyl ether, the solution was vigorously stirred at RT for another 30 mins and filtered through a pad of Celite[®]. The aqueous phase was then extracted with diethyl ether (4 × 20 mL), the organic phase was combined and dried over Na₂SO₄ before removing the solvent under vacuum to give **d-11-en-OH** as a white solid (0.82 g, 77%), which contained 5% **d-11-ex-OH** (measured by integrating the peaks centred at 4.20 ppm and 3.73 ppm in ²H NMR). The alcohol was used directly to synthesize endo-2-d-norbornyl tosylate (**d-11-en-OTs**) without delay.



d-11-en-OTs

Endo-2-d-norbornyl tosylate (d-11-en-OTs)⁶⁵ was synthesized and purified by the same procedure shown for **11-en-OTs**, except for the selective solvolysis to destroy the 5% of the more reactive **d-11-ex-OTs** in 50% aqueous acetone was 25 mins (considering the secondary isotope effect).

¹H NMR (400 MHz, CDCl₃): 7.79 (2H, d, *J* = 8.3 Hz), 7.34 (2H, d, *J* = 8.3 Hz), 2.45 (3H, s), 2.34-2.32 (1H, m), 2.17-2.13 (1H, m), 1.89-1.75 (2H, m), 1.59-1.50 (1H, m), 1.40-1.23 (4H, m), 1.16-1.07 (1H, m). ²H NMR (76.77 MHz, CHCl₃): 4.71 (1²H, s). ¹³C NMR (100

MHz, CDCl₃): 144.5, 134.2, 129.8, 127.8, 82.7 (t, J = 23.4 Hz), 40.9, 37.0, 36.4, 36.2, 29.1, 21.6 and 20.6.

Kinetic analysis

The solvolysis reactions were carried out with 5 mM substrate, 1 M sodium perchlorate or sodium thiocyanate, 6 mM 2,6-di-*tert*-butylpyridine and 0.2 mM 3-nitroacetophenone as the internal standard in 50% aqueous TFE (v/v) at 30 °C. The solutions were immersed in a thermostated water bath, and the progress of the reactions was monitored by analysing aliquots of the reactions mixture using HPLC for 2-3 half-lives. The peak areas in the chromatograms were integrated and a first order equation fitted to these data; in all cases, $R^2 > 0.999$.

Product analysis

The products of the solvolysis of **11-ex-OTs**, **11-en-OTs** and **d-11-en-OTs** were analysed by GC directly after 10 half-lives. The concentrations were the same as shown for Kinetic analysis but 3 mM 3,5-bis(trifluoromethyl)acetophenone was used as the internal standard. Without sodium thiocyanate, there were only two peaks in the chromatogram: the alcohol (**11-ex-OH**) was identified by comparison with an authentic sample; the remaining peak was assumed to be the trifluoroethyl ether (**11-ex-OCH₂CF₃**). The elimination products are below detection limit. In the presence of 1 M sodium thiocyanate, another two peaks (whose areas increased with increasing sodium thiocyanate concentrations) were observed, and assigned to be thiocyanate (**11-ex-SCN**) and isothiocyanate (**11-ex-NCS**). In the presence of 1 M sodium azide, there was another one peak (whose peak area increased with increasing sodium azide concentrations), assigned as the corresponding azide (**11-ex-N₃**).

All the peak areas were integrated and divided by the area of the internal standard to give relative ratios. We could not determine the absolute concentration of those products because of unknown extinction coefficients. However, since we are interested in the relative change, an absolute relative ratio to internal standard is appropriate.

Deuterium scrambling

The solvolysis reaction of **d-11-en-OTs** was carried out with 8 mM substrate, 1 M sodium perchlorate, 10 mM 2,6-di-*tert*-butylpyridine in 50 mL 50% (v : v) TFE at 30 °C. After 10 half-lives, TFE was mostly evaporated under vacuum. The aqueous phase was extracted with diethyl ether (5 × 20 mL) and dried over Na₂SO₄ before removing the solvent under vacuum. The residue was dissolved in 0.7 mL CHCl₃ and subjected to ²H NMR analysis. The solvolysis reaction with 1 M sodium thiocyanate instead of sodium perchlorate was done at the same concentration, but the total reaction volume was 100 mL.

²H NMR spectra were recorded at 76.77 MHz with a Bruker AV 500 instrument, acquired with a 189 receiver gain, 2.667 s acquisition time, 1535.6 Hz sweep width, 4096 data points (0.750 Hz/pt) and a 1.00 s relaxation delay time. Spectra (ca 100 scans) at 25 °C were used to determine the relative concentrations of the isotopic isomers of **11-ex-OH** and **11-ex-SCN**. The ratio of **d-11-ex-OH** and **d'-11-ex-OH** was determined by integrating the peaks centred at 3.75 ppm and 2.14 ppm, respectively. The ratio of **d-11-ex-SCN** and **d'-11-ex-SCN** was determined by integrating the peaks centred at 3.37 ppm and 2.48 ppm, respectively. Chemical shifts are reported relative to TMS.

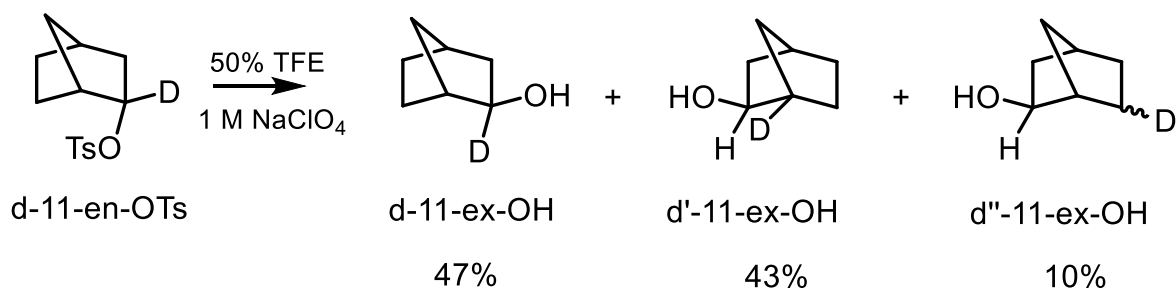
3.3 Results

The pseudo first-order solvolysis rate constant of endo-2-norbornyl tosylate (**11-en-OTs**) in 50% (v : v) TFE with 1 M NaClO₄ at 30 °C was $9.51 \pm 0.07 \times 10^{-6} \text{ s}^{-1}$. When NaClO₄ is replaced by 1 M NaSCN, the observed rate constant ($9.62 \pm 0.06 \times 10^{-6} \text{ s}^{-1}$) did not change within experimental errors. Thus, there is no significant S_N2 acceleration involving NaSCN. A rate constant of $7.93 \pm 0.05 \times 10^{-6} \text{ s}^{-1}$ was obtained when solvolysing 2-d-endo-norbornyl tosylate (**d-11-en-OTs**) with 1 M NaClO₄ under the same conditions, thus the α secondary KIE ($k_{\text{H}} / k_{\text{D}} = 1.20 \pm 0.01$) is consistent with reported values in other solvents^{34c,34f-34h}.

Although 1 M NaSCN did not cause any rate accelerations, exo-2-norbornyl thiocyanate (**11-ex-SCN**) and isothiocyanate (**11-ex-NCS**) were found to be new products (in a combined 52% yield, P. 183) that formed at the expense of exo-2-norborneol (**11-ex-OH**) and exo-2-norbornyl trifluoroethyl ether (**11-ex-OCH₂CF₃**). Solvolysing 2-d-endo-norbornyl tosylate (**d-11-en-OTs**) under the same conditions also gave 52% of these trapping products. This indicates that most of the trapping adducts (**11-ex-SCN + 11-ex-NCS**) result from a step-wise pathway, where the added NaSCN does not affect the ionization step. Otherwise, if the 52% substitution products result from an S_N2 pathway, the pseudo first-order rate constant would increased two fold. On the other hand, 1 M NaN₃ gave only 40% exo-2-norbornyl azide (**11-ex-N₃**) as the trapping adduct (P. 182). The less efficient trapping compared with NaSCN is probably due to the general base catalysis by azide anion⁵⁷, which accelerates solvent attack on the reactive carbon centre. Consistent with this analysis, a larger ratio of $\frac{[\text{11-ex-OCH}_2\text{CF}_3]}{[\text{11-ex-OH}]}$ was observed with NaN₃. This is expected since TFE has a lower pK_a than water.

When solvolysing exo-2-norbornyl tosylate (**11-ex-OTs**) with 1 M NaSCN under the same conditions, 45% **11-ex-SCN** and **11-ex-NCS** were found at the expense of **11-ex-OH** and **11-ex-OCH₂CF₃** (P. 182). The NaN₃ general base effect was also observed for **11-ex-OTs** since only 32% **11-ex-N₃** was formed with a larger ratio of $\frac{[11\text{-ex-OCH}_2\text{CF}_3]}{[11\text{-ex-OH}]}$.

The major products of solvolysing **d-11-en-OTs** with 1 M NaClO₄ under the same conditions were 2-d-exo-norborneol (**d-11-ex-OH**) and 1-d-exo-norborneol (**d'-11-ex-OH**), in a ratio of 1.1 : 1, as determined by ²H NMR (Fig. 3.1) (the ²H NMR chemical shift was assigned to follow the same pattern as non-labelled exo-2-norboeol^{65b}, namely, $\delta(2\text{-}^2\text{H}) > \delta(1\text{-}^2\text{H}) > \delta(6\text{-}^2\text{H})$). About 10% 6-d-exo-norborneol (**d''-11-ex-OH**) was also observed (Scheme 3.3), and attributed to 2,6-hydride transfer. However, with 1 M NaSCN, the ratio of **d-11-ex-OH** and **d'-11-ex-OH** became 1.24 : 1 and the major trapping adducts were 2-d-exo-norbornyl thiocyanate (**d-11-ex-SCN**) and 1-d-exo-norbornyl thiocyanate (**d'-11-ex-SCN**), in a ratio of 1.74 : 1 (Fig. 3.2). Only about 5% **d''-11-ex-OH** and 6-d-exo-norbornyl thiocyanate (**d''-11-ex-SCN**) were visible since the rearrangement pathway competes with additional pathways involving NaSCN (Scheme 3.4).



Scheme 3.3. Major solvolysis products of **d-11-en-OTs** in 50% (v : v) TFE (1 M NaClO₄)

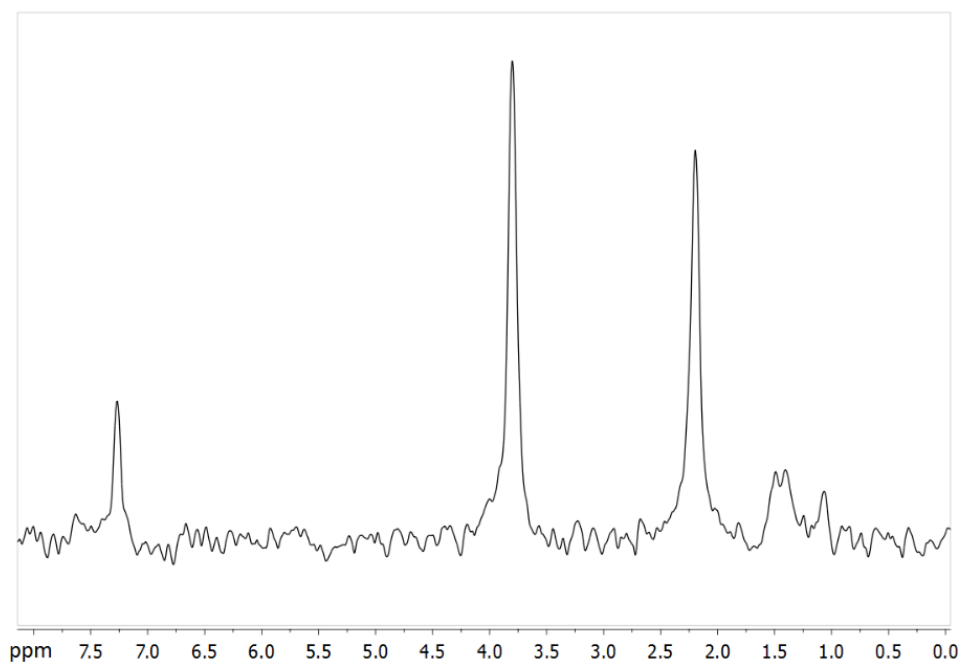
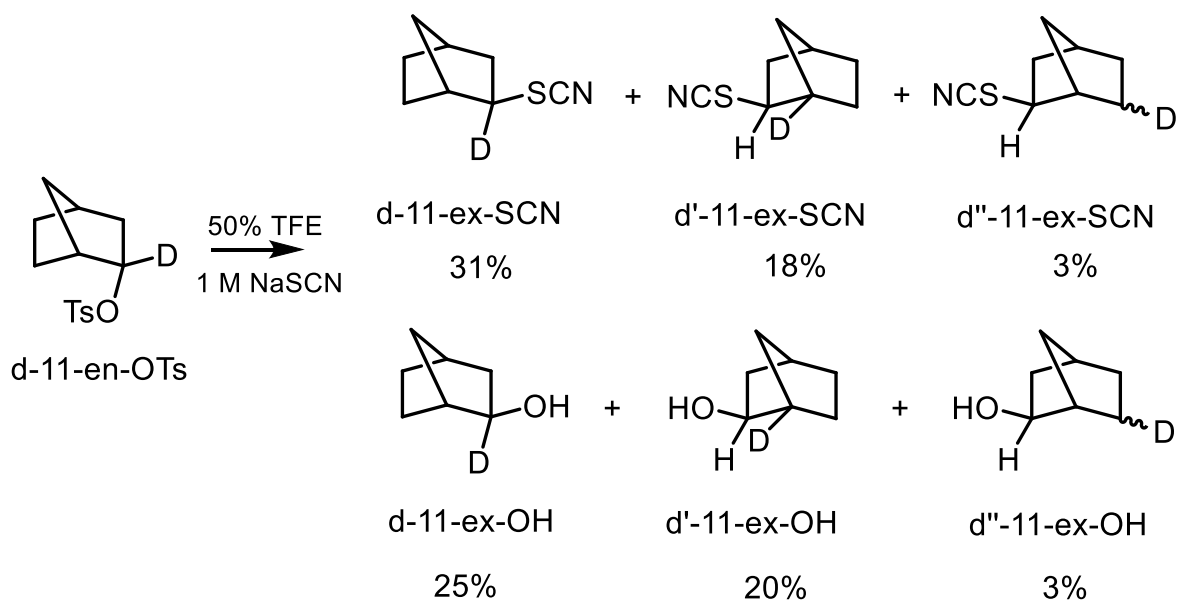


Figure 3.1. ^2H NMR spectra for solvolysis products of **d-11-en-OTs** in 50% TFE (v : v) (1 M NaClO_4)



Scheme 3.4. Major solvolysis products of **d-11-en-OTs** in 50% (v : v) TFE (1 M NaSCN)

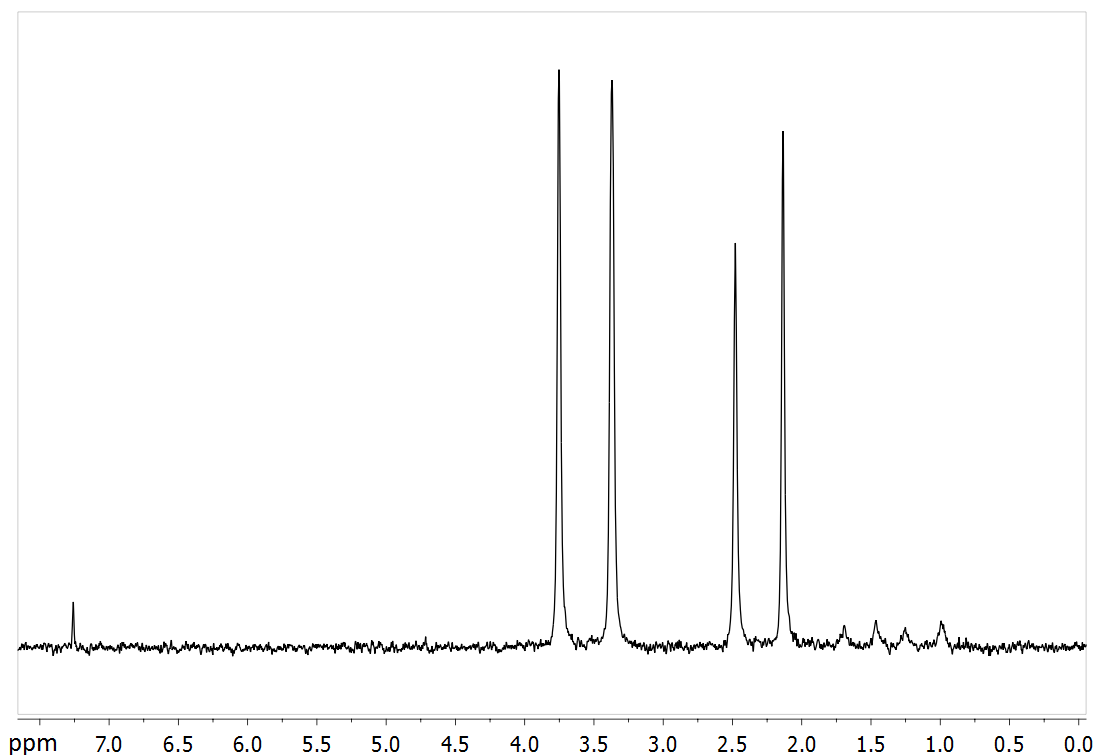


Figure 3.2. ^2H NMR spectra for solvolysis products of **d-11-en-OTs** in 50% TFE (v : v) (1 M NaSCN)

3.4 Discussion

The nearly equal distribution of **d-11-ex-OH** and **d'-11-ex-OH** from the solvolysis of **d-11-en-OTs** in the absence of nucleophilic salts indicated that 95% of the solvolysis products were formed through a non-classical cation intermediate. The 5% excess of **d-11-ex-OH** may result from a minor $\text{S}_{\text{N}}2$ contribution or the capture of a classical 2-norbornyl cation by solvent before rearrangement to a non-classical cation.

The 5% excess of **d-11-ex-OH** should be a valid number rather than an NMR artefact, since in the presence of 1 M NaSCN, the ratio $\frac{[\text{d-11-ex-OH}]}{[\text{d'-11-ex-OH}]}$ became larger. The pathway to generate the excess amount of **d-11-ex-OH** should occur before the formation of the non-classical cation (non-classical cations will only generate 1:1 **d-11-ex-OH** and **d'-11-ex-**

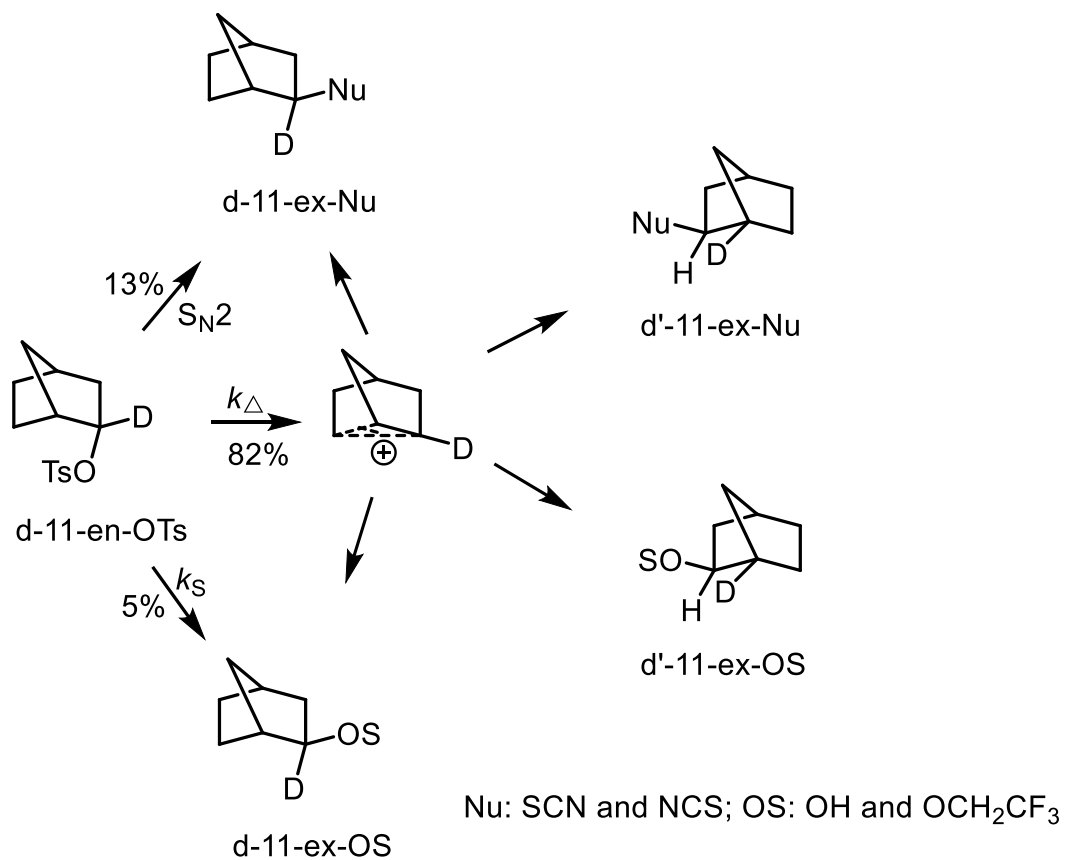
OH, and most of the trapping adducts are from capturing the non-classical cations by NaSCN). Therefore, the added NaSCN will not affect the pathways before of the formation of non-classical cations (solvent direct attack and σ participation) but competed with solvent to trap non-classical cations, then a larger ratio $\frac{[\text{d-11-ex-OH}]}{[\text{d'-11-ex-OH}]}$ in the presence of NaSCN should be expected. If the distribution of **d-11-ex-OH** and **d'-11-ex-OH** is equal but a non-equal ratio is observed due instrumental error, the same ratio (1.1 : 1) should be expected in the presence of 1 M NaClO₄ or NaSCN (NaSCN shows no general base catalysis effects (See Chapters 4 and 5)), which is not consistent with our results.

Considering the distribution of **d-11-ex-SCN** and **d'-11-ex-SCN**, a far larger ratio (1.74 : 1) was found. With 52% total yield of trapping adducts from solvolysis of **d-11-en-OTs**, the excess amount of **d-11-ex-SCN** resulting from 'direct coupling' can be calculated as 13%, which is 2.6 times larger than the excess amount of **11-d-OH** from 'direct coupling' (5%). If we assume that **11-ex-OTs** can be used as a model for a pure S_N1 pathway, which directly generates the non-classical cation as a sole intermediate, then the product selectivity obtained from the product analysis is $\frac{k_{\text{SCN}^-}}{k_{\text{S}}} = 0.82 \text{ M}^{-1}$, indicating $k_{\text{S}} \leq 6.1 \times 10^9 \text{ s}^{-1}$ (as $k_{\text{SCN}^-} \leq 5 \times 10^9 \text{ M}^{-1}\text{s}^{-1}$). A very similar selectivity $\frac{k_{\text{SCN}^-}}{k_{\text{S}}} = 0.89 \text{ M}^{-1}$ is shown by the intermediate generated during the solvolysis of **d-11-en-OTs**, as obtained from both the product and deuterium scrambling analysis. Thus, the consistent selectivity parameters indicate that most of the solvolysis products of **11-en-OTs** are produced via a non-classical cation, which behaves nearly the same as (but not exactly the same, since the tosylate anion's position is different in those two ion-pairs) the non-classical cation generated from **11-ex-OTs**.

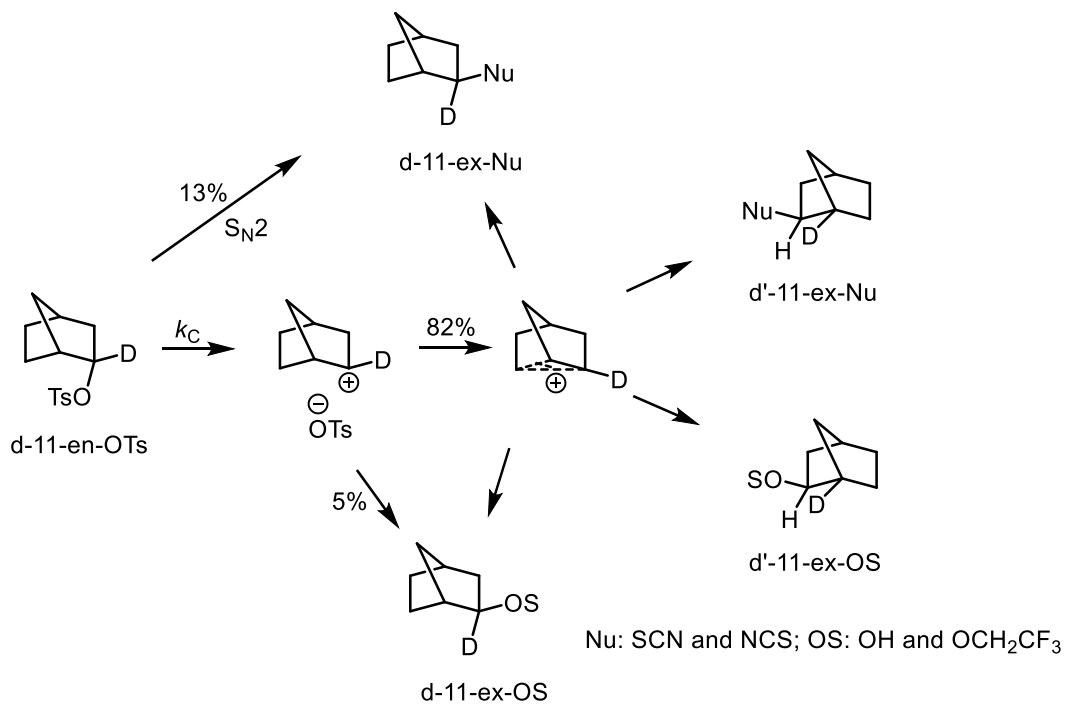
The deuterium effect on the structure disturbance of non-classical norbornyl cation can be ignored. Saunders and Kates⁵⁸ reported that at -150 °C, the isotopic splitting of C1 and C2 in the non-classical norbornyl cation is < 2.3 ppm. At increased temperature, the splitting is expected to be even smaller, resulting in a symmetric and static structure.

Let's now consider the 'direct coupling' product selectivity. The ratio $\frac{k'_{\text{SCN}^-}}{k'_s} = 2.6 \text{ M}^{-1}$ is obtained by analysing the percentage of 'direct coupling' products shown in Scheme 3.4. This ratio is significantly larger than that obtained from the non-classical cations. If the 'direct coupling' products are formed by the capture of classical cations by solvent and NaSCN without pre-association, an even smaller ratio should be expected by applying the localized selectivity-reactivity principle. The classical norbornyl cation should be far more reactive than the non-classical cation, thus the selectivity between strong nucleophiles (NaSCN) and weak nucleophiles (solvents) should be smaller or at least comparable for classical cations. The larger ratio found from 'direct coupling' products then indicates that the excess amount of **d-11-ex-SCN** is most likely to be generated through a bimolecular concerted pathway with NaSCN, which is highly likely to be a classical S_N2 mechanism with a weak bond coupling, which gives a larger $\frac{k_{\text{SCN}^-}}{k_s}$ ratio (but overall, the ratio is still quite small).

However, the mechanism to form 5% excess of **d-11-ex-OH** is still not defined. It can involve a bimolecular pathway (Scheme 3.5) as well or involve capture of the classical cation before it rearranges to the non-classical cation (Scheme 3.6).



Scheme 3.5. The solvolysis mechanism of **d-11-en-OTs** involving only non-classical cation intermediates



Scheme 3.6. The solvolysis mechanism of **d-11-en-OTs** involving classical and non-classical cation intermediates

It is really difficult to exclude the existence of the classical cations since the excess amount of **d-11-ex-OS** is only 5%, and both mechanisms shown in Schemes 3.5 and 3.6 are consistent with our experimental observations.

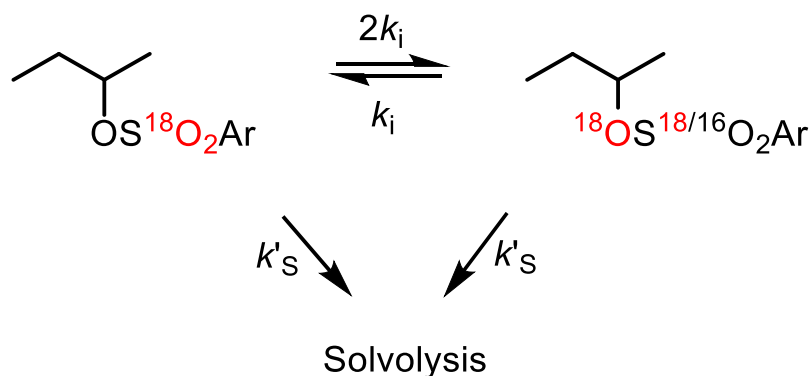
As the rate constant of solvent attack on simple tertiary carbenium ions in 50% (v : v) TFE (See Chapter 5) has been determined as $8 \times 10^{10} \text{ s}^{-1}$, the intrinsic reactivity difference between tertiary and secondary carbenium ions (measured or calculated in gas phase as well as in super acid condition⁵⁹) suggests that the intrinsic bond formation between solvent molecules and simple secondary carbenium ions in 50% (v : v) TFE is barrierless ($> 10^{13} \text{ s}^{-1}$). Therefore, if the classical secondary norbornyl carbenium ions is formed in 50% (v : v) TFE without solvent pre-organization (due to unfavourable entropy), the bond formation step will be dominated by solvent reorganization ($\approx 10^{11} \text{ s}^{-1}$)^{15,35}. If the solvent molecule is pre-organized before substrate ionization, then the solvolysis product formation will be an uncoupled concerted pathway, since the intrinsic bond formation is assumed to be barrierless. Or it even can be a real concerted pathway with mild bond coupling, based on the energy balance between negative entropy and enthalpy. Thus, the pre-organized solvent pathway can be described as an S_N2 mechanism, which is the same as the discussion shown above for NaSCN.

How significant a solvent reorganization dominated step-wise pathway (Scheme 3.4) is depends on the energy cost balance between solvent pre-organization and the intrinsic bond formation barrier. Unfortunately, we cannot find experimental data for the solvent pre-organization energy in 50% (v : v) TFE. Thus, this step-wise pathway dominated by solvent

reorganization remains a reasonable alternative pathway to a concerted solvolysis mechanism.

In order to find more evidence to distinguish between the concerted mechanisms shown in Scheme 3.3 and the step-wise mechanisms shown in Scheme 3.4, two reports that provided indirect data are also analysed and discussed below.

Chang and le Noble³⁴ⁿ reported that after 2.1 half-lives in refluxing ethanol, [ether-¹⁷O]-endo-2-norbornyl mesylate showed no scrambling into the sulfone positions (even 0.5% scrambling should be detected with confidence³⁴ⁿ), indicating an S_N2 mechanism or a step-wise mechanism without detectable internal return. Since even 1 M NaSCN only showed a weak S_N2 contribution ($\approx 13\%$) in 50% (v : v) TFE, pure ethanol, which is more nucleophilic than 50% (v : v) TFE but less nucleophilic than 1 M NaSCN, cannot react with the substrate only through an S_N2 pathway. The major contribution has to be accounted for a step-wise pathway^{60a}. Thus, the absence of isotope exchange after 2.1 half-lives in refluxing ethanol is best explained by a step-wise pathway without internal return. However, isotope exchange in simple secondary tosylates is observable in 50% (v : v) TFE (suggested as an S_N2 mechanism) with a ratio⁵⁴ $k_i = 0.014k'_s$ (Scheme 3.7) and sulfonate anion exchange rate constant^{16,19,41} in 50% (v : v) TFE was suggested as 10^{11} s^{-1} .



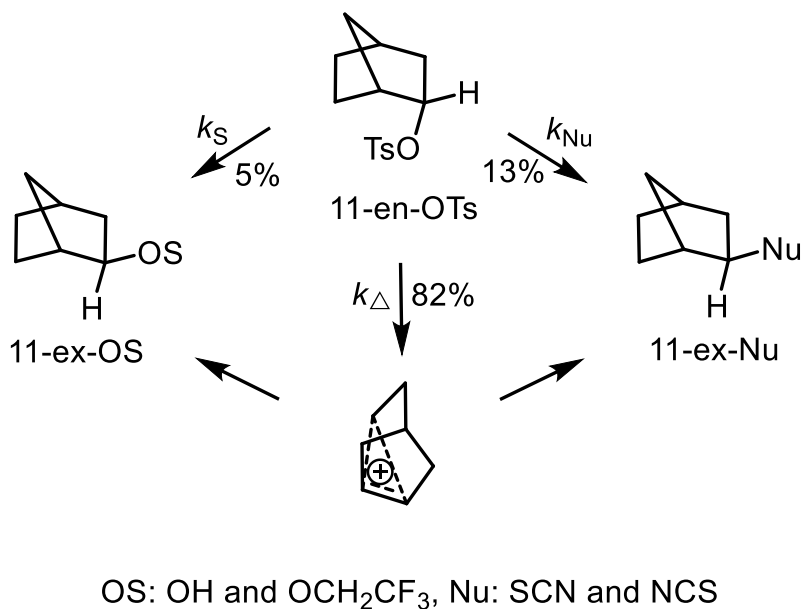
Scheme 3.7. Isotope scrambling of 2-butyl tosylate solvolysis in 50% TFE (v : v)

If the step-wise pathway for **11-en-OTs** proceeds through a classical cation intermediate, then solvent attack and σ participation should be significantly faster than anion exchange (σ participation and anion recombination are assumed to be comparable based on non-classical 2-norpinyl cation-mesylate ion-pair^{60b}). Considering the time scale (10^{13} s^{-1}) for a single bond vibration, this perhaps indicates that the classical cation's lifetime is too short and finally becomes invisible. Ionization and σ participation are enforced to couple in the energy profile, with a transition state that looks like the classical cation. Direct ionization to give a non-classical cation will predict no isotope scrambling, since any internal return by sulfonates to the more reactive exo-2-norbornyl isomers will be more favourable. Thus, no detectable isotope scrambling is consistent with the proposed mechanism shown in Scheme 3.5.

Meanwhile, Kirmse and Siegfried⁶¹ reported the deamination reactions of 2-d-endo-norbornylamine and 2-d-exo-norbornylamine with $\text{NaNO}_2\text{-HNO}_2$ in water (pH = 3.5, adjusted by HClO_4), and found that both substrates gave the same distribution of **d-11-ex-OH** and **d'-11-ex-OH**, in a ratio of 1 : 1.1, determined by ^2H NMR. The non-equal distribution by ^2H NMR integration is unaccounted for⁶¹. Therefore, the deuterium

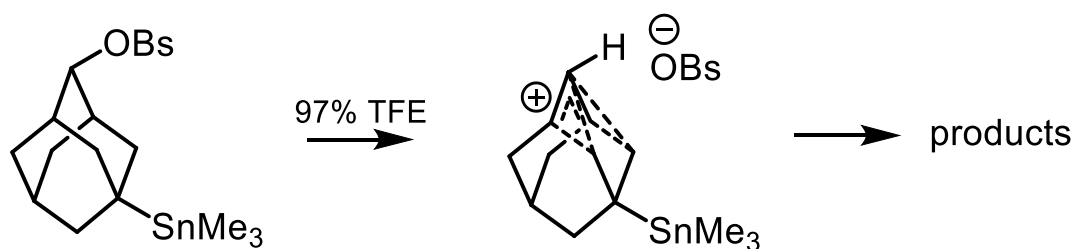
scrambling from more reactive precursors (diazonium salts) in a more nucleophilic solvent (water) did not show different scrambling between exo and endo isomers, against the formation of classical cations from endo isomers. If the exo isomer directly generates the non-classical cation intermediates, this suggests that the same happens for the endo isomer, rather than the formation of a classical cation. Our precursor, tosylate, which is far less reactive than the corresponding a diazonium salt, should suffer from more bond coupling assistance upon solvolysis, and so is not likely to generate the classical cations shown in Scheme 3.6.

Therefore, combining these previous reports with our results, the best description of the solvolysis mechanism of **11-en-OTs** in 50% (v : v) TFE involves only non-classical cation intermediates and is summarized in Scheme 3.8. Without added strong nucleophiles, the solvent induced S_N2 contribution is 5%, and 95% of the solvolysis reactions involve concerted σ participation to form the non-classical cations directly, whose two reactive sites then can be captured by solvents at equal rates.



Scheme 3.8. The solvolysis mechanism of **11-en-OTs** in 50% (v : v) TFE

Further evidence that supports concerted front-side σ participation instead of forming the classical carbenium ion comes from Schleyer *et al.*^{62a,62b} and Firme^{62c}. They reported that by B3LYP/6-311++G* and PBE1PBE/6-311++G** level calculations, respectively, the classical cation cannot be in an energy minimum in aqueous solutions. The ionization of an endo precursor will directly generate the non-classical cation but with a higher barrier than exo isomers. Meanwhile, Shiner Jr. *et al.*⁶³ reported that when solvolysing (*Z*)-5-trimethylstannyl 2-adamantyl brosylate in 97% TFE, ionization will directly give the E-cation in an uncoupled concerted way shown in Scheme 3.9, supporting concerted front-side σ participation. This concerted ionization can also give a large α secondary KIE since at the transition state, the C-H(D) bond will lose most of zero-point energy from the out-of-plane bending vibration at α carbon.



Scheme 3.9. The solvolysis mechanism of (*Z*)-5-trimethylstannyl 2-adamantyl brosylate in 97% TFE

Finally, the observed rate constant of **11-en-OTs** is nearly the same as for simple secondary tosylates in 50% (v : v) TFE⁵⁴, but only about 10% bimolecular reaction with 1 M NaSCN was found (assuming a 10% negative salt effect caused by replacing NaClO₄ with NaSCN). This is significantly smaller than for the reaction of NaSCN with simple secondary substrates, which shows more than 90% bimolecular reaction with 1 M NaSCN. This indicates the ‘neo-pentyl like’ structure slows down the S_N2 reactions by making the α carbon more hindered. We note that α -methyl neo-pentyl substrates solvolyse in weakly

nucleophilic solvents faster than simple secondary substrates, because they can utilise the back-side neighbouring group participation⁶⁴ which significantly lowers the energy barrier to ionization.

3.5 Conclusion

By studying the products, their isotope scrambling in the presence of NaClO₄ or NaSCN, and analysing key literature reports, we suggest that the solvolysis mechanism of **11-en-OTs** is best described as a combination of S_N2 and S_N1 mechanisms. The S_N2 mechanism contributes 5% of the reaction pathways, but becomes more significant with added strong nucleophiles (*ca.* 13% in 1 M NaSCN). The S_N1 mechanism directly generates the non-classical cation through concerted front-side σ participation.

The concerted front-side σ participation is highly likely to be an enforced uncoupled (or slightly coupled) process, since the observed solvolysis rate difference between the exo and endo isomers in weakly nucleophilic solvents is about 1000 (corrected for internal return of exo isomers)^{34a}. This indicates that the energy barrier for the endo isomers to generate the non-classical cation is higher than exo isomers, due to the unfavourable front-side orbital overlap at the transition state. This is consistent with our previous study of simple secondary tosylates in 50% (v : v) TFE⁵⁴, which indicated that the simple secondary cation is too unstable to exist in aqueous solutions.

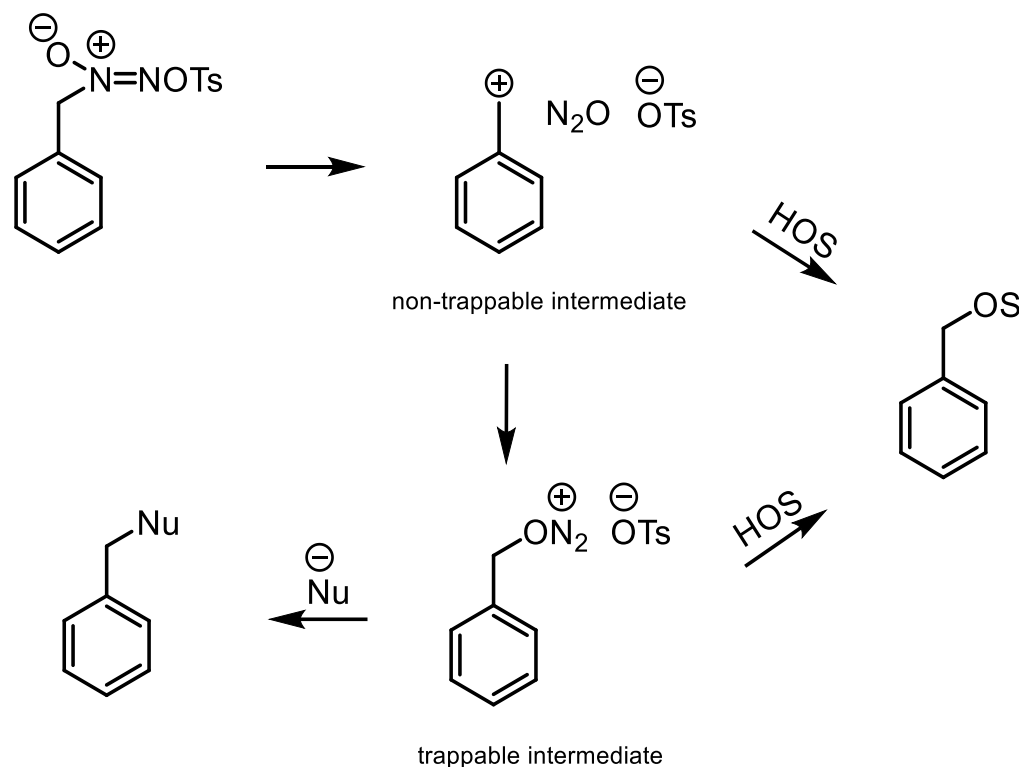
We also conclude that for a ‘neo-pentyl like’ structure which cannot provide too much assistance to ionization, the S_N2 contribution is small compared with simple secondary

structures, since the α carbon is more hindered. The competition between bimolecular pathways and unimolecular ionization is moved more towards S_N1 mechanisms.

Chapter 4: Can 1-(3-nitrophenyl)ethyl cation be formed in 50% (v : v) TFE? On the study of solvolysis reaction of 1-(3-nitrophenyl)ethyl azoxytosylate***

4.1 Introduction

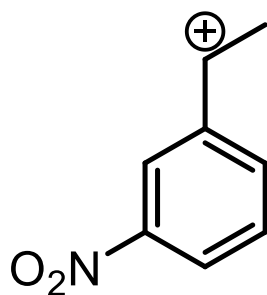
The fact that azoxytosylates can react through a fragmentation type ionization upon solvolysis has been suggested for many years^{32,67-70}. Maskill *et al.* studied the solvolysis mechanism of 2-adamantyl azoxytosylate^{67,69} and substituted benzyl azoxytosylates^{32,68,70} in 50% (v : v) TFE in some detail. He concluded that these substrates undergo step-wise mechanisms without any (or with minor) solvent assistance and two intermediates were involved in the reaction pathway during the solvolysis of benzyl azoxytosylate (Scheme 4.1) in 50% (v : v) TFE³².



Scheme 4.1. The solvolysis mechanism of benzyl azoxytosylate in 50% (v : v) TFE³²

In comparison with tosylates, azoxytosylates seem more likely to react through S_N1 mechanisms (and suffer from less nucleophilic assistance) upon solvolysis. Solvent assistance in the departure of the leaving groups is weak because benzyl azoxytosylate did not show any rate acceleration in the presence of sodium thiocyanate (up to 1 M) but a significant amount of benzyl thiocyanate was found as a new product³². This classic trapping experiment indicates that the bimolecular reaction between the substrate and thiocyanate is not important even for a benzyl electrofuge. However, under the same conditions, benzyl tosylate shows a clear linear relationship between the observed solvolysis rate constant and the concentration of added strong nucleophiles⁷¹. The selectivity parameter $\frac{k_{SCN^-}}{k_S}(M^{-1})$ is also larger for benzyl tosylate than benzyl azoxytosylate³². This evidence indicates that the reaction between strong nucleophiles and benzyl tosylate is a bimolecular pathway⁷¹ but is a unimolecular pathway for benzyl azoxytosylate. Thus, the lack of competition from an S_N2 pathway suggests that azoxytosylates may be a useful nucleofuge for deriving new insights into S_N1 solvolysis mechanisms.

1-(3-Nitrophenyl)ethyl cations (Scheme 4.2) have been predicted to be too unstable to exist as formal intermediates in 50% (v : v) TFE¹², based on extrapolating the linear correlation between stable 1-aryl ethyl cations' lifetimes and σ^+ .



Scheme 4.2. The structure of 1-(3-Nitrophenyl)ethyl cation

Similarly^{16,19}, 1-(3-nitrophenyl)ethyl tosylate appears to undergo an uncoupled concerted pathway, without generating an ion-pair intermediate when solvolysed in 50% (v : v) TFE which is consistent with the estimated lifetime of the cation being $< 10^{-13}$ s. Thus, the conclusion has been drawn that 1-(3-nitrophenyl)ethyl cations in 50% (v : v) TFE cannot exist. However, McClelland *et al.*^{14a} showed that the lifetimes of some triarylmethyl cations did not correlate well with σ^+ . The observed lifetimes of the less stable triarylmethyl cations were found to be longer than predicted by the linear relationship generated from the more stable cations. This was also observed for diarylmethyl cations^{1,2}. In other words, electrofugality and electrophilicity do not always correlate well^{1,2}. Furthermore, although 1-(3-nitrophenyl)ethyl tosylate showed no evidence for an observable S_N1 mechanism, this only indicates that the solvent assisted bimolecular pathway is a lower energy pathway than the S_N1 ionization when solvolysing 1-(3-nitrophenyl)ethyl tosylate in 50% (v : v) TFE (as discussed above for the benzyl systems). This does not necessarily mean that the cation cannot be formed, but that due to the unsuitable cation precursor, an alternative pathway dominates.

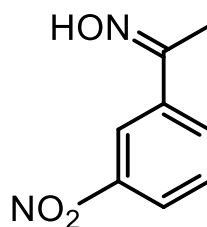
Thus, extrapolating the linear correlation with σ^+ to estimate the lifetime of 1-(3-nitrophenyl)ethyl cations in 50% (v : v) TFE maybe not reliable. Changing the nucleofuge so that the competition from S_N2 pathways is relatively weaker may provide a chance to reveal the 1-(3-nitrophenyl)ethyl cation.

4.2 Experimental

General

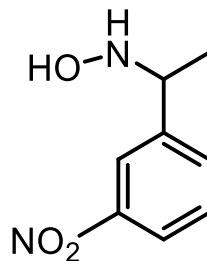
All the chemicals were purchased from Sigma-Aldrich, Alfa Aesar or Acros Organics, those for synthesis purpose were used directly without further purification. TFE was distilled from P₂O₅ and stored over 4Å molecular sieves. UHQ water was obtained from an ELGA PURELAB Option S-R 7-15 system. ¹H NMR and ¹³C NMR spectra were recorded on Bruker AV-HD 400 instrument. HPLC analysis was carried out on Waters 2690 (486 Tunable Absorbance Detector) and 2695 (2487 Dual λ Absorbance Detector) systems with a Hichrom[®] HIRPB-624 C₁₈ column (3.5 μm × 250 mm) and UV detection at 265 nm. A gradient elution was used, changing from 95% water and 5% acetonitrile to 5% water and 95% acetonitrile over 20 mins followed by a further 10 mins of the final eluent mixture.

Syntheses



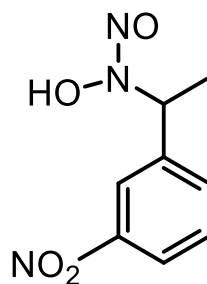
3-nitroacetophenone oxime⁸². Following the procedure reported by Li *et al.*⁸¹ 3.30 g 3-nitroacetophenone (20 mmol) and 1.67 g hydroxylamine hydrochloride (24 mmol) were dissolved in 20 mL ethanol. 27 mL 1 M NaOH was added slowly and then the mixture was stirred at 50 °C under nitrogen overnight before cooling down to room temperature. The white needle precipitate that formed was filtered off and washed with cold water three times before drying under nitrogen, yielding 2.88 g (80%) **3-nitroacetophenone oxime** as a white solid. ¹H NMR (400 MHz, CDCl₃): 8.51 (1H, t, J = 1.9 Hz), 8.23 (1H, ddd, J = 8.2,

2.3, 0.9 Hz), 8.08 (1H, ddd, J = 7.9, 1.6, 1.0 Hz), 7.58 (1H, t, J = 8.0 Hz), 2.36 (3H, s). ¹³C NMR (100 MHz, CDCl₃): 154.1, 148.3, 139.1, 131.9, 129.9, 123.2, 120.2 and 11.6.



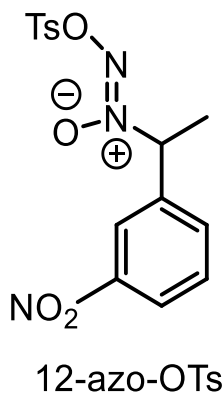
N-(1-(3-nitrophenyl)ethyl)hydroxylamine. Following the procedure reported by Maskill and Jencks.³² 1.80 g 3-nitroacetophenone oxime (10 mmol), 1.26 g sodium cyanoborohydride (20 mmol) and 5 mg methyl orange were added into a 100 mL flask followed by 20 mL of dry methanol. The solution with stirring was cooled to 0 °C and sufficient 35% HCl was added to keep the solution pink. After 30 mins, the ice bath was removed and several drops of 35% HCl were again added to keep the solution pink. The mixture was stirred overnight before quenching with saturated NaHCO₃. Methanol was removed under vacuum and the water phase was extracted with ethyl acetate. The organic layer was separated and dried over Na₂SO₄ before the solvent was evaporated under vacuum to afford 1.18g (65%) of the corresponding hydroxylamine as a white solid. TLC showed only one spot which is more polar than the oxime.

¹H NMR (400 MHz, CDCl₃): 8.27 (1H, t, J = 1.9 Hz), 8.15 (1H, dd, J = 8.1, 1.9 Hz), 7.70 (1H, d, J = 7.7 Hz), 7.54 (1H, t, J = 8.0 Hz), 4.29 (1H, q, J = 6.8 Hz) and 1.41 (3H, d, J = 6.8 Hz). ¹³C NMR (100 MHz, CDCl₃): 148.4, 144.9, 133.5, 129.5, 122.6, 122.2, 61.1 and 19.4.



N-nitroso-N-(1-(3-nitrophenyl)ethyl)hydroxylamine. Following the procedure reported by Maskill and Jencks³². 1.18 g **N-(1-(3-nitrophenyl)ethyl) hydroxylamine** (6.5 mmol) was dissolved in 3 mL methanol at 0 °C. 3 mL water was added, followed by slowly adding 1.1 mL 35% HCl. 2 mL 6 M sodium nitrite solution was added dropwise to the mixture. After 10 mins, the mixture was diluted with cold water and filtered off. The solid was washed twice with cold water before drying under nitrogen to afford 1.02 g crude **N-nitroso-1-(3-nitrophenyl)ethylhydroxylamine** (74%) as a yellow solid.

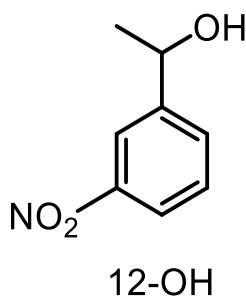
¹H NMR (400 MHz, CDCl₃): 8.38 (1H, t, J = 1.9 Hz), 8.30 (1H, dd, J = 8.0, 1.9 Hz), 7.84 (1H, d, J = 7.7 Hz), 7.62 (1H, t, J = 8.0 Hz), 5.65 (1H, q, J = 7.0 Hz) and 1.97 (3H, d, J = 7.0 Hz). ¹³C NMR (100 MHz, CDCl₃): 148.4, 137.7, 133.4, 130.1, 124.4, 122.6, 70.5 and 18.4.



1-(3-nitrophenyl)ethyl azoxytosylate (12-azo-OTs). Following the procedure reported by Maskill and Jencks³². 1.14 g tosyl chloride (6 mmol) was added portionwise to a stirred

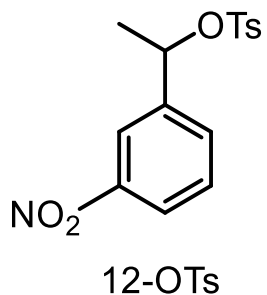
solution of 1.02 g **N-nitroso-N-(1-(3-nitrophenyl)ethyl)hydroxylamine** (4.8 mmol) in 5 mL dry pyridine under nitrogen at 0 °C. The reaction mixture was stirred overnight at RT before quenching with cold water (4 mL). After a brief period of further stirring (15 mins), the mixture was diluted with water and ethyl acetate. The organic phase was separated and dried over Na₂SO₄ before being concentrated under vacuum. The residue was triturated in 10 mL cold diethyl ether and the resulting solid was filtered off and dried under nitrogen to afford 1.10 g of **12-azo-OTs** as a light yellow solid (62%). TLC showed only one movable spot and HPLC showed the small impurity peaks were not solvolysis products.

¹H NMR (400 MHz, CDCl₃): 8.27 (1H, d, J = 8.3 Hz), 8.19 (1H, s), 7.86 (2H, d, J = 8.3 Hz), 7.74 (1H, d, J = 7.8 Hz), 7.57 (1H, t, J = 8.0 Hz), 7.36 (2H, d, J = 8.1 Hz), 5.65 (1H, q, J = 6.9 Hz), 2.47 (3H, s) and 1.88 (3H, d, J = 6.9 Hz). ¹³C NMR (100 MHz, CDCl₃): 148.3, 146.5, 137.0, 133.4, 131.4, 130.0, 128.8, 124.6, 122.7, 73.9, 21.8 and 18.2.



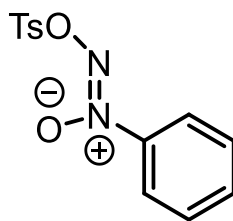
1-(3-nitrophenyl)ethanol (12-OH)⁸⁴. Following the procedure reported by Yu *et al.*⁸³. 1.65 g 3-nitroacetophenone (10 mmol) was dissolved in 30 mL methanol at 0 °C. 1.51 g sodium borohydride (40 mmol) was added portionwise. Further stirring for 2 hours at room temperature and evaporating the methanol gave a yellow solid, which was washed with saturated aqueous NaHCO₃ and extracted with ethyl acetate. The organic phase was separated and dried over Na₂SO₄ before filtration and concentration under vacuum gave 1.02 g **12-OH** as a yellow solid (60%).

^1H NMR (400 MHz, CDCl_3): 8.20 (1H, t, $J = 2.0$ Hz), 8.06 (1H, ddd, $J = 8.2, 2.3, 1.0$ Hz), 7.68 (1H, d, $J = 7.7$ Hz), 7.49 (1H, t, $J = 7.9$ Hz), 4.98 (1H, q, $J = 6.5$ Hz) and 1.50 (3H, d, $J = 6.5$ Hz). ^{13}C NMR (100 MHz, CDCl_3): 148.3, 148.0, 131.7, 129.4, 122.2, 120.4, 69.2 and 25.3.



1-(3-nitrophenyl)ethyl tosylate (12-OTs)^{16,19}. Following the procedure reported by Tsuji and Richard^{16,19}. 1.02 g **12-OH** (6 mmol) was dissolved in 2.5 mL dioxane at 0 °C. 1.53 g tosyl chloride (8 mmol) was added portionwise followed by slow addition of 2.5 mL 5 M NaOH. The mixture was stirred for 6 hours at RT before quenching with cold water (5 mL). The solid was filtered off and collected; diethyl ether (5 mL) was added and the resulting solid was filtered off again and dried under nitrogen, giving 0.50 g **12-OTs** (26%) as a white solid.

^1H NMR (400 MHz, CDCl_3): 8.11 (1H, ddd, $J = 8.2, 2.2, 1.0$ Hz), 7.95 (1H, t, $J = 1.9$ Hz), 7.66 (2H, d, $J = 8.3$ Hz), 7.60 (1H, d, $J = 7.9$ Hz), 7.46 (1H, t, $J = 7.9$ Hz), 7.23 (2H, d, $J = 8.0$ Hz), 5.64 (1H, q, $J = 6.6$ Hz), 2.39 (3H, s) and 1.64 (3H, d, $J = 6.6$ Hz). ^{13}C NMR (100 MHz, CDCl_3): 148.2, 144.9, 141.5, 133.9, 132.2, 131.6, 129.7, 129.6, 123.3, 121.3, 79.0, 23.1 and 21.5.

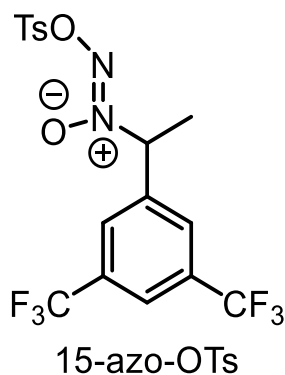


14-azo-OTs

Phenyl azoxytosylate (14-azo-OTs). Following the procedure reported by Stevens⁸⁵. 1.14g tosyl chloride (6 mmol) was added portionwise to a stirred solution of 0.75 g Cupferron (4.8 mmol) in 5 mL dry pyridine under nitrogen at 0 °C. The reaction mixture was stirred overnight at RT before quenching with cold water (4 mL). After a brief period of further stirring (15 mins), the mixture was diluted with water and ethyl acetate. The organic phase was separated, dried over Na₂SO₄ and filtered before being concentrated under vacuum. The residue was triturated in methanol (7 mL) and the resulting solid was filtered off and dried under nitrogen to afford 0.31 g **14-azo-OTs** as a yellow solid (21%). TLC and HPLC both showed only one compound.

¹H NMR (400 MHz, CDCl₃): 7.98 (2H, d, J = 8.4 Hz), 7.95-7.90 (2H, m), 7.63-7.57 (2H, m), 7.54-7.47 (1H, m), 7.42 (2H, d, J = 8.1 Hz), 7.23 (2H, d, J = 8.0 Hz) and 2.48 (3H, s).

¹³C NMR (100 MHz, CDCl₃): 146.5, 143.0, 132.7, 131.6, 130.1, 129.3, 129.0, 121.7 and 21.8.



1-(3,5-bis-trifluoromethylphenyl)ethyl azoxytosylate (15-azo-OTs). This was prepared from 3,5-bis-trifluoromethyl acetophenone by the same method³² shown above for **12-azo-OTs**, to yield an orange solid after crystallization from methanol.

¹H NMR (400 MHz, d₆-DMSO): 8.21 (1H, s), 8.09 (2H, s), 7.79 (2H, d, J = 8.0 Hz), 7.42 (2H, d, J = 8.0 Hz), 6.15 (1H, q, J = 6.9 Hz), 2.39 (3H, s), 1.80 (3H, d, J = 6.9 Hz). ¹⁹F

NMR (400 MHz, d₆-DMSO): -61.3. Due to the low concentration, we could not obtain the ¹³C NMR spectra clearly, however, TLC and HPLC all showed only one compound.

Kinetic analysis

The solvolysis reactions were carried out with 3 mM substrate, 1 M sodium perchlorate or sodium thiocyanate (the total salt concentration was adjusted by sodium perchlorate to 1 M), and 1 mM 4-methoxyacetophenone as the internal standard in 50% aqueous TFE (v/v) at 30 °C. The solutions were immersed in a thermostated water bath, and the progress of the reactions was monitored by analysing aliquots of the reactions mixture using HPLC for 2-3 half-lives. The peak areas in the chromatograms were integrated and a first order equation fitted to these data; in all cases, R² > 0.999.

Product analysis

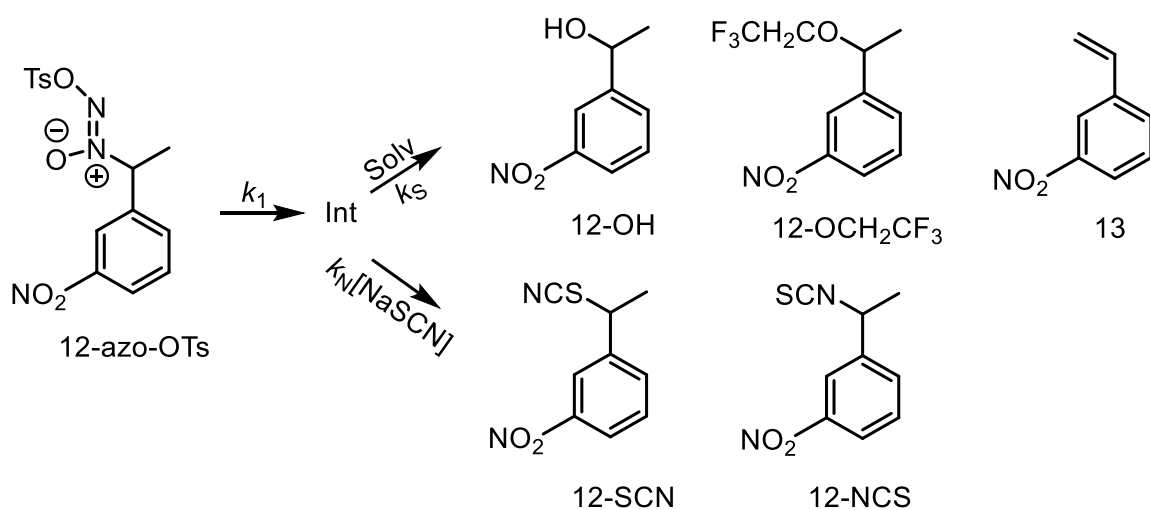
The products from the solvolysis of **12-azo-OTs** were analysed by HPLC after 10 half-lives under the same conditions as shown for **Kinetics**. Without sodium thiocyanate, there are only three peaks in the chromatogram: the corresponding alcohol and styrene were identified and calibrated by comparison with authentic samples. The remaining peak was assumed to be the trifluoroethyl ether (P. 185). The same three peaks were observed as the products of solvolysis of **12-OTs**. In the presence of different concentrations of sodium thiocyanate, there were another two peaks (whose peak areas were increased with increasing sodium thiocyanate concentration), determined as the corresponding thiocyanate and isothiocyanate. The relative concentration of the solvolysis products were normalized by dividing the peak areas by internal standard peak area. We could not determine the absolute concentration of products because of unknown extinction coefficients. However, since we are interested in the relative change, an absolute relative ratio to internal standard is appropriate (See Appendices Chapter 4 P. 186).

The products of solvolysis of **14-azo-OTs** was studied under the same conditions given above. With or without 1 M sodium thiocyanate, the products were the same: N-nitroso phenylhydroxylamine and trifluoroethyl tosylate, which were identified by comparison with authentic samples. Tosylate anion was not detected by our HPLC system. The solvolysis products of **15-azo-OTs** were analysed in the same way.

4.3 Results and Discussions

According to a previous report by Maskill and Jencks³², when buffering the solvolysis reaction of benzyl azoxytosylate in 50% TFE with a general base, a significant amount of

S-O cleavage products are generated, this affected the mass balance relationship for substitution products (since our product analysis is based on an internal standard, see Experimental section). If no base was added, the pH of the solution dropped from 7.0 to 3.0 during solvolysis, but all the products were stable under these acidic conditions (the ratios of all the products did not change between 1 and 10 half-lives). In order to make the product mixture easier to analyse, we generally did not buffer the solution with a non-nucleophilic base, but the effect of 2,6-di-*tert*-butylpyridine will be discussed later. The pseudo first-order solvolysis rate constant of 1-(3-nitrophenyl)ethyl azoxytosylate (**12-azo-OTs**) in 50% (v : v) TFE with 1 M NaClO₄ at 30 °C was $3.6 \pm 0.1 \times 10^{-5} \text{ s}^{-1}$, which is approximately 30 times slower than that of 1-(3-nitrophenyl)ethyl tosylate (**12-OTs**) under the same conditions^{16,19}. When 1 M NaClO₄ is replaced by 1 M NaSCN, the observed rate constant decreased slightly to $3.3 \pm 0.1 \times 10^{-5} \text{ s}^{-1}$ (10% decrease). We attribute this to a non-specific salt effect. Thus, there is no significant S_N2 acceleration involving NaSCN. The variation of product distribution with different NaSCN concentration is shown in Fig. 4.1 and the simplest mechanism that is quantitatively consistent with these data is shown in Scheme 4.3.



Scheme 4.3. The step-wise solvolysis pathway of **12-azo-OTs** in 50% (v : v) TFE with a single intermediate

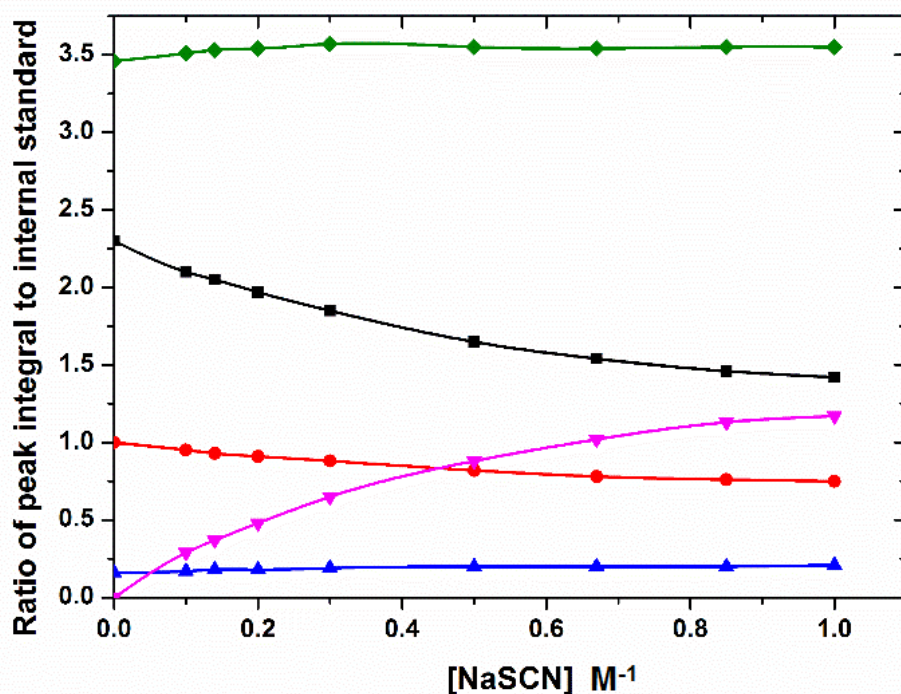


Figure 4.1. Variation in products formed with different [NaSCN]. These data are the ratio of the product peak areas to the internal standard area at 265 nm. Black squares: alcohol (**12-OH**); red circles: trifluoroethyl ether (**12-OCH₂CF₃**); blue triangles: styrene (**13**); purple triangles: sum of RSCN (**12-SCN**) and RNCS (**12-NCS**); green diamonds show the sum of the **12-OH**, **12-OCH₂CF₃**, **13**, **12-SCN** and **12-NCS** data.

The formation of 3-nitro styrene (**13**) is a minor contribution (only 5-6% as established by calibration with authentic samples) to the total product yield and not significantly affected by added NaSCN (blue line with triangles in Fig. 4.1). Thus, a very good mass balance relationship holds to those substitution products using normalized peak integrations against the internal standard. The yield of the two thiocyanate adducts (**12-SCN** + **12-NCS**) then can be obtained by a mass balance with the other two substitution products (alcohol (**12-OH**) and trifluoroethyl ether (**12-OCH₂CF₃**)). This is shown in Fig. 4.2.

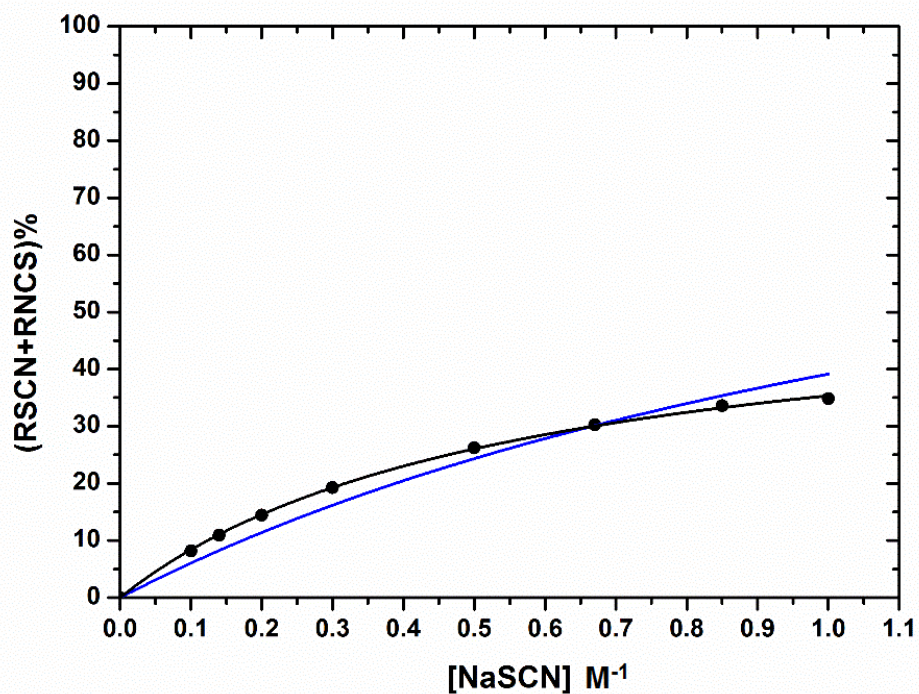


Figure 4.2. Black circles: percentage of **12-SCN** and **12-NCS** obtained as a proportion of total substitution products by mass balance relationship with different [NaSCN]. As the rate constant for loss of substrate does not vary significantly with [NaSCN], these products cannot form through a concerted reaction; they must form through the trapping of an intermediate (Schemes 4.1 and 4.2). Blue line: fitting Equation 13 to the data. Black line: fitting Equation 14 to the data.

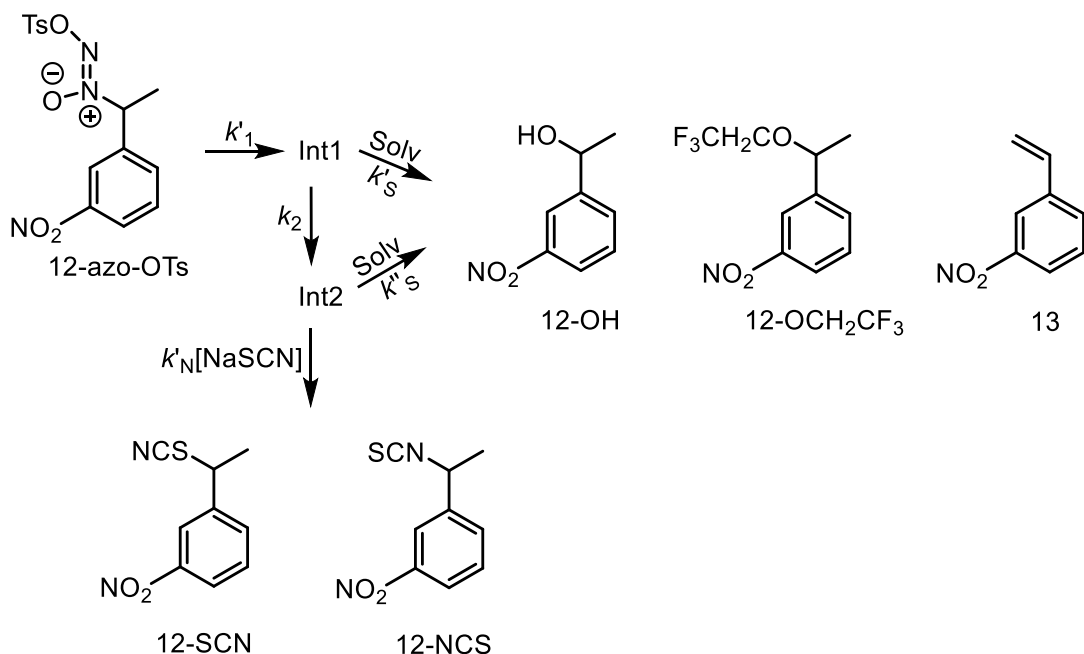
A single intermediate step-wise pathway (Scheme 4.3) leads to the relationship between the percentage of thiocyanate adducts (**12-SCN** + **12-NCS**) and [NaSCN] as shown in Equation 13.

$$\frac{[\mathbf{12-SCN}] + [\mathbf{12-NCS}]}{[\text{total substitution products}]} \times 100\% = \frac{k_N[\text{NaSCN}]}{(k_S + k_N[\text{NaSCN}])} \times 100\% \quad (13)$$

However, this leads to a blue line shown in Fig. 4.2, which does not fit the experimental data well, and thus does not support the mechanism shown in Scheme 4.1.

Note: This fitting method has been checked (See Chapter 4 Appendices P.186-189) for S_N2 (reaction of NaSCN with **12-OTs**) and S_N1 mechanisms (reaction of NaN₃ with benzhydryl chloride and analysis of reported data^{41b,57,72,73}). All these examples predicted 100% trapping when the nucleophile's concentration becomes infinite, indicating the trapping reagent can consume all the starting materials (for S_N2 mechanisms) or intermediates (for S_N1 mechanisms). Thus, the non-100% trapping shown in Fig. 4.2 tells us there are reactive intermediates that cannot be trapped by the strong nucleophiles even when their concentrations are high enough. However, there is an exception; see our succeeding discussions.

The non-100% trapping when [NaSCN] becomes infinite (where $k_N[\text{NaSCN}] \gg k_s$) can be explained if there is another intermediate that only reacts with solvent or rearranges to the second intermediate, but cannot react with NaSCN (Scheme 4.4). This scheme is also used as the preferred mechanism for benzyl azoxytosylates reported by Maskill and Jencks³².



Scheme 4.4. The step-wise solvolysis pathway of **12-azo-OTs** in 50% (v : v) TFE with two intermediates

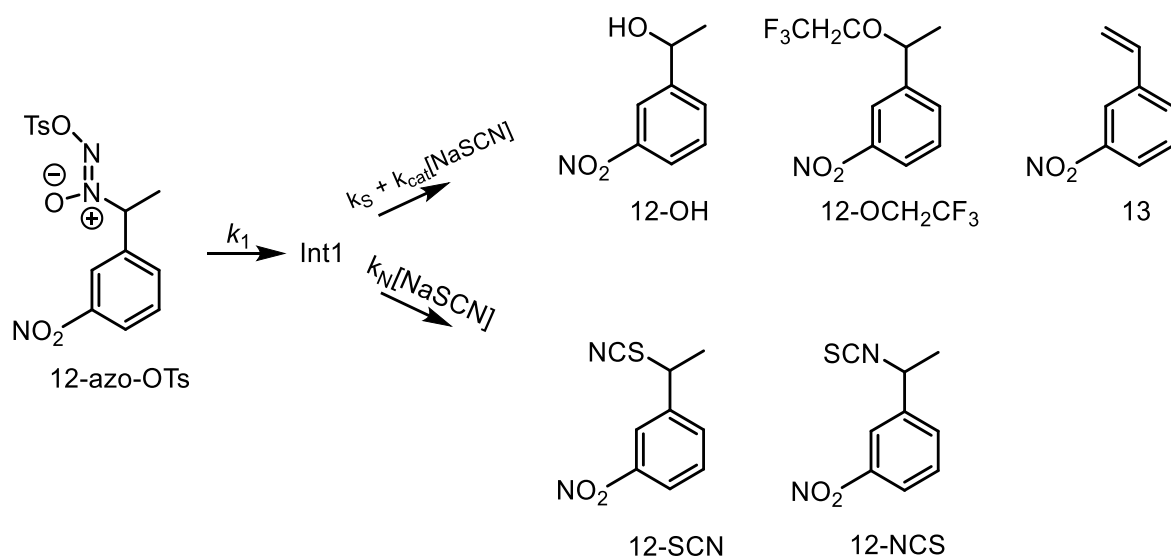
Scheme 4.4 leads to the relationship between the yield of thiocyanate adducts (**12-SCN** + **12-NCS**) and [NaSCN] shown in Equation 14.

$$\frac{[12 - \text{SCN}] + [12 - \text{NCS}]}{[\text{total substitution products}]} \times 100\% = \frac{k_2}{(k_2 + k'_s)} \frac{k'_N[\text{NaSCN}]}{(k''_s + k'_N[\text{NaSCN}])} \times 100\% \quad (14)$$

This leads to a black line shown in Fig. 4.2, which correlates far better than the single intermediate pathway (blue line in Fig. 4.2). The parameter $\frac{k_2}{(k_2 + k'_s)} = 0.55$ indicates that the trapping of intermediate 1 by the surrounding solvent is comparable with its rearrangement to intermediate 2 ($k_2 \approx 1.22k'_s$), which supports the proposed mechanism that intermediate 1 is kinetically visible but too reactive to wait until the diffusion of NaSCN into the solvent shell, namely, $(k_2 + k'_s) \gg 5 \times 10^9 \text{ s}^{-1}$.

Meanwhile, the curve fit also reveals that $\frac{k'_N}{k''_s} = 1.8 \text{ M}^{-1}$ for intermediate 2. If k'_N is assumed to be diffusion controlled ($5 \times 10^9 \text{ s}^{-1} \text{ M}^{-1}$), then k''_s can be estimated as $2.8 \times 10^9 \text{ s}^{-1}$.

An alternative interpretation is that the nucleophile trapping shown in Fig. 4.2 also could be interpreted by Scheme 4.5, where the reaction with NaSCN does not give only **12-SCN** and **12-NCS**, *i.e.* NaSCN acts as a general base to catalyse solvent attack on the intermediate as well as acting as a nucleophile⁷⁴.



Scheme 4.5. The step-wise solvolysis pathway of **12-azo-OTs** in 50% (v : v) TFE with a single intermediate, but catalysed by NaSCN as a base

However, two experimental observations suggest that this is unlikely. The first one is the trapping analysis of **12-OTs** (Fig. 4.3).

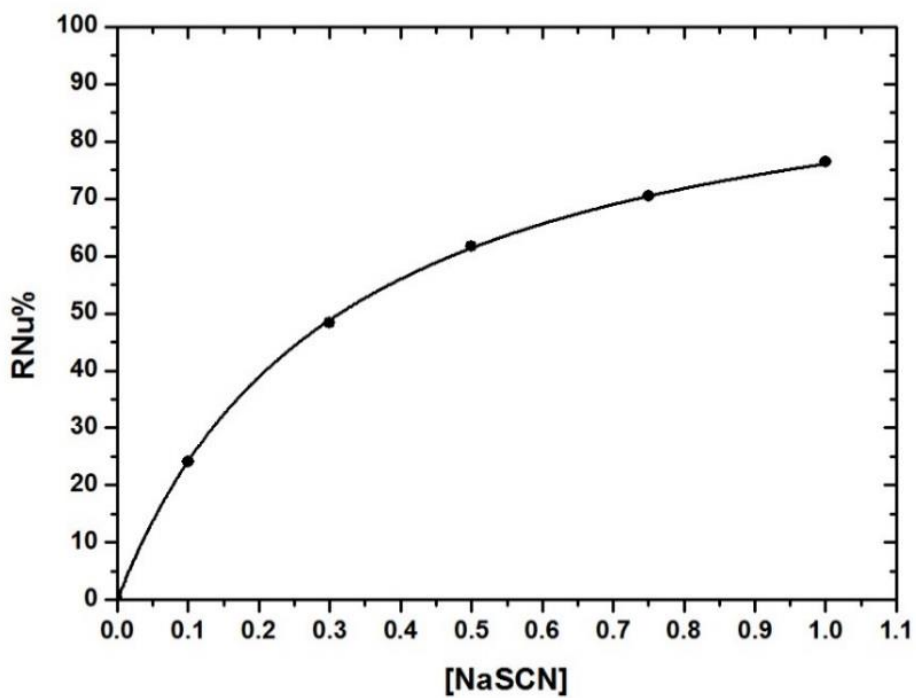
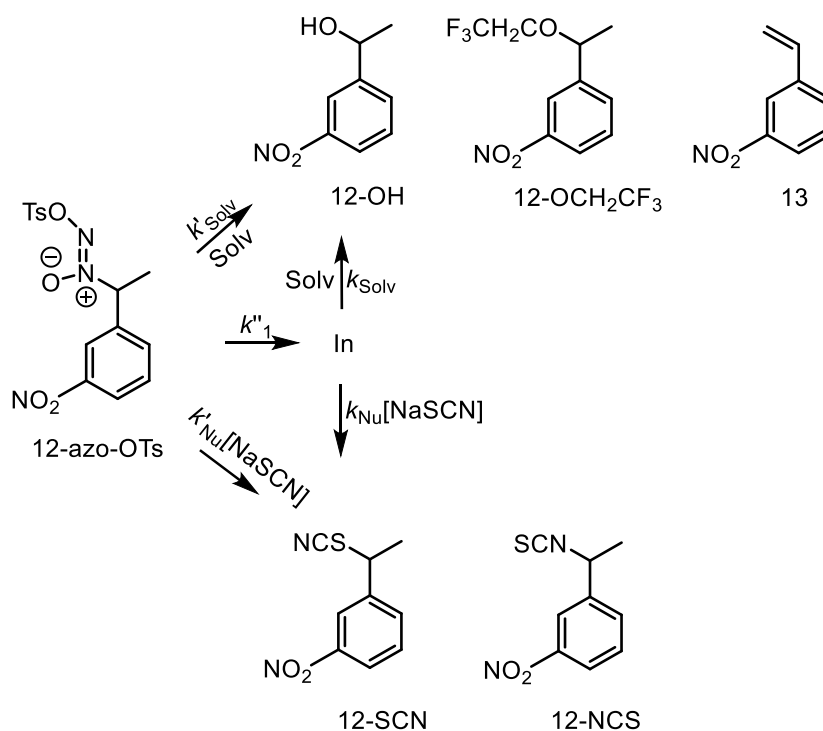


Figure 4.3. Trapping adducts yield with different [NaSCN] when solvolysing **12-OTs** in 50% (v : v) TFE, the black line was fitted by Equation 1 of an S_N2 mechanism

While in the presence of 1 M NaSCN, the B_{AC} hydrolysis pathway was invisible, indicating 1 M NaSCN is much less basic than 3 mM 2,6-di-*tert*-butylpyridine and very unlikely to act as a general base for solvent attack on the carbon centre. Therefore, the lack of complete substitution by NaSCN is unlikely to be explained by a competing base role. The two intermediate mechanism shown in Scheme 4.4 is more credible.

Although the mechanism proposed in Scheme 4.4 seems reasonable, there is still an exception that can give an ‘observed non-100% trapping correlation’ shown in Fig. 4.2, but only with one intermediate. If the reaction took place as a combination of S_N1 (with single intermediate) and pre-association uncoupled concerted pathways, where the pre-association pathway involved with NaSCN is not significant at low concentrations, the observed non-100% correlation up to 1 to 2 M NaSCN still can be achieved. This mechanism is shown in Scheme 4.7.



Scheme 4.7. The step-wise and pre-association pathways of **12-azo-OTs** in 50% (v : v) TFE with a single intermediate

The mechanism shown in Scheme 4.7 leads to the relationship between the percentage of thiocyanate adducts (**12-SCN** + **12-NCS**) and [NaSCN] as described in Equation 15.

$$\begin{aligned}
 & \frac{[12 - \text{SCN}] + [12 - \text{NCS}]}{[\text{total substitution products}]} \times 100\% \\
 &= \frac{[\text{NaSCN}]}{\frac{(k'_{\text{solv}} + k''_1)}{k'_{\text{Nu}}} + [\text{NaSCN}]} \times 100\% \\
 &+ \frac{[\text{NaSCN}]}{\left(\frac{k_{\text{solv}}}{k_{\text{Nu}}} + [\text{NaSCN}]\right) \left(\frac{k'_{\text{solv}} + k''_1 + k'_{\text{Nu}}[\text{NaSCN}]}{k''_1}\right)} \times 100\% \quad (15)
 \end{aligned}$$

Fitting Equation 15 leads to the black line shown in Fig. 4.4, and has no difference with the correlation in Fig. 4.2. The parameter $\frac{k_{\text{solv}}}{k_{\text{Nu}}}$ is still 0.55 M^{-1} for the trappable intermediate, while $k'_{\text{solv}} = k''_1 = 10k'_{\text{Nu}}$ for solvent pre-organization, ionization and NaSCN pre-association pathways. Since it is a weak pre-association, an assumption that $k'_{\text{Nu}} = Kk''_1$ will be reasonable. This indicates that the pre-association constant for NaSCN and the substrate is about 0.1 M^{-1} , which agrees well with other similar reports^{35,75}.

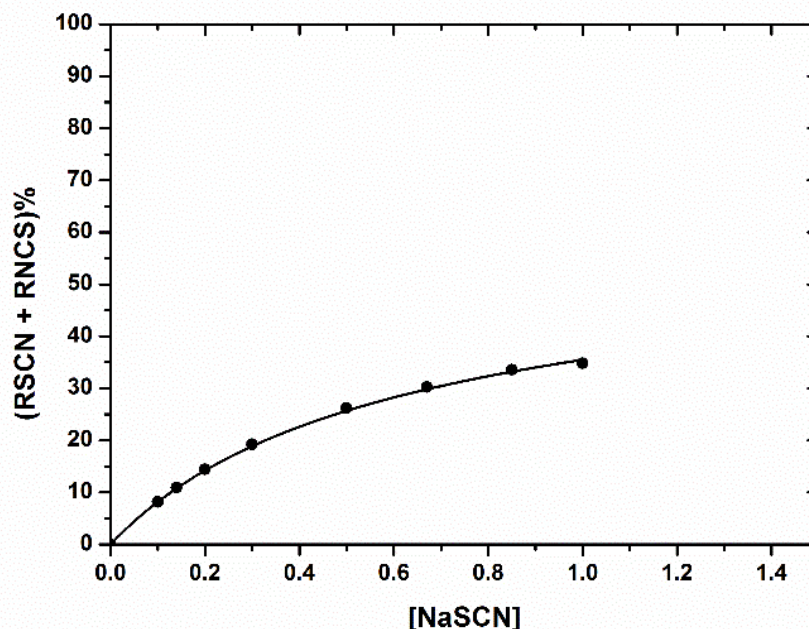
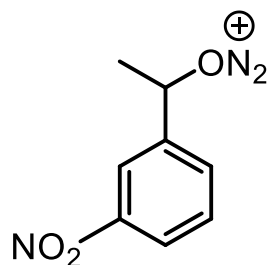


Figure 4.4. Black circles: percentage of substitution products (**12-SCN** and **12-NCS**) obtained by mass balance relationship with different [NaSCN]. Black line: fitting Equation 15 to the data.

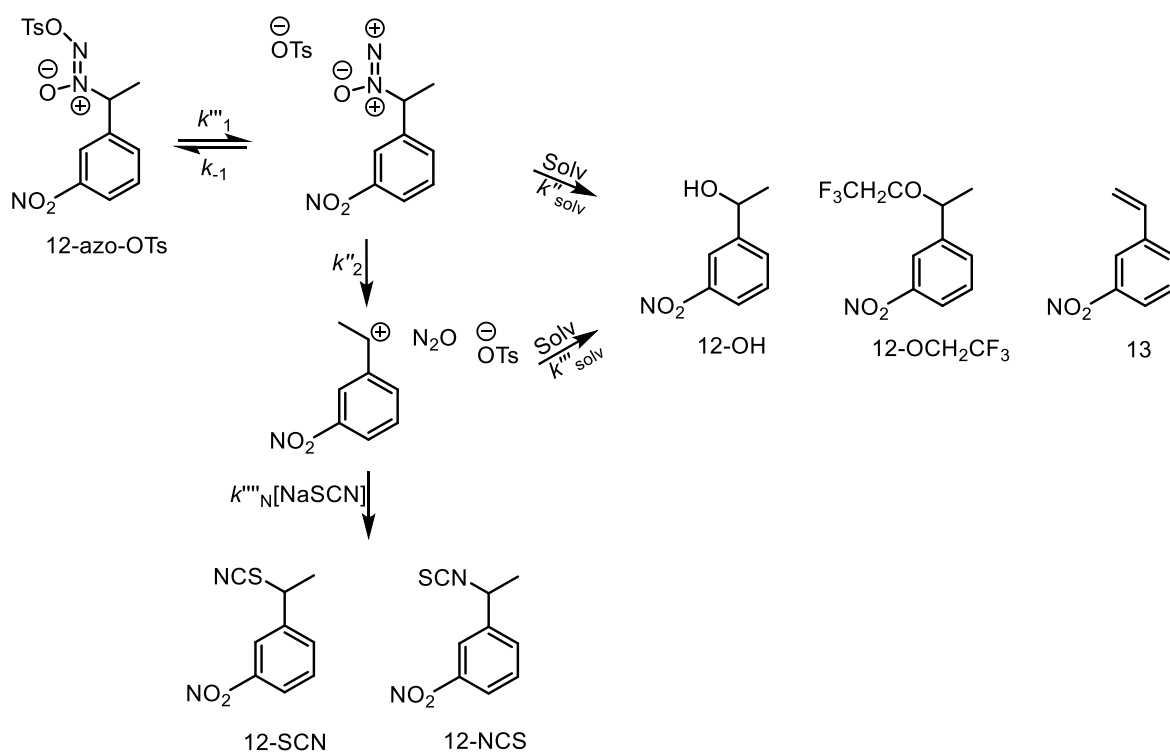
Therefore, the observed ‘non-100%’ trapping curve does not only indicate a step-wise pathway with two different intermediates. A step-wise pathway with a single intermediate accompanied by a pre-association mechanism can also account for the observed results satisfactorily.

In order to gain more information about the structure of intermediate 2 in Scheme 4.4 or the intermediate in Scheme 4.7, we have analysed the product selectivity of **12-OTs** under the same conditions (Scheme 4.8). The tosylate showed $\frac{k_N'''}{k_S'''} = 3.2 \text{ M}^{-1}$ (Fig. 4.3) compared to 0.55 M^{-1} for the trappable intermediate of **12-azo-OTs**. The ratio $\frac{[12\text{-SCN}]}{[12\text{-NCS}]} = 5.1$ is far larger than that obtained from the azoxytosylate (3.5) and the ratio $\frac{[12\text{-OH}]}{[12\text{-OCH}_2\text{CF}_3]} = 3.0$ is also larger than that obtained from the azoxytosylate (2.3). All these data indicate that the



Scheme 4.9. The proposed trappable intermediate of solvolysis of **12-azo-OTs** in 50% (v : v) TFE

White *et al.*⁷⁶ suggested an alternative mechanism (Scheme 4.10) which is consistent with all the observations as well.

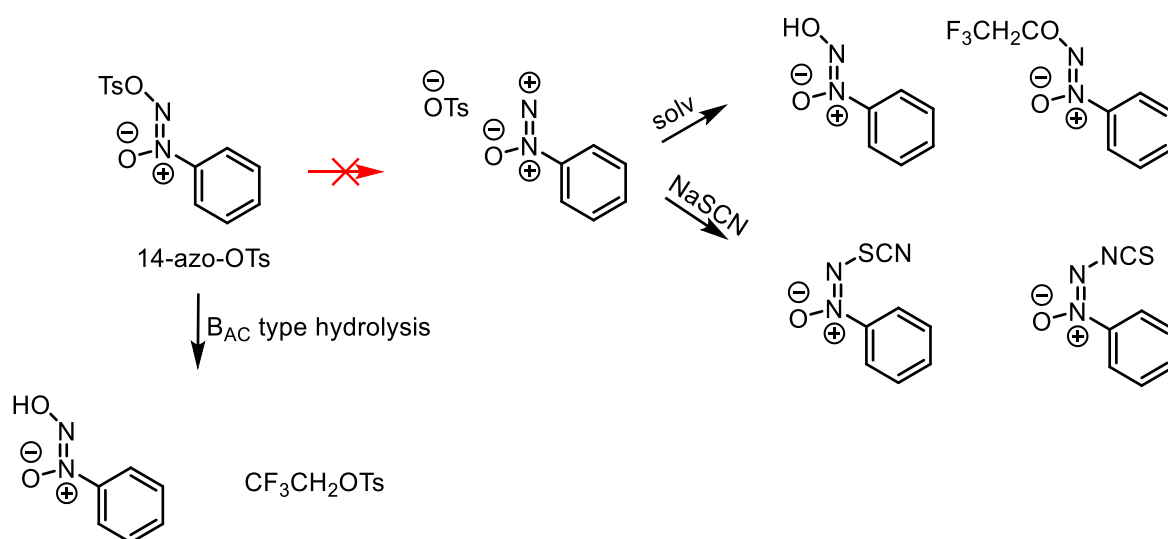


Scheme 4.10. An alternative step-wise mechanism of **12-azo-OTs** with two intermediates in 50% (v : v) TFE

One initial argument against this mechanism is the localized selectivity-reactivity principle. Regarding the α -methyl benzyl carbon centre, intermediate 1 will be more stable and less reactive than intermediate 2. However, our results indicate that intermediate 1 needs to be

more reactive and cannot be trapped by strong nucleophiles. Thus, at the first glance, the proposed mechanism by White *et al.* does not seem consistent with our observations.

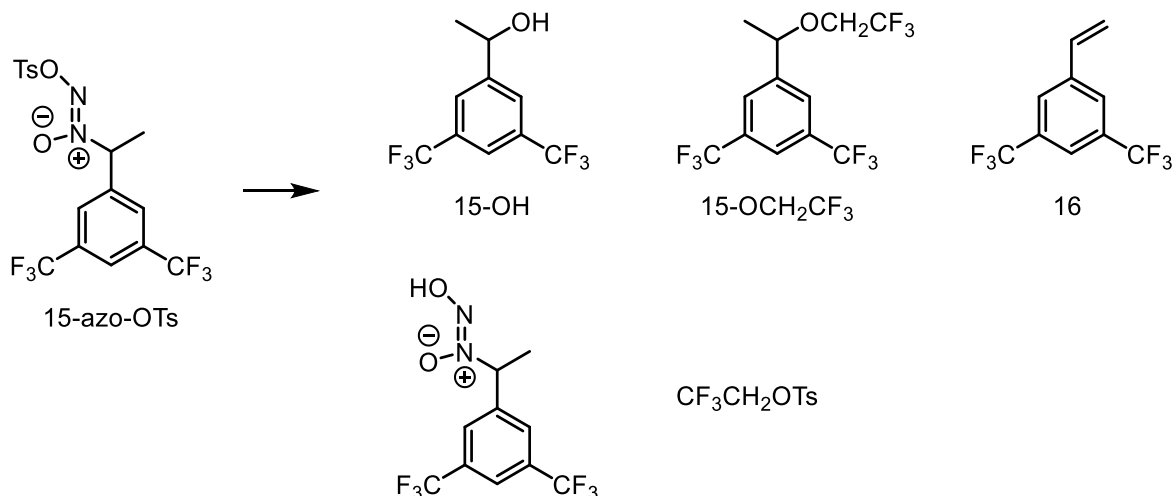
Furthermore, by studying the solvolysis reaction of phenyl azoxytosylate (**14-azo-OTs**) in 50% (v : v) TFE under the same conditions (Scheme 4.11), we cast further doubt on Scheme 4.10.



Scheme 4.11. The solvolysis of **14-azo-OTs** in 50% (v : v) TFE

TsO⁻ could not be detected in our HPLC analysis. However, after 3 days, no phenol or other products from trapping ‘phenyl cation’ could be detected. The only two products were from S-O bond cleavage (B_{AC} type hydrolysis), giving trifluoroethyl tosylate as well as N-nitrosophenyl hydroxylamine. Additionally, in the presence of 1 M NaSCN, no new products could be detected. Thus, this observation further rules out the possible mechanism shown in Scheme 4.10.

Finally, we studied the solvolysis of **15-azo-OTs** in 50% (v : v) TFE (Scheme 4.12) under the same conditions.



Scheme 4.12. The solvolysis of **15-azo-OTs** in 50% (v : v) TFE

The solvolysis rate constant of **15-azo-OTs** is $5.2 \pm 0.2 \times 10^{-6} \text{ s}^{-1}$. The products showed that there was significant S-O cleavage, even when the reaction was not buffered with non-nucleophilic bases. In the presence of 1 M NaSCN, a 36% rate acceleration was observed and more S-O bond cleavage products were obtained. These results showed there was significant S-O cleavage as well as some S_N2 contribution, which now can compete with the slow S_N1 mechanism.

Thus, if White's mechanism is correct, the solvolysis rate expression of the S_N1

contribution in Scheme 4.10 will be $\frac{k_1'''(k_2''+k''_{\text{solv}})}{k_2''+k''_{\text{solv}}+k_{-1}}$ and we should expect very similar rate

constants of k_1''' and k_{-1} for both **12-azo-OTs** and **15-azo-OTs** (since N-O bond cleavage is far from the 1-aryl ethyl group). If we take 50% solvolysis reactions for **15-azo-OTs** as S_N1 into consideration, then $k_{-1} > 10(k_1''' + k''_{\text{solv}})$ can be obtained for **15-azo-OTs**,

indicating that the formation of the first intermediate is highly reversible. However, 2-adamantyl ^{18}O -azoxytosylate solvolyses with a similar rate constant under the same conditions but does not scramble the isotope position in the substrate (personal communication from Maskill⁷⁷), indicating the first ionization step was irreversible, and so the proposed mechanism in Scheme 4.10 is not viable.

Therefore, the mechanism is described as a step-wise mechanism as shown in Scheme 4.4, with an ion-pair ($\text{R}^+\cdot\text{N}_2\text{O}\cdot\text{OTs}^-$) as the logical structure for the non-trappable intermediate. And the trappable intermediate's structure is most likely to be the rearranged azoxy cation RON_2^+ as Maskill *et al.* described³². There is also supportive evidence for RON_2^+ from both experimental⁷⁸ and computational⁷⁹ work. Olah *et al.*⁷⁸ managed to prepare methyl azoxy cation (MeON_2^+) via different precursors, which supports our proposed structure for intermediate 2. On the other hand, Maskill *et al.*⁷⁹ also demonstrated that the oxygen bonded azoxy cation is the most stable species among all the azoxy cation isomers, based on MP4(SDQ)/6-311G(d,p)//MP2(fc)/6-31G(d,p) and G3 level calculations.

Alternatively, the solvolysis mechanism can be described as a step-wise pathway with a single intermediate (RON_2^+) accompanied by an uncoupled concerted pre-association pathway. This can be expected if the ion-pair's ($\text{R}^+\cdot\text{N}_2\text{O}\cdot\text{OTs}^-$) collapse has no barrier, so the formation of $\text{R}^+\cdot\text{N}_2\text{O}\cdot\text{OTs}^-$ and the rotation of N_2O are coupled into one single step. In addition, the solvent trapping of $\text{R}^+\cdot\text{N}_2\text{O}\cdot\text{OTs}^-$ will be shifted to an uncoupled concerted pre-association pathway. In an uncoupled concerted reaction, a weak pre-association between strong nucleophiles and the substrates needs to be taken into account. If the pre-association constant is about 0.1 M^{-1} , this mechanism is consistent with the data.

4.4 Conclusion

By using a thiocyanate trapping method we have identified that there might be two types intermediates with different reactivity involved in the solvolysis of 1-(3-nitrophenyl)ethyl azoxytosylate. Our observations suggest that the first non-trappable intermediate can be regarded as a tight ion-pair, which can only be trapped by the surrounding solvent shell or rearrange to the second intermediate. The trappable intermediate is not the corresponding tosylate, and is probably the rearranged azoxy cation³², which can be trapped by solvent as well as strong nucleophiles. All the results are consistent with previous reports for benzyl azoxytosylate, including the mechanism³².

Alternatively, the results can be interpreted as a combination of an S_N1 pathway with a single intermediate accompanied by pre-association uncoupled concerted pathways. This mechanism will still give a trapping curve that does not react 100% at moderately high NaSCN concentrations but is consistent with the proposal that the ion-pair (R⁺·N₂O·OTs⁻) is too reactive to be an intermediate. All the steps involved with this ion-pair now will be coupled into concerted processes as shown in Scheme 4.7.

Thus, we suggest that the 1-(3-nitrophenyl)ethyl cation may well be formed during the first ionization step as a tight ion-pair, which will undergo a fast rearrangement or be trapped by its surrounding solvents. Alternatively, the ion-pair can be omitted, the solvolysis will directly form the trappable azoxy cation (not the corresponding tosylate) by a concerted fragmentation and suffer from uncoupled concerted substitutions from both solvents and strong nucleophiles. Further confirmation shows that compared with tosylates, azoxytosylates seem to be less reactive and experience less nucleophilic assistance from the

solvent. Therefore, different precursors may suffer different nucleophilic assistance upon solvolysis. However, changing to a poorer nucleofuge that alters the solvolysis in the opposite direction (*i.e.* leading to less nucleophilic assistance) is not well-known, so finally we wish to address that changing from tosylates to azoxytosylates reduces the solvent participation even for benzyl and electro-deficient 1-aryl ethyl systems. This is highly likely due to the different intrinsic barriers between those nucleofuges. A similar observation of different reactivity between sp^2 and sp hybridized carbenium ions that has been attributed to differing intrinsic barriers has been reported by Mayr *et al*⁸⁰.

Chapter 5: The solvolysis mechanism of simple tertiary substrates in 50% (v : v) TFE

5.1 Introduction

The solvolysis mechanism of tert-butyl substrates has been introduced as following one of the most well-known pathways: S_N1 ,^{34b} which displays first-order kinetics. However, S_N1 reactions still cover a range of various mechanistic details.

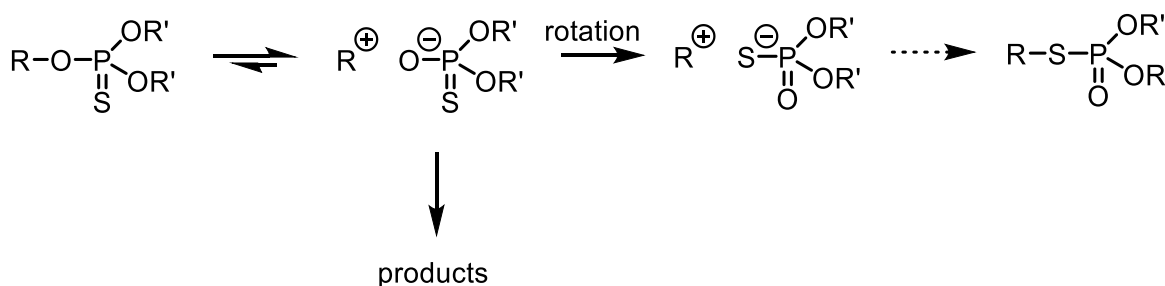
For Ph_3C-X ,⁸⁶ the solvolysis mechanism has been identified as one extreme of S_N1 pathways because Ph_3C^+ is stabilized by significant charge delocalization, thus it is fully equilibrated as a long-lived free cation when generated in solvents, and can be trapped by nucleophiles outside the solvent shell⁸⁶.

On the other hand, Me_3C^+ , lacks such charge delocalization, and the solvolysis mechanism of Me_3C-X still has been subject to debate. Some argue that tert-butyl cations react with solvents within the ion-pair before diffusion apart occurs⁸⁷. Recently, Toteva and Richard³⁵ reported that by extrapolating the linear correlation (Equation 16) of first-order rate constants (k_s) of solvent attack on stable aryl cumyl cations with the solvolysis rates of corresponding chlorides (k_{solv}) in 50% (v : v) TFE, the intrinsic bond formation rate constant (k_s) for capturing the tert-butyl cations in 50% (v : v) TFE is approximately $10^{12} s^{-1}$. Since $10^{12} s^{-1}$ is larger than the solvent reorganization rate constant ($10^{11} s^{-1}$)^{15,35}, then this supported a solvent reorganization dominated step-wise mechanism for solvolytic substitution of simple tertiary substrates. However, the elimination mechanism was suggested as a concerted intramolecular E_i mechanism.

$$\log k_S = -0.53 \log k_{\text{solv}} + 10.6 \quad (16)$$

Isotope exchange between the ether and acyl positions of ester-type nucleofuges has been used as a classical tool to address whether ion-pair formation is possible. Besides ^{18}O labelling⁴¹, thionoesters are another useful nucleofuge family that can provide additional information on ion-pair formation^{27,28}. Among these, thionophosphates whose reactivity is comparable to that of chlorides are particularly suitable to address this issue²⁷.

Replacement of an oxygen by sulfur at the acyl position perturbs the structure as well as the reactivity of thionophosphates. The sulfur atoms at acyl positions in thionoesters are much more nucleophilic than oxygens^{27,28}. The high nucleophilicity of sulfur anions (thiolo anion) means that there is a barrierless combination of the rearranged ion-pair (*i.e.* if the cation's lifetime in 50% TFE is shorter than 100 ns)²⁸, and so the process of rearrangement is dominated by anion exchange (Scheme 5.1). If the rate constant for anion exchange can be measured, this rearrangement will provide an internal clock that can be used to estimate the lifetime of carbenium ion intermediates. For ^{18}O labelling, the lifetime of carbenium ion intermediates cannot be obtained unless the ion-pair recombination rate constant is known, which is very difficult to measure^{41a}.



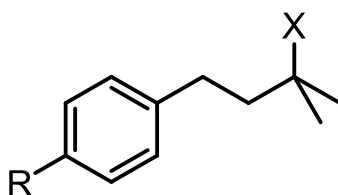
Scheme 5.1. Thiono-thiolo rearrangement of thionophosphates in a step-wise pathway

Additionally, the thiono-thiolo rearrangement product is far more stable than the corresponding thionophosphate due to the lower nucleofugality of thiolo leaving groups^{27,28}, which makes the rearranged product easier to detect by HPLC or ³¹P NMR as it can accumulate (whereas isotopomers continue react at essentially the same rate as the initial substrate).

Therefore, thiono-thiolo rearrangement of thionophosphates during solvolysis is of great advantage compared with isotope exchange by ¹⁸O labelling.

Since the dynamic behaviour of simple tertiary cations (*i.e.* whether it can be generated in 50% (v : v) TFE or not) is still ambiguous and no isotope exchange of non-equivalent oxygens at esters or thiono-thiolo rearrangement of thionophosphates has been reported (except in a 1-adamantyl system²⁶), we wish to revisit this issue to confirm the details of how a simple tertiary substrate behaves when exposed to solvolysis in 50% (v : v) TFE.

We chose a 1-aryl-3-methyl-3-butyl system as a model for simple tertiary structures because the aryl group provides a chromophore, so that all the products could be detected by HPLC,⁴ and with only a very weak electron-withdrawing effect (no neighbouring group participation).



R = OMe or H

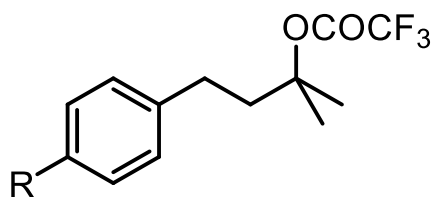
X = Cl, Br, OCOCF₃, SMe₂⁺ or OPS(OEt)₂

5.2 Experimental Section

General

All the chemicals were purchased from Sigma-Aldrich, Alfa Aesar or Acros Organics; those for synthesis purposes were used directly without further purification. TFE was distilled from P₂O₅ and stored over 4Å molecular sieves. UHQ water was obtained from an ELGA PURELAB Option S-R 7-15 system. ¹H NMR and ¹³C NMR spectra were recorded on Bruker AV-HD 400 and AV-HD 500 instruments. HPLC analysis was carried out on Waters 2690 (486 Tunable Absorbance Detector) and 2695 (2487 Dual λ Absorbance Detector) systems with a Hichrom HIRPB-624 C₁₈ column (3.5 μm × 250 mm) and UV detection at 261 nm (1-phenyl-3-methyl-3-butyl substrates) or 277 nm (1-(4-methoxyphenyl)-3-methyl-3-butyl substrates and 1-adamantyl diarylthionophosphate). A gradient elution was used, changing from 95% water and 5% acetonitrile to 5% water and 95% acetonitrile over 20 mins followed by a further 10 mins of the final eluent mixture. Product analysis by GC was determined with a Perkin Elmer ARNEL Auto System XL GC model on Zebron™ ZB-624 GC Column (30 m × 0.32 mm × 1.80 μm). The program started from 50 °C, 6 °C/min to 140 °C (holding for 5 mins) and 45 °C/min to 220 °C (holding for another 9 mins) with a split ratio 20 : 1 for 2-Chloro-2-methylnonane solvolysis; from 70 °C, 10 °C/min to 220 °C (holding for 15 mins) with a split ratio 20 : 1 for 1-(4-methoxyphenyl)-3-methyl-3-butyl chloride and 1-adamantyl bromide solvolysis. Product analysis by chiral GC for (S)-3,7-dimethyl-3-octyl trifluoroacetate solvolysis was determined with the same GC model on β-DEX™ 120 column (30 m × 0.25 mm × 0.25 μm). The program started from 40 °C, 5 °C/min to 140 °C and 45 °C/min to 220 °C (holding for 9 mins) with a split ratio 20 : 1.

Syntheses



17-OCOCF₃, R = OMe

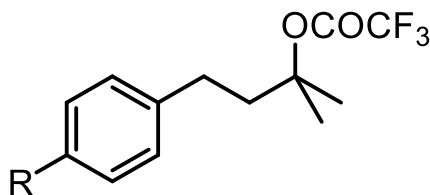
1-(4-Methoxyphenyl)-3-methyl-3-butyl trifluoroacetate (17-OCOCF₃, R = OMe): 1.70 mL 4-(4-methoxyphenyl)-2-butanone (10 mmol) were introduced to an ice-cooled 100 mL round-bottom flask charged with 35 mL anhydrous diethyl ether and a magnetic stirrer bar with stirring. 7 mL of 3 M methylmagnesium bromide solution in diethyl ether (21 mmol) were then added dropwise within 15 mins; after that, the ice bath was removed and the mixture was stirred at RT for further 2 hours. Then ice bath was placed again and 50 mL saturated ammonium chloride solution were introduced slowly to quench the reaction. The ether phase was separated and washed with saturated aqueous NaHCO₃. Aqueous phase was extracted with diethyl ether (4 × 20 mL) and the organic phases were combined and dried over Na₂SO₄. Evaporating the solvent afforded 1.36g 1-(4-methoxyphenyl)-3-methyl-3-butanol (**17-OH, R = OMe**)^{35,102} as a light yellow oil (70%).

¹H NMR (400 MHz, CDCl₃): 7.15 (2H, d, J = 8.7 Hz), 6.86 (2H, d, J = 8.7 Hz), 3.81 (3H, s), 2.70-2.65 (2H, m), 1.81-1.77 (2H, m) and 1.31 (6H, s). ¹³C NMR (100 MHz, CDCl₃): 157.8, 134.7, 129.2, 113.9, 70.9, 55.3, 45.9, 29.8 and 29.3.

The crude **17-OH, R = OMe** was used directly for trifluoroacetate synthesis, using the method reported by Shenvi *et al.*¹⁰³ 0.97 g **17-OH, R = OMe** (5 mmol) and 1.21 mL of pyridine (15 mmol) were added in a 100 mL round flask followed by 30 mL DCM at 0 °C, then 1.41 mL trifluoroacetic anhydride (10 mmol) were introduced dropwise within 10

mins, and the reaction mixture was allowed to warm to RT and stirred for 2 hours before evaporation of the solvent. The residue was directly purified by silica gel chromatography, using 5% EtOAc-95% Petroleum to afford 0.94 g **17-OCOCF₃**, **R = OMe** as a light yellow oil (65%). TLC and HPLC both showed only one compound.

¹H NMR (400 MHz, CDCl₃): 7.12 (2H, d, J = 8.6 Hz), 6.86 (2H, d, J = 8.6 Hz), 3.81 (3H, s), 2.66-2.62 (2H, m), 2.16-2.12 (2H, m) and 1.63 (6H, s). ¹³C NMR (100 MHz, CDCl₃): 158.0, 156.2 (q, J = 41.2 Hz), 133.1, 129.2, 114.0, 114.4 (q, J = 287.0 Hz), 88.9, 55.3, 42.6, 29.2 and 25.6.



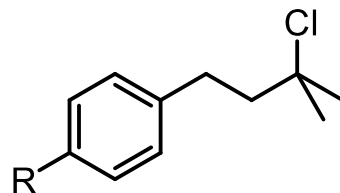
17-OCOCF₃, **R = H**

1-Phenyl-3-methyl-3-butyl trifluoroacetate (17-OCOCF₃, R = H): Commercially available 1-phenyl-3-methyl-3-butanol (**17-OH, R = H**) was used and the method was the same as described in synthesis of **17-OCOCF₃, R = OMe**. TLC and HPLC both showed only one compound.

¹H NMR (400 MHz, CDCl₃): 7.35-7.31 (2H, m), 7.26-7.21 (3H, m), 2.73-2.69 (2H, m), 2.21-2.16 (2H, m) and 1.66 (6H, s). ¹³C NMR (100 MHz, CDCl₃): 156.2 (q, J = 41.2 Hz), 141.1, 128.5, 128.3, 126.1, 114.5 (q, J = 287.0 Hz), 88.7, 42.4, 30.1 and 25.6.

1-Phenyl-3-methyl-3-butyl chloride (bromide): According to the method reported by Cook *et al.*¹⁰² 0.82 g **17-OH, R = H** (5 mmol) and 0.42 g lithium chloride (or 0.87 g lithium bromide) (10 mmol) were added to a 100 mL round bottom flask with a magnetic stirrer bar in an ice-water bath. 30 mL 10 M HCl (or 8 M HBr) were added dropwise within 10 mins,

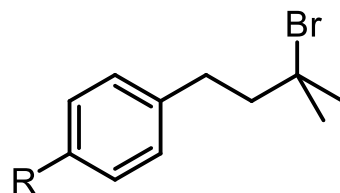
and the mixture was allowed to warm to RT and stirred overnight before quenching with 30 mL cold water and 30 mL diethyl ether. The ether phase was separated and the aqueous phase was extracted with diethyl ether (4 × 20 mL). The combined organic phases were washed with saturated NaHCO₃ and dried over Na₂SO₄. After evaporation of the solvent, the residue was directly purified by silica gel chromatography, using 5% diethyl ether-95% Petroleum, 0.36 g **17-Cl**, **R = H** (40%) and 0.17 g **17-Br**, **R = H** (15%) were obtained as light yellow oils.



17-Cl, **R = H**

1-Phenyl-3-methyl-3-butyl chloride (17-Cl, R = H)¹⁰⁴: ¹H NMR (400 MHz, CDCl₃):

7.36-7.32 (2H, m), 7.26-7.21 (3H, m), 2.89-2.84 (2H, m), 2.11-2.06 (2H, m) and 1.69 (6H, s). ¹³C NMR (100 MHz, CDCl₃): 141.8, 128.4, 128.3, 125.9, 70.5, 48.0, 32.5 and 31.7.

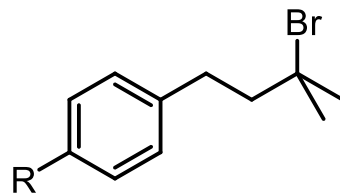


17-Br, **R = H**

1-Phenyl-3-methyl-3-butyl bromide (17-Br, R = H)¹⁰⁵: ¹H NMR (400 MHz, CDCl₃):

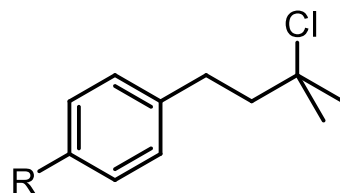
7.37-7.33 (2H, m), 7.27-7.23 (3H, m), 2.93-2.88 (2H, m), 2.16-2.01 (2H, m) and 1.88 (6H, s). ¹³C NMR (100 MHz, CDCl₃): 141.6, 128.5, 128.5, 126.0, 67.6, 49.5, 34.3 and 32.9.

1-(4-Methoxyphenyl)-3-methyl-3-butyl chloride (bromide): They were synthesized from 1-OH, R = OMe by the procedure shown above.



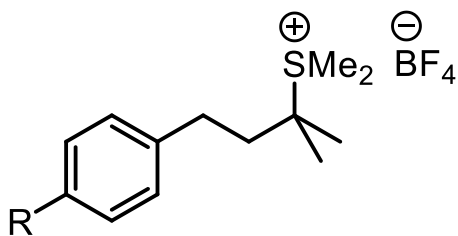
17-Br, R = OMe

1-(4-Methoxyphenyl)-3-methyl-3-butyl bromide (17-Br, R = OMe)^{102,106}: ¹H NMR (400 MHz, CDCl₃): 7.17 (2H, d, J = 8.6 Hz), 6.88 (2H, d, J = 8.6 Hz), 3.83 (3H, s), 2.86-2.82 (2H, m), 2.12-2.08 (2H, m) and 1.86 (6H, s). ¹³C NMR (100 MHz, CDCl₃): 157.9, 133.6, 129.3, 113.9, 67.6, 55.3, 49.7, 34.3 and 32.0.



17-Cl, R = OMe

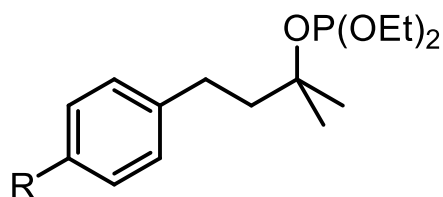
1-(4-Methoxyphenyl)-3-methyl-3-butyl chloride (17-Cl, R = OMe)^{35,102}: ¹H NMR (400 MHz, CDCl₃): 7.16 (2H, d, J = 8.6 Hz), 6.87 (2H, d, J = 8.6 Hz), 3.82 (3H, s), 2.82-2.78 (2H, m), 2.07-2.03 (2H, m) and 1.67 (6H, s). ¹³C NMR (100 MHz, CDCl₃): 157.9, 133.8, 129.3, 113.9, 70.6, 55.3, 48.2, 32.5 and 30.7.



17-SMe₂⁺, R = OMe

1-(4-Methoxyphenyl)-3-methyl-3-butyl dimethylsulfonium tetrafluoroborate (17-SMe₂⁺, R = OMe): According to a literature method reported by Schmitz *et al.*¹⁰⁷ 0.97 g **17-OH**, R = OMe (5 mmol) and 0.44 mL dimethyl sulfide (6 mmol) were added in a 25 mL round flask followed by 10 mL DCM at 0 °C, then 0.75 mL tetrafluoroboric acid-diethyl ether complex (5.5 mmol) were introduced dropwise within 10 mins, and the reaction mixture was allowed to warm to RT and stirred for 2 hours before evaporating the solvent. The residue was directly triturated in cold diethyl ether; the crystalized solid was collected by filtration and dried under N₂. The crude product was purified by silica gel chromatography, using acetonitrile to afford 0.65 g **17-SMe₂⁺**, R = OMe as a white solid (40%). TLC showed only one spot.

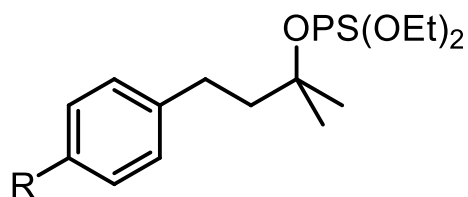
¹H NMR (400 MHz, CD₃CN): 7.21 (2H, d, J = 8.7 Hz), 6.90 (2H, d, J = 8.7 Hz), 3.78 (3H, s), 2.74-2.69 (2H, m), 2.73 (6H, s), 2.06-2.01 (2H, m) and 1.56 (6H, s). ¹⁹F NMR (376 MHz, CD₃CN): -152.0. ¹³C NMR (100 MHz, CD₃CN): 158.0, 131.9, 129.2, 113.6, 57.6, 54.6, 38.8, 28.1, 20.8 and 19.1.



17-OP(OEt)₂, R = H

1-Phenyl-3-methyl-3-butyl diethyl phosphite (17-OP(OEt)₂, R = H): To a stirred solution of 0.82 g **17-OH**, R = H (5 mmol) in 4 mL dry THF at -20 °C were added 3.2 mL 1.6 M n-butyllithium solution in hexane (5.1 mmol) dropwise. The solution at -20 °C was stirred for 1 hour before transfer to a solution of 0.8 g diethyl chlorophosphite in 10 mL dry THF at 0 °C dropwise. The resulting solution was stirred at RT overnight before being concentrated under vacuum. To the residue was added cold diethyl ether and filtered, the fine solid was washed with cold diethyl ether and the combined ether solution was concentrated under vacuum to afford 1.25 g crude **17-OP(OEt)₂**, R = H as a light-yellow oil (88%). Due to the severe instability on silica and neutral alumina, chromatography purification was avoided. TLC showed one movable spot (1 : 9 diethyl ether / hexane) and one faint spot on baseline.

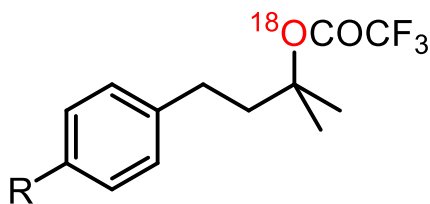
¹H NMR (400 MHz, CDCl₃): 7.34-7.29 (2H, m), 7.26-7.19 (3H, m), 3.93-3.88 (4H, m), 2.83-2.73 (2H, m), 2.01-1.93 (2H, m), 1.50 (6H, s) and 1.31 (6H, t, J = 7 Hz). ³¹P NMR (162 MHz, CDCl₃): 134.9. ¹³C NMR (100 MHz, CDCl₃): 142.5, 128.4, 128.4, 125.7, 77.7 (d, J = 7.9 Hz), 57.1 (d, J = 8.7 Hz), 45.8 (d, J = 5.1 Hz), 30.5, 29.0 (d, J = 9.8 Hz) and 16.9 (d, J = 4.7 Hz).



17-OPS(OEt)₂, R = H

1-Phenyl-3-methyl-3-butyl diethyl thionophosphate (17-OPS(OEt)₂, R = H): To a solution of 256 mg sulfur (8 mmol) in 13 mL dry THF at 25 °C were added 1.25 g crude **17-OP(OEt)₂, R = H** in one portion. The solution under nitrogen was stirred at 25 °C overnight before being concentrated. The residue was dissolved in a small amount of diethyl ether and the solution was filtered to remove excess sulfur. The ether solution was concentrated and the residue was filtered on a short pad of silica, using 60% DCM-40% Petroleum. The filtrate was concentrated to afford 633 mg of **17-OPS(OEt)₂, R = H** as a light-yellow oil (45%). HPLC showed the small impurity peaks were not solvolysis products.

¹H NMR (400 MHz, CDCl₃): 7.33-7.28 (2H, m), 7.26-7.19 (3H, m), 4.20-4.10 (4H, m), 2.80-2.74 (2H, m), 2.10-2.04 (2H, m), 1.62 (6H, s) and 1.36 (6H, t, J = 7.1 Hz). ³¹P NMR (162 MHz, CDCl₃): 59.0. ¹³C NMR (100 MHz, CDCl₃): 142.0, 128.4, 128.4, 125.9, 86.3 (d, J = 9.2 Hz), 63.9 (d, J = 5.8 Hz), 44.8 (d, J = 5.1 Hz), 30.4, 27.6 (d, J = 3.4 Hz) and 16.0 (d, J = 7.7 Hz).

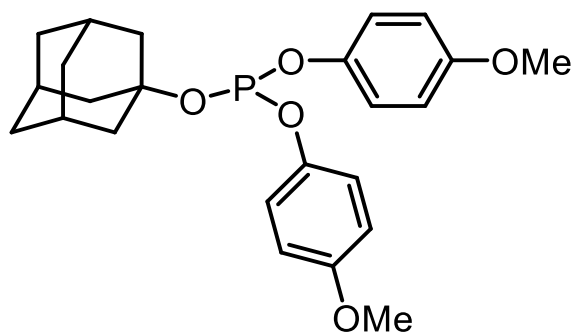


17-¹⁸O-COCF₃, R = H

¹⁸O-1-Phenyl-3-methyl-3-butyl trifluoroacetate (17-¹⁸O-COCF₃, R = H): According to a literature method reported by Sugihara *et al.*,¹⁰⁸ 3.47 mL 4-Phenyl-1-butyne (25 mmol) were introduced to 20 mL of anhydrous acetonitrile in a 100 mL round flask at RT followed by 0.3 mL tetramethylurea (2.5 mmol) and 0.62 g of mercury trifluoromethanesulfonate (1.25 mmol), then 1 mL (50 mmol) 97% labelled H₂¹⁸O was added in one portion followed by 4 mL dry DCM, and the reaction mixture was stirred overnight at RT before evaporating the solvent. 20 mL of saturated aqueous NaHCO₃ and 20 mL diethyl ether were introduced, the mixture was shaken rigorously and filtered; the filtrate was separated and the aqueous phase was extracted by diethyl ether (4 × 10 mL). The organic phases were combined and dried over Na₂SO₄. Evaporating the filtered solution afforded 3.31 g of ¹⁸O-4-phenyl-2-butanone, a light yellow liquid (88%), with 55% labelling detected by GC-MS.

Following by reaction with methyl Grignard reagent, trifluoroacetic anhydride and silica chromatography purification, **17-¹⁸O-COCF₃, R = H** was obtained as a light yellow oil (70%).

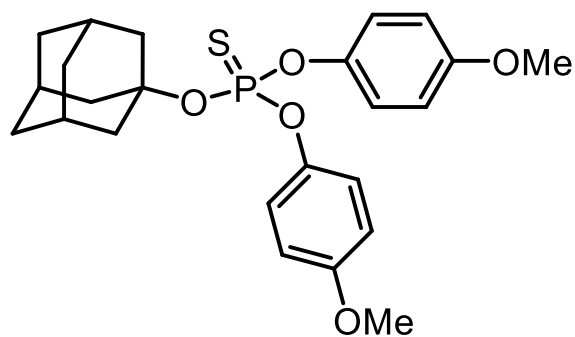
¹H NMR (400 MHz, CDCl₃): 7.35-7.31 (2H, m), 7.26-7.21 (3H, m), 2.73-2.69 (2H, m), 2.21-2.16 (2H, m) and 1.66 (6H, s). ¹³C NMR (100 MHz, CDCl₃): 156.2 (q, J = 41.2 Hz), 141.1, 128.5, 128.3, 126.1, 114.5 (q, J = 287.0 Hz), 88.66 (¹⁶O-¹³C), 88.61 (¹⁸O-¹³C), 42.4, 30.1 and 25.6.



20-OP(OAr)₂

1-Adamantyl di-4-methoxyphenyl phosphite (20-OP(OAr)₂): In an ice-cooled 100 mL flask under nitrogen, 13 mL dry THF were added, followed by 0.46 mL PCl₃ (5.27 mmol). 802 mg 1-adamantanol (**20-OH**) (5.27 mmol) and 0.74 mL triethyl amine (5.31 mmol) were dissolved in 5 mL dry THF and added into the solution dropwise. After that the ice-bath was removed and the mixture was stirred at RT for 2 hours. Ice bath was placed again, 1.31 g 4-methoxyphenol (10.60 mmol) and 1.48 mL triethyl amine (10.62 mmol) were dissolved in 5 mL dry THF and added into the solution dropwise. After that the ice-bath was removed and the mixture was stirred at RT for 2.5 hours before evaporating the solvent. The residue was dissolved in enough 80% DCM-20% Petroleum mixture and filtered through a pad of silica gel quickly. The filtrate was concentrated to afford 1.18 g **20-OP(OAr)₂** (52%) as a pale oil. Due to the instability on silica gel, chromatography purification was avoided. TLC showed only one spot.

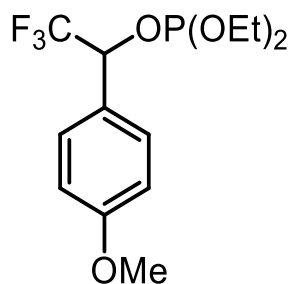
¹H NMR (400 MHz, CDCl₃): 7.05 (4H, d, J = 8.9 Hz), 6.84 (4H, d, J = 8.9 Hz), 3.80 (6H, s), 2.19 (4H, br), 2.06 (6H, br) and 1.66 (6H, br). ³¹P NMR (162 MHz, CDCl₃): 136.4. ¹³C NMR (100 MHz, CDCl₃): 155.7, 145.7 (d, J = 2.5 Hz), 121.8 (d, J = 6.7 Hz), 114.4, 78.2 (d, J = 6.9 Hz), 55.6, 45.0 (d, J = 8.2 Hz), 35.9 and 31.0.



20-OPS(OAr)₂

1-Adamantyl di-4-methoxyphenyl thionophosphate (20-OPS(OAr)₂): Following the same procedure as for **20-OPS(OEt)₂**, the residue after removing THF and excess sulfur was dissolved in enough 1 : 1 DCM-Petroleum and filtered through a pad of silica gel quickly. The filtrate was concentrated to afford 202 mg **20-OPS(OAr)₂** as a pale oil (15.8 %). Due to the instability on silica gel, chromatography purification was avoided. TLC and HPLC showed only one compound.

¹H NMR (400 MHz, CDCl₃): 7.16 (4H, dd, J = 9.0, 1.6 Hz), 6.88 (4H, d, J = 9.0 Hz), 3.80 (6H, s), 2.30 (6H, br), 2.24 (4H, br) and 1.68 (6H, br). ³¹P NMR (162 MHz, CDCl₃): 50.0. ¹³C NMR (100 MHz, CDCl₃): 156.8, 144.7 (d, J = 8.3 Hz), 122.0 (d, J = 4.7 Hz), 114.4, 86.7 (d, J = 10.1 Hz), 55.6, 43.4 (d, J = 3.8 Hz), 35.7 and 31.4.

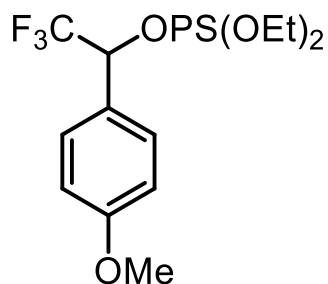


21-OP(OEt)₂

1-(4-Methoxyphenyl)-2,2,2-trifluoroethyl diethyl phosphite (21-OP(OEt)₂): 1.03 g 1-(4-methoxyphenyl)-2,2,2-trifluoroethanol (**21-OH**) (5 mmol) obtained by reducing the corresponding ketone with NaBH₄ in methanol were added to 25 mL dry THF at 0 °C followed by 0.75 mL diethyl chlorophosphite (5.2 mmol) dropwise. The solution was stirred for 10 mins before adding 0.73 mL triethylamine (5.2 mmol) dropwise. The ice-water bath was removed and the resulting mixture was stirred at RT for 2 hours before concentration under vacuum. The residue was dissolved in 60% DCM-40% Petroleum and filtered through a pad of silica gel quickly. The filtrate was concentrated to afford 0.82g (50%) **21-OP(OEt)₂** as a pale oil. TLC showed only one spot.

¹H NMR (400 MHz, CDCl₃): 7.42 (2H, d, J = 8.7 Hz), 6.93 (2H, d, J = 8.7 Hz), 5.36 (1H, dq, J = 13.5, 6.7 Hz), 3.92-3.78 (2H, m), 3.84 (3H, s), 3.71-3.61 (2H, m), 1.21 (3H, t, J = 7.1 Hz) and 1.15 (3H, t, J = 7.1 Hz). ³¹P NMR (162 MHz, CDCl₃): 139.0 (q, J = 3.1 Hz).

¹⁹F NMR (377 MHz, CDCl₃): -77.3 (d, J = 3.0 Hz). ¹³C NMR (100 MHz, CDCl₃): 160.4, 129.3, 125.9, 123.9 (dq, J = 281.3, 5.1 Hz), 113.8, 71.2 (dq, J = 32.7, 10.2 Hz), 59.0 (d, J = 12.3 Hz), 55.3, 16.6 (d, J = 5.6 Hz) and 16.5 (d, J = 5.6 Hz).

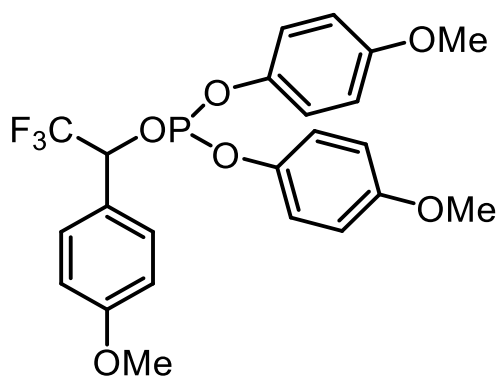


21-OPS(OEt)₂

1-(4-Methoxyphenyl)-2,2,2-trifluoroethyl diethyl thionophosphate (21-OPS(OEt)₂):

Following the same procedure as for **21-OPS(OEt)₂**, the residue after removing THF and excess sulfur was dissolved in 1 : 1 DCM-Petroleum and quickly filtered through a pad of silica gel. The filtrate was concentrated to afford 0.36 g **21-OPS(OEt)₂** (50%) as a colourless oil. HPLC showed only one compound.

¹H NMR (400 MHz, CDCl₃): 7.43 (2H, d, J = 8.7 Hz), 6.94 (2H, d, J = 8.7 Hz), 5.72 (1H, dq, J = 13.2, 6.6 Hz), 4.26-4.07 (2H, m), 3.98-3.73 (2H, m), 3.83 (3H, s), 1.34 (3H, t, J = 7.1 Hz) and 1.12 (3H, t, J = 7.1 Hz). ³¹P NMR (162 MHz, CDCl₃): 68.0. ¹⁹F NMR (377 MHz, CDCl₃): -76.8. ¹³C NMR (100 MHz, CDCl₃): 160.9, 129.7, 123.5, 123.2 (dq, J = 281.0, 12.4 Hz), 114.0, 76.6 (dq, J = 33.7, 2.7 Hz), 64.7 (d, J = 5.4 Hz), 64.6 (d, J = 5.4 Hz), 55.3, 15.7 (d, J = 8.0 Hz) and 15.6 (d, J = 8.0 Hz).

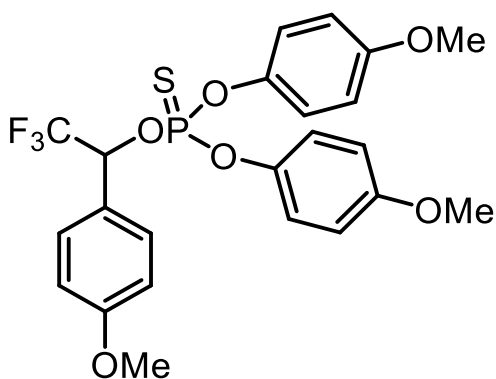


21-OP(OAr)₂

1-(4-Methoxyphenyl)-2,2,2-trifluoroethyl di(4-methoxyphenyl) phosphite (21-

OP(OAr)₂): 0.44 mL PCl₃ (5 mmol) were added into 25 mL dry THF at 0 °C followed by 1.03 g 1-(4-methoxyphenyl)-2,2,2-trifluoroethanol (**21-OH**) (5 mmol) and 0.41 mL dry pyridine (5.1 mmol) dissolved in 3 mL dry THF dropwise. The solution was stirred for 3 hours at RT before cooling down to 0 °C again. 1.24 g 4-methoxyphenol (10 mmol) and 0.82 mL dry pyridine (10.2 mmol) dissolved in 5 mL dry THF were added to the solution dropwise and the mixture was allowed to stir for another 3 hours at RT before being concentrated. The residue was dissolved in 60% DCM-40% Petroleum and filtered through a pad of silica gel quickly. The filtrate was concentrated to afford 0.97g (40%) **21-OP(OAr)₂** as a pale oil. TLC showed only one movable spot (1 : 1 DCM / hexane) and a faint spot on baseline.

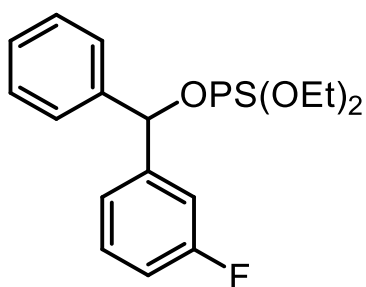
¹H NMR (400 MHz, CDCl₃): 7.47 (2H, d, J = 8.7 Hz), 7.03 (2H, d, J = 8.6 Hz), 6.94 (2H, d, J = 8.6 Hz), 6.86 (2H, d, J = 8.7 Hz), 6.76 (4H, s), 5.82 (1H, dq, J = 13.2, 6.5 Hz), 3.85 (3H, s), 3.80 (3H, s) and 3.77 (3H, s). ³¹P NMR (162 MHz, CDCl₃): 129.7. ¹⁹F NMR (377 MHz, CDCl₃): -76.8. ¹³C NMR (100 MHz, CDCl₃): 160.6, 156.3, 156.1, 145.2 (d, J = 6.8 Hz), 145.0 (d, J = 6.8 Hz), 129.5, 125.4, 123.6 (dq, J = 281.3, 4.2 Hz), 121.4 (d, J = 7.0 Hz), 121.2 (d, J = 7.0 Hz), 114.7, 114.6, 113.9, 71.9 (q, J = 33.2 Hz), 55.6, 55.5 and 55.3.



21-OPS(OAr)₂

1-(4-Methoxyphenyl)-2,2,2-trifluoroethyl di(4-methoxyphenyl) thionophosphate (21-OPS(OAr)₂): 128 mg sulfur (4 mmol) were dissolved in 10 mL dry pyridine followed by 0.97 g **21-OP(OAr)₂** (2 mmol). The mixture under nitrogen was stirred at 30 °C overnight before being concentrated. The residue was dissolved in 1 : 1 DCM-Petroleum and quickly filtered through a pad of silica gel. The filtrate was concentrated to afford 0.52 g **21-OPS(OAr)₂** (50%) as a colourless oil. HPLC showed the impurity peaks were not solvolysis products.

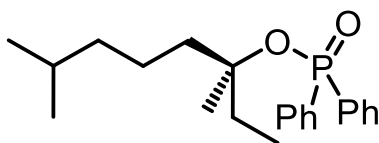
¹H NMR (400 MHz, CDCl₃): 7.45 (2H, d, J = 8.7 Hz), 7.19 (2H, dd, J = 9.0, 1.8 Hz), 6.93 (2H, d, J = 8.7 Hz), 6.92 (2H, d, J = 9.0 Hz), 6.80 (2H, dd, J = 9.0, 1.8 Hz), 6.73 (2H, d, J = 9.0 Hz), 5.86 (1H, dq, J = 12.8, 6.3 Hz), 3.85 (3H, s), 3.82 (3H, s) and 3.76 (3H, s). ³¹P NMR (162 MHz, CDCl₃): 60.9. ¹⁹F NMR (377 MHz, CDCl₃): -76.3. ¹³C NMR (100 MHz, CDCl₃): 161.1, 157.3 (d, J = 1.2 Hz), 157.1 (d, J = 1.2 Hz), 144.0 (d, J = 8.2 Hz), 143.9 (d, J = 8.2 Hz), 130.1, 123.8 (dq, J = 281.2, 12.2 Hz), 122.8, 122.1 (d, J = 4.7 Hz), 121.8 (d, J = 4.7 Hz), 114.6, 114.4, 114.1, 77.8 (dq, J = 34.1, 2.3 Hz), 55.6, 55.5 and 55.3.



22-OPS(OEt)₂

3-Fluorobenzhydryl diethyl thionophosphate (22-OPS(OEt)₂): 22-OPS(OEt)₂ was obtained as a colourless oil following the procedure shown for 21-OPS(OEt)₂. TLC and HPLC showed one compound.

¹H NMR (400 MHz, CDCl₃): 7.44-7.27 (6H, m), 7.22-7.14 (2H, m), 7.05-6.99 (1H, m), 6.60 (1H, d, J = 11.4 Hz), 4.14-4.00 (2H, m), 4.00-3.83 (2H, m), 1.24 (3H, t, J = 7.0 Hz) and 1.19 (3H, t, J = 7.0 Hz). ³¹P NMR (162 MHz, CDCl₃): 67.5. ¹⁹F NMR (377 MHz, CDCl₃): -112.4. ¹³C NMR (100 MHz, CDCl₃): 162.8 (d, J = 246.5 Hz), 143.1 (t, J = 6.6 Hz), 139.9 (d, J = 5.2 Hz), 130.0 (d, J = 8.2 Hz), 128.6, 128.3, 127.2, 122.7 (d, J = 2.8 Hz), 114.9 (d, J = 21.2 Hz), 114.0 (d, J = 22.6 Hz), 80.8 (d, J = 2.6 Hz), 64.3 (d, J = 5.3 Hz), 15.74 (d, J = 8.0 Hz) and 15.69 (d, J = 8.0 Hz).

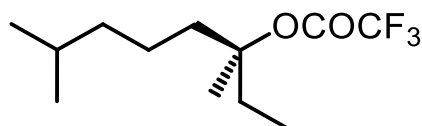


S-23-OPOPh₂

(S)-3,7-Dimethyl-3-octyl diphenylphosphinate (S-23-OPOPh₂): Commercially available R-linalool was converted to (S)-3,7-dimethyl-3-octanol (**S-23-OH**) by palladium carbon catalysed hydrogenation in ethyl acetate at RT by autoclave. 0.79 g **S-23-OH** (5 mmol) and 1.22 g 4-dimethylaminopyridine (10 mmol) were added to a 100 mL round flask followed

by 20 mL DCM, the solution with stirring was cooled to 0 °C before adding 1.43 mL diphenylphosphinic chloride (7.5 mmol) dropwise. The solution was allowed to warm to RT and stirred overnight before evaporating the solvent, then the residue was dissolved in enough ethyl acetate and filtered through a short pad of Celite[®]. The filtrate was concentrated and the residue was purified by silica gel chromatography, using 5% acetonitrile-95% DCM to afford 0.92 g *S*-23-OPOPh₂ as a colourless oil (50%). Using Daicel CHIRALPAK[®] IA with 3% isopropanol-97% hexane (1.0 mL/min), the ee value was determined as 98.4%. HPLC and TLC showed one compound.

¹H NMR (400 MHz, CDCl₃): 7.77-7.71 (4H, m), 7.35-7.27 (6H, m), 1.81-1.64 (4H, m), 1.49-1.40 (1H, m), 1.37 (3H, s), 1.32-1.22 (2H, br), 1.11-1.04 (2H, m), 0.99-0.84 (3H, m) and 0.81-0.75 (6H, m). ³¹P NMR (162 MHz, CDCl₃): 24.9. ¹³C NMR (100 MHz, CDCl₃): 135.7, 134.3, 131.3 (d, J = 2.2 Hz), 131.2 (d, J = 10.1 Hz), 89.2 (d, J = 8.9 Hz), 40.6 (d, J = 3.6 Hz), 39.1, 33.6 (d, J = 3.9 Hz), 27.7, 25.9 (d, J = 2.8 Hz), 22.5, 21.7 and 8.6.



S-23-OCOCF₃

(*S*)-3,7-Dimethyl-3-octyl trifluoroacetate (*S*-23-OCOCF₃): this was synthesized in the way shown for **17-OCOCF₃**, **R = OMe** (P. 106), after evaporation of the DCM, the residue was dissolved in hexane, filtered on silica gel and the product was isolated as a colourless oil. The only impurities determined by GC were several elimination products of both *E* and *Z* configurations, but none of the corresponding alcohol (*S*-23-OH) was detected. ¹H NMR and ¹³C NMR data are not reported here.

¹⁹F NMR (376.6 MHz, CDCl₃): -75.8.

Kinetics: All the rate constant determination except for the solvolysis of **17-SMe₂⁺**, **R = OMe** and **20-OPS(OAr)₂** were done by HPLC at 30 °C. A 1 mL solution containing 1:1 (v : v) water-TFE, 7 mM 2,6-di-*tert*-butylpyridine, 0.2 mM 3-nitroacetophenone (internal standard) and 1 M sodium perchlorate (or other nucleophiles with the total salt concentration adjusted by sodium perchlorate to afford a 1 M concentration) was made. 10 μL 0.5 M or 0.2 M substrate in acetonitrile was then introduced to the solution and quickly placed into the sample box. The progress of the reactions was monitored by analysing aliquots of the reactions mixture for 2-3 half-lives. The peak areas in the chromatograms were integrated and a first order equation fitted to these data; in all cases, $R^2 > 0.999$.

The slow solvolysis reaction of **17-SMe₂⁺**, **R = OMe** in 50% (v : v) TFE was done by UV-Vis at 30 °C. The conditions were as described in **Kinetics** above, except that 0.2 mM 2,6-dimethyl-3-hydroxypyridine ($\lambda_{\text{max}} = 323 \text{ nm}$) was used as a pH indicator to follow the first 5-10% reaction. (No 2,6-di-*tert*-butylpyridine or 3-nitroacetophenone)

Product analysis: All the product analyses were done by GC-MS with the same concentrations as under **Kinetics** and the yield was detected by HPLC after 10 half-lives except **17-SMe₂⁺**, **R = OMe** (1 half-life), assuming all the products had the same absorbance coefficient under a specified wavelength (261 nm for 1-phenyl-3-methyl-3-butyl and 277 nm for 1-(4-methoxyphenyl)-3-methyl-3-butyl substrates), which was confirmed by mass balance of peak areas and previous work⁴.

To those products that not be separated or detected by HPLC, GC method was used to determine the relative concentration ratio by using 6-undecanone as the internal standard

and normalized to absolute yield by comparing with HPLC yield or to relative yield against the internal standard, if the coefficient was unknown.

The products of solvolysis of 1-adamantyl bromide in 50% (v : v) TFE with different additives were determined by GC with the same concentrations as under **Kinetics**, except the substrate concentration was 1 mM, the base used was 1.4 mM and using 1.4 mM 1,3-dimethoxybenzene as an internal standard. The relative concentrations of solvolysis products were normalized by dividing the peak areas by internal standard peak area.

The products of solvolysis of **S-23-OCOCF₃** in 50% (v : v) TFE were determined by chiral GC with the same concentrations as under **Kinetics** (total volume: 60 mL), but no internal standard was used. After 8 half-lives, most of TFE was evaporated under vacuum, the aqueous phase was extracted with 5 × 20 mL diethyl ether, the combined organic phase was then separated and dried over Na₂SO₄ before being concentrated under vacuum; the residue was dissolved in 1 mL chloroform and subjected to chiral GC analysis. The ratio of alcohol enantiomers was directly measured by comparing their peak areas.

Under these nearly neutral solvolysis conditions, all the products were stable.

Solvolysis of 20-OPS(OAr)₂: A 1 mL solution containing 1:1 (v : v) water-TFE, 0.4 mM 2,6-di-*tert*-butylpyridine, 0.25 mM 3-nitroacetophenone (internal standard) and 1 M NaClO₄ was made, then 10 μL 0.05 M substrate in chloroform was introduced and the solution was quickly immersed in a thermostatic water bath. During the solvolysis, another peak accumulated with the same rate constant as that of the starting material's decay. It was demonstrated that this new product was stable under solvolysis conditions after 8 half-lives.

The extinction coefficients of both **20-SPO(OAr)₂** and **20-OPS(OAr)₂** were determined in a ratio of 1.4 : 1, thus the yield of **20-SPO(OAr)₂** determined by HPLC was 20%.

A large scale solvolysis was carried out with 2 mM substrate, 1.1 mM triphenylphosphine sulfide (³¹P NMR internal standard), 2 mM 2,6-di-*tert*-butylpyridine and 1 M NaClO₄ in 150 mL 1:1 (v : v) water-TFE at 30 °C. After 8 half-lives, most TFE was evaporated and the aqueous phases was extracted with chloroform (6 × 20 mL) and diethyl ether (4 × 20 mL). The organic phases were combined, dried over Na₂SO₄, and filtered before being concentrated. The residue was directly dissolved in 0.7 mL CDCl₃ and analysed by NMR. In addition to the internal standard peak at 43.27 ppm, ³¹P NMR showed a new peak at 18.57 ppm, whose integrated peak area was 0.37 : 1 compared with the internal standard, indicating a 20% thiono-thiolo rearrangement. Proton coupled ³¹P NMR showed the new peak at 18.57 ppm was singlet. ¹³C NMR showed only two doublet peaks below 80 ppm at 55.03 (J = 4.4 Hz) and 44.88 (J = 6.2 Hz). Those characterizations support the formation of **20-SPO(OAr)₂** as the rearranged product.

The thiono-thiolo rearrangements of **17-OPS(OEt)₂**, **21-OPS(OAr)₂**, **21-OPS(OEt)₂** and **22-OPS(OEt)₂** were analysed in the way shown above, giving 4%, 30%, 44% and 46% rearranged products, respectively.

¹⁸O scrambling of 17-¹⁸OCOCF₃, R = H: 7.5 mmol of 17-¹⁸OCOCF₃, R = H (with 55% ¹⁸O enrichment) were added to 150 mL 1:1 water-TFE, containing 10 mmol 2,6-di-*tert*-butylpyridine and 1 M sodium perchlorate at 30 °C (substrate concentration 0.05 M). After 16 h, 24 h, 40 h and 48 h, aliquots were withdrawn (50 mg of starting material should be

recovered for ^{13}C NMR analysis) and extracted with diethyl ether (5×20 mL); the combined organic phases were dried and evaporated under reduced pressure. The whole residue was dissolved in 0.7 mL CDCl_3 for ^{13}C NMR analysis by using reported methods⁴¹. ^{13}C NMR at 125 MHz (pulse angle 45° , 2228 transients at 25°C acquired with a 103 Hz sweep width, 8192 data points (0.025 Hz/pt) and a 0.1 s relaxation delay time) gave the relative concentrations of trifluoroacetate esters with ^{18}O in the bridging and nonbridging positions. The tertiary ^{13}C signals were at 88.74 (^{18}O non-bridging) and 88.69 (^{18}O bridging) ppm, respectively. The peaks were sufficiently resolved (0.05 ppm difference) to allow the ratio of ^{13}C bonded to ^{18}O or ^{16}O to be calculated by integration of the signals (P. 191).

5.3 Results and Discussion

The first-order rate constant of 1-phenyl-3-methyl-3-butyl trifluoroacetate (**17-OCOCF₃**, **R = H**) in 50% (v : v) TFE at 30°C is $1.61 \pm 0.05 \times 10^{-5} \text{ s}^{-1}$ and in the presence of 1 M NaSCN, the rate constant reduces to $1.25 \pm 0.06 \times 10^{-5} \text{ s}^{-1}$. This is attributed to non-specific salt effects (medium effects). The first-order rate constant of 1-(4-methoxyphenyl)-3-methyl-3-butyl trifluoroacetate (**17-OCOCF₃**, **R = OMe**) in 50% (v : v) TFE is $1.58 \pm 0.06 \times 10^{-5} \text{ s}^{-1}$ and is reduced to $1.27 \pm 0.04 \times 10^{-5} \text{ s}^{-1}$ in the presence of 1 M NaSCN. Since a similar product distribution to 2-chloro-2-methylnonane was observed (see Tables 5.1 and 5.4), no neighbouring group participation by the aryl groups is observed, as concluded by Toteva and Richard⁴.

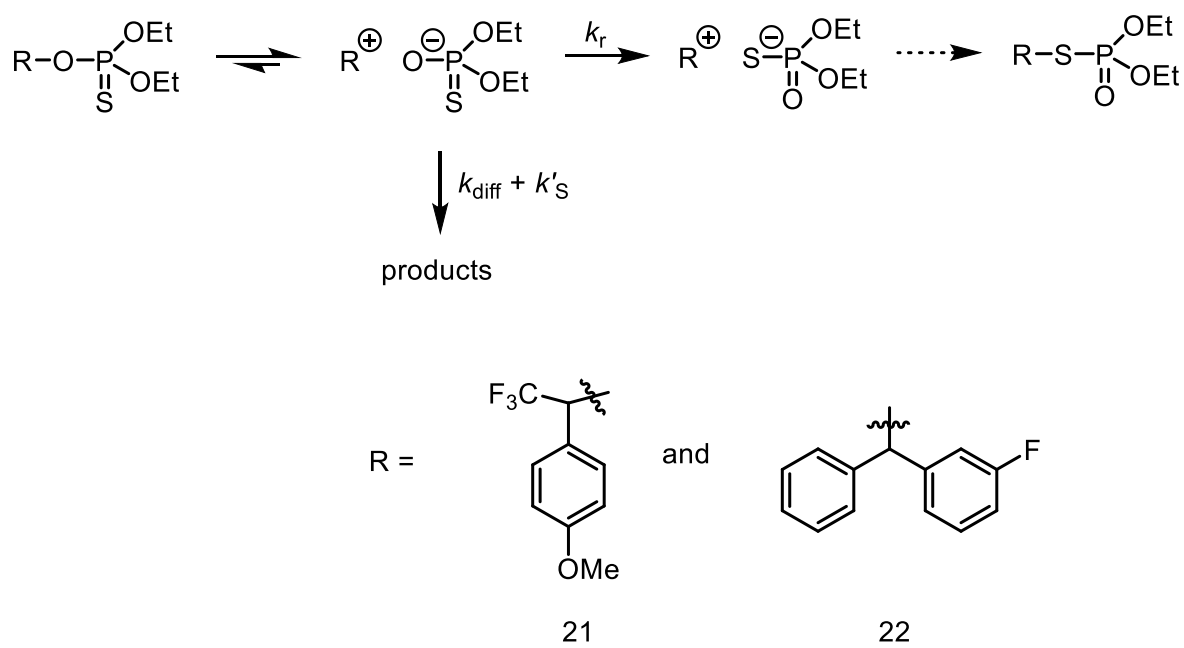
Table 5.1. Product yield of 2-chloro-2-methylnonane with different additives in 50% (v : v) TFE

substrate	additives [1 M]	relative product yield [†] (± 0.002)		
		ROH	ROCH ₂ CF ₃	C=C
CH ₃ (CH ₂) ₆ C(Me) ₂ Cl	NaClO ₄	0.292	0.120	0.421
	NaSCN	0.225	0.090	0.373
	NaN ₃	0.243	0.103	0.372
	NaSCH ₂ CH ₂ OH	0.213	0.099	NG ^{††}
	HOCH ₂ CH ₂ SH	0.301	0.120	NG ^{††}

[†]: relative product yield was determined by GC and normalized against internal standard; R = CH₃(CH₂)₆C(Me)₂ and C=C are the mixture of two alkene isomers

^{††}: not given, due to the peak overlap with HOCH₂CH₂SH

Solvolysis of 1-(4-methoxyphenyl)-2,2,2-trifluoroethyl diethylthionophosphate (**21-OPS(OEt)₂**) (with a solvent attack rate constant of $3 \times 10^7 \text{ s}^{-1}$ on **21**⁺ in 50% (v : v) TFE⁸⁸) and 3-fluorobenzhydryl diethylthionophosphate (**22-OPS(OEt)₂**) (with a solvent attack rate constant of 10^9 s^{-1} on **22**⁺ in 50% (v : v) TFE^{2,89}) gave 44% and 46% thiono-thiolo rearranged products, respectively (Scheme 5.2). Since these two precursors with substantially different reactivity give the same yield of thiono-thiolo rearranged products, it is reasonable to conclude that the thiono-thiolo rearrangement takes place in a step-wise pathway and is faster than ion-pair separation²⁸. Taking the ion-pair separation rate constant (k_{diff}) $1.6 \times 10^{10} \text{ s}^{-1}$ into consideration, the rearrangement of diethylthionophosphate can be calculated as $1.4 \times 10^{10} \text{ s}^{-1}$, which is about 7 times slower than thionobenzoate rearrangement²⁸. This is reasonable since the tetracoordinated thionophosphate needs to move one additional group upon exchange compared with a tricoordinated thionocarboxylate.

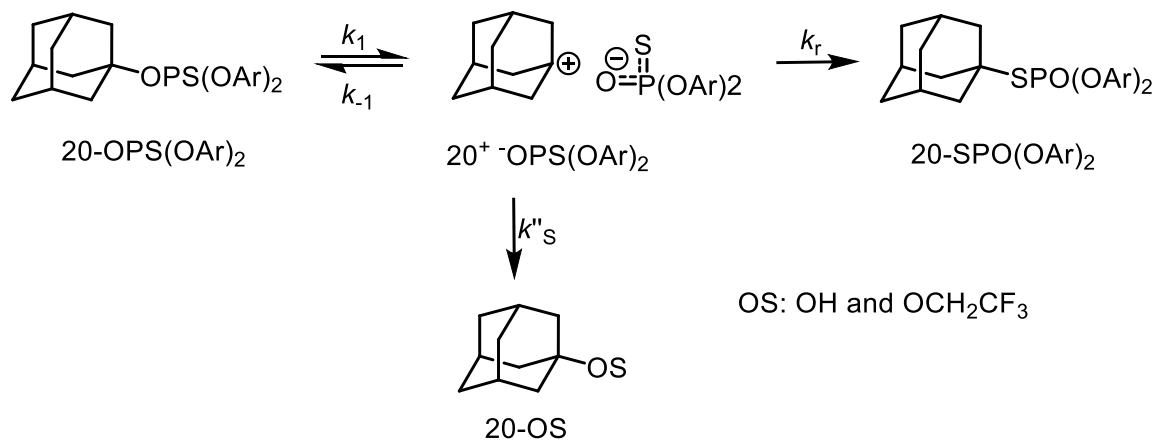


Scheme 5.2. Thiono-thiolo rearrangement of **21-OPS(OEt)₂** and **22-OPS(OEt)₂** in 50% TFE

Solvolyzing 1-(4-Methoxyphenyl)-2,2,2-trifluoroethyl di(4-methoxyphenyl)thionophosphate (**21-OPS(OAr)₂**) in 50% (v : v) TFE only gave 30% thiono-thiolo rearrangement, indicating a slower exchange rate constant compared with diethylthionophosphate. Therefore, the anion exchange rate constant of diarylthionophosphate was calculated as $7 \times 10^9 \text{ s}^{-1}$, which is about 14 times slower than thionobenzoate²⁸. This is presumably because changing OEt to OAr requires the movement of a heavier group for exchange.

Solvolyzing 1-adamantyl di(4-methoxyphenyl) thionophosphate (**20-OPS(OAr)₂**) in 50% (v : v) TFE gave 20% rearranged products (Scheme 5.3). Therefore, using the calibrated anion exchange rate constant of thiophosphates, and if all the thiono-thiolo rearrangement results from the corresponding ion-pair (it has been previously suggested that the thiono-

thiolo exchange is a step-wise pathway for another cation whose lifetime is similar to this²⁸), k''_s in Scheme 5.3 can be calculated as $1.2 \times 10^{10} \text{ s}^{-1}$.



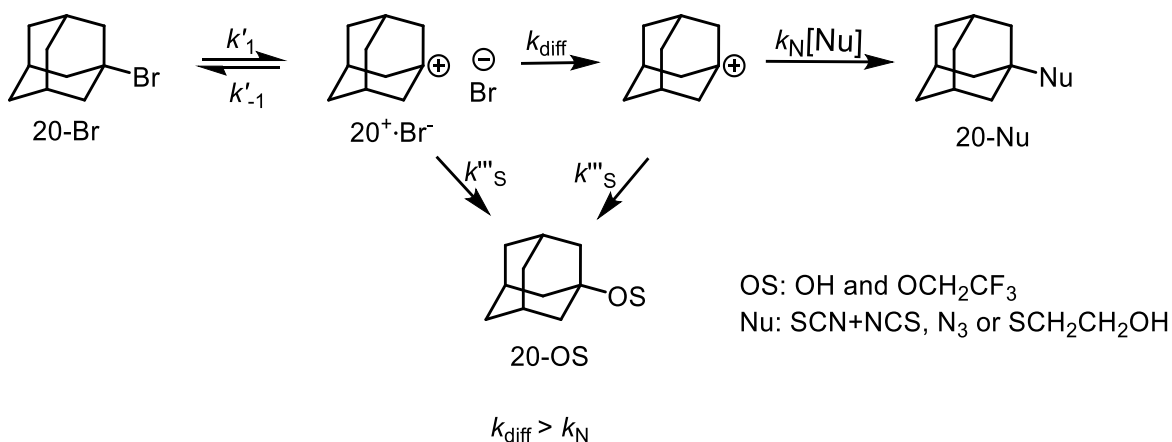
Scheme 5.3. Thiono-thiolo rearrangement of **20-OPS(OAr)₂** in 50% (v : v) TFE

In order to test whether the thiono-thiolo rearrangement probe is valid or not, another classical trapping method was used. The solvolysis of 1-adamantyl bromide (**20-Br**) in the presence of 1 M strong nucleophiles yielded 8-10% substitution products from an external nucleophile (except **20-N₃**) (Table 5.2).

Table 5.2. Product yield of **20-Br** with different additives in 50% (v : v) TFE

substrate	additives [1 M]	product yield (%) (± 0.2)	
		20-OH + 20-OCH ₂ CF ₃	20-Nu
20-Br	NaClO ₄	100	
	NaSCN	92.4	7.6
	NaN ₃	95.5	4.5
	NaSCH ₂ CH ₂ OH	92.3	7.7
	HOCH ₂ CH ₂ SH	90.1	9.9

Due to the unavailability of rear-side approach, unfavorability of front-side concerted substitution, and unfavourable (or very weak) front-side pre-association of anion nucleophiles with **20-Br**, the nucleophile adducts must primarily result from trapping of the reactive ion-pair intermediate (Scheme 5.4). The rate constant of solvent attack on **20⁺ Br⁻** can be estimated to have a lower limit $k''_s = 1.2\text{-}1.4 \times 10^{10} \text{ s}^{-1}$ (Equation 17), by using the statistically corrected diffusion-controlled rate constant ($2.5 \times 10^9 \text{ M}^{-1} \text{ s}^{-1}$) for nucleophile trapping¹¹⁻¹³, if no pre-association is considered.



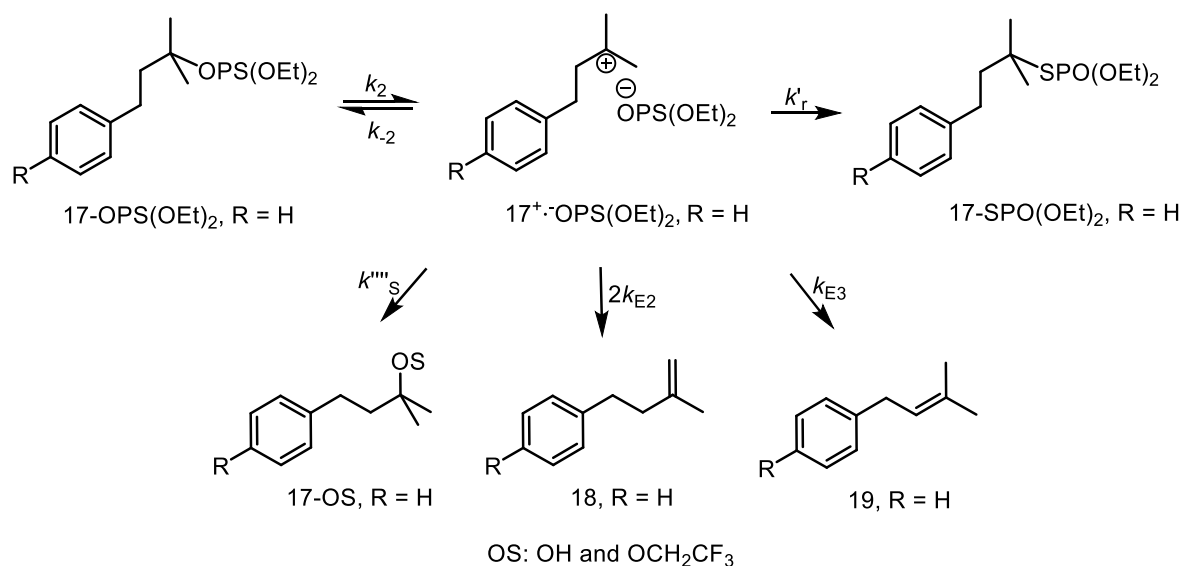
Scheme 5.4. Solvolysis of **20-Br** in 50% (v : v) TFE with added nucleophiles

$$\frac{[20 - \text{Nu}]}{[20 - \text{Nu}] + [20 - \text{OS}]} = \frac{k_{\text{diff}}}{k_{\text{diff}} + k'''_s} \frac{k_{\text{N}}[\text{Nu}]}{k_{\text{N}}[\text{Nu}] + k'''_s} \quad (17)$$

Thus, $k''_s = 1.2 \times 10^{10} \text{ s}^{-1}$ obtained from thiono-thiolo rearrangement agrees very well with the trapping experiment ($1.2\text{-}1.4 \times 10^{10} \text{ s}^{-1}$). This indicates that anion pre-association at the front side of the 1-adamantyl analogue is unlikely to be a significant contribution to the substitution reaction and an earlier report by Sommer and Carey was found to support our assumption⁹⁰. The facial selectivity of azide attack on a cumyl carboxylate in MeOH was

reported as 1: 4, so the expected trapping adduct yield for 1-adamantyl bromide with 1 M anion-type nucleophiles is less than 2%.

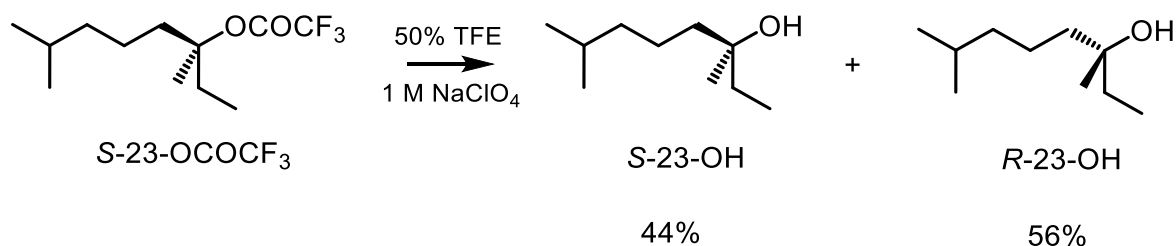
Solvolysing 1-phenyl-3-methyl-3-butyl diethylthionophosphate (**17-OPS(OEt)₂**, **R = H**) in 50% (v : v) TFE only gave 4% thiono-thiolo rearrangement (Scheme 5.5). Therefore, the lower limit for the solvent attack rate constant (k''''_s) on **17⁺ ·OPS(OEt)₂** can be calculated as $3.2 \times 10^{11} \text{ s}^{-1}$, if no concerted rearrangement is taken into consideration. Since this is of the same order as the solvent reorganization rate constant¹⁵, it is not clear whether the decay of **17⁺ ·OPS(OEt)₂** is dominated by solvent reorganization or not. However, if the intrinsic barrier to form the covalent bond between **17⁺ ·OPS(OEt)₂** and solvents is lower than the solvent reorganization barrier, the solvent attack on **20⁺ ·OPS(OAr)₂** also should be dominated by solvent reorganization (due to the structure similarity), and will produce less than 6% rearranged product. In contrast, 20% of the rearranged product was found. Therefore, the decay of **17⁺ ·OPS(OEt)₂** in 50% (v : v) TFE should be governed by bond formation rather than solvent reorganization, which indirectly indicates that the intrinsic rate of capturing simple tertiary cations by solvent molecules reported by Toteva and Richard³⁵ is too fast.



Scheme 5.5. Thiono-thiolo rearrangement of **17-OPS(OEt)₂**, **R = H** in 50% (v : v) TFE

Since the proportion of elimination product (75%) from diethylthionophosphate is only slightly higher than for diphenylphosphate (68%) which does not contain a sulfur atom, we do not think there is any significant contribution from concerted elimination pathways. This is in strong contrast to thionocarboxylates, which enormously accelerate elimination pathways⁹¹ relative to substitutions. Meanwhile, if proton extraction from **17⁺·SPO(OEt)₂** is also barrierless, and so can compete efficiently with ion-pair combination, we would expect a near quantitative formation of elimination products from the diphenylphosphate precursor, which has the same oxygen basicity as diethylthionophosphate but does not require the exchange atom positions. The fact that only 68% elimination products are observed indicates that there are no other barrierless processes except ion-pair combination on **17⁺·SPO(OEt)₂**. Therefore, it is credible that the normalized solvolysis products (25% **17-OS** + 32% **18** + 43% **19**) result from step-wise pathways, so $k''''S$, k_{E2} and k_{E3} in Scheme 5.5 can be obtained as $8.0 \times 10^{10} \text{ s}^{-1}$, $5.2 \times 10^{10} \text{ s}^{-1}$ and $1.3 \times 10^{11} \text{ s}^{-1}$, respectively.

Furthermore, the solvolysis of (*S*)-3,7-dimethyl-3-octyl trifluoroacetate (**S-23-OCOCF₃**) in 50% (v : v) TFE showed the facial selectivity of alcohol products was 56 : 44 (inversion : retention) (Scheme 5.6), which agreed very well with previous reports of solvolysing chiral 3,7-dimethyl-3-octyl substrates in pure TFE⁹².



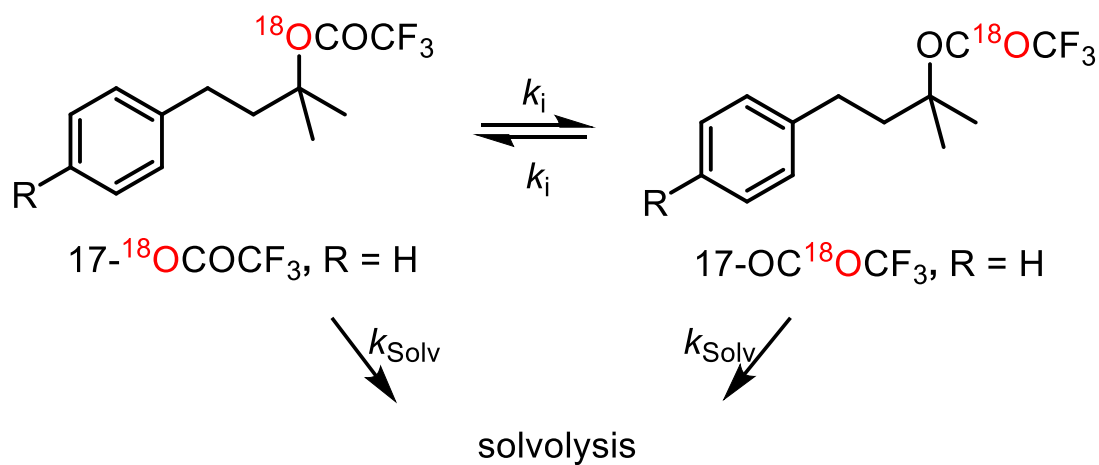
Scheme 5.6. The solvolysis of **S-23-OCOCF₃** in 50% TFE

Based on the facial selectivity determined from **S-23-OCOCF₃**, if assuming the leaving group has a minor effect on the facial selectivity, the solvent back-side attack rate constant on **17⁺ ·OPS(OEt)₂** can be calculated as $4.5 \times 10^{10} \text{ s}^{-1}$ and the front-side attack rate constant is $3.5 \times 10^{10} \text{ s}^{-1}$. Thus, the best estimation of k^{front} (Scheme 5.5) for **17⁺ X⁻** is $8.0 \times 10^{10} \text{ s}^{-1}$, which is one order magnitude smaller than Toteva and Richard's calculation³⁵, one order magnitude larger than McClelland's extrapolation⁹³, but very close to Mayr's calculation^{12,89} based on $\log k (25 \text{ }^\circ\text{C}) = s \times (N + E)$. The estimated lifetime of simple tertiary ion-pairs is also consistent with the 500 fs (0.5 ps) lifetime of tert-butyl cation found in aqueous sulfuric acid⁹⁴.

The reason why the front-side attack rate constant on **17⁺ ·OPS(OEt)₂** is three times faster than that of **20⁺ ·OPS(OAr)₂** is unknown, and maybe due to different solvation environments around **17⁺ ·OPS(OEt)₂** and **20⁺ ·OPS(OAr)₂**. However, the very similar

results indicate that the 1-adamantyl system can be used as a valid model for front-side substitution of simple tertiary substrates.

The observable isotope exchange when $17\text{-}^{18}\text{O}\text{COCF}_3$, $\mathbf{R} = \mathbf{H}$ solvolyses in 50% (v : v) TFE provides further information about ion-pair formation (Scheme 5.7).



Scheme 5.7. ^{18}O scrambling of $17\text{-}^{18}\text{O}\text{COCF}_3$, $\mathbf{R} = \mathbf{H}$ in 50% (v : v) TFE

The fraction of isotope exchanged substrate $\frac{[17\text{-}^{18}\text{O}\text{COCF}_3]}{[17\text{-}^{18}\text{O}\text{COCF}_3] + [17\text{-}^{16}\text{O}\text{COCF}_3]}$ when solvolysing 0.05 M $17\text{-}^{18}\text{O}\text{COCF}_3$, $\mathbf{R} = \mathbf{H}$ (with 55% initial ^{18}O enrichment) was analysed by quantitative ^{13}C NMR (Table 5.3) and fitted by Equation 18 to obtain the pseudo first-order isotope exchange rate constant $k_i = 0.1k_{\text{Solv}} = 1.60 \times 10^{-6} \text{ s}^{-1}$ (Scheme 5.7 and Fig. 5.1).

$$\frac{[17\text{-}^{18}\text{O}\text{COCF}_3]_t}{[17\text{-}^{18}\text{O}\text{COCF}_3]_t + [17\text{-}^{16}\text{O}\text{COCF}_3]_t} = \frac{0.5[17\text{-}^{18}\text{O}\text{COCF}_3]_0}{[17\text{-}^{18}\text{O}\text{COCF}_3]_0 + [17\text{-}^{16}\text{O}\text{COCF}_3]_0} (1 + e^{-2k_i t}) \quad (18)$$

Table 5.3. Results of isotope exchange of 17-¹⁸O COCF₃, R = H in 50% (v : v) TFE

Reaction time/s	$\frac{[17 - ^{18}\text{OCOCF}_3]_t}{[17 - ^{18}\text{OCOCF}_3]_t + [17 - ^{16}\text{OCOCF}_3]_t}$
0	0.553
57600	0.502
86400	0.484
144000	0.456
172800	0.435

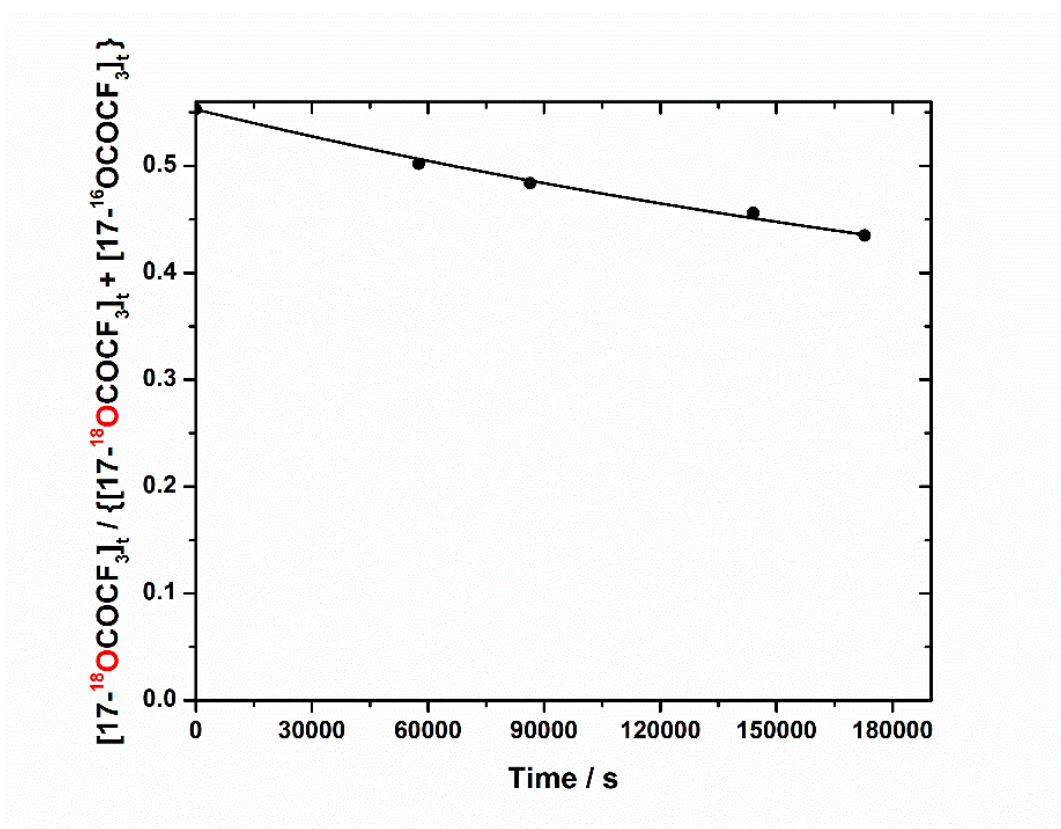


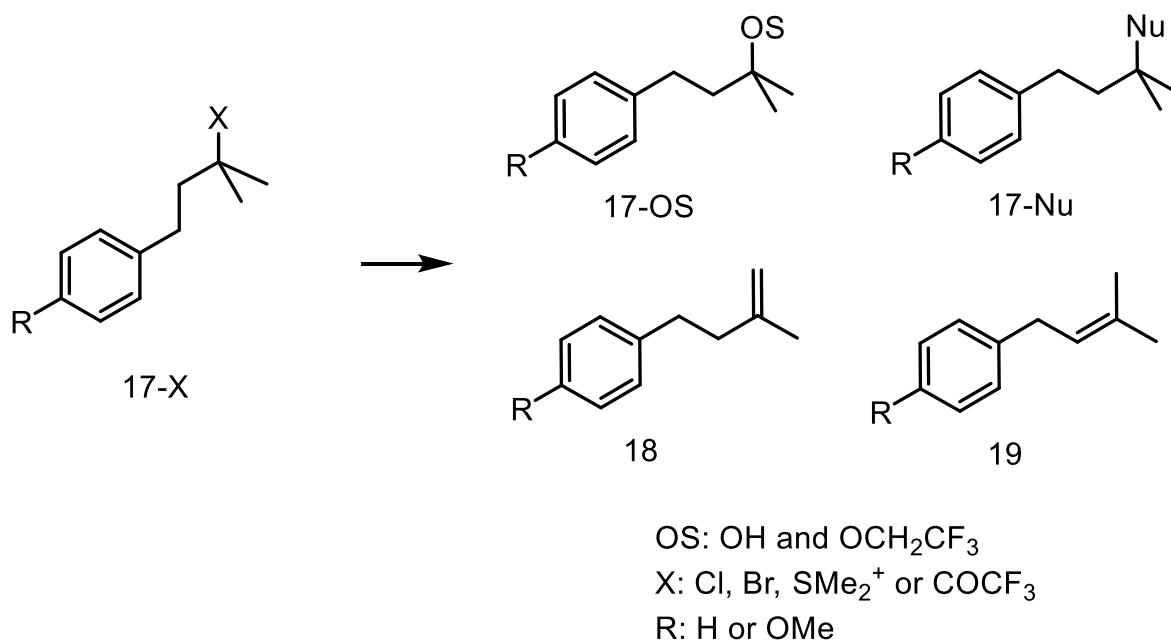
Figure 5.1. Least square fitting to Equation 18 of ¹⁸O scrambling of 17-¹⁸O COCF₃, R = H in 50% (v : v) TFE

Since $k_i = 0.1k_{\text{Solv}}$, this indicates a reversible ionization that hardly competes with other partitioning processes, consistent with the lifetime estimated above. On the other hand, solvolysing (*S*)-3,7-dimethyl-3-octyl diphenylphosphinate (*S*-23-OPOPh₂) in 50% (v : v) TFE revealed less than 0.6% accumulation of *R*-23-OPOPh₂ after 7 half-lives. Due to the

presence of other impurities with similar retention times, this figure is a maximum value and implies that the ion-pair $17^+ X^-$ has a very short lifetime that does not allow the electrophile part to rotate, consistent with the estimated lifetime shown above. The absence of visible racemization has also been reported for *S*-**23-Cl** in TFE after 1 half-life⁹².

Therefore, based on the lifetime of simple tertiary cations in 50% TFE discussed above, the mechanism of the reaction of **17-X** with different additives needs to be further discussed.

The products (Scheme 5.8) and their absolute yields are summarized in Table 5.4.



Scheme 5.8. Products of **17-X** with different additives in 50% (v : v) TFE

Table 5.4. Product yield of **17-X** with different additives in 50% (v : v) TFE

substrate	additives [1 M]	product yield (%) (± 0.2)			
		17-OH	17-OCH ₂ CF ₃	18 + 19	17-Nu
R = OMe 17-Cl	NaClO ₄	44.9	12.2	42.7	
	NaSCN	32.6	8.8	36.0	22.6
	NaN ₃	35.5	10.5	41.0	13.0
	HOCH ₂ CH ₂ NH ₂	45.4	10.5	43.4	ND ^{†††}
	0.5 M NaOH + 0.5 M NaClO ₄	43.8	11.2	45.0	
	NaSCH ₂ CH ₂ OH	32.0	10.0	58.0	< 2.0%
	HSCH ₂ CH ₂ OH	43.4	11.8	44.8	< 1.8%
R = OMe 17-SMe ₂ ⁺	NaClO ₄	57.3	23.0	19.8	
	NaSCN	33.4	13.4	26.2	26.9
	NaOH	19.4	8.0	72.6	
	NaSCH ₂ CH ₂ OH	16.0	ND ^{†††}	84.0	ND ^{†††}
R = OMe 17-Br	NaClO ₄	51.3	14.4	34.3	
	0.5 M NaOH + 0.5 M NaClO ₄	51.2	13.1	35.7	
	NaSCN	36.0	9.7	28.8	25.4
R = OMe 17-OCOFC ₃	NaClO ₄	41.8	13.2	45.0	
	NaSCN	31.0	9.8	39.5	19.7
R = H 17-Cl	NaClO ₄	42.7	11.1	46.2	
	NaSCN	32.3	8.0	38.7	21.0
	0.5 M NaOH + 0.5 M NaClO ₄	42.1	10.6	47.3	
R = H	NaClO ₄	52.3	14.0	33.7	
	NaSCN	38.8	10.1	27.7	25.4

17-Br	0.5 M NaOH + 0.5 M NaClO ₄	50.5	12.5	37.0	
R= H	NaClO ₄	42.3	12.9	44.8	
17-OCOCF ₃	NaSCN	32.4	9.4	38.7	19.5

†††: Not detected

The very small amount of thiocyanate trapping adducts (20%-25%) of **17-X** with a 20% solvolysis rate decrease can be accounted for either by a pre-association step-wise pathway or a true concerted pathway combined with a negative salt effect on the solvolysis rate compared with NaClO₄. The expected trapping adduct yield resulting from the common ion-pair intermediate will be less than 1%.

However, the large selectivity difference between NaSCN and HOCH₂CH₂SH ($k_{\text{SCN}} / k_{\text{RSH}} > 18$) does not support the pre-association step-wise pathway. Both are of equal nucleophilicity towards **20⁺ Br⁻**, but almost no trapping products result from the presence of 1 M HOCH₂CH₂SH with **17-X**, in contrast to 20-25% trapping products when 1 M NaSCN is present. The large selectivity difference indicates that the bond coupling of nucleophiles and **17-X** is relatively significant, which is not consistent with a pre-association step-wise pathway. We suggest that the reaction of strong nucleophiles with **17-X** should be best described as a concerted pathway with a weak bond coupling, but due to the steric congestion, it does not compete efficiently with step-wise solvolysis⁹⁵. The concerted bimolecular reaction of nucleophiles with tertiary substrates will be more significant when the step-wise pathway is slowed down^{96,97}.

It is obvious that NaN_3 does not act as a nucleophile only, otherwise the ratio of solvolytic substitution and solvolytic elimination ($\frac{[17-\text{OH}] + [17-\text{OCH}_2\text{CF}_3]}{[18] + [19]}$) should be a constant regardless of added nucleophiles (assuming the different salt effects on product distribution are not significant). However, replacing NaClO_4 by NaSCN increased the proportion of elimination slightly (Table 5.4). Since NaSCN does not show general base effects (see Chapters 3 and 4), this small change must be attributed to different salt effects on the product determining steps. In the presence of NaN_3 , the change is more significant than the medium effect (Table 5.4), which indicates that NaN_3 also acts as a base.

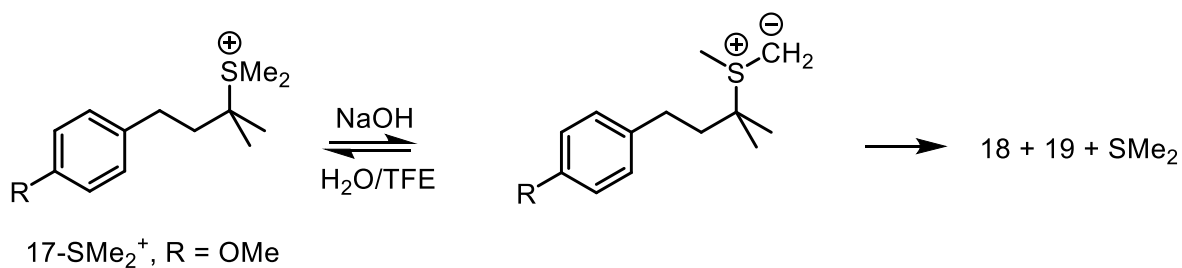
Based on the insensitivity of alkene formation towards the added bases, Richard *et al.* proposed an intramolecular E_i mechanism³⁵. However, Meng and Thibblin⁹⁸ as well as Creary *et al.*⁹⁹ showed that it was the *anti*-proton which was extracted to give the elimination products in some substrates that have similar structures. We also observed that the base strength-insensitive elimination process was not affected by different leaving groups, although bromide gave a lower yield of elimination products (dimethylsulfonium salt will be discussed separately below). We do not think the intramolecular E_i mechanism is needed to explain the base strength-insensitive elimination pathway for simple tertiary substrates. We still prefer the classical E_2 pathway, but the solvation of the corresponding bases plays a more important role than their basicity.

Since the base-induced elimination reaction for simple tertiary substrates in 50% TFE lies towards a unimolecular pathway (but cannot be an E_1 pathway, due to the short lifetime of simple tertiary carbenium ions in 50% TFE), the bond coupling of added bases and C-H cannot be very strong, which makes the competition between added bases and solvents less

favourable. This is clearly shown in Table 5.4. Therefore, the basicity is not important during the base-promoted elimination reactions, so the solvation energy that needs to be overcome becomes the dominated factor. This observation is consistent with Bunnett and Migdal's proposal¹⁰⁰ and changing the solvent to one which has a lower Y_{Cl} value (weaker 'anion solvation' power), the effects of added base on simple tertiary substrates will be more significant, which is consistent with a continuous change from uncoupled E2 (basicity is not as important as desolvation) to classical coupled E2 (basicity is more important than desolvation) pathways. The different solvation energy of added bases then explains why NaOH or HOCH₂CH₂NH₂ have nearly no effect on the product distribution^{88a,101a}, while NaN₃, which is a much weaker base but with less solvation, can accelerate elimination. Furthermore, it is not surprising that HOCH₂CH₂SNa, which has a similar pK_b to HOCH₂CH₂NH₂ but is more weakly solvated^{101b}, becomes the best base to promote elimination reactions of simple tertiary substrates in 50% TFE.

The dimethylsulfonium tetrafluoroborate salt showed a higher sensitivity to the different additives. Without additives, elimination is less significant than for halides or trifluoroacetate. This indicates that the solvolytic elimination pathway is dependent on the leaving groups. For example, added NaSCN now accelerates the elimination slightly, in contrast to halides or trifluoroacetates, indicating that the salt effect is more significant for the sulfonium leaving group. 1 M NaOH or NaSCH₂CH₂OH significantly accelerate the elimination process but with an opposing regioselectivity. NaOH favours formation of 18 (anti-Saytzeff product) while NaSCH₂CH₂OH favours formation of 19 (Saytzeff product). This opposite regioselectivity again indicates the mechanisms of elimination induced by NaOH and NaSCH₂CH₂OH are different. NaOH induced elimination can be accounted by

the E_i pathway through an ylide intermediate (Scheme 5.9), but NaSCH₂CH₂OH induced elimination is best accounted for by an uncoupled E2 mechanism (which may include a small proportion of E_i pathway), which also supports the observation of additive effects on elimination reactions of tertiary halides.



Scheme 5.9. E_i elimination pathway of **17-SMe₂⁺**, **R = OMe** through an ylide intermediate in the presence of NaOH

5.4 Conclusion

(1) The solvolysis mechanism of simple tertiary substrates in 50% (v : v) TFE is best described as a step-wise pathway, with $k''''_s = 8.0 \times 10^{10} \text{ s}^{-1}$ and $k_E = 0.7\text{-}2.4 \times 10^{11} \text{ s}^{-1}$ (leaving group dependent) in Scheme 5.5. Solvent pre-organization is not needed since the rate constant is no larger than (or just close to) the solvent re-organization rate constant¹⁵. The lifetime of a simple tertiary cation has been estimated as 3-7 ps, which is consistent with Mayr's calculation^{12,89}. The ionization mechanism via a reactive intermediate also supports the slow but observable isotope exchange observed in **17-¹⁸O**COCF₃, **R = H**.

(2) The small amount of trapping adducts with NaSCN indicates that the intermediate, if it forms, is quite reactive and cannot be trapped efficiently by strong nucleophiles. This is in contrast with the idea that a simple tertiary cation is stable. The large selectivity ($k_{\text{SCN}} / k_{\text{RSH}}$) indicates that nucleophile trapping should be best described as a concerted pathway, and partial bonding between nucleophiles and tertiary carbon explains the large selectivity

between thiols and NaSCN. Due to steric hindrance as well as weak bonding, a low trapping yield (less efficient compared to solvent) is expected⁹⁵.

(3) For tertiary halides in 50% (v : v) TFE, strongly solvated bases have no effect on the solvolysis behaviour. Only weakly solvated bases can provide an additional E2 pathway for elimination reactions, whose effect still depends on their basicity if the desolvation energy is similar.

(4) With a dimethylsulfonium leaving group, there is greater sensitivity to the added base but generally the same behaviour to non-basic nucleophiles as halides or trifluoroacetate leaving groups. The weakly nucleophilic base favours the intramolecular E_i pathway through an ylide intermediate, however, the nucleophilic base still favours E2 mechanism, which is consistent with their opposite regioselectivity.

Chapter 6: Solvolysis of 3,5-Bis(trifluoromethyl)cumyl substrates and on the search for thiono-thiolo rearrangement of thionophosphates in 50% (v : v) TFE

6.1 Introduction

The lifetime of 3,5-bis(trifluoromethyl) cumyl cations^{95,109} in 50% (v : v) TFE has been calculated as 10^{-13} s by extrapolating the linear correlation (Equation 19)³⁵ of first-order rate constants (k_S) of solvent attack on stable aryl cumyl cations with the solvolysis rates of corresponding chlorides (k_{solv}) in 50% (v : v) TFE.

$$\log k_S = -0.53 \log k_{\text{solv}} + 10.6 \quad (19)$$

Since the extrapolated lifetime of 3,5-bis(trifluoromethyl) cumyl cations in 50% (v : v) TFE is close to the bond vibration time scale, which suggests it is too unstable to exist; the solvolysis mechanism has been described as an enforced uncoupled concerted mechanism without any intermediates^{11-13,95,109}.

Intramolecular ether-acyl positional exchange for ester-type leaving groups has been used as a criterion for S_N1 mechanisms *i.e.* to infer the presence of a carbenium intermediate. Recent reports^{16,19} showed that the intramolecular exchange is also visible in a concerted solvolysis mechanism. In order to test the possible ether-acyl exchange of a tertiary substrate that was believed to solvolyse in a concerted pathway^{95,109}, a suitable ester nucleofuge that can distinguish between ether and acyl positions is required.

Besides ^{18}O labelling^{16,19,41}, thionoesters are another type of nucleofuge which can be used as a probe²⁸. Among these, thionophosphates have a reactivity comparable to chlorides and are suitable to address this issue²⁷. The advantage of using thiono-thiolo rearrangement rather than ^{18}O labelling has been already discussed in Chapters 1 and 5.

We wish to report here that by solvolysing 3,5-bis(trifluoromethyl) cumyl diethylthionophosphate in 50% (v : v) TFE, the O-S migration is visible and may be used to estimate the corresponding ion-pair's lifetime.

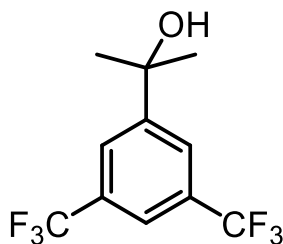
The formation of 3,5-bis(trifluoromethyl)- α -methyl styrene when solvolysing 3,5-bis(trifluoromethyl)cumyl chloride in 50% (v : v) TFE has been attributed to an intramolecular E_i mechanism¹¹⁰ since neither 0.5 M NaN_3 nor NaOAc show any effects on the elimination reactions and the azide adduct was only formed at the expense of solvent substitution products. However, Meng and Thibblin⁹⁸ as well as Creary *et al.*⁹⁹ demonstrated that it was the *anti*-proton which was extracted to generate alkene products in the solvolysis of some tertiary cyclic substrates. Using different nucleophiles and bases together with product analysis, we re-examined the elimination mechanism as well as the role of the added nucleophiles in these elimination reactions. Herein, we describe the elimination mechanism as a normal E_2 pathway, where the nucleophiles provide an additional pathway leading to the elimination product, which depends on the basicity and the desolvation energy of those nucleophiles.

6.2 Experimental Section

General

All the chemicals were purchased from Sigma-Aldrich, Alfa Aesar or Acros Organics, those for synthesis purpose were used directly without further purification. TFE was distilled from P₂O₅ and stored over 4Å molecular sieves. UHQ water was obtained from an ELGA PURELAB Option S-R 7-15 system. ¹H NMR and ¹³C NMR spectra were recorded on Bruker AV-HD 400 instrument. HPLC analysis was carried out on Waters 2690 (486 Tunable Absorbance Detector) and 2695 (2487 Dual λ Absorbance Detector) systems with a Hichrom C₁₈ column (HIRPB-624) and UV detection at 260 nm. A gradient elution was used, changing from 95% water and 5% acetonitrile to 5% water and 95% acetonitrile over 20 mins followed by a further 10 mins of the final eluent mixture.

Syntheses

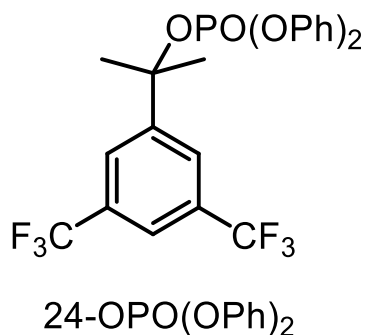


24-OH

3',5'-Bis(trifluoromethyl)cumyl alcohol (24-OH)¹¹⁴: Followed by the method reported by Wen and Crich¹¹³. 10 mL 3 M methylmagnesium bromide solution in diethyl ether (30 mmol) were introduced to an ice-cooled 200 mL round-bottom flask charged with 30 mL anhydrous diethyl ether and a magnetic stirrer bar with stirring. 1.80 mL 3',5'-bis(trifluoromethyl)acetophenone (10 mmol) dissolved in 5 mL diethyl ether were then added dropwise within 10 mins; after that the ice bath was removed and the mixture was stirred at RT for further 2 hours. Then ice bath was placed again and 50 mL saturated

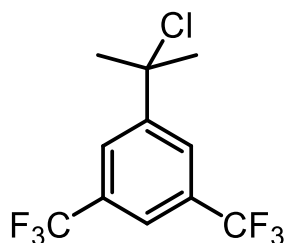
ammonium chloride solution was introduced slowly to quench the reaction. The ether phase was separated and washed with saturated aqueous NaHCO₃. Aqueous phase was extracted with diethyl ether (4 × 20 mL) and the combined organic phase was dried over Na₂SO₄ and evaporated under vacuum to afford 2.09 g **24-OH** as a white solid (77%).

¹H NMR (400 MHz, CDCl₃): 7.97 (2H, s), 7.79 (1H, s) and 1.66 (6H, s). ¹⁹F NMR (376.5 MHz, CDCl₃): -62.8. ¹³C NMR (100 MHz, CDCl₃): 151.6, 131.5 (q, J = 33.0 Hz), 124.9, 123.4 (q, J = 272.8 Hz), 120.9, 72.3 and 31.8.



3',5'-Bis(trifluoromethyl)cumyl diphenyl phosphate (24-OPO(OPh)₂): 1.36 g **24-OH** (5 mmol) and 1.22 g DMAP (10 mmol) were added into a 100-mL round flask followed by 20 mL DCM at 0 °C, then 1.66 mL diphenylphosphoryl chloride (8 mmol) were introduced dropwise within 10 mins, and the reaction mixture was allowed to warm to RT and stirred for 2 hours before evaporating the solvent. The residue was dissolved in enough ethyl acetate and the solution was filtered through a pad of Celite[®]. The filtrate was then evaporated and the residue was directly purified by silica gel chromatography using 30% diethyl ether-70% petroleum. The phosphate was not stable on silica gel, however, so only the last two fractions were collected as pure **24-OPO(OPh)₂** (15 mg), as a colourless oil. TLC and HPLC showed only one compound.

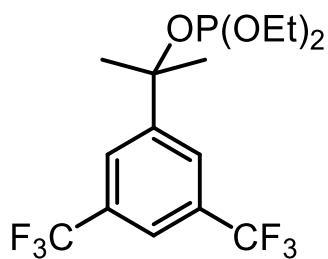
^1H NMR (400 MHz, CDCl_3): 8.09 (2H, s), 7.86 (1H, s), 7.37-7.25 (8H, m), 7.19-7.14 (2H, m) and 1.98 (6H, s). ^{19}F NMR (376.5 MHz, CDCl_3): -62.8. ^{31}P NMR (162 MHz, CDCl_3): -17.2. ^{13}C NMR (100 MHz, CDCl_3): 150.6 (d, $J = 7.6$ Hz), 148.0 (d, $J = 8.3$ Hz), 131.8 (q, $J = 33.3$ Hz), 129.8, 125.5, 124.9 (d, $J = 2.5$ Hz), 123.2 (q, $J = 273.0$ Hz), 121.7 (dt, $J = 7.0$, 3.5 Hz), 120.0 (d, $J = 5.1$ Hz), 85.3 (d, $J = 6.1$ Hz) and 29.8 (d, $J = 2.3$ Hz).



24-Cl

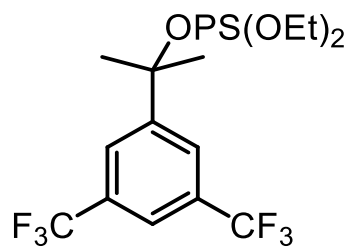
3',5'-Bis(trifluoromethyl)cumyl chloride (24-Cl)¹¹⁶: Followed by the method reported by Cook *et al.*¹¹⁵ 1.36 g **24-OH** (5 mmol) and 0.64 g lithium chloride (15 mmol) were added into a 50 mL round flask followed by 3 mL DCM at 0 °C, then 20 mL 35% concentrated HCl (200 mmol) was introduced dropwise within 10 mins, and the reaction mixture was allowed to warm to RT and stirred overnight before dilution with 20 mL cold water and 30 mL diethyl ether. The ether phase was separated, and the aqueous phase was extracted with more diethyl ether (4 × 15 mL); the organic phases were combined and dried over Na_2SO_4 before being concentrated. The residue was directly purified by silica gel chromatography, using 100% petroleum to afford 0.58 g **24-Cl** (40%) as a colourless oil, which only contains 1% alkene shown by ^1H NMR.

^1H NMR (400 MHz, CDCl_3): 8.06 (2H, s), 7.84 (1H, s) and 2.06 (6H, s). ^{19}F NMR (376.5 MHz, CDCl_3): -62.8. ^{13}C NMR (100 MHz, CDCl_3): 148.9, 131.7 (q, $J = 33.3$ Hz), 125.9, 123.2 (q, $J = 272.9$ Hz), 121.6 (dt, $J = 7.4$, 3.7 Hz), 67.4 and 34.1.



24-OP(OEt)₂

3',5'-Bis(trifluoromethyl)cumyl diethyl phosphite (24-OP(OEt)₂): Followed by the method reported by Dahl *et al.*¹¹⁷ 1.36 g **24-OH** (5 mmol) was added into a 100-mL round flask followed by 20 mL DCM at 0 °C, then 0.64 mL diethyl chlorophosphite (4.5 mmol) was introduced dropwise within 10 mins, followed by 0.69 mL triethylamine (5 mmol) dropwise within 10 mins. The reaction mixture was allowed to warm to RT and stirred for 1.5 hours before evaporation of the solvent. The residue was dissolved in diethyl ether and filtered through a pad of silica gel quickly; the solvent was then evaporated and the crude **24-OP(OEt)₂** (1.47 g, 75%) was obtained as a light yellow oil with satisfactory purity. Due to the instability on silica gel, the crude product was used directly for next step without chromatography purification. TLC showed one movable spot and a faint spot on baseline. ¹H NMR (400 MHz, CDCl₃): 7.94 (2H, s), 7.78 (1H, s), 3.95-3.87 (4H, m), 1.80 (6H, s) and 1.27 (t, J = 7.1 Hz). ¹⁹F NMR (376.5 MHz, CDCl₃): -62.9. ³¹P NMR (162 MHz, CDCl₃): 135.7. ¹³C NMR (100 MHz, CDCl₃): 150.8, 131.5 (q, J = 33.1 Hz), 125.3, 123.4 (q, J = 272.7 Hz), 120.9 (dt, J = 7.1, 3.5 Hz), 77.5 (d, J = 9.9 Hz), 57.7 (d, J = 9.0 Hz), 31.2 (d, J = 10.7 Hz) and 16.7 (d, J = 4.7 Hz).



24-OPS(OEt)₂

3',5'-Bis(trifluoromethyl)cumyl diethyl thionophosphate (24-OPS(OEt)₂): The crude 1.47 g **24-OP(OEt)₂** (3.75 mmol) and 0.24 g sulfur (7.5 mmol) were added into a 50-mL round flask followed by 20 mL dry THF. The solution under nitrogen was stirred at 35 °C for 24 hours before evaporating the solvent. The residue was dissolved in cold diethyl ether and filtered through a pad of silica gel quickly. The filtrate was concentrated, giving 1.27 g desired **24-OPS(OEt)₂** (80%) as a light yellow oil with satisfactory purity. Due to the instability on silica gel, chromatography purification was avoided. HPLC showed the impurity peaks were not solvolysis products.

¹H NMR (400 MHz, CDCl₃): 7.92 (2H, s), 7.82 (1H, s), 4.12 (4H, dq, J = 9.8, 7.1 Hz), 1.96 (6H, s) and 1.31 (t, J = 7.1 Hz). ¹⁹F NMR (376.5 MHz, CDCl₃): -62.9. ³¹P NMR (162 MHz, CDCl₃): 59.6. ¹³C NMR (100 MHz, CDCl₃): 148.8 (d, J = 5.4 Hz), 131.5 (q, J = 33.3 Hz), 125.3 (d, J = 2.5 Hz), 123.3 (q, J = 272.7 Hz), 121.3 (dt, J = 7.1, 3.5 Hz), 84.1 (d, J = 7.9 Hz), 64.2 (d, J = 5.6 Hz), 29.7 (d, J = 3.6 Hz) and 15.8 (d, J = 7.7 Hz).

Kinetics: All the rate determinations were done by HPLC at 30 °C. A 1 mL solution containing 1:1 (v : v) water-TFE, 7 mM 2,6-di-*tert*-butylpyridine, 1 mM 1,3-dimethoxybenzene (internal standard) and 1 M NaClO₄ (or other nucleophiles that the total salt concentration was adjust by NaClO₄ to afford a 1 M salt concentration) was made, then 10 μL 0.5 M substrate in acetonitrile or chloroform was introduced to the solution which

was quickly immersed in a thermostatic water bath. The progress of the reactions was monitored by analysing aliquots of the reactions mixture using HPLC for two to three half-lives, focusing on accumulation of the alcohol product. The peak areas in the chromatograms were integrated and a first order equation fitted to these data; in all cases, $R^2 > 0.999$.

Product analysis: The products from the solvolysis of **24-Cl** and **24-OPO(OPh)₂** were analysed by HPLC after 8 half-lives under the conditions shown in **Kinetics** above. With 1 M NaClO₄, there are only three peaks in the chromatogram of solvolysis of both substrates. The corresponding alcohol (**24-OH**) was identified by comparing with the authentic sample; the remaining two peaks were assumed to be the trifluoroethyl ether (**24-OCH₂CF₃**) and alkene (**25**). In the presence of different concentrations of NaSCN, there were another two peaks (whose areas increased with increasing NaSCN concentrations), determined as the corresponding thiocyanate (**24-SCN**) and isothiocyanate (**24-NCS**). In the presence of NaN₃, an additional peak was detected and was assigned as the corresponding azide adduct (**24-N₃**). In the presence of NaOH, NaOAc or HOCH₂CH₂NH₂, no additional peaks could be detected.

Solvolysis of 24-OPS(OEt)₂: a 1 mL solution of 1:1 (v : v) water-TFE, containing 7 mM 2,6-di-*tert*-butylpyridine, 0.2 mM 3-nitroacetophenone (internal standard) and 1 M NaClO₄ was made; 10 μL 0.5 M substrate in acetonitrile was introduced to the solution which was quickly immersed in a thermostatic water bath. During the solvolysis, another peak accumulated with the same rate constant as that of the starting material's decay. It was demonstrated that this new product was stable under solvolysis conditions after 8 half-lives.

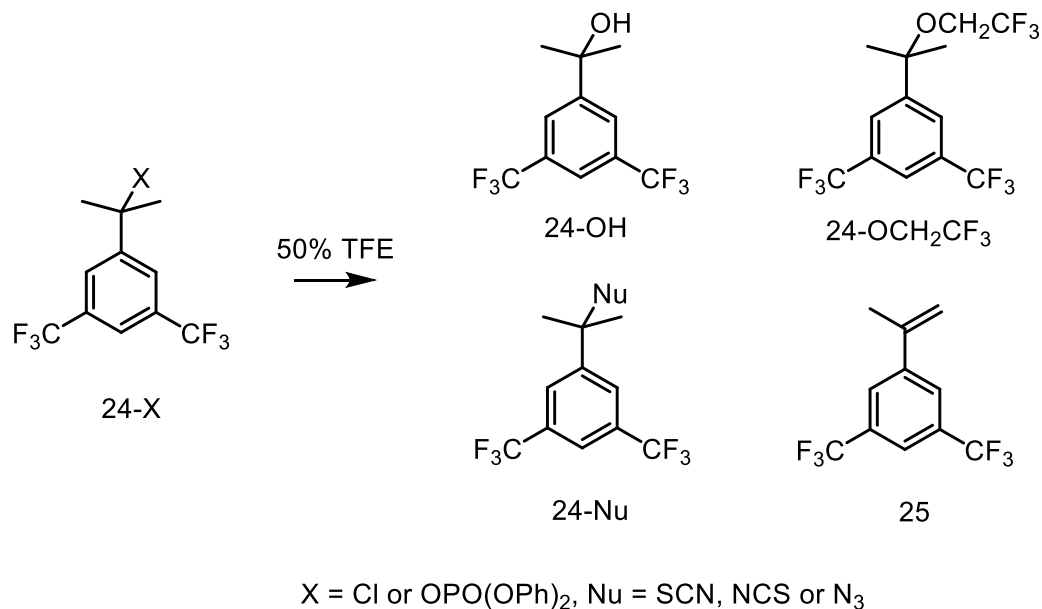
A large scale solvolysis was carried out with 8 mM substrate, 0.64 mM triphenylphosphine sulfide (^{31}P NMR internal standard), 10 mM 2,6-di-*tert*-butylpyridine and 1 M NaClO_4 in 250 mL 1:1 (v : v) water-TFE at 30 °C. After 8 half-lives, most TFE was evaporated and the aqueous phase was extracted with chloroform (5×20 mL) and 20 mL ethyl acetate. The organic phases were combined, dried over Na_2SO_4 , and filtered before being concentrated. The residue was directly dissolved in 0.7 mL CDCl_3 and analysed by NMR. ^{31}P NMR showed the internal standard peak at 43.31 ppm, and a peak at 22.42 ppm, whose integrated peak areas were 1 : 1. Coupled ^{31}P NMR showed the peak at 22.42 ppm was a pentet. ^{13}C NMR showed only four doublet peaks below 80 ppm at 63.61 (J = 6.6 Hz), 52.07 (J = 4.2 Hz), 31.5 (J = 7.0 Hz) and 15.78 (J = 7.2 Hz).

6.3 Results

'Thiocyanate clock' and 'azide clock' methods

The pseudo first-order rate constant of solvolysis of 3,5-bis(trifluoromethyl)cumyl chloride (**24-Cl**) in 50% (v : v) TFE at 30 °C (1 M NaClO_4) is $3.6 \pm 0.1 \times 10^{-5} \text{ s}^{-1}$. In the presence of 1 M NaSCN , the rate constant increases to $4.5 \pm 0.1 \times 10^{-5} \text{ s}^{-1}$; while in the presence of 1 M NaN_3 , the rate constant reduces to $3.0 \pm 0.1 \times 10^{-5} \text{ s}^{-1}$. This is attributed to different non-specific salt effects (medium effects). Product analysis shows **24-Cl** and 3,5-Bis(trifluoromethyl)cumyl diphenyl phosphate (**24-OPO(OPh)₂**) in 1 M NaClO_4 generated only three products: alcohol (**24-OH**), trifluoroethyl ether (**24-OCH₂CF₃**) and alkene (**25**). The yields were measured by HPLC using an internal standard of known concentration. In the presence of 1 M NaSCN , another two new compounds could be detected. These are assigned as thiocyanate (**24-SCN**) and isothiocyanate (**24-NCS**). In the presence of 1 M

NaN₃, one new compound was detected and assigned as the azide adduct (**24-N₃**). The solvolysis products and their yields are shown in Scheme 6.1 and Table 6.1.



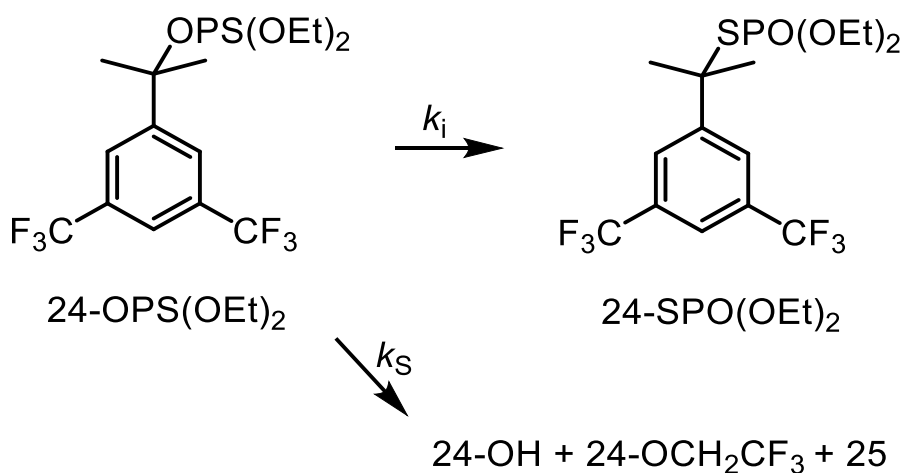
Scheme 6.1. Products from solvolysis of **24-X** in 50% (v : v) TFE

Table 6.1. Product yield of solvolysing **24-X** in 50% (v : v) TFE with NaClO₄, NaSCN and NaN₃

substrate	salt [1 M]	yield of product (%) (± 0.2)			
		24-OH	24-OCH ₂ CF ₃	25	24-Nu
24-Cl	NaClO ₄	57.0	13.1	29.9	
	NaSCN	33.7	7.7	25.1	33.5 (two products)
	NaN ₃	34.8	9.3	31.4	24.5
24-OPO(OPh) ₂	NaClO ₄	30.1	10.0	59.9	
	NaSCN	19.0	6.5	44.6	29.9

Thiono-thiolo rearrangement

The yield of the assigned rearranged product of solvolysis of 3,5-Bis(trifluoromethyl)cumyl diethyl thionophosphate (**24-OP(S)(OEt)₂**) in 50% (v : v) TFE ($t_{1/2} \approx 20$ h) detected by HPLC was 9%, assuming the extinction coefficients of both **24-OP(S)(OEt)₂** and **24-SP(O)(OEt)₂** are the same (Scheme 6.2). ³¹P NMR spectra of the products recovered from a larger scale solvolysis of **24-OP(S)(OEt)₂** are consistent with the structure of **24-SP(O)(OEt)₂**. ³¹P NMR showed two peaks centred at 43.31 ppm (triphenylphosphine sulfide as the internal standard) and 22.42 ppm. The new signal at 22.42 ppm might be **24-SP(O)(OEt)₂** or **O=P(SEt)(OEt)₂** (from bimolecular ethyl transfer between **24-OP(S)(OEt)₂** and **SP(O)(OEt)₂** generated in the course of solvolysis of **24-OP(S)(OEt)₂**). However, the proton coupled ³¹P NMR spectrum showed the peak at 22.42 ppm was a pentet; and the reported ³¹P NMR chemical shift of **O=P(SEt)(OEt)₂** in CDCl₃ was 27.00-27.90 ppm¹¹¹. Previous work²⁷ also confirmed the very slow bimolecular methyl transfer between dimethylthionophosphates and **SP(O)(OMe)₂**, and so overall, we rule out the formation of **O=P(SEt)(OEt)₂**. Furthermore, proton decoupled ¹³C NMR showed only four signals below 80 ppm that are doublets, the expected doublet ¹³C peak for **O=P(SEt)(OEt)₂** at 25.0 ppm¹¹² (CH₃CH₂S-) was undetectable. The doublet peaks at 52.09 and 31.55 ppm are assigned to be the tertiary carbon and its adjacent methyl group in **24-SPO(OEt)₂**. Using triphenylphosphine sulfide as the internal standard, the yield of **24-SP(O)(OEt)₂** was ~8%. The formation of ~8% **24-SPO(OEt)₂** thus represents $k_i \approx 0.1k_s$ in Scheme 6.2.



Scheme 6.2. Thiono-thiolo rearrangement of **24-OP(S)(OEt)₂** in 50% (v : v) TFE

The effects of different additives on product distribution

Other additives have also been studied to elucidate the effects on product composition (substitution vs elimination) and are summarized in Table 6.2.

Table 6.2. Product yield of solvolysing **24-Cl** with different additives in 50% (v : v) TFE

substrate	additives [1 M]	product yield (%) (± 0.2)			
		24-OH	24-OCH ₂ CF ₃	25	24-Nu
24-Cl	NaClO ₄	57.0	13.1	29.9	
	NaOAc	46.8	13.8	36.9	< 2.5
	HOCH ₂ CH ₂ NH ₂	52.0	11.4	36.6	ND ^{†††}
	NaOH	46.6	10.8	42.6	
	NaSCH ₂ CH ₂ OH	31.9	8.6	51.6	< 7.9
	HSCH ₂ CH ₂ OH	50.5	10.4	0	39.2

^{†††}: Not detected

6.4 Discussion

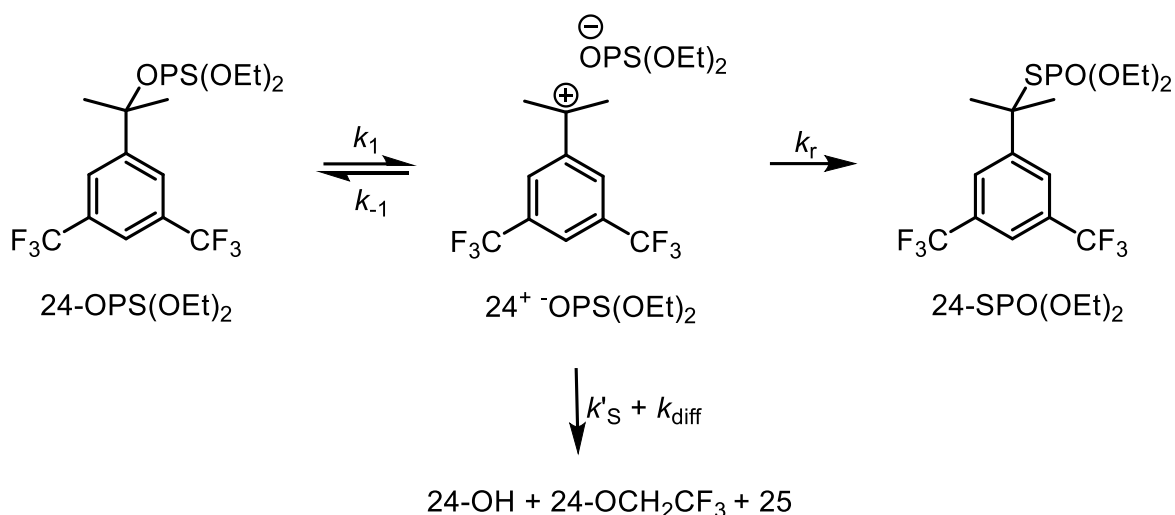
The ‘thiocyanate clock’ and ‘azide clock’ methods did not provide useful information. Similar to simple tertiary substrates (Chapter 5), the relatively low yield of trapping products if all result from S_N2 pathways should accelerate the solvolysis reaction by 40%. However, there is either an 18% rate decrease or a 25% rate increase by NaN_3 or NaSCN . Therefore, the different salt effects make these data impossible to interpret clearly—a simple S_N2 contribution may be occurring, or the reaction is unhelpfully sensitive to the medium.

Since the reaction of simple tertiary substrates with NaN_3 or NaSCN is assigned to be a concerted mechanism (Chapter 5), **24-X**, which is less reactive than simple tertiary compounds, should also react with strong nucleophiles in a concerted pathway. This is confirmed independently by the large selectivity difference between NaSCN and $\text{NaSCH}_2\text{CH}_2\text{OH}$ on **24-Cl**.

The small amount (~8%) of visible thiono-thiolo rearrangement during solvolysis of **24-OP(S)(OEt)₂** in 50% (v : v) TFE may indicate a short-lived intermediate that can partition between solvent trapping (k'_s) and leaving group exchange (k_r) (Scheme 6.3), or the ‘leaving group exchange’ could follow a concerted pathway that does not go through an intermediate, since concerted ^{18}O exchange has been already reported by Richard *et al.*^{16,19} Using Equation 19, the lifetime of **24⁺** was calculated as $10^{-13} \text{ s}^{95,109}$, which means it cannot exist as an intermediate in 50% (v : v) TFE. However, the extrapolation predicts that the lifetime of a simple tertiary cation is only 0.5 ps in 50% (v : v) TFE, which is one order magnitude shorter than our experimental analysis (Chapter 5). If we use the current experimental data $k'_s = 8 \times 10^{10} \text{ s}^{-1}$ for simple tertiary chlorides, then 1 ps ($k'_s \approx 10^{12} \text{ s}^{-1}$)

can be obtained for the lifetime of **24**⁺ in 50% (v : v) TFE based on Equation 19, which is still not consistent with ~8% thiono-thiolo rearrangement occurring by a step-wise pathway ($k_r \approx 1.4 \times 10^{10} \text{ s}^{-1}$, see Chapter 5). The predicted lifetime of 1 ps ($k'_s \approx 10^{12} \text{ s}^{-1}$) for such an intermediate will only generate $\approx 1\%$ rearranged product. If all the rearrangement took place by a step-wise pathway, k'_s can be obtained as $1.4 \times 10^{11} \text{ s}^{-1}$, which is comparable to that of simple tertiary cations in 50% (v : v) TFE (Chapter 5).

Since an even lower rearranged product yield was found for simple tertiary substrates (4%) (Chapter 5), whose thiono-thiolo rearrangement was assigned to be step-wise, we think that all the 8% rearranged product should result from a step-wise pathway, which leads $k'_s = 1.4 \times 10^{11} \text{ s}^{-1}$. As Mayr pointed out^{1,2}, the linear relationship between the solvolysis rates and the lifetime of the corresponding carbenium ions does not hold for less reactive precursors and their corresponding cations. Thus, it is reasonable that compared with simple tertiary chlorides, **24-Cl** solvolyses one order magnitude slower but generates an intermediate with a similar lifetime to simple tertiary cations in 50% (v : v) TFE. The reason why the relationship breaks down for less reactive precursors or precursors with different structures is attributed to different intrinsic barriers⁸⁰.



Scheme 6.3. Thiono-thiolo rearrangement of **24-OPS(OEt)₂** in 50% (v : v) TFE by step-wise pathway

It is obvious that NaN₃ does not act as a nucleophile only, otherwise the ratio of

$\frac{[\text{24-OH}] + [\text{24-OCH}_2\text{CF}_3]}{[\text{25}]}$ should be a constant regardless of added nucleophiles (assuming that

the different salt effects on product distribution are not significant). However, replacing

NaClO₄ by NaSCN increased the elimination reactions slightly (Table 6.2). Since NaSCN

shows no general base effects (Chapter 4), this small change must be attributed to different

salt effects on the product determining steps. In the presence of NaN₃, the change is more

significant than the medium effect alone, which indicates that NaN₃ also acts as a base.

Since there is no direct evidence for the solvolytic E_i mechanisms proposed by Richard *et*

al.^{109,110}, and Meng and Thibblin⁹⁸ already reported the anti-periplanar elimination

mechanism of a similar substrate, we do not think a new E_i mechanism is needed here for

the base strength-insensitive elimination. However, a clear explanation for this base

strength-insensitive elimination seems necessary.

We suggest that a slightly coupled conventional E2 pathway, which is not sensitive to basic additives, can account for the observation summarized in Table 6.2. Since the solvent's concentration is ≈ 35 M for 50% (v : v) TFE, the competition between 1 M additives and 35 M solvent molecules cannot be strong (if the transition state is just slightly coupled by the bases). Even the strongest base (NaSCH₂CH₂OH) only gives 20% more elimination product (70% increase) than for simple solvolysis. Our results agree with Bunnett and Migdal's reports¹⁰⁰ that in aqueous solvent, the elimination of some tertiary halides is not sensitive to the added bases, but related to their desolvation energy. If those bases have a similar pK_b , the less solvated the base, the larger the effect on elimination reactions will be. When changing the solvent to one which has a lower Y_{Cl} value, the base-induced elimination will become more visible, which is consistent with a continuous mechanistic shift from uncoupled concerted E2/S_N2 (where desolvation is more important than basicity) to classical E2/S_N2 (basicity dominated).

Finally, the instability of **25** in the presence of a thiol indicates that radical addition is significant. The radical addition cannot be initiated by single electron transfer, since **25** is stable in the presence of thiolate, which is a stronger reduction reagent. We prefer to suggest that hydrogen atom transfer is the initiation step (Scheme 6.4), then the radical pair formed within the solvent cage collapses quickly to give **24-Nu** at the expense of **25**. Therefore, due to this radical addition reaction, we do not encourage people to use thiol as the trapping reagent if the solvolysis involves a significant amount of elimination products.

or exchange rate is much faster than the solvolysis rate^{26,81}, it is clear evidence for a reversible ion-pair formation. If the scrambling is completely invisible⁶³, it is clear evidence for either irreversible ion-pair generation or a classical concerted pathway. For those compounds whose solvolysis mechanisms are uncoupled concerted pathways or with unstable intermediates (the borderline region), slow rearrangement cannot be used as a criterion to support the ion-pair existence^{16,19,54}.

(3) Similar to simple tertiary chlorides, the effect of bases on elimination reactions of **24-Cl** is not significant but is related to their desolvation energy. If they have a similar pK_b , the less solvated the base, the larger the effect on elimination will be, which is consistent with Bunnett and Migdal's E2 mechanism picture¹⁰⁰. In addition, we confirm that the most powerful elimination reagent so far is thiolate, rather than hydroxide, for tertiary substrates in aqueous solvents. There is no need to explain the base strength-insensitive elimination mechanism by an E_i pathway, since Meng and Thibblin⁹⁸ as well as Creary *et al.*⁹⁹ provided steric evidence for an *anti*-periplanar elimination pathway. A slightly coupled E2 pathway can account for the observation satisfactorily.

(4) The significant radical addition between thiol and alkenes reduced the potential value of using thiol as an efficient trapping reagent. The best neutral nucleophile could be used only if the reaction does not involve significant elimination products, otherwise, the trapping product yield will be masked by the side reaction, which will generate trapping adducts at the expense of elimination products.

In conclusion, the solvolysis reaction of **24-X** in 50% (v : v) TFE can be interpreted by a step-wise pathway dominated by solvent reorganization with an intermediate whose lifetime is approximately 1 ps by extrapolation, but predicts only 1% thiono-thiolo exchange, which does not agree well with our experimental data. The ~8% rearrangement found gives $k'_s = 1.4 \times 10^{11} \text{ s}^{-1}$, which might support a step-wise pathway and indicates that the extrapolation based on stable cations is not valid. Both elimination and substitution reactions are not very sensitive to the added nucleophiles or bases (still more sensitive than simple tertiary substrates, see Chapter 5), but react in concerted pathways, indicating that the bond coupling in the transition state is not as strong as that for classical S_N2 and $E2$ reactions (highly likely due to steric reasons and solvent effects). Changing the solvents to those which have a lower Y_{Cl} value, the effects of added bases and nucleophiles will become larger, which is consistent with a continuous mechanism spectrum of $E1/S_N1$ to $E2/S_N2$. The concerted solvolysis mechanism is also possible but the bond coupling will be very weak and is not necessary to explain the observations here.

Chapter 7: Summary and Perspective

The simple secondary carbenium ions controversy might be considered resolved since the classical 2-norbornyl cation is not suggested as an intermediate with sufficient lifetime to be trapped in solvents ($\tau < 10^{-13}$ s) that are more nucleophilic than 50% (v : v) TFE. It will be even less likely that 2-alkyl carbenium ions will be intermediates in these solvents, as the precursors are more prone to solvent nucleophilic assistance. Although the calculated k_S (intrinsic rate constant of trapping 2-alkyl cations in solvents) can support a pre-association step-wise pathway for 2-butyl or endo-2-norbornyl tosylate in 50% (v : v) TFE, the k_S for simple secondary carbenium ions is not much larger than the best estimated k_S for simple tertiary carbenium ions in the same aqueous solvent. The energy difference between simple secondary and tertiary carbenium ions is about 15.7 kcal·mol⁻¹ in the gas phase and about 9.5 kcal mol⁻¹ in SO₂ClF solution⁵⁹; and the best estimated k_S for simple tertiary carbenium ions in 50% (v : v) TFE is $\approx 10^{11}$ s⁻¹, leading to a value of k_S for simple secondary carbenium ions in 50% (v : v) TFE $> 10^{13}$ s⁻¹. Therefore, any reactions involved simple secondary precursors ought to be excluded from step-wise mechanisms. It is better to view this behaviour as a consequence of an enforced concerted uncoupled dynamic process, since some classical criteria used to support the ion-pair formation still can be observed.

Among those criteria, the most important observation that needs to be addressed is oxygen scrambling in ester-type leaving groups. Previous work^{16,19,43} as well as our analysis indicate that this probe is no longer definitive evidence for reversible step-wise pathways. It could also take place through an uncoupled concerted mechanism without ion-pair formation. The thiono-thiolo rearrangement of thiono esters is more useful, if the upper

limit of the concerted rearrangement can be measured. Upon the development of organic synthetic strategies, more reactive thiono ester nucleofuges (not only thionocarboxylates or thionophosphates) may be obtained in the future, such as thionosulfonates, which will make this probe a relatively robust and widely applicable tool. However, since the concerted thiono-thiolo rearrangement cannot be avoided, this probe has its own detection limit. The faster the anion rotates, the higher the detection limit will be.

Whether a carbenium ion intermediate can be formed or not seems insensitive to the corresponding nucleofuge. According to Mayr's view¹⁻³, the nucleofuge will only (or mainly) affect the general reactivity of the corresponding precursors but cannot shift the mechanism from concerted to step-wise if the intrinsic barrier to form the corresponding cation intermediate is too high. Therefore, consistent with previous reports, azoxytosylate, a type of nucleofuge that requires less nucleophilic assistance than the tosylate, still cannot drive the pathway from uncoupled concerted to step-wise, if the electrophile itself is kinetically too reactive to become an intermediate. The reason why azoxytosylate precursors are generally less reactive than tosylate precursors but also suffer less nucleophilic assistance from strong nucleophiles might be due to different intrinsic barriers rather than thermodynamic considerations. The observation of similar reactivity of sp^2 and sp hybridized carbenium ions generated from precursors of significantly different solvolysis rates reported by Mayr *et al.*⁸⁰ was also attributed to intrinsic barriers.

The best estimated lifetime for solvent trapping of simple tertiary carbenium ions in 50% (v : v) TFE, based on 1-adamantyl structures and thiono-thiolo rearrangement is between 3 and 7 ps. This unambiguously supports a step-wise solvolysis mechanism without solvent

pre-association for simple tertiary precursors. On the other hand, the reaction between strong nucleophiles (NaSCN or NaN₃) and simple tertiary substrates is suggested as an enforced concerted pathway, indicating the intermediate is too kinetically reactive to be trapped by nucleophiles that need to diffuse into the solvent shell. Therefore, only the trapping products from concerted pathways can be observed but inefficiently compete with solvolysis products from step-wise pathways. Meanwhile, simple tertiary halides in 50% (v : v) TFE are quite insensitive to the strength of strong bases¹¹⁸. Only the nucleophilic base thiolate can accelerate the elimination pathway (but with very little substitution), consistent with previously proposed E2 pathways¹⁰⁰, in which the desolvation energy is more important than basicity. However, thiolate still cannot compete efficiently with step-wise solvolysis in aqueous solvents, since the transition state is E1-like and the coupling between base and C-H is weak.

However, the estimated lifetime of simple tertiary carbenium ions is still based on indirect measurements and kinetic parameters. The best solution to this problem may be the direct observation of carbenium ions' decay by laser flash photolysis methods. Current laser flash photolysis can only measure those cations mainly and reliably by time-resolved UV-vis spectroscopy; as the development of other more accurate spectroscopy methods with ultra-fast laser (*i.e.* picosecond time-resolved IR) in the future, the dream of direct observation of those simple cations may come true and can finally solve this problem.

Pessimistically, the writer does not think the laser flash photolysis can be useful to determine the lifetime of those very unstable cations (*ca.* lifetime less than 10 ps, borderline region, whose precursors are suspected to go through uncoupled concerted

solvolysis pathways). The first reason is the quantum yield of cation formation will be significantly decreased as the cation become less stable¹¹⁹, because other competing processes now will dominate (*i.e.* light-induced radical pair formation). Thus, the detection limit thus will prevent any observations of weak signals¹²⁰. The second reason (perhaps more important) is that when the cation become less stable, the rate limiting step to consume those photo-generated cations is no longer bond formation, and other slower processes (*ca.* solvent reorganization) will become dominant, which sets the lowest lifetime limit for all the photo-generated cations in solutions. Therefore, a carbenium ion with lifetime between 0.1 and 10 ps for solvent trapping cannot be determined experimentally. Chemists still have to use correlations and extrapolations based on other lifetime-known carbeniums to ‘estimate’ whether the target carbenium ion can exist or not, namely, how fast intrinsic bond formation is. Currently, the most widely used and well-known correlation methods are solvolysis rates-lifetime^{11-13,95,109} and electrophilicity-nucleophilicity equations¹⁻³. Both have been criticized^{1-3,14,80} as only useful within a local structure family, with the later one more robust. To improve the accuracy and scope of those extrapolation methods, more universal parameters related to carbenium ions’ lifetime need to be found in the future and this (together with theoretical calculation) may provide a solution for chemists to predict changes from S_N1 to S_N2 mechanisms.

In conclusion, we think the topic of solvolysis mechanisms of simple secondary substrates should be closed and people would better not talk about the existence of simple secondary cations from their precursors in nucleophilic solutions anymore, even for endo-2-norbornyl or 2-adamantyl precursors. As for simple tertiary substrates, the classical tools finally can only narrow the window down to 3 to 7 ps for the lifetime of simple tertiary cations in 50%

(v : v) TFE but unambiguously indicate the step-wise solvolysis mechanism. The more accurate lifetime will come from direct laser flash photolysis observation in the future.

References

- * This article is published in Journal of Physical Organic Chemistry as a special issue on the 15th European Symposium on Organic Reactivity (ESOR), Kiel, Germany, 2015.
See full article: D. Li, N. H. Williams, *J. Phys. Org. Chem.* **2016**, 29, 709.
- ** This work is in memory of Professors P. v. R. Schleyer and H. C. Brown, for their long-time contribution to the non-classical cation issue.
- ***This work is dedicated to Professors J. P. Richard, H. Maskill as well as W. P. Jencks, for their contribution to ion-pair dynamics.
- [1] H. Mayr, A. R. Ofial, *Acc. Chem. Res.* **2016**, 49, 952.
- [2] H. Mayr, *Tetrahedron* **2015**, 71, 5095.
- [3] N. Streidl, B. Denegri, O. Kronja, H. Mayr, *Acc. Chem. Res.* **2010**, 43, 1537.
- [4] S. Minegishi, S. Kobayashi, H. Mayr, *J. Am. Chem. Soc.* **2004**, 126, 5174.
- [5] R. D. Guthrie, W. P. Jencks, *Acc. Chem. Res.* **1989**, 22, 343.
- [6] a) IUPAC GOLD BOOK, <http://goldbook.iupac.org/N04246.html> (accessed February 2017). b) IUPAC GOLD BOOK, <http://goldbook.iupac.org/E01965.html> (accessed February 2017)
- [7] IUPAC GOLD BOOK, <http://goldbook.iupac.org/S05762.html> (accessed February 2017).
- [8] E. V. Anslyn, D. A. Dougherty, *Modern Physical Organic Chemistry*, University Science Books, Sausalito, CA **2006**.
- [9] W. P. Jencks, *Acc. Chem. Res.* **1980**, 13, 161.
- [10] F. A. Carey, R. J. Sundberg, *Advanced Organic Chemistry* (5th ed., Springer, Berlin **2008**).

- [11] a) J. P. Richard, W. P. Jencks, *J. Am. Chem. Soc.* **1984**, *106*, 1373. b) J. P. Richard, W. P. Jencks, *J. Am. Chem. Soc.* **1984**, *106*, 1396.
- [12] J. P. Richard, M. E. Rothenberg, W. P. Jencks, *J. Am. Chem. Soc.* **1984**, *106*, 1361.
- [13] J. P. Richard, W. P. Jencks, *J. Am. Chem. Soc.* **1984**, *106*, 1383.
- [14] a) R. A. McClelland, V. M. Kanagasabapathy, N. S. Banait, S. Steenken, *J. Am. Chem. Soc.* **1989**, *111*, 3966. b) F. L. Cozens, V. M. Kanagasabapathy, R. A. McClelland, S. Steenken, *Can. J. Chem.* **1999**, *77*, 2069.
- [15] U. Kaatze, R. Pottel, A. Schumacher, *J. Phys. Chem.* **1992**, *96*, 6017.
- [16] Y. Tsuji, J. P. Richard, *J. Am. Chem. Soc.* **2006**, *128*, 17139.
- [17] T. L. Amyes, J. P. Richard, *J. Am. Chem. Soc.* **1990**, *112*, 9507.
- [18] a) C. Lim, S. Kim, S. Yoh, M. Fujio, Y. Tsuno, *Tetrahedron Lett.* **1997**, *38*, 3423. b) S. Kim, S. Yoh, C. Lim, M. Mashima, M. Fujio, Y. Tsuno, *J. Phys. Org. Chem.* **1998**, *11*, 254. c) S. Yoh, D. Cheong, C. Lee, S. Kim, J. Park, M. Fujio, Y. Tsuno, *J. Phys. Org. Chem.* **2001**, *14*, 123.
- [19] Y. Tsuji, M. M. Toteva, T. L. Amyes, J. P. Richard, *Org. Lett.* **2004**, *6*, 3633.
- [20] Y. Tsuji, T. Mori, M. M. Toteva, J. P. Richard, *J. Phys. Org. Chem.* **2003**, *16*, 484.
- [21] C. Paradisi, J. F. Bunnett, *J. Am. Chem. Soc.* **1985**, *107*, 8223.
- [22] Y. Tsuji, K. Yatsugi, M. Fujio, T. Tsuno, *Tetrahedron Lett.* **1995**, *36*, 1461.
- [23] Y. Tsuji, S. H. Kim, Y. Saeki, K. Yatsugi, M. Fujio, Y. Tsuno, *Tetrahedron Lett.* **1995**, *36*, 1465.
- [24] A. D. Allen, M. Fujio, O. S. Tee, T. T. Tidwell, Y. Tsuji, Y. Tsuno, K. Yatsugi, *J. Am. Chem. Soc.* **1995**, *117*, 8974.
- [25] S. Chang, W. J. le Noble, *J. Am. Chem. Soc.* **1984**, *106*, 810.
- [26] D. T. Stoelting, V. J. Shiner, Jr. *J. Am. Chem. Soc.* **1993**, *115*, 1695.

- [27] C. D. Poulter, D. S. Mautz, *J. Am. Chem. Soc.* **1991**, *113*, 4895.
- [28] J. P. Richard, Y. Tsuji, *J. Am. Chem. Soc.* **2000**, *122*, 3963.
- [29] J. P. Richard, *J. Am. Chem. Soc.* **1989**, *111*, 6735.
- [30] T. L. Amyes, J. P. Richard, *J. Am. Chem. Soc.* **1991**, *113*, 8960.
- [31] J. P. Richard, T. L. Amyes, T. Vontor, *J. Am. Chem. Soc.* **1991**, *113*, 5871.
- [32] H. Maskill, W. P. Jencks, *J. Am. Chem. Soc.* **1987**, *109*, 2062.
- [33] a) P. E. Dietze, R. Hariri, J. Khattak, *J. Org. Chem.* **1989**, *54*, 3317. b) P. E. Dietze, W. P. Jencks, *J. Am. Chem. Soc.* **1986**, *108*, 4549. c) A. D. Allen, I. C. Ambidge, T. T. Tidwell, *J. Org. Chem.* **1983**, *48*, 4527. d) J. J. Dannenberg, J. K. Barton, B. Bunch, B. J. Goldberg, T. Kowalski, *J. Org. Chem.* **1983**, *48*, 4524. e) D. Farcașiu, *J. Chem. Soc., Chem. Commun.* **1994**, *22*, 2611.
- [34] a) H. C. Brown, *The Non-classical Ion Problem* (with comments by P. v. R. Schleyer), Plenum Press, New York, **1977**. b) T. H. Lowry, K. S. Richardson, *Mechanism and Theory in Organic Chemistry*, Harper & Row Publishers, New York, **1987**. c) L. Ma, E. H. Sweet, P. G. Schultz, *J. Am. Chem. Soc.* **1999**, *121*, 10227. d) R. Bruckner, *Advanced Organic Chemistry*, Harcourt/Academic Press, Burlington, Massachusetts, **2002**. e) R. A. McClelland, Carbocations, in *Reactive Intermediate Chemistry* (Eds. R. A. Moss, M. S. Platz, M. Jones, Jr.), John Wiley & Sons, Inc., Hoboken, New Jersey, 2004 f) C. C. Lee, E. W. C. Wong, *Can. J. Chem.* **1965**, *43*, 2254. g) J. M. Harris, R. E. Hall, P. v. R. Schleyer, *J. Am. Chem. Soc.* **1971**, *93*, 2551. h) V. J. Shiner, Jr., R. D. Fisher, *J. Am. Chem. Soc.* **1971**, *93*, 2553. i) D. J. Raber, J. M. Harris, R. E. Hall, P. v. R. Schleyer, *J. Am. Chem. Soc.* **1971**, *93*, 4821. j) J. M. Harris, D. L. Mount, D. J. Raber, *J. Am. Chem. Soc.* **1978**, *100*, 3139. k) C. C. Lee, L. K. M. Lam, *J. Am. Chem. Soc.* **1965**, *88*, 2831. l) C. C. Lee, B. Hahn, L. K. M. Lam, D. J. Woodcock, *Can. J.*

- Chem.* **1970**, *48*, 3831. m) J. B. Stothers, C. T. Tan, *J. Am. Chem. Soc.* **1972**, *94*, 8581.
- n) S. Chang, W. J. le Noble, *J. Am. Chem. Soc.* **1984**, *106*, 810.
- [35] M. M. Toteva, J. P. Richard, *J. Am. Chem. Soc.* **1996**, *118*, 11434.
- [36] P. E. Dietze, R. Hariri, J. Khattak, *J. Org. Chem.* **1989**, *54*, 3317.
- [37] P. E. Dietze, W. P. Jencks, *J. Am. Chem. Soc.* **1986**, *108*, 4549.
- [38] A. D. Allen, I. C. Ambidge, T. T. Tidwell, *J. Org. Chem.* **1983**, *48*, 4527.
- [39] J. J. Dannenberg, J. K. Barton, B. Bunch, B. J. Goldberg, T. Kowalski, *J. Org. Chem.* **1983**, *48*, 4524.
- [40] D. Farcașiu, *J. Chem. Soc., Chem. Commun.* **1994**, *22*, 2611.
- [41] a) Y. Tsuji, T. Mori, J. P. Richard, T. L. Amyes, M. Fujio, Y. Tsuno, *Org. Lett.* **2001**, *3*, 1237; b) M. Teshima, Y. Tsuji, J. P. Richard, *J. Phys. Org. Chem.* **2010**, *23*, 730.
- [42] a) T. W. Bentley, C. T. Bowen, D. H. Morten, P. V. R. Schleyer, *J. Am. Chem. Soc.* **1981**, *103*, 5466; b) P. E. Peterson, R. E. Kelley Jr, R. Belloli, K. A. Sipp, *J. Am. Chem. Soc.* **1965**, *87*, 5169; c) T. W. Bentley, P. V. R. Schleyer, *J. Am. Chem. Soc.* **1976**, *98*, 7658.
- [43] P. E. Dietze, M. Wojciechowski, *J. Am. Chem. Soc.* **1990**, *112*, 5240.
- [44] B. K. Carpenter in *Reactive Intermediate Chemistry* (Eds: R. A. Moss, M. S. Platz, M. Jones Jr.), John Wiley and Sons: Hoboken, NJ, 2004; pp. 925–960.
- [45] J. Javier Ruiz Pernía, I. Tuñón, I. H. Williams, *J. Phys. Chem. B*, **2010**, *114*, 5769.
- [46] T. L. Amyes, W. P. Jencks, *J. Am. Chem. Soc.* **1989**, *111*, 7888.
- [47] D. H. Burns, J. D. Miller, H. K. Chan, M. O. Delaney, *J. Am. Chem. Soc.* **1997**, *119*, 2125.
- [48] Y. Muraki, T. Taguri, R. Yamakawa, T. Ando, *J. Chem. Ecol.* **2014**, *40*, 250.
- [49] X. Ma, Y. Zhang, Y. Zhang, C. Peng, Y. Che, J. Zhao, *Adv. Mater.* **2015**, *27*, 7746.

- [50] M. Pohmakotr, W. Ieawsuwan, P. Tuchinda, P. Kongsaree, S. Prabpai, V. Reutrakul, *Org. Lett.* **2004**, *6*, 4547.
- [51] Y. Nitta, Y. Arakawa, N. Ueyama, *Chem. Pharm. Bull.* **1986**, *34*, 2710.
- [52] C. Chiappe, D. Pieraccini, *Green Chem.* **2003**, *5*, 193.
- [53] a) H. Veisi, R. Ghorbani-Vaghei, J. Mahmoodi, *Bull. Korean Chem. Soc.* **2011**, *32*, 3692; b) H. Veisi, A. Sedrpoushan, S. Hemmati, D. Kordestani, *Phosphorus, Sulfur, Silicon Relat. Elem.* **2012**, *187*, 769.
- [54] D. Li, N. H. Williams, *J. Phys. Org. Chem.* **2016**, *29*, 709.
- [55] H. C. Brown, M. Ravindranathan, F. J. Chloupek, I. Rothberg, *J. Am. Chem. Soc.* **1978**, *100*, 3143.
- [56] a) M. L. Sinnott, M. C. Whiting, *J. Chem. Soc., Perkin Trans. 2*, **1975**, 1446. b) J. A. Bone, J. R. Pritt, M. C. Whiting, *J. Chem. Soc., Perkin Trans. 2*, **1975**, 1447.
- [57] Y. Tsuji, D. Hara, R. Hagimoto, J. P. Richard, *J. Org. Chem.*, **2011**, *76*, 9568.
- [58] M. Saunders, M. R. Kates, *J. Am. Chem. Soc.* **1980**, *102*, 6868.
- [59] a) E. M. Arnett, T. C. Hofelich, *J. Am. Chem. Soc.*, **1983**, *105*, 2889. b) J. W. de M. Carneiro, P. v. R. Schleyer, W. Koch, K. Raghavachari, *J. Am. Chem. Soc.*, **1990**, *112*, 4064. c) S. Sieber, P. Buzek, P. v. R. Schleyer, W. Koch, J. W. de M. Carneiro, *J. Am. Chem. Soc.*, **1993**, *115*, 259. d) M. Boronat, P. Viruela, A. Corma, *J. Phys. Chem.*, **1996**, *100*, 633.
- [60] a) J. P. Richard, personal communication (2016). b) T. W. Bentley, S. J. Norman, R. Kemmer, M. Christl, *Liebigs Ann.* **1995**, 599.
- [61] W. Kirmse, R. Siegfried, *J. Am. Chem. Soc.* **1983**, *105*, 950.

- [62] a) P. R. Schreiner, P. v. R. Schleyer, H. F. Schaefer, III, *J. Org. Chem.* **1997**, *62*, 4216;
b) J. Kong, D. Roy, D. Lenoir, X. Zhang, J. Zou, P. v. R. Schleyer, *Org. Lett.* **2009**,
11, 4684. c) C. L. Firme, *J. Braz. Chem. Soc.* **2012**, *23*, 513.
- [63] W. Adcock, N. A. Trout, D. Vercoe, D. K. Taylor, V. J. Shiner, Jr., T. S. Sorensen, *J. Org. Chem.* **2003**, *68*, 5399.
- [64] T. W. Bentley, P. v. R. Schleyer, *J. Am. Chem. Soc.* **1976**, *98*, 7658.
- [65] a) S. P. McManus, M. R. Smith, J. M. Shankweiler, R. V. Hoffman, *J. Org. Chem.* **1988**, *53*, 141. b) R. J. Abraham, J. J. Byrne, L. Griffiths, Manuel Perez, *Magn. Reson. Chem.* **2006**, *44*, 491.
- [66] M. C. Barden, J. Schwartz, *J. Org. Chem.* **1995**, *60*, 5963.
- [67] H. Maskill, J. T. Thompson, A. A. Wilson, *J. Chem. Soc., Perkin Trans. 2* **1984**, 1693.
- [68] I. M. Gordon, H. Maskill, *J. Chem. Soc., Chem. Commun.* **1989**, 1358.
- [69] J. K. Conner, J. Haider, M. N. S. Hill, H. Maskill, M. Pestman, *Can. J. Chem.* **1998**, *76*, 862.
- [70] I. M. Gordon, H. Maskill, *J. Chem. Soc., Perkin Trans. 2* **2001**, 2059.
- [71] H. Maskill, *J. Chem. Soc., Perkin Trans. 2* **1986**, 1241.
- [72] M. Novak, M. J. Poturalski, W. L. Johnson, M. P. Jones, Y. T. Wang, S. A. Glover, *J. Org. Chem.* **2006**, *71*, 3778.
- [73] X. C. Huang, K. S. E. Tanaka, A. J. Bennet, *J. Am. Chem. Soc.* **1998**, *120*, 1405.
- [74] J. P. Richard, personal communication (2016). Thiocyanic acid, Wikipedia,
https://en.wikipedia.org/wiki/Thiocyanic_acid (accessed January 2017).
- [75] J. I. Finneman, J. C. Fishbein, *J. Am. Chem. Soc.* **1995**, *117*, 4228.
- [76] E. H. White, K. W. Field, W. H. Hendrickson, P. Dzadzic, D. F. Roswell, S. Paik, P. W. Mullen, *J. Am. Chem. Soc.* **1992**, *114*, 8023.

- [77] H. Maskill, personal communication (2016).
- [78] G. A. Olah, R. Herges, K. Laali, G. A. Segal, *J. Am. Chem. Soc.* **1986**, *108*, 2054.
- [79] M. Eckert-Maksić, Z. Glasovac, H. Maskill, I. Zrinski, *J. Phys. Org. Chem.* **2003**, *16*, 491.
- [80] P. A. Byrne, S. Kobayashi, E.-U. Würthwein, J. Ammer, H. Mayr, *J. Am. Chem. Soc.* **2017**, *139*, 1499.
- [81] P. Li, J. J. Zhao, C. G. Xia, F. W. Li, *Org. Lett.* **2014**, *16*, 5992.
- [82] R. Ray, A. D. Chowdhury, D. Maiti, G. K. Lahiri, *Dalton Trans.* **2014**, *43*, 38.
- [83] B. Wang, L. Jiang, J. Wang, J. Ma, M. Liu, H. Yu, *Tetrahedron: Asymmetry* **2011**, *22*, 980.
- [84] J. L. N. Fernandes, M. C. de Souza, E. C. S. Brenelli, J. A. Brenelli, *Synthesis* **2009**, 4058.
- [85] T. E. Stevens, *J. Org. Chem.* **1964**, *29*, 311.
- [86] N. S. Isaacs, *Physical Organic Chemistry*, Prentice Hall, New Jersey, **1996**.
- [87] M. Cocivera, S. Winstein, *J. Am. Chem. Soc.* **1963**, *85*, 1702.
- [88] a) J. P. Richard, *J. Chem. Soc., Chem. Commun.* **1987**, 1768. b) J. P. Richard, *J. Am. Chem. Soc.* **1989**, *111*, 1455. c) J. P. Richard, *J. Org. Chem.* **1992**, *57*, 625. d) J. P. Richard, T. L. Amyes, T. Vontor, *J. Am. Chem. Soc.* **1992**, *114*, 5626. e) R. A. McClelland, F. L. Cozens, S. Steenken, T. L. Amyes, J. P. Richard, *J. Chem. Soc., Perkin Trans. 2* **1993**, 1717.
- [89] S. Minegishi, S. Kobayashi, H. Mayr, *J. Am. Chem. Soc.* **2004**, *126*, 5174.
- [90] J. P. Richard, personal communication (2016). The facial selectivity 1 : 4 of azide attack on a cumyl carboxylate in MeOH was reported by Sommer and Carey (L. H.

- Sommer, F. A. Carey, *J. Org. Chem.* **1967**, *32*, 800.), the expected trapping adduct yield for 1-adamantyl bromide with 1 M anion-type nucleophiles is less than 2%.
- [91] a) R. L. Buckson, S. G. Smith, *J. Org. Chem.* **1967**, *32*, 634. b) S. G. Smith, D. J. W. Goon, *J. Org. Chem.* **1969**, *34*, 3127.
- [92] P. Müller, J. Rossier, *J. Chem. Soc., Perkin Trans. 2* **2000**, 2232.
- [93] a) Y. Chiang, W. K. Chwang, A. J. Kresge, M. F. Powell, S. Szilagyi, *J. Org. Chem.* **1984**, *49*, 5218. b) Y. Chiang, A. J. Kresge, *J. Am. Chem. Soc.* **1985**, *107*, 6363. c) R. A. McClelland, V. M. Kanagasabapathy, N. S. Banait, S. Steenken, *J. Am. Chem. Soc.* **1989**, *111*, 3966.
- [94] D. Watanabe, H. Hamaguchi, *Chem. Phys.* **2008**, *354*, 27.
- [95] T. L. Amyes, M. M. Toteva, J. P. Richard, Crossing the Borderline Between S_N1 and S_N2 Nucleophilic Substitution at Aliphatic Carbon, in *Reactive Intermediate Chemistry* (Eds. R. A. Moss, M. S. Platz, M. Jones, Jr.), John Wiley & Sons, Inc., Hoboken, New Jersey, 2004
- [96] S. W. Paine, J. H. Ridd, *J. Chem. Soc., Perkin Trans. 2* **1996**, 2571.
- [97] M. Mascal, N. Hafezi, M. D. Toney, *J. Am. Chem. Soc.* **2010**, *132*, 10662.
- [98] Q. Meng, A. Thibblin, *J. Chem. Soc., Perkin Trans. 2* **1999**, 1397.
- [99] X. Creary, V. P. Casingal, C. E. Leahy, *J. Am. Chem. Soc.* **1993**, *115*, 1734.
- [100] a) J. F. Bunnett, C. A. Migdal, *J. Org. Chem.* **1989**, *54*, 3037. b) J. F. Bunnett, C. A. Migdal, *J. Org. Chem.* **1989**, *54*, 3041. c) D. S. Bailey, W. H. Saunders, Jr, *J. Org. Chem.* **1973**, *38*, 3363. d) J. F. Bunnett, S. Sridharan, W. P. Cavin, *J. Org. Chem.* **1979**, *44*, 1463.

- [101] a) R. A. McClelland, V. M. Kanagasabapathy, N. S. Banait, S. Steenken, *J. Am. Chem. Soc.* **1992**, *114*, 1816. b) R. A. McClelland, N. S. Banait, S. Steenken, *J. Am. Chem. Soc.* **1986**, *108*, 7023.
- [102] T. C. Atack, R. M. Lecker, S. P. Cook, *J. Am. Chem. Soc.* **2014**, *136*, 9521.
- [103] S. V. Pronin, C. A. Reiher, R. A. Shenvi, *Nature* **2013**, *501*, 195.
- [104] B. Gaspar, E. M. Carreira, *Angew. Chem. Int. Ed.* **2008**, *47*, 5758.
- [105] H. Someya, H. Yorimitsu, K. Oshima, *Tetrahedron* **2010**, *66*, 5993.
- [106] S. Yoshida, H. Yorimitsu, K. Oshima, *J. Organomet. Chem.* **2007**, *692*, 3110.
- [107] B. Badet, M. Julia, J. M. Mallet, C. Schmitz, *Tetrahedron* **1988**, *44*, 2913.
- [108] M. Nishizawa, M. Skwarczynski, H. Imagawa, T. Sugihara, *Chem. Lett.* **2002**, *31*, 12.
- [109] J. P. Richard, T. L. Amyes, T. Vontor, *J. Am. Chem. Soc.* **1991**, *113*, 5871.
- [110] T. L. Amyes, J. P. Richard, *J. Am. Chem. Soc.* **1991**, *113*, 8960.
- [111] B. Mlotkowska, M. Wartalowska-Graczyk, *J. Prakt. Chem.* **1987**, *329*, 735.
- [112] J. L. Mundy, J. M. Harrison, P. Watts, C. M. Timperley, *Phosphorus, Sulfur, Silicon Relat. Elem.* **2006**, *181*, 1847.
- [113] P. Wen, D. Crich, *J. Org. Chem.* **2015**, *80*, 12300.
- [114] F. Hoffmann-Emery, H. Hilpert, M. Scalone, P. Waldmeier, *J. Org. Chem.* **2006**, *71*, 2000.
- [115] T. C. Atack, R. M. Lecker, S. P. Cook, *J. Am. Chem. Soc.* **2014**, *136*, 9521.
- [116] K. Takeuchi, T. Kurosaki, K. Okamoto, *Tetrahedron*, **1980**, *36*, 1557.
- [117] T. Boesen, C. Madsen, D. S. Pedersen, B. M. Nielsen, A. B. Petersen, M. Å. Petersen, M. Munck, U. Henriksen, C. Nielsen, O. Dahl, *Org. Biomol. Chem.* **2004**, *2*, 1245.
- [118] J. P. Richard, personal communication (2016)

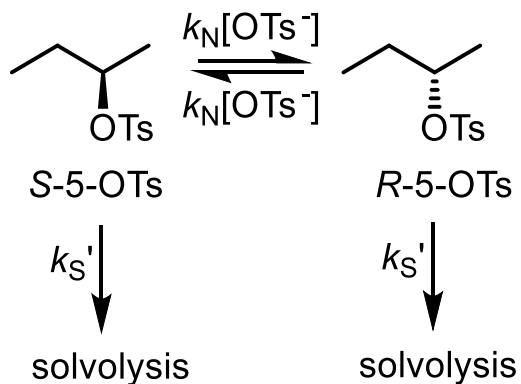
[119] J. Ammer, C. Nolte, H. Mayr, *J. Am. Chem. Soc.* **2012**, *134*, 13902.

[120] H. Mayr, personal communication (2015)

Appendices

Chapter 2

Derivation of Equation 3:



$$\frac{d[S - 5 - \text{OTs}]}{dt} = k_N[\text{OTs}^-][R - 5 - \text{OTs}] - (k_N[\text{OTs}^-] + k_S')[S - 5 - \text{OTs}]$$

$$\frac{d[R - 5 - \text{OTs}]}{dt} = k_N[\text{OTs}^-][S - 5 - \text{OTs}] - (k_N[\text{OTs}^-] + k_S')[R - 5 - \text{OTs}]$$

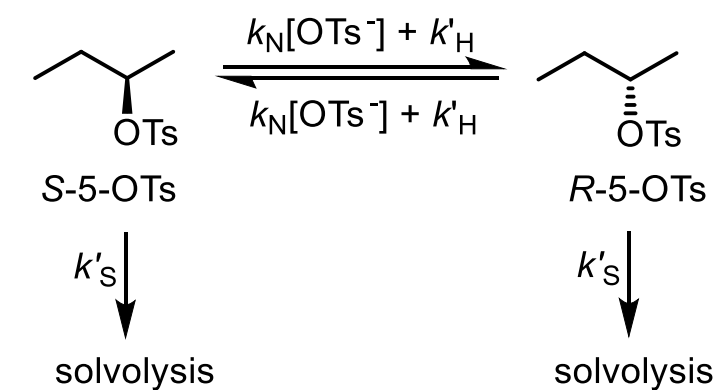
$$\frac{d[S - 5 - \text{OTs} + R - 5 - \text{OTs}]}{dt} = -k_S'[S - 5 - \text{OTs} + R - 5 - \text{OTs}]$$

$$[S - 5 - \text{OTs} + R - 5 - \text{OTs}]_0 = [A]_0, \quad [R - 5 - \text{OTs}]_0 = \frac{1 - ee}{2} [A]_0$$

Using Mathematica^a gives Equation 3:

$$\frac{[R - 5 - \text{OTs}]}{[S - 5 - \text{OTs} + R - 5 - \text{OTs}]} = 0.5 - \frac{ee}{2} \exp\left(-2k_N[A]_0\left(t - \frac{1 - e^{-k_S't}}{k_S'}\right)\right)$$

Derivation of Equation 4:



$$\frac{d[S - 5 - \text{OTs}]}{dt}$$

$$= (k_N[\text{OTs}^-] + k'_H)[R - 5 - \text{OTs}] - (k_N[\text{OTs}^-] + k'_H + k'_S)[S - 5 - \text{OTs}]$$

$$\frac{d[R - 5 - \text{OTs}]}{dt}$$

$$= (k_N[\text{OTs}^-] + k'_H)[S - 5 - \text{OTs}] - (k_N[\text{OTs}^-] + k'_H + k'_S)[R - 5 - \text{OTs}]$$

$$\frac{d[S - 5 - \text{OTs} + R - 5 - \text{OTs}]}{dt} = -k'_S[S - 5 - \text{OTs} + R - 5 - \text{OTs}]$$

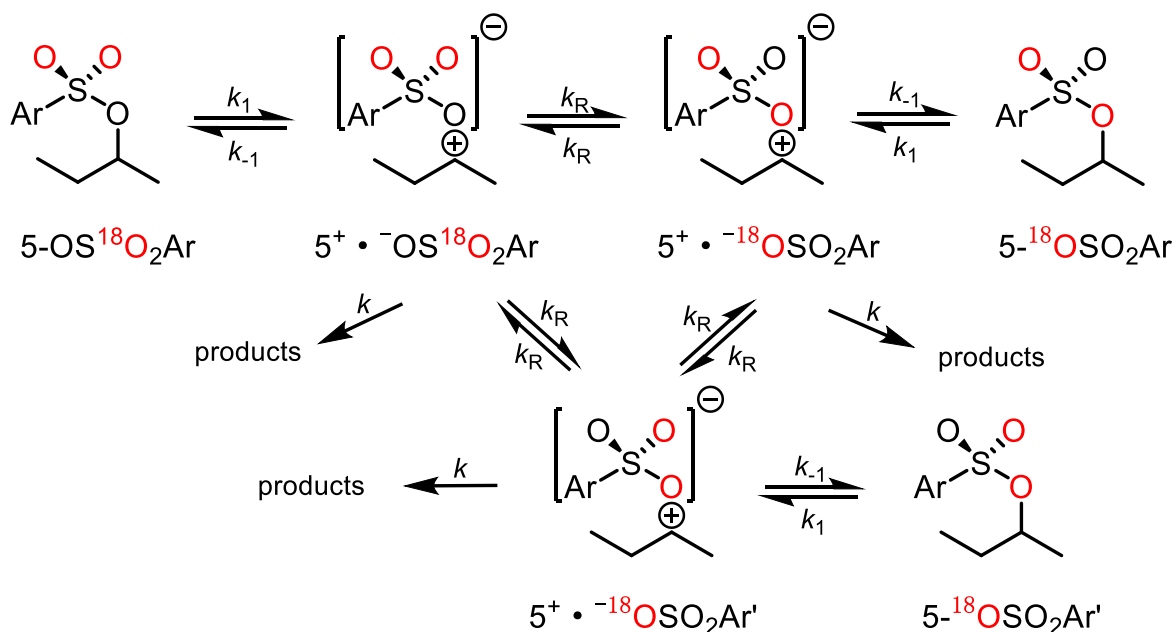
$$[S - 5 - \text{OTs} + R - 5 - \text{OTs}]_0 = [A]_0,$$

$$[R - 5 - \text{OTs}]_0 = \frac{1 - ee}{2} [A]_0$$

Using Mathematica^a gives Equation 4:

$$\frac{[R - 5 - \text{OTs}]}{[S - 5 - \text{OTs} + R - 5 - \text{OTs}]} = 0.5 - \frac{ee}{2} \exp(-2k_N[A]_0(t - \frac{1 - e^{-k'_S t}}{k'_S})) - 2k'_H t$$

Derivation of Equation 6:



$$\frac{d[5 - \text{OS}^{18}\text{O}_2\text{Ar}]}{dt} = k_{-1}[5^+ \cdot ^-\text{OS}^{18}\text{O}_2\text{Ar}] - k_1[5 - \text{OS}^{18}\text{O}_2\text{Ar}]$$

$$\frac{d[5 - ^{18}\text{OSO}_2\text{Ar}]}{dt} = k_{-1}[5^+ \cdot ^{-18}\text{OSO}_2\text{Ar}] - k_1[5 - ^{18}\text{OSO}_2\text{Ar}]$$

$$\frac{d[5 - ^{18}\text{OSO}_2\text{Ar}']}{dt} = k_{-1}[5^+ \cdot ^{-18}\text{OSO}_2\text{Ar}'] - k_1[5 - ^{18}\text{OSO}_2\text{Ar}']$$

$$\frac{d[5^+ \cdot ^-\text{OS}^{18}\text{O}_2\text{Ar}]}{dt}$$

$$= k_1[5 - \text{OS}^{18}\text{O}_2\text{Ar}] + k_R[5^+ \cdot ^{-18}\text{OSO}_2\text{Ar} + 5^+ \cdot ^{-18}\text{OSO}_2\text{Ar}']$$

$$- (k_{-1} + 2k_R + k_S)[5^+ \cdot ^-\text{OS}^{18}\text{O}_2\text{Ar}] = 0$$

$$\frac{d[5^+ \cdot ^{-18}\text{OSO}_2\text{Ar}]}{dt}$$

$$= k_1[5 - ^{18}\text{OSO}_2\text{Ar}] + k_R[5^+ \cdot ^-\text{OS}^{18}\text{O}_2\text{Ar} + 5^+ \cdot ^{-18}\text{OSO}_2\text{Ar}']$$

$$- (k_{-1} + 2k_R + k_S)[5^+ \cdot ^{-18}\text{OSO}_2\text{Ar}] = 0$$

$$\frac{d[5^+ \cdot \text{}^{-18}\text{OSO}_2\text{Ar}']}{dt} = k_1[5 - \text{}^{18}\text{OSO}_2\text{Ar}'] + k_R[5^+ \cdot \text{}^{-}\text{OS}^{18}\text{O}_2\text{Ar} + 5^+ \cdot \text{}^{-18}\text{OSO}_2\text{Ar}] - (k_{-1} + 2k_R + k_S)[5^+ \cdot \text{}^{-18}\text{OSO}_2\text{Ar}'] = 0$$

$$[5 - \text{OS}^{18}\text{O}_2\text{Ar}]_0 = [A]_0,$$

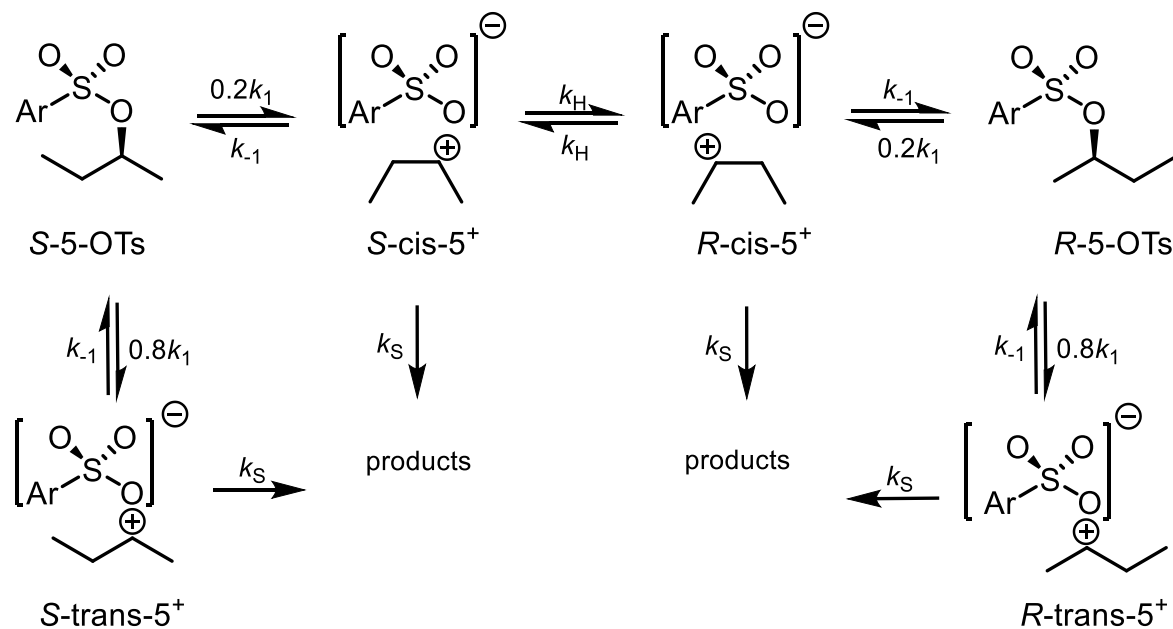
$$[5 - \text{}^{18}\text{OSO}_2\text{Ar}]_0 = [5 - \text{}^{18}\text{OSO}_2\text{Ar}']_0 = 0$$

Using Mathematica^a gives Equation 6:

$$\frac{[5 - \text{}^{18}\text{OSO}_2\text{Ar} + 5 - \text{}^{18}\text{OSO}_2\text{Ar}']}{[5 - \text{}^{18}\text{OSO}_2\text{Ar} + 5 - \text{}^{18}\text{OSO}_2\text{Ar}' + 5 - \text{OS}^{18}\text{O}_2\text{Ar}]} = \frac{2}{3}(1 - e^{-k_i t}) \text{ where}$$

$$k_i = \frac{3k_1k_{-1}k_R}{(k_{-1} + k_S)(k_{-1} + k_S + 3k_R)} = 5.4 \times 10^{-7} \text{ s}^{-1}$$

Derivation of Equation 7:



$$\frac{d[S - 5 - \text{OTs}]}{dt} = k_{-1}[S - \text{cis} - 5^+ + S - \text{trans} - 5^+] - k_1[S - 5 - \text{OTs}]$$

$$\frac{d[R - 5 - \text{OTs}]}{dt} = k_{-1}[R - \text{cis} - 5^+ + R - \text{trans} - 5^+] - k_1[R - 5 - \text{OTs}]$$

$$\frac{d[S - \text{trans} - 5^+]}{dt} = 0.8k_1[S - 5 - \text{OTs}] - (k_{-1} + k_S)[S - \text{trans} - 5^+] = 0$$

$$\frac{d[R - \text{trans} - 5^+]}{dt} = 0.8k_1[R - 5 - \text{OTs}] - (k_{-1} + k_S)[R - \text{trans} - 5^+] = 0$$

$$\begin{aligned} \frac{d[S - \text{cis} - 5^+]}{dt} &= 0.2k_1[S - 5 - \text{OTs}] + k_H[R - \text{cis} - 5^+] \\ &\quad - (k_{-1} + k_S + k_H)[S - \text{cis} - 5^+] = 0 \end{aligned}$$

$$\begin{aligned} \frac{d[R - \text{cis} - 5^+]}{dt} &= 0.2k_1[R - 5 - \text{OTs}] + k_H[S - \text{cis} - 5^+] \\ &\quad - (k_{-1} + k_S + k_H)[R - \text{cis} - 5^+] = 0 \end{aligned}$$

$$[R - 5 - \text{OTs}]_0 = \frac{1 - ee}{2} [S - 5 - \text{OTs} + R - 5 - \text{OTs}]_0 = 0.045[A]_0$$

Using Mathematica^a gives Equation 7:

$$\frac{[R - 5 - \text{OTs}]}{[S - 5 - \text{OTs} + R - 5 - \text{OTs}]} = \frac{1}{2} (1 - 0.91e^{-2k'_H t}) \text{ where}$$

$$2k'_H = \frac{0.4k_1k_{-1}k_H}{(k_{-1} + k_S)(k_{-1} + k_S + 2k_H)} = 4.2 \times 10^{-7} \text{ s}^{-1}$$

Table A2.1 Rearrangement of **7-OTs** to **6-OTs** when solvolysing **7-OTs** in 50% aqueous (v : v) TFE

Time/s	[6-OTs] / [7-OTs]
0	0.00
165600	0.39
180000	0.56
194400	0.84
252000	1.48
280800	2.01
340200	6.98

Table A2.2 Racemization of *S*-5-OTs (10 mM) in 50% aqueous (v : v) TFE at different time intervals

Reaction time/h	Peak area for <i>S</i> -5-OTs /mV·s	Peak area for <i>R</i> -5-OTs /mV·s	[5-OTs] / [<i>R</i> -5-OTs]
0	790.416	37.143	22.3:1
17	605.824	35.487	18.1:1
24.5	526.297	36.283	15.5:1
41	342.526	28.671	12.9:1
48.5	257.423	24.804	11.4:1
65	128.900	14.745	9.7:1
73.5	183.281	20.816	9.6:1

Table A2.3 Observed racemization rate of *S*-5-OTs (10 mM) against the tosylate anion presented in 50% aqueous (v : v) TFE

[OTs ⁻] (M)	k in [<i>R</i> -5-OTs] / [5-OTs] = $0.5 - 0.455e^{-kt}$
0	$0.46 \pm 0.03 \times 10^{-6} \text{ s}^{-1}$
0.1	$0.75 \pm 0.05 \times 10^{-6} \text{ s}^{-1}$
0.5	$2.31 \pm 0.07 \times 10^{-6} \text{ s}^{-1}$

a: <http://www.wolfram.com/mathematica/index.en.html?footer=lang>

Chapter 3

Table A3.1 Product analysis of solvolysis of **11-ex-OTs** in 50% (v : v) TFE with different salts

Salts [1 M]	11-ex-OH/inter	average	11-ex-OCH ₂ CF ₃ /inter	average	average 11-ex-OH/ 11-ex-OCH ₂ CF ₃	11-ex-Nu%
NaClO ₄	1.075	1.070± 0.005	0.226	0.220± 0.003	4.86	
	1.074		0.217			
	1.061		0.218			
	1.066		0.220			
	1.072		0.222			
NaSCN	0.588	0.582± 0.005	0.125	0.125± 0.001	4.66	45.2
	0.582		0.125			
	0.577		0.126			
	0.583		0.124			
	0.579		0.125			
NaN ₃	0.712	0.706± 0.006	0.175	0.174± 0.002	4.05	31.8
	0.709		0.176			
	0.700		0.176			
	0.705		0.174			
	0.706		0.172			

inter: internal standard

Table A3.2 Product analysis of solvolysis of **11-en-OTs** in 50% (v : v) TFE with different salts

Salts [1 M]	11-ex-OH/inter	average	11-ex-OCH ₂ CF ₃ /inter	average	average 11-ex-OH/ 11-ex-OCH ₂ CF ₃	11-ex-Nu%
NaClO ₄	1.034	1.034±	0.229	0.227±	4.55	
	1.035		0.228			
	1.035	0.002	0.228	0.002		
	1.031	0.226				
	1.034	0.226				
NaSCN	0.481	0.478±	0.121	0.120±	4.00	52.7
	0.478		0.120			
	0.477	0.002	0.120	0.001		
	0.478	0.120				
	0.478	0.129				
NaN ₃	0.598	0.593±	0.162	0.163±	3.64	40.2
	0.596		0.162			
	0.588	0.003	0.165	0.001		
	0.593	0.162				
	0.593	0.162				

inter: internal standard

Table A3.3 Product analysis of solvolysis of **d-11-en-OTs** in 50% (v : v) TFE with different salts

Salts [1 M]	11-ex-OH/inter	average	11-ex-OCH ₂ CF ₃ /inter	average	average 11-ex-OH/ 11-ex-OCH ₂ CF ₃	11-ex-Nu%
NaClO ₄	1.287	1.278± 0.004	0.282	0.282± 0.003	4.53	
	1.277		0.285			
	1.274		0.280			
	1.277		0.281			
NaSCN	0.598	0.600± 0.002	0.148	0.148± 0.001	4.06	52.1
	0.602		0.149			
	0.599		0.148			
	0.601		0.147			

inter: internal standard

Chapter 4

Table A4.1 12-azo-OTs solvolysis products peak integrals against the internal standard with different [NaSCN]

[NaSCN]/ M	Ionic strength	12-OH	12-OCH ₂ CF ₃	13	12-SCN + 12-NCS	Total products
0	1.0	2.30	1.00	0.16	0.00	3.46
0.1	1.0	2.10	0.95	0.17	0.29	3.51
0.14	1.0	2.05	0.93	0.18	0.37	3.53
0.2	1.0	1.97	0.91	0.18	0.48	3.54
0.3	1.0	1.85	0.88	0.19	0.65	3.57
0.5	1.0	1.65	0.82	0.20	0.88	3.55
0.67	1.0	1.54	0.78	0.20	1.02	3.54
0.85	1.0	1.46	0.76	0.20	1.13	3.55
1.0	1.0	1.42	0.75	0.21	1.17	3.55

Individual error bar: ± 0.01

Table A4.2 Absolute yield of trapping adducts (**12-SCN** + **12-NCS**) with different [NaSCN] during solvolysis of **12-azo-OTs** in 50% TFE

[NaSCN]/M	Ionic strength	(12-SCN+ 12-NCS)% ($\pm 0.2\%$)
0	1.0	0.0
0.1	1.0	8.2
0.14	1.0	10.9
0.2	1.0	14.5
0.3	1.0	19.3
0.5	1.0	26.2
0.67	1.0	30.3
0.85	1.0	33.6
1.0	1.0	34.8

Table A4.3 **12-OTs** solvolysis products peak integrals against the internal standard with different [NaSCN]

[NaSCN]/M	Ionic strength	12-OH	12-OCH ₂ CF ₃	12-SCN + 12-NCS
0	1.0	3.60	1.05	0.00
0.1	1.0	2.73	0.79	1.18
0.3	1.0	1.87	0.54	2.37
0.5	1.0	1.38	0.40	3.00
0.75	1.0	1.06	0.31	3.43
1.0	1.0	0.85	0.25	3.72

Individual error bar: ± 0.01

Table A4.4 Absolute yield of trapping adducts (**12-SCN** + **12-NCS**) with different [NaSCN] during the solvolysis of **12-OTs** in 50% TFE

[NaSCN]/M	Ionic strength	(12-SCN + 12-NCS)% ($\pm 0.2\%$)
0	1.0	0.0
0.1	1.0	24.0
0.3	1.0	48.3
0.5	1.0	61.7
0.75	1.0	70.5
1.0	1.0	76.4

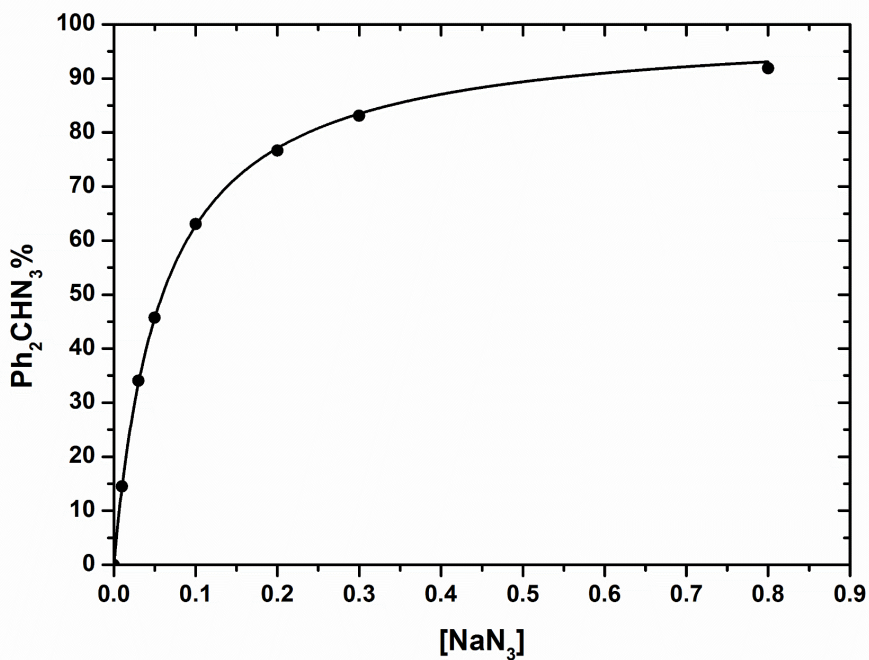


Figure A4.1 Benzhydryl azide yield with different [NaN₃] when solvolysing benzhydryl chloride in 50% (v : v) TFE, the black line was fitted by Equation 13 of an S_N1 mechanism (single intermediate)

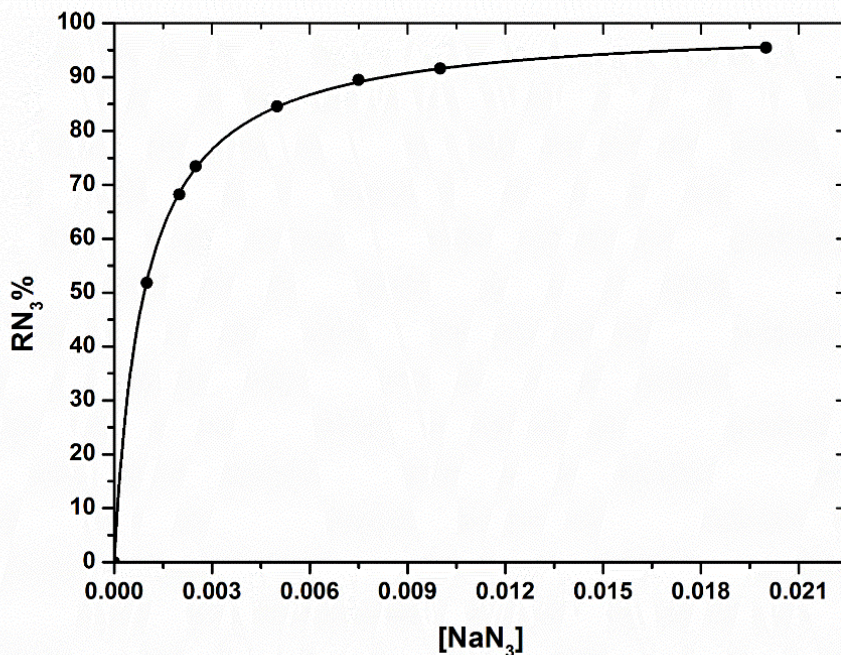


Figure A4.2 Azide adduct yield with different [NaN₃] when solvolysing 4-(p-methylphenyl)-4-acetoxy-2,5-cyclohexadienone in water, the black line was fitted by Equation 13 of an S_N1 mechanism (single intermediate)⁷²

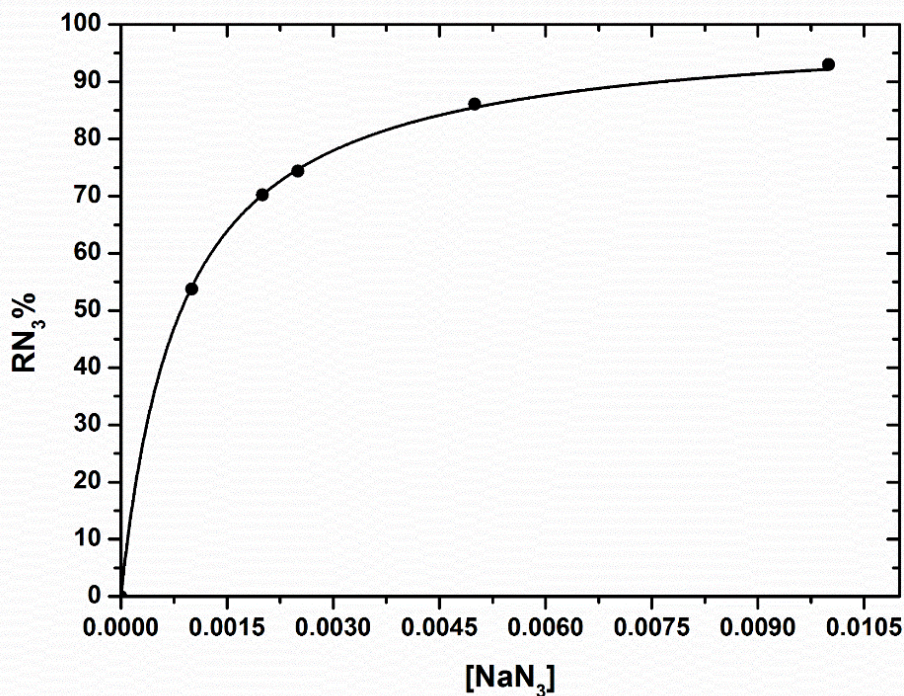


Figure A4.3 Azide adduct yield with different [NaN₃] when solvolysing O-(4-(p-methylphenyl)phenyl)-N-methanesulfonylhydroxylamine in water, the black line was fitted by Equation 13 of an S_N1 mechanism (single intermediate)⁷²

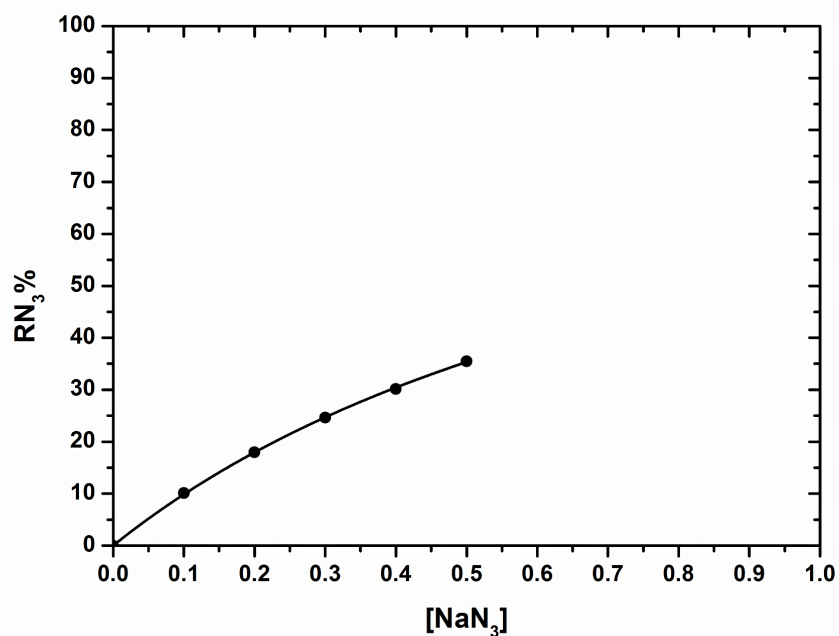


Figure A4.4 Azide adduct yield with different $[\text{NaN}_3]$ when solvolysing 1-(p-methylphenyl)-2,2,2-trifluoroethyl tosylate in 50% (v : v) TFE, the black line was fitted by Equation 13 of an $\text{S}_{\text{N}}1$ mechanism (single intermediate)^{41b}

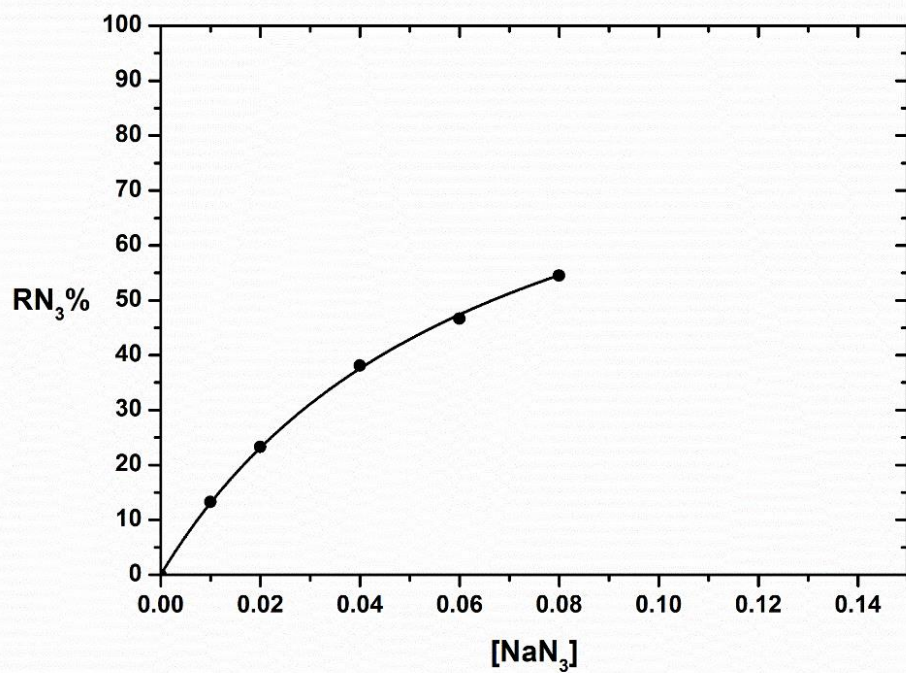


Figure A4.5 Azide adduct yield with different $[\text{NaN}_3]$ when solvolysing adamantylideneadamantyl bromide in 60% ethanol-40% water, the black line was fitted by Equation 13 of an $\text{S}_{\text{N}}1$ mechanism (single intermediate)⁷³

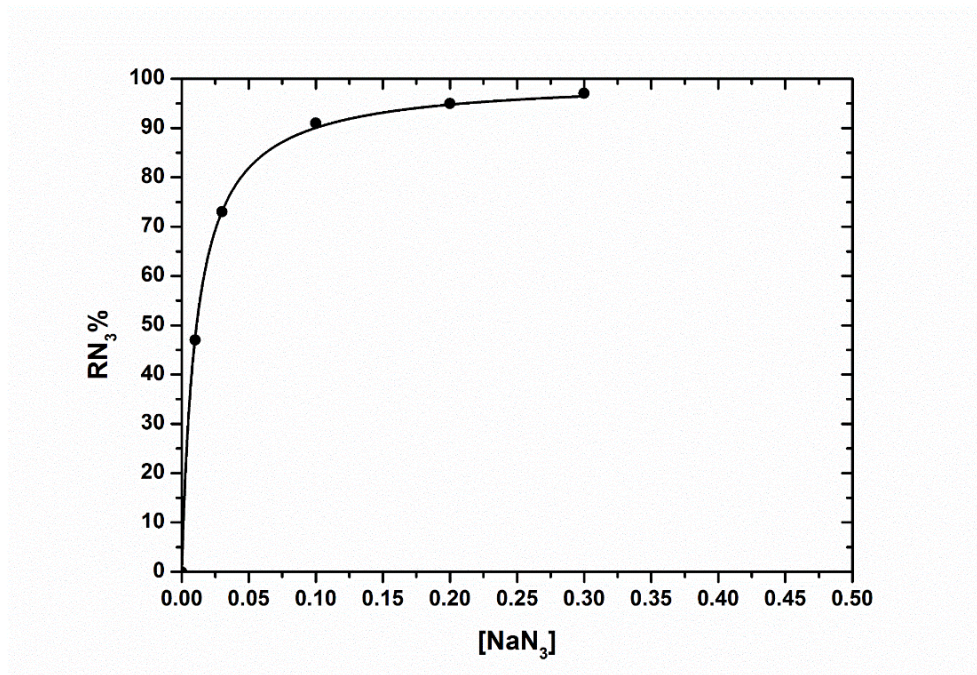


Figure A4.6 Azide adduct yield with different [NaN₃] when solvolysing 2-(p-methoxyphenyl)ethyl tosylate in 50% (v : v) TFE, the black line was fitted by Equation 13 of a combination of S_N1 and S_N2 mechanisms (single intermediate)⁵⁷

Chapter 5

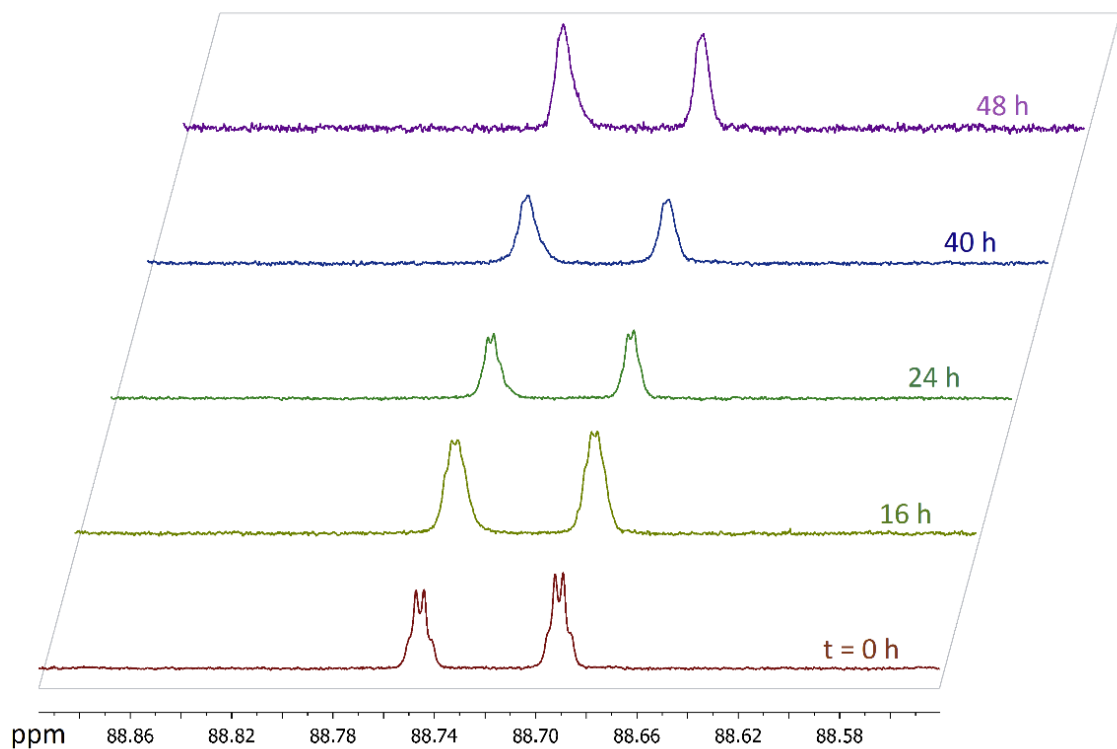


Figure A5.1 ^{13}C NMR spectra of recovered $17\text{-}^{18}\text{O}\text{COCF}_3$, $\text{R} = \text{H}$ and $17\text{-}^{16}\text{O}\text{COCF}_3$, $\text{R} = \text{H}$ at different solvolysis time in 50% TFE. The first three spectra were recorded on 400 MHz NMR, the coupling between the tertiary central carbon and F is observable